9. SITE 664[1]

Shipboard Scientific Party[2]

HOLE 664A

Date occupied: 30 March 1986, 2250 UTC

Date departed: 30 March 1986, 2330 UTC

Time on hole: 0.7 hr

Position: 0°06.44′N, 23°13.65′W

Water depth (sea level; corrected m, echo-sounding): 3806

Water depth (rig floor; corrected m, echo-sounding): 3816.5

Bottom felt (rig floor; m, drill pipe measurement): (subsurface core)

Distance between rig floor and sea level (m): 10.5

Total depth (rig floor, m): 3845.7

Penetration (m): 28.9

Number of cores (including cores with no recovery): 1

Total length of cored section (m): 9.5

Total core recovered (m): 9.64

Core recovery (%): 101.0

Oldest sediment cored:
Depth (mbsf): 28.9
Nature: calcareous nannofossil ooze
Age: Pleistocene (0.7 Ma)

HOLE 664B

Date occupied: 31 March 1986, 0130 UTC

Date departed: 31 March 1986, 2309 UTC

Time on hole: 21.7 hr

Position: 0°06.44′N, 23°13.65′W

Water depth (sea level; corrected m, echo-sounding): 3806

Water depth (rig floor; corrected m, echo-sounding): 3816.5

Bottom felt (rig floor; m, drill pipe measurement): 3816.8

Distance between rig floor and sea level (m): 10.5

Total depth (rig floor, m): 4063.8

Penetration (m): 247.0

Number of cores (including cores with no recovery): 26

Total length of cored section (m): 247.0

Total core recovered (m): 244.9

Core recovery (%): 99.1

Oldest sediment cored:
Depth (mbsf): 247.0
Nature: calcareous nannofossil ooze
Age: early Pliocene (~4.5 Ma)

HOLE 664C

Date occupied: 1 April 1986, 0145 UTC

Date departed: 1 April 1986, 0730 UTC

Time on hole: 5.75 hr

Position: 0°06.44′N, 23°16.5′W

Water depth (sea level; corrected m, echo-sounding): 3810

Water depth (rig floor; corrected m, echo-sounding): 3820.5

Bottom felt (rig floor; m, drill pipe measurement): 3817.3

Distance between rig floor and sea level (m): 10.5

Total depth (rig floor, m): 3878.5

Penetration (m): 61.2

Number of cores (including cores with no recovery): 7

Total length of cored section (m): 61.2

Total core recovered (m): 57.1

Core recovery (%): 93.3

Oldest sediment cored:
Depth (mbsf): 61.2
Nature: calcareous nannofossil ooze
Age: middle Pleistocene (1.4 Ma)

HOLE 664D

Date occupied: 1 April 1986, 1000 UTC

Date departed: 2 April 1986, 1040 UTC

Time on hole: 24.7 hr

Position: 0°06.44′N, 23°13.65′W

Water depth (sea level; corrected m, echo-sounding): 3807.0

Water depth (rig floor; corrected m, echo-sounding): 3817.5

Bottom felt (rig floor; m, drill pipe measurement): 3812.2

[1] Ruddiman, W., Sarnthein, M., Baldauf, J., et al., 1988. *Proc., Init. Repts. (Pt. A), ODP*, 108.

[2] William Ruddiman (Co-Chief Scientist), Lamont-Doherty Geological Observatory, Palisades, NY 10964; Michael Sarnthein (Co-Chief Scientist), Geologisch-Paläontologisches Institut, Universität Kiel, Olshausenstrasse 40, D-2300 Kiel, Federal Republic of Germany; Jack Baldauf, ODP Staff Scientist, Ocean Drilling Program, Texas A&M University, College Station, TX 77843; Jan Backman, Department of Geology, University of Stockholm, S-106 91 Stockholm, Sweden; Jan Bloemendal, Graduate School of Oceanography, University of Rhode Island, Narragansett, RI 02882-1197; William Curry, Woods Hole Oceanographic Institution, Woods Hole, MA 02543; Paul Farrimond, School of Chemistry, University of Bristol, Cantocks Close, Bristol BS8 1TS, United Kingdom; Jean Claude Faugeres, Laboratoire de Géologie-Océanographie, Université de Bordeaux I, Avenue des Facultés, Talence 33405, France; Thomas Janacek, Lamont-Doherty Geological Observatory, Palisades, NY 10964; Yuzo Katsura, Institute of Geosciences, University of Tsukuba, Ibaraki 305, Japan; Hélène Manivit, Laboratoire de Stratigraphie des Continents et Océans, (UA 319) Université Paris VI, 4 Place Jussieu, 75230 Paris Cedex, France; James Mazzullo, Department of Geology, Texas A&M University, College Station, TX 77843; Jürgen Mienert, Geologisch-Paläontologisches Institut, Universität Kiel, Olshausenstrasse 40, D-2300 Kiel, Federal Republic of Germany, and Woods Hole Oceanographic Institution, Woods Hole, MA 02543; Edward Pokras, Lamont-Doherty Geological Observatory, Palisades, NY 10964; Maureen Raymo, Lamont-Doherty Geological Observatory, Palisades, NY 10964; Peter Schultheiss, Institute of Oceanographic Sciences, Brook Road, Wormley, Godalming, Surrey GU8 5UG, United Kingdom; Rüdiger Stein, Geologisch-Paläontologisches Institut, Universität Giessen, Senckenbergstrasse 3, 6300 Giessen, Federal Republic of Germany; Lisa Tauxe, Scripps Institution of Oceanography, La Jolla, CA 92093; Jean-Pierre Valet, Centre de Faibles Radioactivités, CNRS, Avenue de la Terrasse, 91190 Gif-sur-Yvette, France; Philip Weaver, Institute of Oceanographic Sciences, Brook Road, Wormley, Godalming, Surrey GU8 5UG, United Kingdom; Hisato Yasuda, Department of Geology, Kochi University, Kochi 780, Japan.

Distance between rig floor and sea level (m): 10.5

Total depth (rig floor, m): 4109.0

Penetration (m): 296.8

Number of cores (including cores with no recovery): 32

Total length of cored section (m): 296.8

Total core recovered (m): 302.8

Core recovery (%): 102.0

Oldest sediment cored:
Depth (mbsf): 296.8
Nature: clayey calcareous nannofossil ooze
Age: late Miocene (~9 Ma)

Principal results: Site 664 is located at 0°06.44′N, 23°13.65′W, in a water depth of 3806.3 m in the central equatorial Atlantic on the upper-middle flank of the east side of the mid-Atlantic Ridge just north of the Romanche Fracture Zone (see "Background and Scientific Objectives" section, this chapter). The site is situated in a sediment pond with about 0.3–0.4 s of relatively transparent layering (see "Background and Scientific Objectives" section, this chapter). Although basement outcroppings are common in the surrounding terrain, the region immediately adjacent to Site 664 is largely covered with sediments. Our primary objective at this site was to obtain late Neogene records of the equatorial divergence and of eolian sedimentation.

From Holes 664A, 664B, 664C, and 664D, we recovered a total of 66 advanced piston corer (APC) cores to depths of 28.9, 247.0, 61.2, and 296.8 meters below the seafloor (mbsf), respectively. Holes 664B, 664C, and 664D were cored continuously. We recovered only one core from Hole 664A below the mud line because of miscounting the pipe stands. Recovery averaged 101.0% for Hole 664A, 99.1% for Hole 664B, 93.3% for Hole 664C, and 102.0% for Hole 664D.

The entire cored section (0–296.8 mbsf) consisted of one lithologic unit composed of nannofossil and foraminifer-nannofossil oozes of late Miocene, Pliocene, and Pleistocene age (Fig. 1). Secondary components are clay (including zeolitic clay in Cores 108-664D-31H and -664D-32H), diatoms, and radiolarians. Two deeper holes (Holes 664B and 664D) contain many slump units, as well as several other partially deformed layers (see "Composite-Depth Section," this chapter).

Paleomagnetic reversal boundaries provided a useful stratigraphy down to the Jaramillo subchron only (see "Paleomagnetism" section, this chapter). Below this level, the decreasing natural remanent magnetization precluded the use of paleomagnetic results. The nannofossil and planktonic-foraminifer biostratigraphy also provided numerous datums to constrain the age-depth curve throughout the sequence (see "Sediment-Accumulation Data" section, this chapter).

Preservation of calcareous fossils is generally good, although it becomes worse at about 200 mbsf (4.4 Ma; early Pliocene). This change in carbonate preservation agrees with similar evidence from previous Leg 108 sites, providing additional confirmation of a major change in bottom-water chemistry in the early Pliocene.

Preservation of diatoms is moderate to poor in the upper 200 mbsf, and sediments have no diatoms below this depth. This suggests a much lower supply of biogenic silica from surface waters because of lower productivity before about 4.0 to 4.5 Ma.

The depositional rate of pelagic sediments varied and, in those parts of the sequences with frequent slumps, was difficult to determine. The upper Pleistocene pelagic sequence (0–55 mbsf) in Holes 664A, 664B, and 664C was deposited at average rates of about 49 m/m.y. The late Pliocene rates farther down in Hole 664B were difficult to determine owing to frequent slump interruption, but appeared to be slightly lower (see "Sediment-Accumulation Rates" section, this chapter). In the less disrupted lower Pliocene to Pleistocene sequence in Hole 664D, rates average 32–51 m/m.y. down to a slump at 185 mbsf, and then decrease to less than 20 m/m.y in the Miocene and early Pliocene sequence from 208 mbsf to the bottom of the hole.

Neither paleomagnetic-susceptibility nor *P*-wave measurements were useful for between-hole correlations, so we used carbonate layering from core photographs to provide these links. We succeeded in correlating the uppermost pelagic unit (0–55 mbsf; 0 to 1.25 Ma) between Holes 664B and 664D, thus tracing a continuous composite-depth section throughout that entire upper Pleistocene sequence (see "Composite-Depth Section," this chapter).

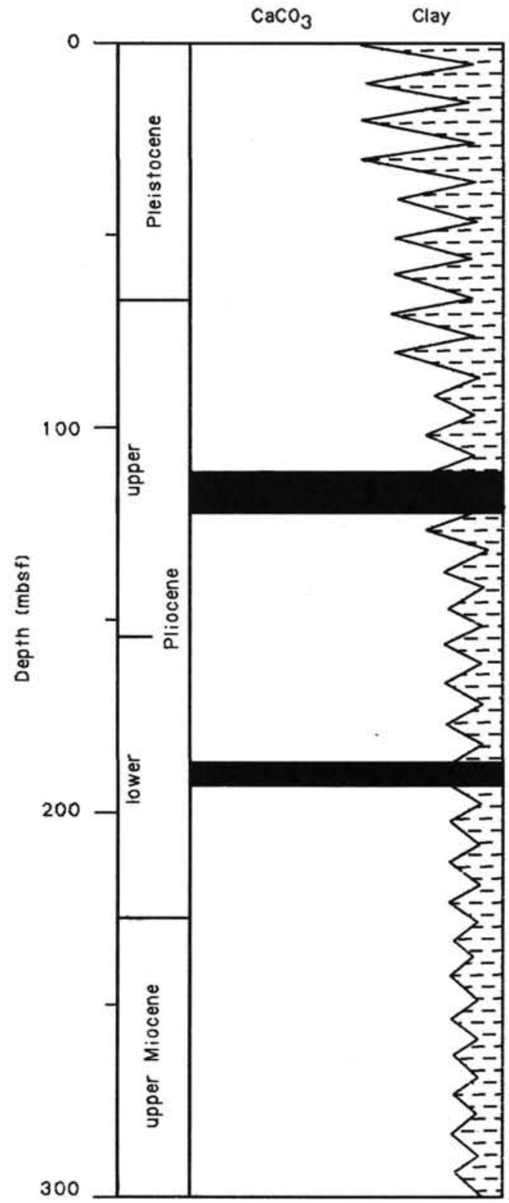

Figure 1. Lithostratigraphic and biostratigraphic summary of Site 664, based on Hole 664D. Black layers are badly deformed gravity-flow mass deposits (mostly slumps); slightly deformed bedding from 49 to 87 mbsf and 190 to 208 mbsf indicates possible slump deformation, but with little or no disturbance of the age-depth sequence; remainder of section is pelagic-nannofossil ooze. Schematic representation of $CaCO_3$ cycles shows general range of percentage of $CaCO_3$ variations increasing upward. Actual timing of this increase cannot be determined from widely spaced shipboard $CaCO_3$ analyses.

Slumps at 55 to 97 mbsf in Hole 664B and 49 to 87 mbsf in Hole 664D interrupt this continuous sequence. The slump in Hole 664B brought in disturbed allochthonous sediments of late to early Pliocene age, older than the underlying upper Pliocene pelagic layer (see "Sediment-Accumulation Rates" section, this chapter). In contrast, the sediments at equivalent depths in Hole 664D were disturbed much less (slightly tilted, with bioturbation and mottling partially obscured), and their age fits directly on the age-depth curve interpolated from over- and underlying pelagic sequences. This indicates that the "slumped" unit in Hole 664D may be nearly *in situ*. These results show a surprising variability in degree of deformation and in age of slumped units over very small lateral scales (1000 m) within the same sediment pond.

Below these slumps, we were able to correlate only a short (10-m) sequence near 100 mbsf, which represents a short upper Pliocene (2.4 Ma) section. Below 110 mbsf, the $CaCO_3$ layering was too faint to use core photographs for correlations. The high recovery and the relatively undisturbed condition of the sections below 200 mbsf at Hole 664D suggest that we recovered a valuable upper Miocene sequence deposited at high rates.

As at Sites 662 and 663, there was an intensification of the $CaCO_3$ cycles from the late Pliocene to the late Pleistocene (see "Organic Geochemistry" section, this chapter). This increased amplitude occurred because of stronger $CaCO_3$ minima, accompanied by increased silica and clay contents in grayish green sediment layers. Because of interruptions from slumps and aliasing of the true signal by our limited shipboard sampling resolution, we were unable to ascertain whether this increase in amplitude was gradual or abrupt. Possible explanations for this change include increased carbonate dissolution, decreased carbonate productivity, increased silica productivity, or increased eolian sedimentation.

The slump at approximately 1.25 Ma may coincide with mid-Pleistocene deformation at Sites 662 and 663. All three sites are located adjacent to the active transform-fault section of the Romanche Fracture Zone. The almost simultaneous occurrence of slump deformation at these sites could indicate that a major seismic event within the Romanche Fracture Zone dislodged pelagic sediments over a broad region of the upper flanks of the mid-Atlantic Ridge, sending slumps and turbidites down into sediment ponds in many areas.

BACKGROUND AND SCIENTIFIC OBJECTIVES

Site 664 (target Site Eq-9) was the last of three Leg 108 sites designed to retrieve a late-Neogene record of climatic variability from near the equator (see Fig. 2, Site 662 chapter). For a discussion of our overall scientific criteria and rationale for these sites, see "Background and Scientific Objectives" section, Site 662 chapter (this volume). Because of its location more than 1100 km to the west-northwest of Sites 662 and 663, we felt Site 664 should contain a climatic record dominated primarily by equatorial divergence and influenced less by advection of cold water in the Benguela Current flow from the Southern Hemisphere.

Our primary scientific objectives at Site 664 were as follows:

1. To determine the late-Neogene history of variations in equatorial surface-ocean circulation, using estimated sea-surface temperatures from planktonic foraminifers, as well as fluxes of opaline silica, $CaCO_3$, and organic carbon.
2. To reconstruct the late-Neogene history of variations in African aridity, as indicated by biogenic material and wind-blown terrigenous dust from the African continent.

Our secondary objectives for Site 664 were the following:

1. To obtain a continuous, late-Neogene sequence for high-resolution paleomagnetic, biostratigraphic, and stable-isotope analyses.
2. To obtain a calcareous sequence for analysis of late-Neogene dissolution trends.

Geologic and Topographic Setting

Site 664 is located in the central equatorial Atlantic on the upper-middle flank of the east side of the mid-Atlantic Ridge (Fig. 2; see also Fig. 2, Site 662 chapter, this volume). The ridge topography in this region is complex, with major east-west jumps of the rift valley between fracture zones separated by an average north-south distance of about 40 km. Just 120 km south of Site 664, the rift valley shifts some 1000 km to the east across the Romanche Fracture Zone, the largest such jump in the equatorial Atlantic Ocean.

Air-gun records from the Site 664 region reveal a fairly complex topography, with areas of outcropping or near-outcropping basement alternating with ponds of thin sediment fill on a scale of miles to tens of miles. The sediment fill averages about 0.2 s (about 150 m) and reaches maximum values of about 0.4 s (about 300 m).

The appearance of the fill in the sediment ponds varies considerably. V3004 cruise seismic lines some 25 to 50 km to the east of the proposed site are similar to those obtained in the region of Sites 662 and 663, with small ponds of reflective, flat-lying sediments in larger areas of basement outcropping. Based on drilling results at those sites, these sediments frequently may be disturbed by turbidites and slumps. The several hours of seismic record from the immediate vicinity of Site 664, however, are somewhat different in character from the surrounding region (Fig. 3). These sediments are faintly layered, more conformable to basement topography, and, generally, have more of the "draped" character typical of pelagic deposition, with only minor amounts of redeposition in thicker sediment ponds. Based on data obtained during the GEOTROPEX '85 cruise of the *Polarstern*, the location of Site 664 was adjusted to an area of thick, moderately reflective sediment cover (Fig. 2).

The basement age at Site 662 is estimated as late Miocene, based on regional magnetic lineations. The anticipated sedimentary section is a cyclical alternation of upper Miocene, Pliocene, and Pleistocene nannofossil ooze and mud.

OPERATIONS

After departing Site 663, we steamed at a speed of 13 kt on a course of 290° toward the location of Site 664. On 30 March at 1200 UTC, we slowed to 5 kt and streamed out 80-in.^{3} water guns and a magnetometer. (All times are UTC, Universal Time Coordinated, formerly GMT, Greenwich Mean Time.) We continued on the same course until 1350, when we turned to a course of 305° to position our track over the sediment pond we wished to core (see Fig. 2; "Background and Scientific Objectives" section, this chapter). All navigation during this survey was controlled by our global positioning system (GPS). At 1452, we turned to a course of 270°. At this point, we finally selected the Site 664 location at a position about 2 nmi east-northeast of the approved position; we chose a position we had crossed earlier at 1440 on the *JOIDES Resolution* line 108-8, shown in Figure 2. At 1515, we steamed on a course of 100° and returned to the Site 664 location at 0°06.44′N, 23°13.65′W.

We arrived at the site at 1605 on 30 March and dropped a beacon. We then slowed to 2 kt, retrieved our geophysical gear, and returned to the beacon. We began running drill pipe into the hole by 1640 and finished at 2200. The first and only advanced piston corer (APC) core from Hole 664A came on deck at 2330 (Table 1), by which time we discovered that we had miscounted one pipe stand and that the core actually was shot below the mud line. We moved 15 m south to try again. Our first attempt produced a water core, but our second attempt gave us our first core from Hole 664B, which was brought on deck at 0205 on 31 March. We continued APC coring to a total penetration depth of 247 meters below the seafloor (mbsf) and brought the final core (108-664B-26H) on deck at 2309.

We then pulled out of Hole 664B and offset the drill string 15 m to the north. We spudded in Hole 664C on 1 April at 0145. The first APC core from Hole 664C came on deck at 0205. We continued APC coring until Core 108-664C-7H, which came on deck at 0730. We then pulled out of Hole 664C and offset the drill string 1000 m to the north at Hole 664D, hoping to avoid some of the slumped sections encountered in Hole 664B.

We spudded in Hole 664D at 1000 on 1 April. The first APC core from Hole 664D came on deck at 1030. We oriented Cores 108-664D-3H through -664D-6H. We continued APC coring until Core 108-664D-32H came on deck at 1040 on 2 April. One final core attempted as we neared the acoustic basement stroked out completely, but became stuck in the stiffer sediment. The core

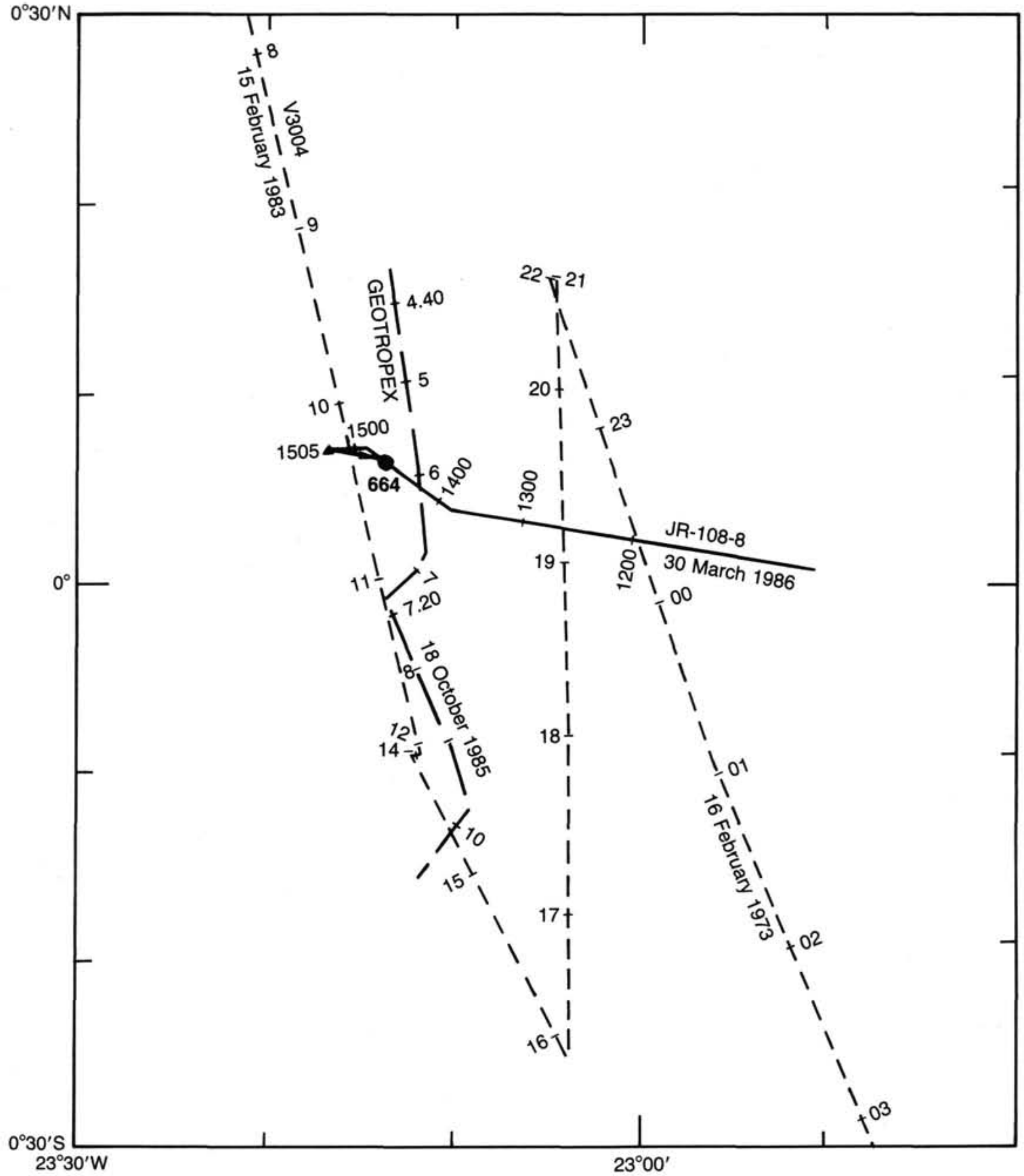

Figure 2. Seismic track lines near Site 664.

barrel parted at 145,000 lb of overpull during our attempts to retrieve it. At 1300, we began pulling out of the hole, and the drill string was back on deck by 1945. We got under way from Site 664 at 1945 on 2 April and headed for Site 665. The weather was favorable—warm and sunny throughout all operations, with weak to moderate winds and swell.

LITHOSTRATIGRAPHY AND SEDIMENTOLOGY

Introduction

One major lithologic unit was recognized at Site 664 (Fig. 4). It is composed primarily of calcareous-nannofossil ooze and is late Miocene through Pleistocene in age. The unit is further subdivided on the basis of distinct variations in carbonate content in Hole 664B. Subunits are described in detail in the following sections.

Subunit IA

Cores 108-664A-1H-1 through -664A-1H, CC; depth, 19.4–28.9 mbsf; age, Pleistocene.
Cores 108-664B-1H through -664B-6H-4, 70 cm; depth, 0–52.7 mbsf; age, Pleistocene.
Cores 108-664C-1H through -664C-6H-5, 90 cm; depth, 0–49.1 mbsf; age, Pleistocene.
Cores 108-664D-1H through -664C-7H-1, 130 cm; depth, 0–51.1 mbsf; age, Pleistocene.

Subunit IA is composed primarily of clay- and foraminifer-bearing nannofossil ooze interbedded with foraminifer-nannofossil and muddy nannofossil oozes. This subunit is characterized by carbonate concentrations ranging from 60% to 90%, with a few intervals having values of less than 50%. The sediments range in color from white (5Y 8/1, 7.5YR 8/0) and light

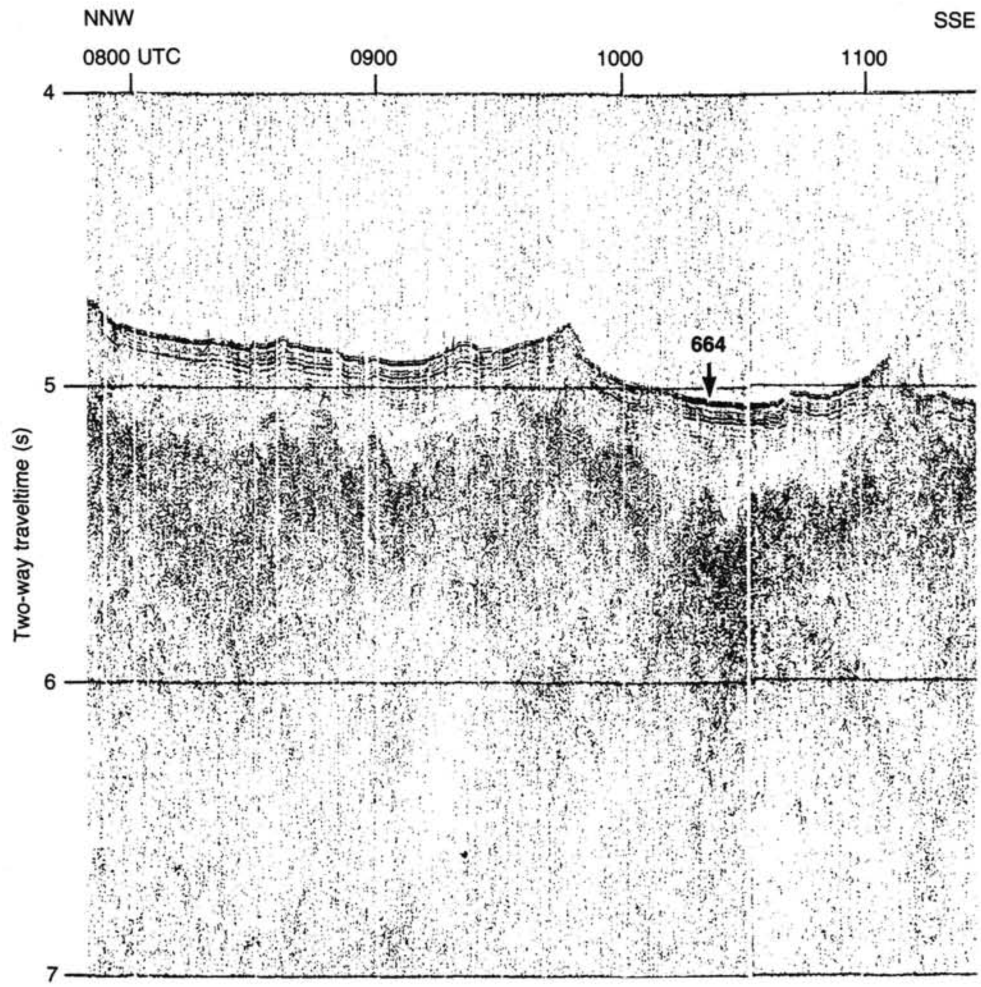

Figure 3. Seismic-reflection record from cruise V3004 near Site 664.

gray (5Y 7/1) to gray (5Y 6/1). The darker intervals (gray to light gray) generally have higher terrigenous concentrations. The calcareous component is composed primarily of nannofossils (55% to 70%) and foraminifers (5% to 30%). The terrigenous component of the sediments is primarily clay (10% to 25%) and quartz (trace to 5%). Siliceous material is present in minor concentrations (trace to 5%) and is composed primarily of diatoms and radiolarians. These sediments are weakly to moderately bioturbated, and green, purple, and black laminations are present throughout the subunit. The nannofossil ooze is interrupted by scattered sandy foraminifer turbidites or contourites, ranging from 2 to 10 cm thick.

Subunit IB

Cores 108-664B-6H-4, 70 cm, through -664B-26H, CC; depth, 52.7–247.0 mbsf; age, Pliocene through Pleistocene.
Cores 108-664C-6H-5, 90 cm, through -664C-7H, CC; depth, 49.1–61.2 mbsf; age, Pleistocene.
Cores 108-664D-7H-1, 130 cm, through -664D-32H, CC; depth, 51.1–296.8 mbsf; age, late Miocene through Pleistocene.

Subunit IB is composed primarily of mud and foraminifer-bearing nannofossil oozes. Muddy nannofossil and foraminifer-nannofossil oozes are scattered. The subunit is characterized by high carbonate concentrations, generally 85% to 90%. The sediments are predominantly white (2.5Y 8/0, 7.5YR 8/0), with scattered light gray (5Y 7/1) intervals. Nannofossils range in concentration from 75% to 90%, with foraminifers making up 5% to 20% of the sediments, except in a few intervals, where concentrations are as high as 45%. Clay content is generally less than 10%, with a few intervals as high as 25%. Siliceous material, mostly diatoms and radiolarians, is present in trace amounts.

This subunit is characterized by slumped and folded sediments of lithology similar to normal pelagic sediments. Microfaults and turbidites commonly occur in the slumped intervals. In Hole 664B, these slumped intervals are characterized by carbonate values greater than 85%, similar to those values observed in the older (>2.6 Ma) sediments at Sites 662 and 663. In intervals not affected by slumping (100–116, 147–163, 170–180, and 204–220 mbsf), carbonate concentrations are more variable and range from 75% to 90%.

Depositional Environment

The stratigraphic sequences recovered at Site 664 are similar to those recovered at Sites 662 and 663. The depositional history of these sediments is typical of equatorial Atlantic high-productivity regions. As at Sites 662 and 663, the normal pelagic sedimentation was interrupted by slumps and turbidites of similar lithology. The remarkably uniform age-depth curve for Hole 664D (see "Sediment-Accumulation Rates" section, this chapter) suggests that the slumped intervals in this hole may represent sediment deformed *in situ*, rather than material originating from topographic highs. In some cases, the degree of deformation is slight.

Table 1. Site 664 coring summary (drilling depths).

Core no.	Date (1986)	Time (UTC)	Depths (mbsf)	cored (m)	Length recovered (m)	Length Recovery (%)
108-664A-1H	30 March	2330	19.4–28.9	9.5	9.6	101.0
108-664B-1H	31 March	0205	0–9.5	9.5	9.6	101.0
108-664B-2H	31 March	0304	9.5–19.0	9.5	9.3	97.3
108-664B-3H	31 March	0355	19.0–28.5	9.5	9.5	100.0
108-664B-4H	31 March	0432	28.5–38.0	9.5	9.5	100.0
108-664B-5H	31 March	0530	38.0–47.5	9.5	9.7	101.0
108-664B-6H	31 March	0627	47.5–57.0	9.5	9.5	99.8
108-664B-7H	31 March	0718	57.0–66.5	9.5	9.4	99.1
108-664B-8H	31 March	0800	66.5–76.0	9.5	9.5	100.0
108-664B-9H	31 March	0845	76.0–85.5	9.5	9.7	102.0
108-664B-10H	31 March	0930	85.5–95.0	9.5	9.2	96.5
108-664B-11H	31 March	1010	95.0–104.5	9.5	9.5	99.7
108-664B-12H	31 March	1050	104.5–114.0	9.5	9.5	100.0
108-664B-13H	31 March	1145	114.0–123.5	9.5	9.7	102.0
108-664B-14H	31 March	1240	123.5–133.0	9.5	9.2	96.4
108-664B-15H	31 March	1326	133.0–142.5	9.5	9.4	99.2
108-664B-16H	31 March	1417	142.5–152.0	9.5	9.8	103.0
108-664B-17H	31 March	1502	152.0–161.5	9.5	9.5	100.0
108-664B-18H	31 March	1548	161.5–171.0	9.5	9.5	100.0
108-664B-19H	31 March	1643	171.0–180.5	9.5	8.5	89.7
108-664B-20H	31 March	1725	180.5–190.0	9.5	9.6	101.0
108-664B-21H	31 March	1819	190.0–199.5	9.5	9.4	98.4
108-664B-22H	31 March	1919	199.5–209.0	9.5	9.7	101.0
108-664B-23H	31 March	2012	209.0–218.5	9.5	9.6	101.0
108-664B-24H	31 March	2059	218.5–228.0	9.5	9.9	104.0
108-664B-25H	31 March	2149	228.0–237.5	9.5	8.7	91.1
108-664B-26H	31 March	2309	237.5–247.0	9.5	8.8	92.5
108-664C-1H	1 April	0205	0–4.2	4.2	4.2	100.0
108-664C-2H	1 April	0305	4.2–13.7	9.5	9.5	100.0
108-664C-3H	1 April	0351	13.7–23.2	9.5	8.5	89.9
108-664C-4H	1 April	0450	23.2–32.7	9.5	8.5	88.9
108-664C-5H	1 April	0559	32.7–42.2	9.5	9.3	97.6
108-664C-6H	1 April	0650	42.2–51.7	9.5	7.8	82.2
108-664C-7H	1 April	0730	51.7–61.2	9.5	9.4	98.8
108-664D-1H	1 April	1030	0–2.3	2.3	2.3	98.7
108-664D-2H	1 April	1115	2.3–11.8	9.5	9.9	103.0
108-664D-3H	1 April	1227	11.8–21.3	9.5	9.7	102.0
108-664D-4H	1 April	1320	21.3–30.8	9.5	9.5	100.0
108-664D-5H	1 April	1415	30.8–40.3	9.5	9.7	102.0
108-664D-6H	1 April	1508	40.3–49.8	9.5	9.6	101.0
108-664D-7H	1 April	1559	49.8–59.3	9.5	9.5	100.0
108-664D-8H	1 April	1649	59.3–68.8	9.5	9.7	102.0
108-664D-9H	1 April	1732	68.8–78.3	9.5	9.6	101.0
108-664D-10H	1 April	1826	78.3–87.8	9.5	9.6	101.0
108-664D-11H	1 April	1912	87.8–97.3	9.5	9.8	103.0
108-664D-12H	1 April	1959	97.3–106.8	9.5	9.8	103.0
108-664D-13H	1 April	2048	106.8–116.3	9.5	9.6	101.0
108-664D-14H	1 April	2137	116.3–125.8	9.5	9.4	99.2
108-664D-15H	1 April	2228	125.8–135.3	9.5	9.9	104.0
108-664D-16H	1 April	2315	135.3–144.8	9.5	10.0	105.3
108-664D-17H	2 April	0001	144.8–154.3	9.5	9.8	103.0
108-664D-18H	2 April	0048	154.3–163.8	9.5	9.6	101.0
108-664D-19H	2 April	0130	163.8–173.3	9.5	9.6	101.0
108-664D-20H	2 April	0220	173.3–182.8	9.5	9.5	100.0
108-664D-21H	2 April	0258	182.8–192.3	9.5	9.5	100.0
108-664D-22H	2 April	0345	192.3–201.8	9.5	9.7	102.0
108-664D-23H	2 April	0425	201.8–211.3	9.5	9.8	103.0
108-664D-24H	2 April	0510	211.3–220.8	9.5	9.7	102.0
108-664D-25H	2 April	0555	220.8–230.3	9.5	9.8	103.0
108-664D-26H	2 April	0630	230.3–239.8	9.5	9.7	102.0
108-664D-27H	2 April	0715	239.8–249.3	9.5	9.7	102.0
108-664D-28H	2 April	0750	249.3–258.8	9.5	9.8	103.0
108-664D-29H	2 April	0830	258.8–268.3	9.5	9.9	104.0
108-664D-30H	2 April	0910	268.3–277.8	9.5	9.8	103.0
108-664D-31H	2 April	1000	277.8–287.3	9.5	9.7	102.0
108-664D-32H	2 April	1040	287.3–296.8	9.5	9.7	101.0

H = hydraulic piston. UTC = Universal Time Coordinated.

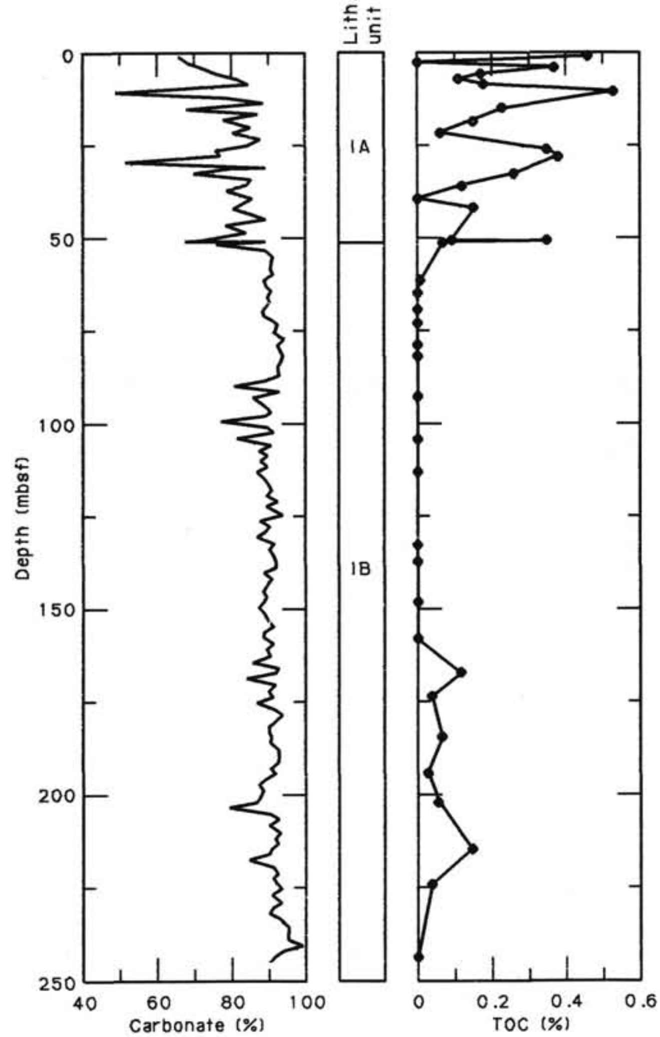

Figure 4. Carbonate and total-organic-carbon (TOC) concentrations for Hole 664B. Also shown are subunits observed at this site.

BIOSTRATIGRAPHY

Four holes were drilled at Site 664, but Hole 664A was abandoned after only drilling one core because the mud line could not be recovered. All other holes were cored continuously. Hole 664B reached a depth of 247 mbsf and Hole 664C penetrated to 61.2 mbsf. Hole 664D attained a depth of 296.8 mbsf, with a maximum age of about 9 Ma (late Miocene). Although Hole 664D is within 1 km of the other three holes, it shows much less stratigraphic disturbance than the other deep hole, Hole 664B. Age and zonal assignments for Holes 664B and 664D are shown in Figures 5 and 6.

Calcareous nannofossils and planktonic foraminifers were generally abundant and well preserved, except that planktonic foraminifers show poor preservation in the Miocene and lower Pliocene of Hole 664D, and discoasters exhibit overgrowths of calcium. Discoasters are substantially more numerous at Site 664 than at Sites 662 and 663, located farther east. The planktonic-foraminifer fauna is characterized by a greater percentage of tropical vs. temperate species than that found at Sites 662 and 663. Benthic foraminifers are rare to few, with preservation generally moderate to poor. Diatom abundances fluctuate markedly, but are generally few to common. No diatoms were observed in the Miocene and lower Pliocene sediments.

The presence of extensive slumps and turbidites in Hole 664B leads to considerable stratigraphic complexity, and fossil-based age assignments were often reversed (see "Sediment-Accumulation Rates" section, this chapter). Hole 664D, however, contains slumps and turbidites, but no alterations to the normal stratigraphic sequence. A number of marker taxa occur only sporadically near the limits of their ranges, restricting the number of useful biostratigraphic zones in both holes.

Calcareous Nannofossils

Discoasters are substantially more abundant at Site 664 than at Sites 662 and 663. At Site 664, placoliths are dissolved mod-

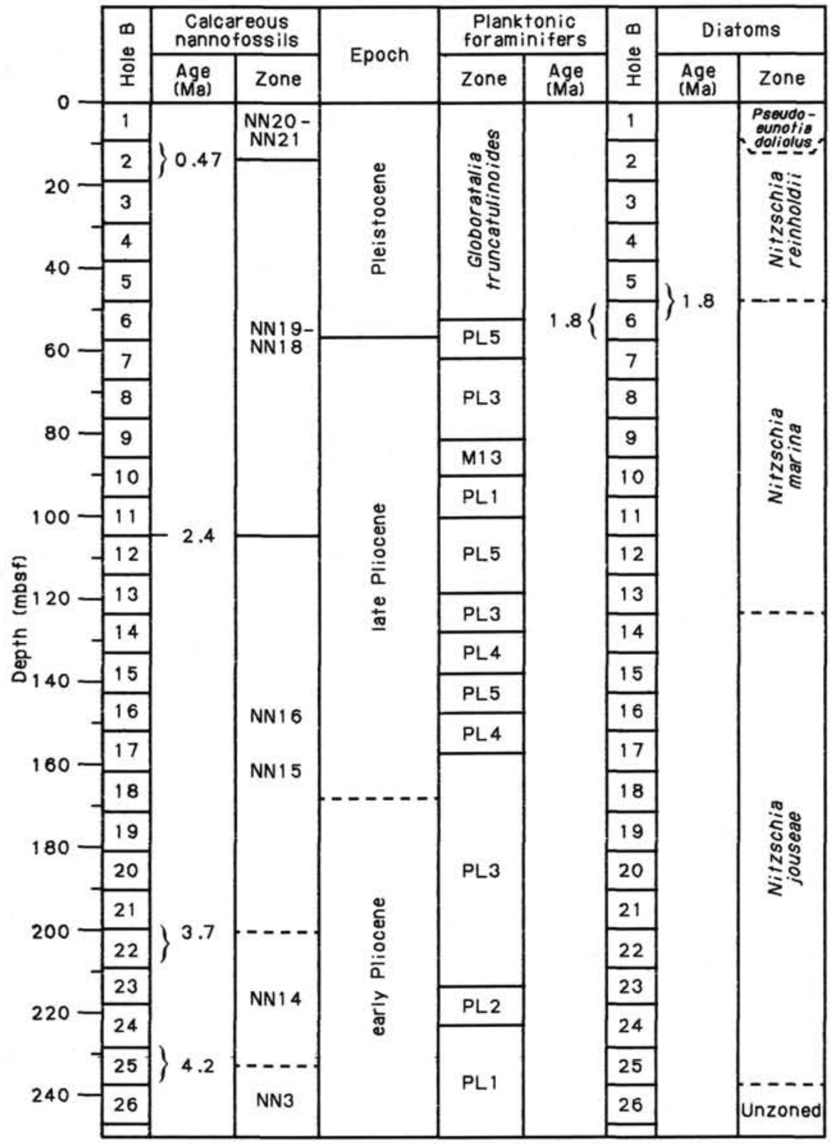

Figure 5. Zonal assignments for cores recovered from Hole 664B.

erately in the latest Miocene through Pleistocene and are dissolved severely in the earliest late Miocene. Discoasters show moderate overgrowth in the latest Miocene through Pliocene. Overgrowth increases in the late Miocene, and most primary morphological characters in the earliest late Miocene are blurred severely by secondary calcium.

Holes 664A and 664C

Pseudoemiliania lacunosa was observed at both the top and bottom of Core 108-664A-1H. Both levels lacked *Calcidiscus macintyrei*, placing this core in the middle part of the Pleistocene. In Hole 664C, the extinction of *P. lacunosa* was observed in Core 108-664C-3H. Sample 108-664C-6H, CC still contained a typical Pleistocene assemblage without either *C. macintyrei* or *Helicosphaera sellii*. Sample 108-664C-7H, CC yielded these species as well as common reworked Pliocene species (e.g., *Sphenolithus abies*), making the presence of *C. macintyrei* biostratigraphically valueless in this sample.

Hole 664B

Emiliania huxleyi has its first occurrence (FO) in Section 108-664B-1H-6, and its acme interval seems restricted to the uppermost few tens of centimeters in Section 108-664B-1H-1. The disappearance of *P. lacunosa* occurs either in lower Section 108-664B-2H-3 or in upper Section 108-664B-2H-4. The first major slump was encountered in Core 108-664B-6H, and all samples investigated above the slump in Core 108-664B-6H had no occurrences of *H. sellii* and *C. macintyrei.*

Sample 108-664B-6H-4, 30 cm, was taken from the uppermost part of the slump and contained abundant Pliocene discoasters, including *Discoaster asymmetricus* and *Discoaster tamalis.* This upper Pliocene assemblage also was observed in Cores 108-664B-8H and -664B-9H, whereas Cores 108-664B-9H and -664B-10H contained an assemblage suggesting an early Pliocene age, with common *Reticulofenestra pseudoumbilica* and sphenoliths.

The discoaster assemblages in Core 108-664B-11H represent the late Pliocene, with common *Discoaster brouweri* and rare *Discoaster pentaradiatus.* The latter species is significantly more abundant in Core 108-664B-12H. Neither Core 108-664B-11H nor Core -664B-12H shows early Pliocene reworking. The sediments from Cores 108-664B-11H and -664B-12H are not disturbed by slumping. Therefore, we can place the evolutionary last occurrence (LO) of *D. pentaradiatus* within Core 108-664B-

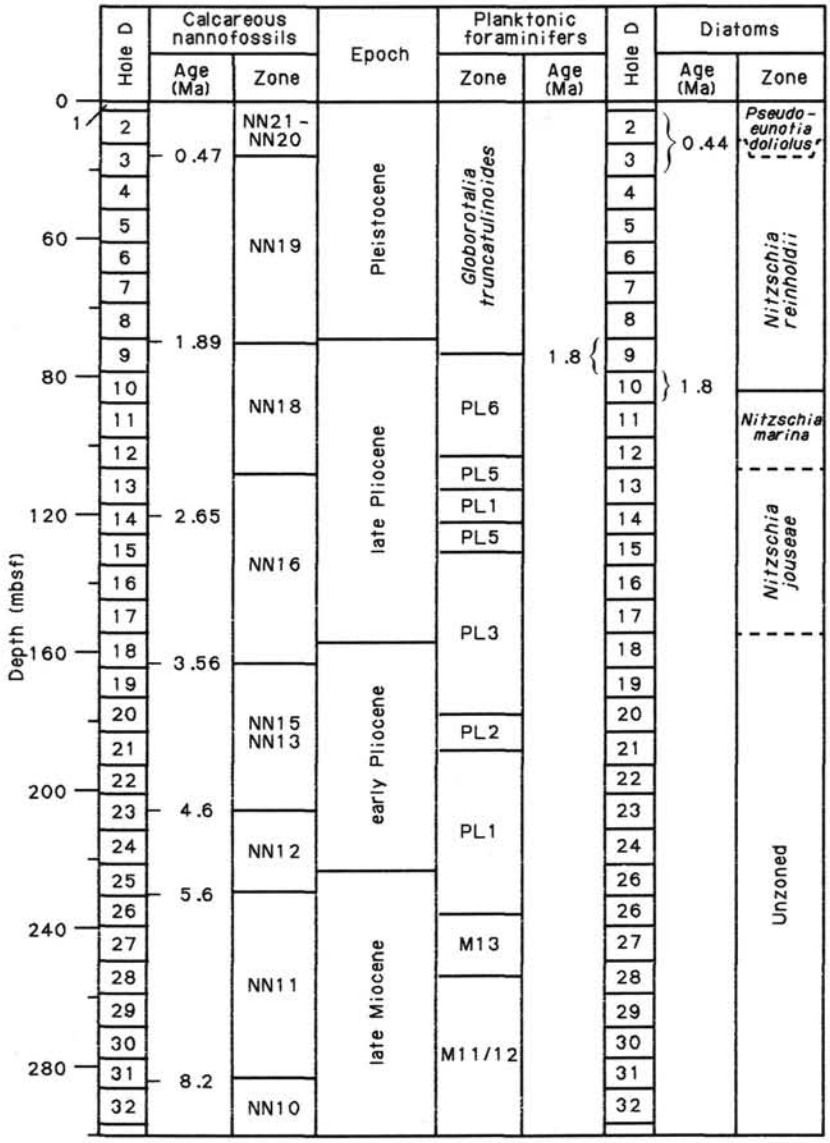

Figure 6. Zonal assignments for cores recovered from Hole 664D. The intervals representing calcareous-nannofossil Zones NN14 and NN17 were not identified at this hole.

12H, despite its high abundances upsection within slumped intervals.

Cores 108-664B-13H through -664B-19H all contain late-Pliocene discoaster assemblages typical of those that thrived during the time of the existence of *D. tamalis.* A few samples in this interval yielded rare early-Pliocene nannofossils, probably because several cores from this interval contain turbidites, debris flows, or slumps.

Although Cores 108-664B-20H and -664B-21H were retrieved from within a slumped unit, they are in biostratigraphic sequence and seemingly undisturbed, in that sphenoliths disappear in Core 108-664B-20H, and *R. pseudoumbilica* disappears in Core 108-664B-21H. The first downhole observation of *Amaurolithus* spp. was in Core 108-664B-24H.

Ceratolithus rugosus was present throughout the lower part of Hole 664B and occurred with *Ceratolithus acutus* in the deepest core (Core 108-664B-26H).

Hole 664D

Cores 108-664D-1H and -664D-2H show typical late-Pleistocene assemblages, characterized by low species diversity and strong dominance by gephyrocapsids. The extinction of *P. lacunosa* occurs in Section 108-664D-3H-3, whereas the early Pleistocene markers *H. sellii* and *C. macintyrei* disappear in Cores 108-664D-7H and -664D-8H, respectively.

Discoaster brouweri and *D. triradiatus* are present at the base of Core 108-664D-9H, but are not found farther upsection, indicating a position for the Pliocene/Pleistocene boundary within Core 108-664D-9H (about midway between the extinction levels of *C. macintyrei* and *D. brouweri*). Both core-catcher samples of Cores 108-664D-9H and -664D-10H displayed high proportions (>20%) of *D. triradiatus* relative to *D. brouweri.* This percentage decreased to 3% in Section 108-664D-11H-4, implying that the upper one-half of Core 108-664D-11H has an age of about 2.0 to 2.1 Ma. *Discoaster pentaradiatus* does not occur above Section 108-664D-12H-3; Section 108-664D-12H, CC contains *Discoaster surculus,* which disappears in the lower one-half of Core 108-664D-12H.

The succession of late Pliocene assemblages is broken in Core 108-664D-13H by a slump representing sediment of early Pliocene age. Sphenoliths and small reticulofenestrids are abundant in this assemblage, and discoasters, *Calcidiscus leptoporus,* and

Dictyococcites productus also are common. The biostratigraphically important *C. acutus* is rare, but nevertheless indicates that this assemblage can be referred to basal Pliocene (the upper one-half of Zone NN12). Discoasters show substantial overgrowth, and placoliths have rather strong etching.

Cores 108-664D-14H through -664D-17H all contain *D. tamalis* and *D. asymmetricus*, but no sphenoliths or *R. pseudoumbilica* were observed. Sphenoliths disappear in Section 108-664D-18H-3, and *R. pseudoumbilica* disappears immediately above 108-664D-18H, CC. The first downhole occurrence of *Amaurolithus* spp. was observed in Core 108-664D-21H, presumably indicating that we missed the extinction event of this genus owing to its low abundance. This suggestion is supported by planktonic-foraminifer data, as well as by the anomalously high sedimentation rates that would be required if amaurolithids had their extinction within Core 108-664D-21H.

Ceratolithus rugosus is present down to the top of Section 108-664D-23H-2. This species is never abundant or even common and often is overgrown severely with diagenetic calcium, which, in several samples, caused problems regarding the separation between *C. rugosus* and its predecessor, *C. acutus*. Rare, but distinct, *C. acutus* was observed between Sections 108-664D-23H-5 and -664D-25H-2. The LO of *C. rugosus* was observed in Section 108-664D-25H-5.

Overgrowth of the central areas of the discoasters made recognition of *Discoaster quinqueramus* difficult in many samples. Therefore, the LO of this species is placed tentatively in Section 108-664D-26H-2; it co-occurs with *A. amplificus* in Section 108-664D-26H-4. *Amauroliths* spp. and *D. quinqueramus* have overlapping ranges down through Core 108-664D-28H, below which *D. quinqueramus* continues its range to Section 108-664D-31H-4. The central-area/ray-length ratio increases markedly toward the earliest part of the range of *D. quinqueramus*; however, we have not attempted to distinguish between those ranges showing high central-area/ray-length ratios (*Discoaster berggrenii*) and those having lower ratios (*D. quinqueramus*), mainly because diagenetic alterations have blurred the critical morphological parameters in most specimens observed.

Dissolution has strongly biased the composition of the nannofossil assemblages in the early part of the late Miocene, with abundant discoasters and few placoliths. Three important biostratigraphic events occurred in Core 108-664D-32H; *Discoaster bollii* disappeared in Section 108-664D-32H-3, whereas *Discoaster hamatus* and *Catinaster calyculus* have their last occurrences in Section 108-664D-32H-6. The core-catcher sample contained all three species, but *C. coalitus* was absent.

Planktonic Foraminifers

The record of planktonic foraminifers extends to the lower Pliocene in Hole 664B, through the upper Pleistocene in Hole 664C, and to the upper Miocene in Hole 664D. All three holes contained slumps, identified by the presence of anomalous biostratigraphic markers or other reworked species. A complete late-Pleistocene record was recovered from each hole, and two holes, 664B and 664D, exhibit good recovery before 3.0 Ma. This site is characterized by numerous tropical species (including *Globigerinoides ruber, Neogloboquadrina dutertrei, Globigerinoides trilobus, Dentogloboquadrina altispira*, and *Globigerina decoraperta*), more so than Sites 662 and 663, which contained more temperate *Globorotalia inflata, Globigerina bulloides*, and *Neogloboquadrina pachyderma* (right-coiling). Thus, it appears that the influence of the Benguela Current or equatorial divergence lessens toward the west along the equator.

Planktonic foraminifers were abundant, with moderate-to-good preservation, in the Pleistocene. In Holes 664B and 664C, the FO of *Globorotalia truncatulinoides* lies directly above slumped sediments belonging to Zone PL5 (2.2 to 2.9 Ma). Part of the lowermost Pleistocene may be missing in these holes along with all of Zone PL6, which was not recorded. In Hole 664D, the entire Pleistocene record appears to be present, with the *Globorotalia truncatulinoides*/PL6 boundary, indicated by the LO of *G. obliquus*, found between Samples 108-664D-9H, CC and -664D-8H, CC. Zone PL6 continues through Sample 108-664D-12H, CC, which contains *Globorotalia miocenica* and thus is placed in Zone PL5.

Holes 664B and 664D contain extensive slumped material within the upper Pliocene. Between Samples 108-664B-6H, CC and -664B-14H, CC in Hole 664B, zonal assignments appear to be random, changing with almost every core-catcher sample. Only after Sample 108-664B-15H, CC (assigned to Zone PL5), does a normal stratigraphic section appear. Zone PL4, found between the last occurrences of *Sphaerodinellopsis seminulina* and *D. altispira*, occurs in Sample 108-664B-16H, CC. Zone PL3, between the last occurrences of *G. margaritae* and *S. seminulina*, encompasses Samples 108-664B-17H, CC through -664B-22H, CC. This zone is characterized by good preservation and numerous *N. humerosa, G. trilobus*, and *D. altispira*. In Hole 664D, Zone PL3 is found directly below slumped material and, hence, may be missing a few meters of sediment at its top. Zone PL3 was identified in Samples 108-664D-15H, CC through -664D-19H, CC.

In both Holes 664B and 664D, Zone PL2 is short, occurring only in Samples 108-664B-23H, CC and -664D-20H, CC, respectively. The apparent truncation of this zone may be an artifact of the unreliability of the LO of *G. margaritae*, which defines the top of this zone.

The lowermost samples in Hole 664B (108-664B-24H, CC through -664B-26H, CC), can be assigned to Zone PL1, based on the presence of *Globigerina nepenthes*. As in the late Pliocene, *D. altispira* and *G. trilobus* are the dominant members of the fauna. *Neogloboquadrina humerosa* is slightly less abundant. In Hole 664D, Zone PL1 occurs in Samples 108-664D-21H, CC through -664D-25H, CC, and the bottom of this zone begins to reflect the poor preservation that continues into the upper Miocene. The LO of *Globoquadrina dehiscens* (in Sample 108-664D-26H, CC) marks the top of Miocene Zone M13, and the FO of *Globorotalia cibaoensis* (in Sample 108-664D-27H, CC) marks the base of this zone. The Miocene fauna is characterized by abundant *N. pachyderma* (left-coiling), with lesser amounts of *S. seminulina, G. nepenthes, D. altispira*, and *G. trilobus*. The deepest cores recovered, Samples 108-664D-28H, CC through -664D-32H, CC, were assigned to Zones M11/M12, which could not be differentiated.

Diatoms

Diatoms were examined from all core-catcher samples recovered from Site 664. Abundance and preservation varied from sample to sample and were less consistent than at previous sites. Marine diatoms were generally present in upper to lower Pliocene through Holocene sediments. Freshwater *Melosira* spp. were generally few to common in all samples from Holes 664A, 664B, and 664C, and in Samples 108-664D-1H, CC through -664D-20H, CC. No diatoms were observed in lowermost Pliocene or Miocene sediments.

Core-catcher Samples 108-664C-1H, -664C-2H, and -664D-1H contain *Pseudoeunotia doliolus* without *Nitzschia reinholdii*, which allows us to assign these samples to the *Pseudoeunotia doliolus* Zone (<0.65 Ma). *Nitzschia reinholdii* and *P. doliolus* were observed in core-catcher Samples 108-664A-1H, 108-664B-1H through -664B-5H, 108-664C-3H through -664C-7H, and 108-664D-3H through -664D-10H, indicating that these samples can be placed in the *Nitzschia reinholdii* Zone. The LO of the silicoflagellate *Mesocena quadrangula* occurs in Samples 108-664B-4H, CC and -664D-5H, CC, which suggests an approximate age of 0.79 Ma for these samples.

The FO of *P. doliolus*, which defines the base of the *Nitzschia reinholdii* Zone, occurs in Sample 108-664D-9H, CC. Because of the occurrence of slump deposits and/or a decrease in diatom preservation and abundance, this zonal boundary was not recognized in Holes 664B.

Core-catcher Samples 108-664B-11H through -664B-13H and 108-664D-10H through -664D-12H are tentatively placed in the *Nitzschia marina* Zone. The LO of *Thalassiosira convexa* s. ampl. occurs in Samples 108-664B-12H, CC and -664D-13H, CC.

The *Nitzschia jouseae* Zone, which is defined by the total range of *N. jouseae*, occurs from core-catcher Samples 108-664B-14H through -664B-23H and 108-664D-14H through -664D-17H. Although core-catcher Samples 108-664B-24H, 108-664B-25H, and 108-664D-18H through -664D-20H contained diatoms, no age-diagnostic species were observed. Diatoms were not observed in Samples 108-664B-26H, CC and 108-664D-21H, CC through -664D-32H, CC. This abrupt decrease and eventual absence downcore of biogenic silica (indicated by strewn-slide analysis) occurs between Samples 108-664D-20H, CC and -664D-21H, CC, suggesting that equatorial divergence at Site 664 may have been less intense before ~3.5 Ma.

Benthic Foraminifers

Rare-to-common benthic foraminifers occur in core-catcher samples examined from Holes 664B and 664D; preservation is generally poor to moderate. The characteristic species throughout the stratigraphic interval examined are *Oridorsalis tener, Globocassidulina subglobosa, Eggerella bradyi, Pyrgo murrhyna, Pyrgo lacernula, Melonis pompilioides, Melonis barleeanus*, and *Gyroidinoides soldanii*. The abundance of these species varies from sample to sample. *Spiroplectammina* sp. was observed only in Sample 108-664B-10H, CC and -664D-23H, CC. Several specimens of *Gyroidinoides soldanii acuta* are observed in Samples 108-664B-10H, CC and -664D-25H, CC. The first occurrence of *Uvigerina hispida* occurs in Sample 108-664D-23H, CC.

PALEOMAGNETISM

Magnetostratigraphy

We measured the archive halves from Cores 108-664B-1H through -664B-6H, 108-664C-1H through -664C-6H, and 108-664D-1H through -664D-6H. Based on results from previous sites, the natural remanent magnetization was not measured, and all sections were demagnetized directly to 50 Oe.

Results obtained from Holes 664B, 664C, and 664D are similar. As an example, in Figures 7A through 7E we show the declination, inclination, and intensity variations recorded in Sections 108-664D-2H through -664D-6H. At the equatorial latitude of the site, polarity intervals cannot be identified from the inclination values, which fluctuate near 0°. Nonetheless, these inclination records are useful for ascertaining the reliability of remanence; i.e., scattered inclinations suggest a poor record. Interpretation of the results in terms of polarity intervals can be obtained only from changes in the declination record. No orientation of cores was attempted at Hole 664B; however, Cores 108-664C-3H and -664C-4H were oriented, and the declinations reported in Figures 7B and 7C were corrected.

At this equatorial site, declination data obtained from the five upper cores provided an exceptionally good record. This is illustrated in Figures 7C and 7D by the records of the Brunhes-Matuyama, lower and upper Jaramillo transitions. The stratigraphic position of each reversal is well delimited, and no further sampling was necessary to establish the magnetostratigraphy of these sections. Figures 7A through 7E also show that the remanent-magnetization intensity decreases as a function of depth and is just above the noise level at the bottom of Core 108-664B-6H. No reliable record could be obtained between 40 and 296.8 mbsf. After the promising results of the upper 40 m at Site 664, we were forced to the same conclusions we reached at Sites 662 and 663—no magnetic record was available. Lithology of the three sites is similar, and the absence of magnetism could result from the same unknown processes.

Magnetic Susceptibility

Whole-core volume susceptibilities from Hole 664B were measured for Cores 108-664B-1H through -664B-6H. Susceptibility values averaged around 20×10^{-6} SI units; from previous experience at Sites 662 and 663, we knew this was too low to provide reliable stratigraphy.

SEDIMENT-ACCUMULATION RATES

Sediment-accumulation rates were calculated for Holes 664B and 664D, the two holes with the greatest penetration. Stratigraphic control for Hole 664B consisted of 25 biostratigraphic and magnetostratigraphic events (Tables 2 and 3). Diatom datums were excluded for both Holes 664B and 664D because most were poorly constrained from sporadic diatom occurrences. Because of the extensive disturbance of the sediments in Hole 664B, stratigraphic zones were plotted based on the overlapping of key taxa at specific depths in each core. As is evident in Figure 8, a number of displaced stratigraphic units occur in Hole 664B because of slumps (see "Composite-Depth Section," this chapter). We have, therefore, replotted the age-depth curve after removing recognizable slumps and by ignoring biostratigraphic events within the disturbed sections. The resulting curve (Fig. 9), which uses 14 stratigraphic events, reveals that normal, pelagic sediments accumulated at a rate of 49 m/m.y. during most of the Pleistocene (~1.35 Ma to the present) and that approximately 10 m of sediment is missing from the top of the section. A hiatus spans the time interval from ~1.35 to 2.27 Ma. From 2.27 Ma to the base of the section (~4.6 Ma), the sediment-accumulation rate averaged 37 m/m.y.

Stratigraphic control for Hole 664D was based on 21 nannofossil, planktonic-foraminifer, and paleomagnetic events (Table 4). The resulting curve (Fig. 10) suggests a continuous, average accumulation rate of 32 m/m.y. for the late Pleistocene (<0.47 Ma). Between 4.3 and 0.47 Ma, the accumulation rate averaged 51 m/m.y., whereas the average accumulation rate from 4.3 Ma to the bottom of the hole (~8.85 Ma) was 19 m/m.y. Inspection of the core reveals numerous turbidites and slumps concentrated between 50 and 220 mbsf (see "Composite-Depth Section," this chapter). These apparently contribute to the high accumulation rates observed between 4.3 and 0.47 Ma. Because of their large numbers and generally small vertical extension, we have not attempted to construct a revised, "no-turbidite/slump" section.

No biostratigraphic datums fall below the line in Figure 10; however, several fall slightly above the line. These are the last occurrences of *Discoaster brouweri, D. pentaradiatus, Sphaeroidinellopsis seminulina*, and *Globorotalia crassaformis*, all of which occur slightly higher up in the section than would be expected, based on other stratigraphic data. These anomalies may be the result of upward reworking.

INORGANIC GEOCHEMISTRY

Interstitial-water samples were squeezed from five sediment samples recovered routinely approximately every 50 m from Site 664. Values for pH and alkalinity were measured in conjunction, using a Metrohm 605 pH-meter, followed by titration with 0.1N HCl, and salinities were measured using an optical refractometer. Cl^-, Ca^{2+}, and Mg^{2+} concentrations were determined by the titrations described in Gieskes and Peretsman (1986). SO_4^{2-} analyses were conducted by ion chromatography using a Dionex 2120i instrument. Results from all analyses are presented in Table 5.

ORGANIC GEOCHEMISTRY

At Site 664, Holes 664B and 664D, 185 samples were used to determine carbonate content. Of these, 40 samples also were analyzed for total-organic-carbon (TOC) contents, and 12 samples were measured by Rock-Eval pyrolysis.

Organic and Inorganic Carbon

Inorganic carbon (IC) was measured using the Coulometrics Carbon Dioxide Coulometer, while total carbon (TC) was determined using the Perkin Elmer 240C Elemental Analyser. TOC values were calculated by difference. Analytical methods are discussed, and data listed in the Appendix (this volume).

According to the carbonate record, the sediment sequence at Site 664 can be divided into two parts that correspond to lithologic Subunits IA and IB (see "Lithostratigraphy and Sedimentology" section, this chapter). The upper 51 mbsf (i.e., Hole 664B, Cores 108-664B-1H through 664B-6H-3) is characterized by high-amplitude variations ranging from about 50% to 90% $CaCO_3$ (Fig. 11). The lower part of the sequence (i.e., Hole 664B, Cores 108-664B-6H-4 through 664B-26H [Fig. 11], and Hole 664D, down to Core 108-664D-32H) is characterized by constantly high carbonate values of about 90%, with one exception: lower values of 77% to 81% $CaCO_3$ occur in Core 108-664D-11H (at about 100 mbsf).

TOC values fluctuate from 0% to 0.53% in the upper 51 m, whereas most of the lower part of the sequence has a TOC content of about 0%. TOC values for 165 to 220 mbsf range between 0.05% and 0.15% (Fig. 11). According to results of Rock-Eval pyrolysis (Table 6), samples with higher TOC values are dominated by lower hydrogen-index values (i.e., possibly by a higher content of terrigenous organic matter).

Discussion

The high-amplitude variations of $CaCO_3$ possibly are caused by changes in carbonate dissolution and/or by the input of noncarbonate (i.e., biogenic silica and terrigenous) material. A higher content of terrigenous organic matter during intervals of low carbonate content may support a higher input of terrigenous matter during these times. However, more data are required to verify this preliminary interpretation. The intervals of slumps (see "Lithostratigraphy and Sedimentology" section, this chapter) are characterized by constantly high carbonate values of about 90% and TOC values of 0% (Fig. 11).

PHYSICAL PROPERTIES

The techniques used for shipboard physical-properties measurements at Site 664 are outlined in the "Introduction and Explanatory Notes" (this volume). Hole 664A consisted of only one core (108-664A-1H), which will be used for a detailed study of the *P*-wave logger (see following section). Physical-properties measurements were conducted on four holes: 664A, 664B, 664C, and 664D. Data for Holes 664B and 664D are presented here.

Tables 7 and 8 show the index-properties and vane-shear-strength data for Holes 664B and 664D, respectively. Figures 12 through 18 show downhole plots of these data. Continuous *P*-wave-velocity and GRAPE records were obtained from Holes 664A, 664B, and 664C. Only a partial record was obtained from Hole 664D because of time constraints. Table 9 shows a synthesis of the *P*-wave-logger velocity data for Hole 664B, which are plotted in Figure 15. The calcium carbonate content for Hole 664B is plotted in Figure 14. No data presented here were screened for bad data points.

The carbonate content in lithologic Unit IA varies from 50% to 90% (see "Lithostratigraphy and Sedimentology" section, this chapter). Changes in carbonate content determine the index properties for Unit IA. For example, the sharp increase in carbonate content from about 50% to 90% at 11 mbsf results in an increase in the wet-bulk density (approximately 1.3 to 1.5 g/cm^3) and other related parameters (e.g., dry density changes from 0.5 to 0.9 g/cm^3, water content changes from 50% to 60%, and porosity changes from 70% to 80%). Grain density has an average value of 2.6 g/cm^3.

Below 52 mbsf (in lithologic Unit IB), a high calcium carbonate content prevails, with an average value of 95%. In contrast, the index properties, vane shear strength, and *P*-wave velocities are highly variable. This variability is caused by seven slumped intervals (52–96, 106–128, 142–147, 163–170, 179–189, 191–204, and 220–225 mbsf; see "Lithostratigraphy and Sedimentology" section, this chapter) that interrupted the undisturbed pelagic sediment sequence. The major slump (52–96 mbsf) is characterized by an abrupt decrease in water content and porosity and a sharp increase in wet- and dry-bulk densities (Fig. 12). This caused a distinctive sequence of high *P*-wave-velocity variations (1520–1640 m/s) and an increase in vane shear strength from the top of the slump to its base (from approximately 40 to 80 kPa).

To reconstruct the depositional history of the slump, the water content at the top of the slump was extrapolated to the depth reaching the water content of the undisturbed pelagic sequence. If one assumes that no significant dewatering occurred, then the top of the slump probably originated from sediments that previously had been buried to a depth of about 100 mbsf. However, some dewatering possibly may have occurred if significant pore pressures were developed during the shearing process when the slump was mobile.

Figure 19 shows the *P*-wave logger record for Core 108-664A-1H measured across four different axes at 45° intervals. The "physical noise" is restricted to low-amplitude, high-frequency excursions. We anticipate that this core will be sampled in detail to investigate the primary cause of the velocity fluctuations. In particular, detailed profiles of grain-size distribution and carbonate content will be compared with velocity profiles.

SEISMIC STRATIGRAPHY

Water-gun seismic profiler records were obtained both during the initial crossing of Site 664 and during a return approach to the site (see "Operations" section, this chapter). The record shown in Figure 20 is from the first crossing. Four seismic units can be discerned:

Seismic unit 1 (0–0.05 s) is an upper unit with a false acoustic signal caused by water guns. This unit should equate to about the upper 38 m of sediment.

Seismic unit 2 (0.05–0.18 s) is a unit with regular, moderately reverberant reflectors almost parallel to the seafloor. This unit should equate to the interval from about 38 to 136 mbsf.

Seismic unit 3 (0.18–0.34 s) is a nearly transparent, lower unit with faint scattered reflections. This unit should equate to the interval at 136 to 258 mbsf.

Seismic unit 4 ($>$0.34 s) is the acoustic basement.

These unit thicknesses apply specifically to Holes 664A, 664B, and 664C. Hole 664D was positioned 1000 m to the north of this location, but no seismic record from directly over this hole is available. This hole is near the bracketed section of the seismic record in Figure 20. The sediment pond deepens in this region, and the acoustic basement lies at a depth of approximately 0.4 s or greater (300 mbsf).

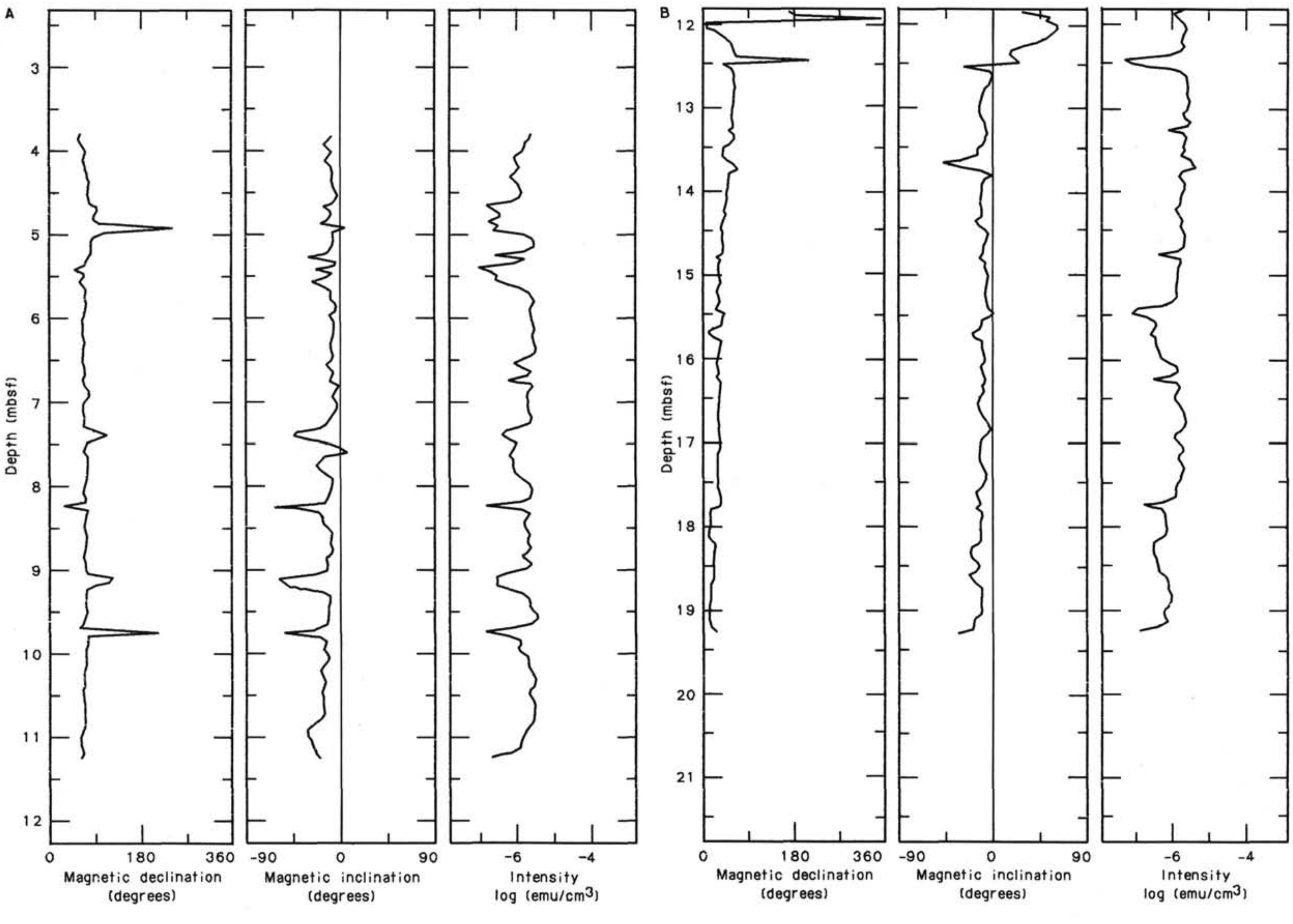
A
Depth (mbsf)
Magnetic declination (degrees)
Magnetic inclination (degrees)
Intensity log (emu/cm3)
B
Depth (mbsf)
Magnetic declination (degrees)
Magnetic inclination (degrees)
Intensity log (emu/cm3)

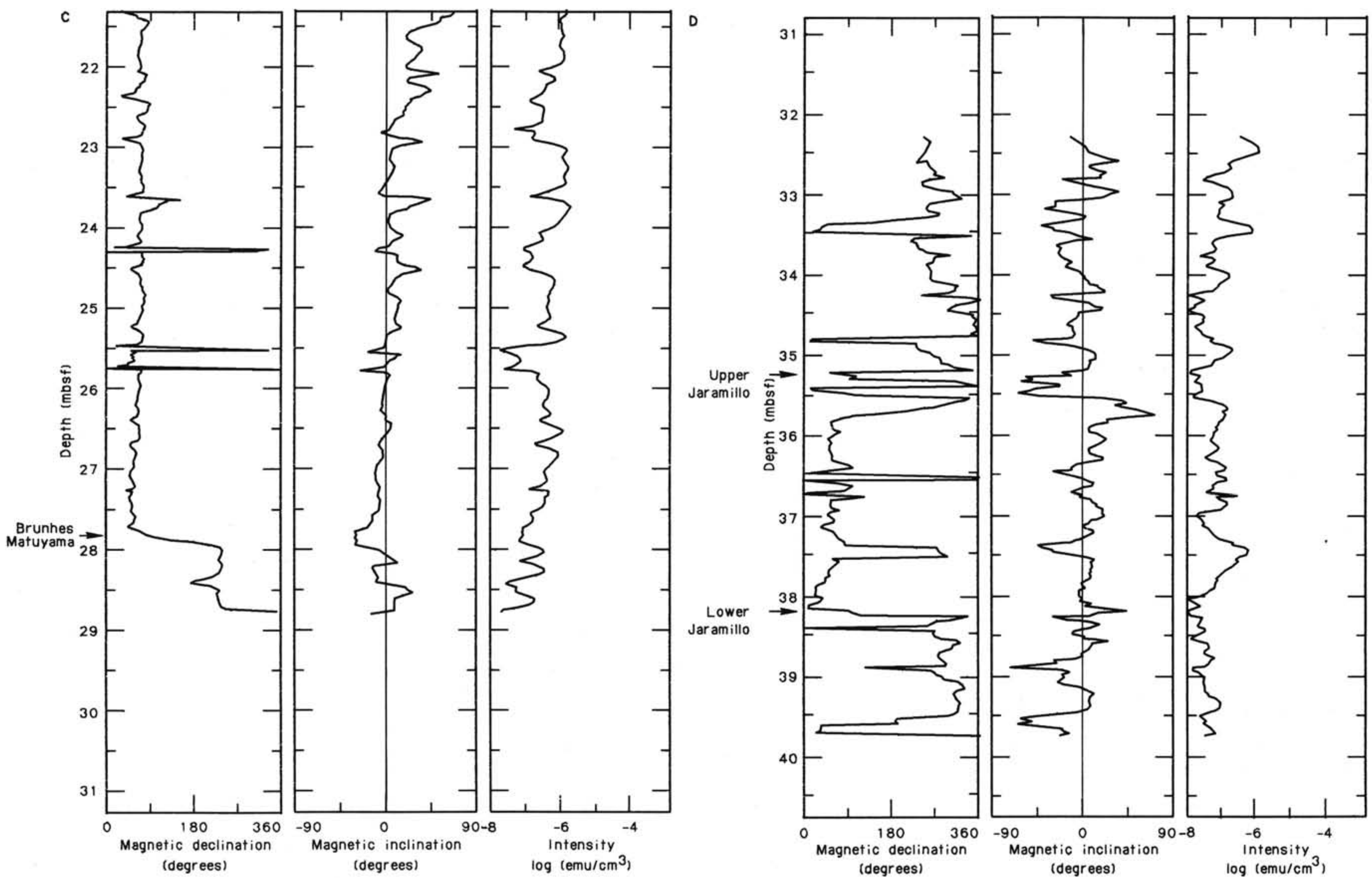

Figure 7. Declination, inclination, and intensity variations obtained from *A, B, C, D,* and *E:* Cores 108-664B-1H through -664B-6H. The stratigraphic positions of the reversals in Figures 7C and 7D are indicated by arrows. For a better representation of results, declination values have been rotated arbitrarily in Figure 7C, adjusting the mean normal data to 90° and the mean reversed data to 270°.

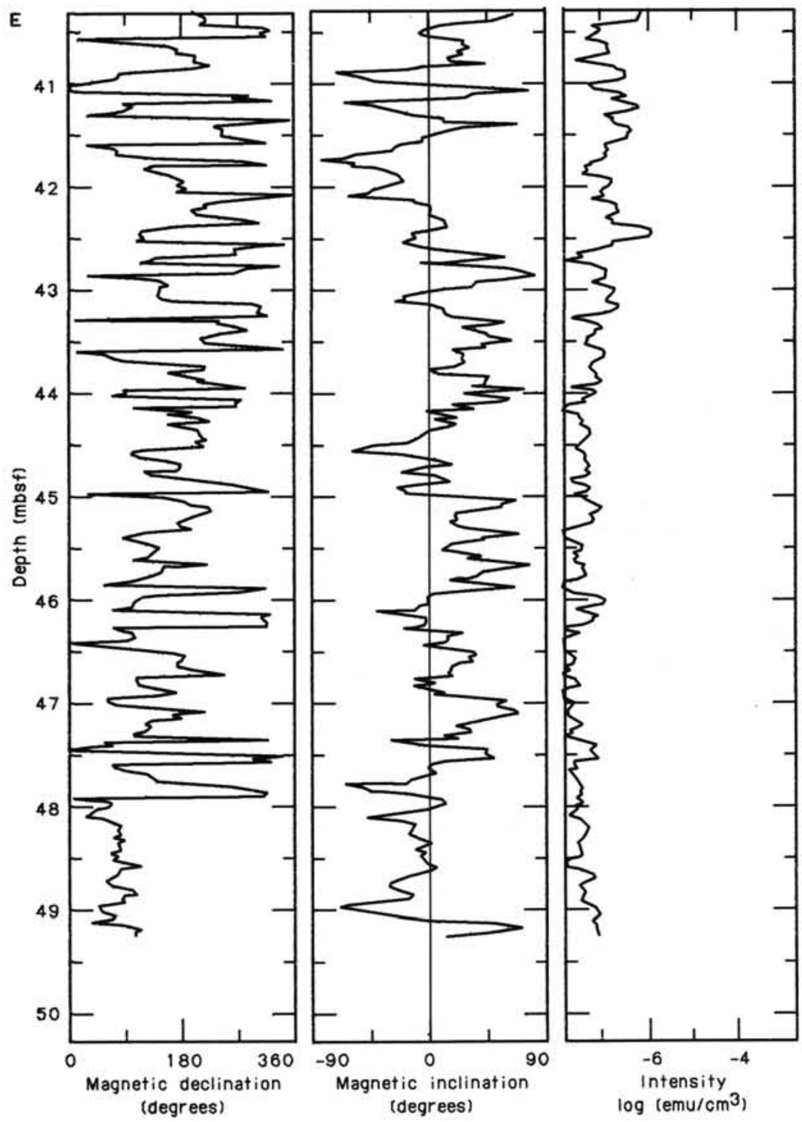

Figure 7 (continued).

We used a mean sound velocity of 760 m/s for the entire sediment section at Site 664 (see "Physical Properties" section, this chapter) to evaluate the correlations of the seismic units with lithologic units (Fig. 20). Seismic unit 1 is an artifact.

Seismic unit 2 encompasses both the lower part of lithologic Subunit IA, in which maximum variations in $CaCO_3$ occur, as well as the upper part of lithologic Subunit IB, in which only a few $CaCO_3$ changes are evident (see "Lithostratigraphy and Sedimentology" section, this chapter). The carbonate layering (or some correlative property), thus, does not appear to cause the changes in acoustical reflectivity, nor is any correlation apparent between the seismic units and the position of slumps in lithologic Subunit IB (see "Principal Results" section, this chapter).

Seismic unit 3 is equivalent to the lower Pliocene and upper Miocene nannofossil oozes cored in Hole 664D; despite increasing depth below the seafloor, these layers showed no obvious tendencies toward lithification (see "Physical Properties" section, this chapter).

Seismic unit 4 is basement, presumably the altered basalts of the mid-Atlantic Ridge. The last coring attempted in Hole 664D was fired to full stroke, but became stuck; the core barrel broke at an overpull of 145,000 lb (see "Operations" section, this chapter). This suggests that firm sediments just above the basement were encountered. The last two cores recovered (108-664D-32H and -664D-33H) consisted of clay-bearing nannofossil ooze. The age of the deepest sediments (8–9 Ma; see "Biostratigraphy" section, this chapter) agrees with the basement age estimated from magnetic lineations (see "Background and Scientific Objectives" section, this chapter). The depth to acoustic basement at the approximate offset position of Hole 664D in Figure 20 also is consistent with this conclusion.

COMPOSITE-DEPTH SECTION

As at Sites 662 and 663, Site 664 contains a rapidly deposited pelagic section interrupted by several slumps. In Figures 21 and 22, the depths below the seafloor of the slumps in Holes 664A and 664D are plotted in relation to the sections marked by pelagic deposition. The two holes were plotted separately because they had somewhat different sedimentation histories. The ages of biostratigraphic datum levels in the pelagic intervals are shown by triangles (see "Biostratigraphy" section, this chapter).

Table 2. Depth and age estimates of biostratigraphic and magnetostratigrahic indicators used to establish accumulation rates for Hole 664B.

Datum	Depth (mbsf)	Age 1[1] (Ma)	Age 2[2] (Ma)
LO *Pseudoemiliania lacunosa*	14.0	0.47	0.47
Brunhes/Matuyama	27.0	0.73	0.73
Matuyama/Jaramillo	35.5	0.91	0.91
LO *P. lacunosa* to LO *Calcidiscus macintyrei*	56.0	0.47	1.45
Discoaster tamalis (p), Dentogloboquadrina altispira (a)	57.0	2.65	2.90
D. altispira (p), Sphaerodinellopsis seminulina (a)	66.5	2.90	3.00
Pulleniatina (p), Sphenolithus abies (a)	76.0	3.30	3.45
D. tamalis (p), S. abies (a)	85.5	2.65	3.45
D. tamalis (p), S. abies (a)	95.0	2.65	3.45
D. pentaradiatus (p), D. surculus (a)	104.5	2.35	2.45
D. pentaradiatus (p), D. surculus (a)	114.0	2.35	2.45
D. altispira (p), S. seminulina (a)	123.5	2.90	3.00
D. altispira (p), S. seminulina (a)	133.0	2.90	3.00
D. tamalis (p), D. altispira (a)	142.5	2.65	2.90
D. altispira (p), S. seminulina (a)	152.0	2.90	3.00
Pulleniatina (p), Sphenolithus abies (a)	161.5	3.30	3.45
Pulleniatina (p), S. abies (a)	171.0	3.30	3.45
Sphaerodinellopsis seminulina (p), Pulleniatina (a)	180.5	3.00	3.30
Sphenolithus abies (p), Reticulofenestra pseudoumbilica (a)	190.0	3.45	3.56
R. pseudoumbilica (p), Amaurolithus (a)	199.5	3.56	3.70
R. pseudoumbilica (p), Amaurolithus (a)	209.0	3.56	3.70
R. pseudoumbilica (p), Amaurolithus (a)	218.5	3.56	3.70
Globigerina nepenthes (p), G. crassaformis (a)	228.0	3.90	4.20
G. crassaformis (p), Ceratolithus rugosus (a)	237.5	4.20	4.60
C. rugosus (p), C. acutus (a)	247.0	4.50	4.70

[1] Age 1 = youngest possible age.
[2] Age 2 = oldest possible age.
Note: (*p*) = present; (*a*) = absent.

Table 3. Depth and age estimates of biostratigraphic and magnetostratigraphic indicators used to establish accumulation rates in the absence of identifiable slumps and turbidites.

Datum	Depth (mbsf)	Age 1[1] (Ma)	Age 2[2] (Ma)
LO *Pseudoemiliania lacunosa*	14.0	0.47	0.47
Brunhes/Matuyama	27.0	0.73	0.73
Matuyama/Jaramillo	35.5	0.91	0.91
LO *P. lacunosa* to LO *Calcidiscus macintyrei*	56.0	0.47	1.45
Globorotalia miocenica (p), Discoaster pentaradiatus (a)	58.0	2.20	2.35
D. pentaradiatus (p), D. surculus (a)	67.5	2.35	2.45
Dentogloboquadrina altispira (p), Sphaerodinellopsis seminulina (a)	87.5	2.90	3.00
Pulleniatina (p), Reticulofenestra pseudoumbilica (a)	97.0	3.30	3.56
Pulleniatina (p), R. pseudoumbilica (a)	98.8	3.30	3.56
R. pseudoumbilica (p), Globigerina nepenthes (a)	111.8	3.56	3.90
R. pseudoumbilica (p), G. nepenthes (a)	121.3	3.56	3.90
G. nepenthes (p), G. crassaformis (a)	126.3	3.90	4.20
G. crassaformis (p), Ceratolithus rugosus (a)	135.8	4.20	4.60
C. rugosus (p), C. acutus (a)	145.3	4.50	4.70

[1] Age 1 = youngest posssible age.
[2] Age 2 = oldest possible age.
Note: (*p*) = present; (*a*) = absent.

We attempted between-hole correlations for the uppermost pelagic sections of Holes 664B and 664C. For pelagic sections below 100 mbsf, we attempted correlations between Holes 664A and 664D. However, no useful magnetic susceptibility data existed for this, nor were *P*-wave records entirely suitable because of the limited analyses for Hole 664D. Thus, we used the $CaCO_3$ layering visible in core photographs to make these correlations.

Table 10 shows the correlation levels we used as a pathway to produce the continuous composite-depth sections within the intervals of pelagic deposition in Holes 664B, 664C, and 664D. These composite-depth sections were chosen so as to use short sequences in Holes 664C and 664D for spanning core-break gaps in the Hole 664B record.

The first correlated interval covered the pelagic sequence (0–54.7 mbsf) in the upper six cores at Holes 664B and 664D and

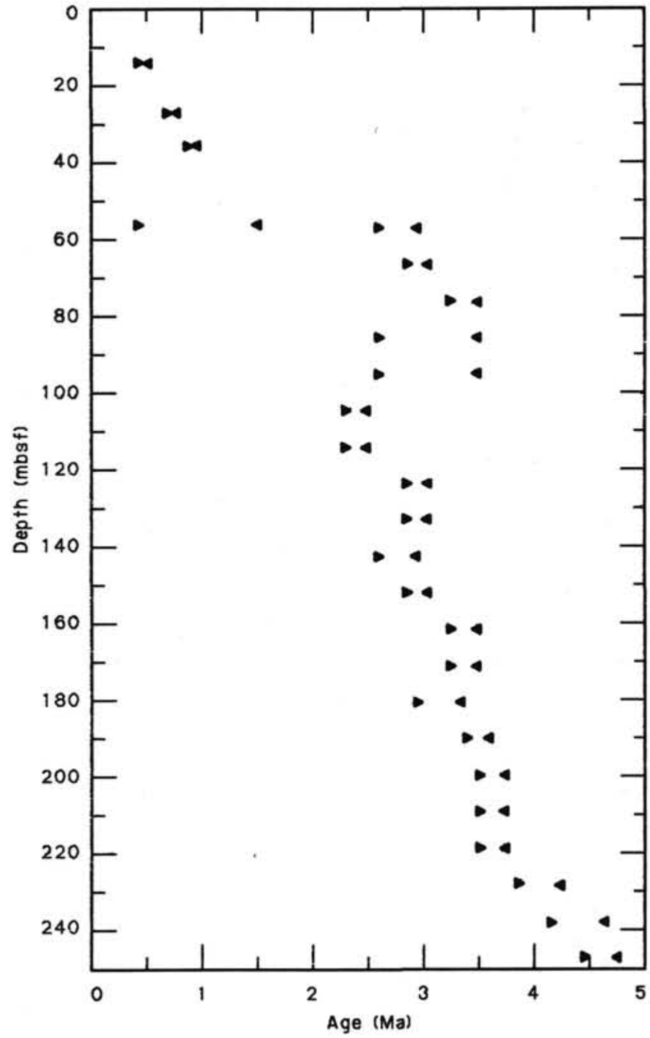

Figure 8. Sediment-accumulation rates for Hole 664B.

ended at the top of a large slumped unit (Table 10, Figs. 21 and 22). This pelagic interval covers roughly the last 1.25 m.y.

Unlike the slumps at the previous two sites, the slump in Hole 664B caused the loss of the section. Anomalously old (lower Pliocene) sediment was brought in by the slump (54.7–97 mbsf; Fig. 21). The first undisturbed sediment beneath the slump dates to about 2.4 Ma, indicating the loss of all material between 1.25 and 2.4 Ma. In Hole 664D, however, the "slumped" material at nearly the same depths below the seafloor as at Hole 664B is not anomalously old, based on the age-depth curve (Fig. 22), but seems to be part of a nearly continuous stratigraphic section and is relatively undisturbed.

The only remaining part of the sediment section that could be correlated by photographs was a short section in Core 108-664B-12H through a section in Cores 108-664D-12H and -664D-13H (Table 10). This section provided correlations of a lower Pleistocene interval roughly 10 m long. For this interval, we used the listed ODP depth below the seafloor of the top of Core 108-664B-12H as a reference point to begin the short composite-depth section.

Some suggestion of a correlation for Cores 108-664B-11H and -664D-11H is also apparent, but would require laboratory $CaCO_3$ analyses for confirmation. At and below Cores 108-664B-14H and -664D-14H, the $CaCO_3$ layering is too faint for

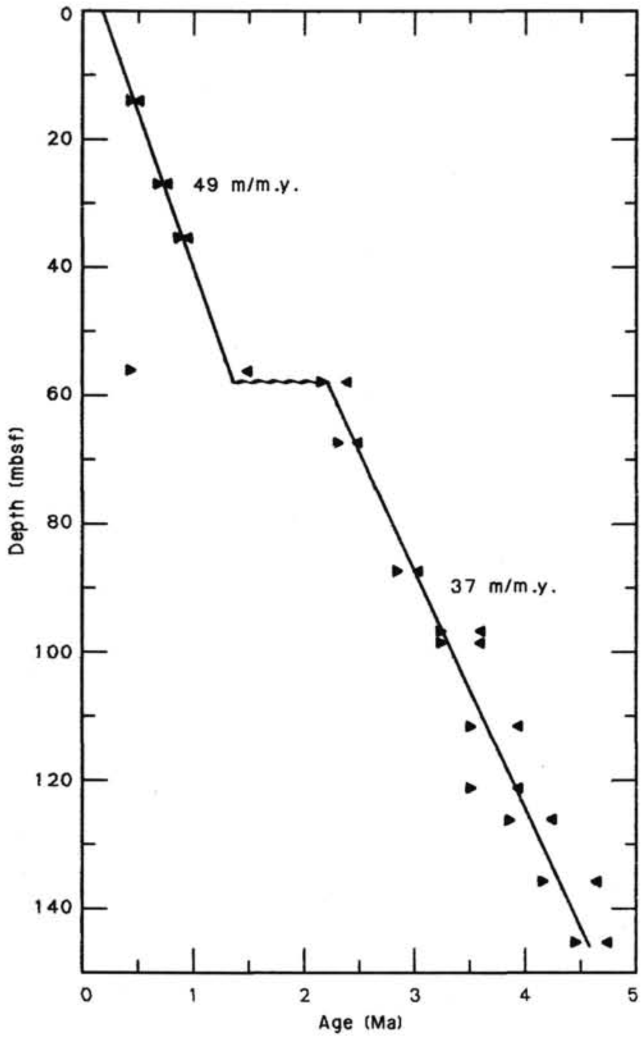

Figure 9. Sediment-accumulation rates for Hole 664B in the absence of identifiable slumps and turbidites.

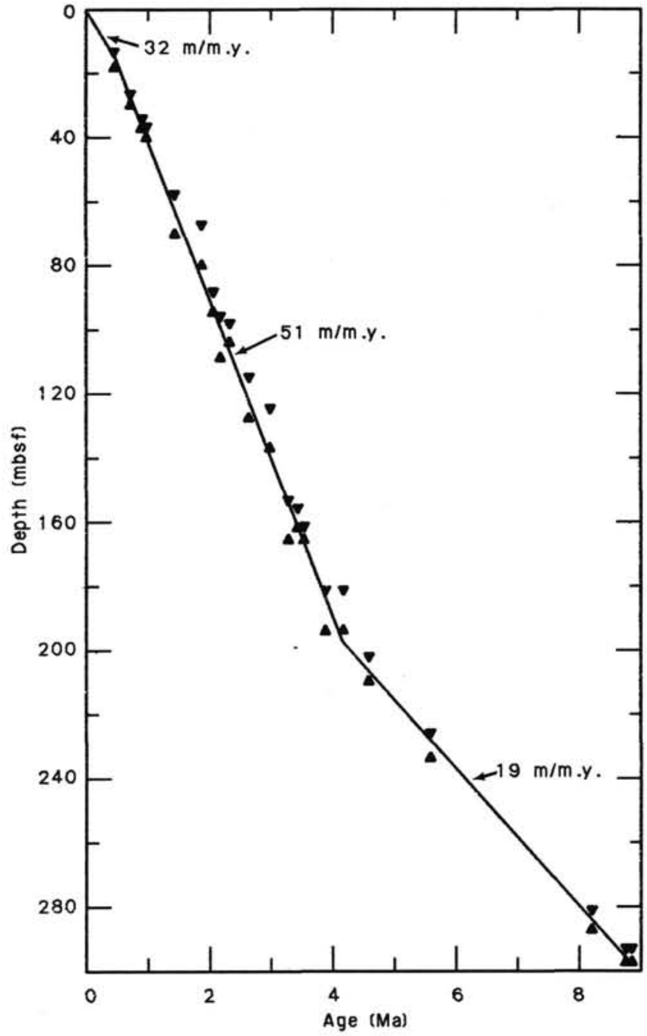

Figure 10. Sediment-accumulation rates for Hole 664D.

Table 4. Depth and age estimates of biostratigraphic and magnetostratigraphic indicators used to establish accumulation rates for Hole 664D.

Datum	Depth (mbsf)	Age (Ma)
LO *Pseudoemiliania lacunosa*	14.9–16.4	0.47
Brunhes/Matuyama	27.9–28.0	0.73
Matuyama/Jaramillo	35.8–35.8	0.91
Jaramillo/Matuyama	38.3–38.3	0.99
LO *Calcidiscus macintyrei*	59.3–68.8	1.45
LO *Discoaster brouweri*	68.8–78.3	1.89
FO *D. triradiatus* acme	89.6–92.6	2.07
LO *Globorotalia miocenica*	97.3–106.8	2.20
LO *Discoaster pentaradiatus*	99.4–102.4	2.35
LO *D. tamalis*	116.3–125.8	2.65
LO *Sphaerodinellopsis seminulina*	125.8–135.3	3.00
LO *Pulleniatina*	154.3–163.8	3.30
LO *Sphenolithus abies*	157.0–160.0	3.45
LO *Reticulofenestra pseudoumbilica*	163.0–163.8	3.56
LO *Globigerina nepenthes*	182.8–192.3	3.90
FO *G. crassaformis*	182.8–192.3	4.20
FO *Ceratolithus rugosus*	203.4–207.9	4.60
LO *Discoaster quinqueramus*	227.1–231.9	5.60
FO *D. quinqueramus*	282.5–285.5	8.20
LO *Catinaster calyculus*	294.4–295.9	8.75
LO *Discoaster hamatus*	294.4–295.9	8.85

LO = last occurrence. FO = first occurrence.

photographs to be useful for correlations, and the pelagic record at Hole 664B is interrupted by numerous slumps. Laboratory analyses of other properties might provide some correlation between Holes 664B and 664D in this part of the section.

Discussion

Because of numerous slumps, Site 664 added little to the Pleistocene or late-Pliocene history of the equatorial divergence. In particular, slumps again disrupted the pelagic sequence in the 1.3 to 1.2 Ma interval that was disturbed at both earlier sites. However, the slightly deformed sediments between 49 and 87 mbsf in Hole 664D possibly will prove useful for studying this interval. We did collect a continuous upper Pleistocene section (0–1.25 Ma), which can be compared with results from the more easterly Sites 662 and 663.

We also retrieved from Hole 664D an excellent upper Miocene and lower Pliocene section that extends the results at earlier sites well back into the Neogene. Although continuity of this section cannot be confirmed by shipboard results, the excellent recovery from Holes 664B (99%) and 664D (102%) suggests that sediment loss at core breaks was minimal.

REFERENCES

Gieskes, J. M., and Peretsman, G., 1986. Water chemistry procedures aboard *JOIDES Resolution*. ODP Technical Note No. 5.

Table 5. Results of inorganic-geochemical analyses conducted for Site 664.

Core/ section	pH	Alkalinity (mmol/L)	Salinity (‰)	Chlorinity (mmol/L)	SO_4^{2-} (mmol/L)	Mg^{2+} (mmol/L)	Ca^{2+} (mmol/L)
1-5	7.88	2.22	33.9	559.0	18.15	52.88	8.50
6-5	7.49	3.49	34.1	564.9	17.02	52.85	8.91
11-5	7.66	4.42	34.1	565.4	16.62	51.83	9.77
16-5	7.76	3.96	34.9	562.3	16.78	52.10	9.38
21-5	7.60	4.55	34.3	567.5	16.51	51.37	10.23

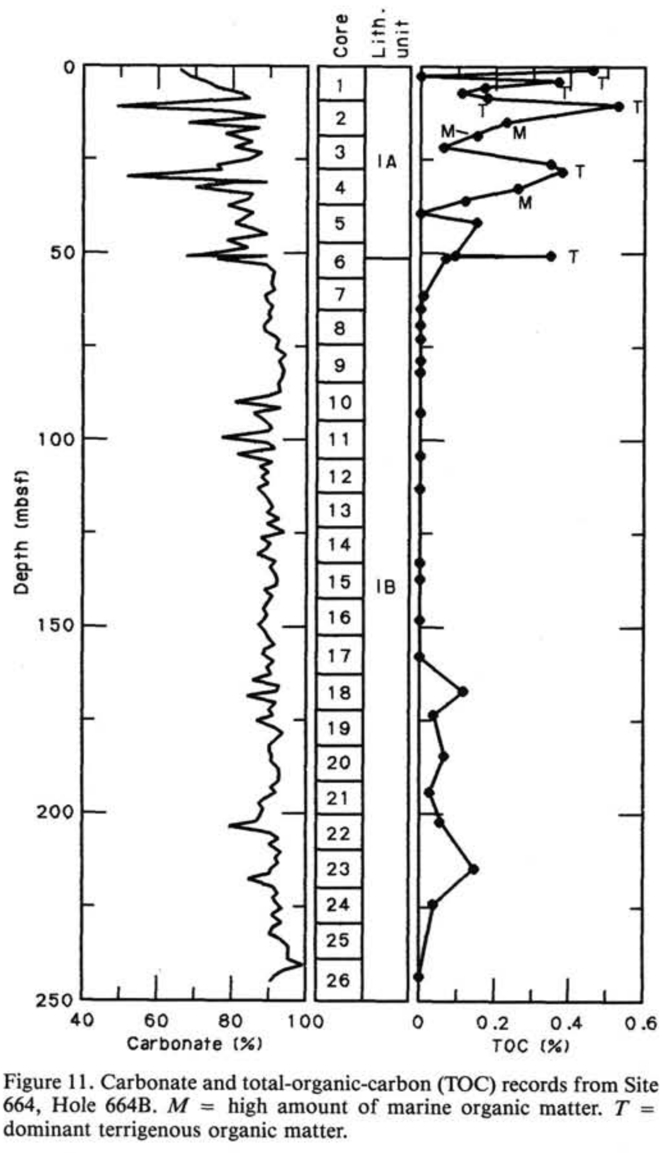

Figure 11. Carbonate and total-organic-carbon (TOC) records from Site 664, Hole 664B. *M* = high amount of marine organic matter. *T* = dominant terrigenous organic matter.

Table 6. Results of Rock-Eval pyrolysis for Site 664.

Sample no. (cm)	TOC (%)	Hydrogen index	Oxygen index	T_{max}
1-1, 120	0.46	74	743	372
1-3, 120	0.37	95	903	401
1-4, 120	0.17	171	1900	—
1-6, 120	0.18	122	1177	—
2-1, 120	0.53	98	847	465
2-4, 120	0.23	257	1526	429
2-6, 120	0.15	313	1593	—
3-5, 130	0.35	69	686	—
3-6, 130	0.38	108	692	463
4-3, 120	0.26	215	1173	466
5-3, 120	0.16	206	1475	—
6-3, 33	0.35	31	—	—

Table 7. Index-properties and vane-shear-strength data for Hole 664B.

Core/ section	Interval (cm)	Depth (mbsf)	Grain density (g/cm^3)	Wet-water content (%)	Dry-water content (%)	Dry-bulk density (g/cm^3)	Wet-bulk density (g/cm^3)	Porosity (%)	Vane shear strength (kPa)
1-1	121	1.21	2.64	36.47	129.72	1.39	0.64	77.24	17.00
1-2	121	2.65	2.39	32.57	110.85	1.43	0.71	73.98	25.00
1-3	121	4.15	2.87	39.41	146.37	1.38	0.38	70.93	15.00
1-4	121	5.65	2.34	31.93	108.04	1.40	0.73	71.47	30.00
1-5	121	7.15	2.64	31.03	104.19	1.46	0.77	73.19	30.00
1-6	121	8.63	2.39	49.01	99.24	1.47	0.77	71.81	30.00
2-1	121	10.71	2.42	62.32	165.40	1.30	0.34	79.93	18.00
2-2	121	12.21	2.47	32.19	109.15	1.42	0.72	72.79	20.00
2-3	121	13.71	2.36	45.70	84.15	1.32	0.87	65.09	23.00
2-4	121	13.21	2.61	35.32	123.82	1.40	0.67	70.26	25.00
2-5	111	16.61	2.87	45.43	83.26	1.82	0.38	67.90	36.00
2-6	111	18.11	2.81	47.93	92.04	1.48	0.01	69.39	31.00
3-1	121	20.21	2.63	40.75	87.78	1.51	0.84	69.54	26.00
3-2	121	21.71	2.49	49.41	97.66	1.45	0.78	70.67	39.00
3-3	121	23.21	2.32	47.70	91.22	1.48	0.82	69.45	35.00
3-4	121	24.71	2.60	46.86	87.11	1.51	0.86	69.19	20.00
3-5	121	26.21	2.35	31.92	107.98	1.43	0.73	73.22	28.00
3-6	121	27.71	2.76	83.60	115.52	1.44	0.71	75.96	30.00
4-1	121	29.71	2.44	39.21	145.18	1.34	0.39	77.92	39.00
4-2	131	31.29	2.49	84.97	122.08	1.39	0.67	75.14	24.00
4-3	121	32.69	2.59	31.89	107.84	1.44	0.73	73.43	29.00
4-4	121	34.19	2.70	46.74	95.07	1.30	0.80	71.73	29.00
4-5	121	35.69	2.71	44.25	79.38	1.56	0.91	68.05	38.00
4-6	121	37.19	2.72	47.78	91.49	1.51	0.83	71.12	36.00
5-1	121	39.21	2.67	45.30	82.82	1.54	0.89	68.65	30.00
5-2	121	40.71	2.66	46.19	85.85	1.53	0.86	69.34	29.00
5-3	121	42.21	2.64	51.27	105.22	1.45	0.74	73.34	30.00
5-4	121	43.71	2.66	45.69	84.11	1.53	0.86	68.90	31.00
5-5	116	45.16	2.53	46.37	86.47	1.30	0.85	68.41	26.00
5-6	121	46.71	2.34	47.53	90.59	1.49	0.81	69.34	34.00
6-1	121	46.71	2.52	47.61	90.89	1.48	0.83	69.41	36.00
6-2	121	50.21	2.61	44.80	81.17	1.54	0.89	67.68	41.00
6-3	121	51.71	2.64	49.11	96.52	1.48	0.80	71.59	35.00
6-4	121	53.21	2.78	43.30	76.37	1.39	0.93	67.74	26.00
6-5	121	54.71	2.60	39.81	66.13	1.61	1.02	62.97	41.00
6-6	121	56.21	2.62	40.47	67.99	1.60	0.99	63.81	41.00
7-1	121	58.21	2.54	40.67	68.55	1.58	0.98	63.25	39.00
7-2	121	59.71	3.87	16.74	20.11	2.52	1.35	41.40	35.00
7-3	121	61.21	2.66	39.87	66.30	1.62	0.99	63.55	38.00
7-4	121	62.71	2.62	39.05	64.06	1.62	1.03	62.38	32.00
7-5	121	64.21	2.75	39.23	64.55	1.65	1.04	63.69	38.00
7-6	121	65.71	2.77	40.95	69.34	1.63	0.99	65.48	32.00
8-1	51	67.01	2.67	40.74	68.74	1.61	0.98	64.44	40.00
8-2	121	68.91	2.61	40.76	68.81	1.60	0.99	63.95	31.00
8-3	121	70.41	2.52	39.84	64.57	1.60	1.03	61.62	34.00
8-4	121	71.91	2.63	39.04	64.05	1.63	1.02	62.47	34.00
8-5	51	72.71	2.36	38.81	62.62	1.62	1.03	61.29	35.00
8-6	121	74.39	2.59	41.67	71.43	1.58	0.96	64.68	38.00
9-1	121	77.21	2.60	42.37	73.53	1.57	0.94	65.38	30.00
9-2	121	78.71	2.49	38.83	63.49	1.60	1.03	60.96	42.00
9-3	121	80.21	2.70	36.90	58.47	1.68	1.10	60.95	48.00
9-4	121	81.71	2.66	35.94	56.10	1.68	1.11	59.54	56.00
9-5	121	83.21	2.64	36.82	87.53	1.67	1.09	60.04	50.00
9-6	121	84.71	2.00	37.78	60.73	1.71	1.07	63.33	51.00
10-1	121	86.71	2.57	35.41	54.82	1.67	1.11	58.21	54.00
10-2	121	88.21	2.58	34.40	62.44	1.69	1.15	57.20	54.00
10-3	121	89.71	2.60	36.45	57.37	1.66	1.11	69.57	78.00
10-4	121	91.21	2.60	34.92	53.66	1.69	1.13	57.91	80.00
10-5	121	92.71	2.61	34.26	82.11	1.70	1.10	57.32	63.00
10-6	121	94.09	2.63	31.38	45.74	1.76	1.24	54.23	84.00
11-1	116	96.16	2.62	35.93	56.09	1.68	1.11	59.22	0.00
11-1	121	96.21	2.56	34.36	52.34	1.69	1.14	56.97	45.00
11-1	131	96.31	2.52	45.61	83.85	1.51	0.86	67.70	0.00
11-2	121	97.71	2.56	40.16	67.11	1.59	1.01	62.91	26.00
11-3	121	99.21	2.64	42.72	74.57	1.57	0.95	66.04	34.00
11-4	121	100.71	2.57	38.41	62.37	1.62	1.05	61.28	41.00
11-5	121	102.21	2.66	38.35	62.20	1.65	1.05	62.07	30.00
11-6	121	103.61	2.60	40.34	67.61	1.60	1.00	63.47	43.00
12-1	121	105.71	2.63	39.06	64.11	1.63	1.03	62.45	34.00
12-2	121	107.21	2.66	42.04	72.53	1.59	0.95	65.61	35.00
12-3	121	108.71	2.36	40.06	66.82	1.55	1.00	60.96	45.00
12-4	121	110.21	2.61	39.05	64.07	1.62	1.02	62.33	32.00
12-5	116	111.66	2.62	40.18	67.16	1.61	0.99	63.52	35.00
12-6	111	112.81	2.54	38.25	61.93	1.62	1.04	60.90	47.00
13-1	121	115.21	2.49	40.75	68.78	1.57	0.97	62.85	34.00
13-2	121	116.71	2.34	45.98	85.12	1.47	0.83	66.40	35.00
13-3	121	118.21	2.63	40.44	67.89	1.61	1.00	63.83	41.00
13-4	121	119.71	2.68	39.81	66.13	1.63	1.00	63.63	42.00

Table 7 (continued).

Core/ section	Interval (cm)	Depth (mbsf)	Grain density (g/cm^3)	Wet-water content (%)	Dry-water content (%)	Dry-bulk density (g/cm^3)	Wet-bulk density (g/cm^3)	Porosity (%)	Vane shear strength (kPa)
13-5	121	121.21	2.60	37.31	59.50	1.65	1.08	60.46	46.00
13-6	121	122.71	2.55	39.31	64.77	1.60	1.01	61.97	41.00
14-1	111	124.61	2.58	41.29	70.33	1.58	0.97	64.17	21.00
14-2	121	126.06	2.82	40.70	68.65	1.58	0.97	63.13	36.00
14-3	121	127.51	2.55	36.54	62.71	1.62	1.03	61.23	38.00
14-4	121	129.01	2.62	38.24	61.93	1.64	1.04	61.61	40.00
14-5	121	130.51	2.70	39.23	64.56	1.64	1.06	63.29	48.00
14-6	121	132.01	2.73	39.12	64.25	1.65	1.05	63.43	31.00
15-1	119	134.19	2.52	40.36	67.67	1.38	0.99	62.79	48.00
15-2	121	135.60	2.61	38.21	61.84	1.63	1.05	61.42	30.00
15-3	121	137.10	2.62	35.64	55.38	1.68	1.11	38.90	51.00
15-4	121	138.60	2.47	40.18	67.17	1.57	1.00	62.16	45.00
15-5	111	140.00	2.58	39.48	65.23	1.61	1.03	62.41	50.00
15-6	119	141.58	2.65	37.37	59.67	1.66	1.06	60.94	40.00
16-1	121	143.71	2.66	38.51	62.64	1.64	1.04	62.24	36.00
16-2	121	145.17	2.45	39.07	64.11	1.58	1.00	60.80	55.00
16-3	121	146.67	2.61	38.87	63.57	1.62	1.03	62.08	60.00
16-4	121	148.17	2.65	38.40	62.34	1.64	1.06	61.97	60.00
16-5	121	149.67	2.47	38.25	61.94	1.60	1.06	60.17	62.00
16-6	121	151.17	2.61	37.33	59.57	1.65	1.08	60.60	57.00
17-1	121	153.21	2.72	35.63	55.36	1.71	1.13	59.79	55.00
17-2	121	154.71	2.64	39.08	64.14	1.63	1.02	62.58	33.00
17-3	121	156.21	2.61	41.05	69.64	1.59	0.98	64.27	45.00
17-4	121	157.71	2.59	38.08	61.50	1.63	1.06	61.18	40.00
17-5	121	159.21	2.61	39.33	64.81	1.62	1.02	62.54	39.00
17-6	121	160.71	2.66	38.84	63.50	1.64	1.03	62.55	32.00
18-1	121	162.71	2.65	38.87	63.58	1.65	1.02	61.67	38.00
18-2	121	164.13		37.53	60.08	1.67	1.05	60.35	42.00
18-3	121	165.63		37.83	60.84	1.66	1.04	60.64	50.00
18-4	121	167.13		39.13	64.30	1.64	1.01	61.93	37.00
18-5	111	168.53		37.35	59.62	1.67	1.06	60.17	35.00
18-6	121	170.13		38.66	63.03	1.65	1.02	61.47	32.00
19-1	121	172.21		40.74	68.75	1.62	0.97	63.46	41.00
19-2	121	173.61		39.66	65.74	1.64	1.00	62.44	39.00
19-3	121	175.11		40.67	68.54	1.62	0.97	63.39	37.00
19-4	121	176.61		39.06	64.11	1.64	1.01	61.86	40.00
19-5	121	178.11		38.28	62.03	1.66	1.03	61.09	40.00
20-1	121	181.71		30.94	58.59	1.68	1.07	59.76	41.00
20-2	121	183.19		35.66	55.43	1.70	1.10	58.45	47.00
20-3	121	184.69		36.77	58.16	1.68	1.07	59.59	47.00
20-4	121	186.19		39.54	65.41	1.64	1.00	62.32	32.00
20-5	121	187.69		39.42	65.06	1.64	1.00	62.20	35.00
20-6	121	189.19		37.97	61.21	1.66	1.04	60.78	32.00
21-1	121	191.21		39.20	64.48	1.64	1.01	61.99	21.00
21-2	121	192.64		38.03	61.36	1.66	1.04	60.84	42.00
21-3	121	194.12		39.54	65.39	1.64	1.00	62.31	55.00
21-4	121	195.62		38.48	62.56	1.65	1.03	61.29	52.00
21-5	121	197.12		38.12	61.60	1.66	1.04	60.93	48.00
21-6	121	198.52		39.87	66.32	1.63	0.99	62.64	36.00
22-1	121	200.71		39.11	64.23	1.64	1.01	61.90	50.00
22-2	121	202.21		38.85	63.53	1.65	1.02	61.65	60.00
22-3	121	203.68		38.94	63.78	1.65	1.01	61.74	46.00
22-4	121	205.18		34.08	64.15	1.64	1.01	61.87	45.00
22-5	111	206.38		34.58	65.50	1.64	1.00	62.35	42.00
22-6	121	208.18		40.49	68.04	1.62	0.97	63.22	38.00
23-1	121	210.21		39.69	65.82	1.63	0.99	62.46	24.00
23-2	121	211.71		38.62	62.91	1.65	1.02	61.42	31.00
23-3	121	213.19		37.94	61.12	1.66	1.04	60.75	32.00
23-4	121	214.67		36.56	62.76	1.65	1.02	61.37	40.00
23-5	121	216.17		37.49	59.96	1.67	1.05	60.30	42.00
23-6	121	217.67		36.37	62.26	1.66	1.03	61.18	53.00
24-1	121	219.64		32.84	48.91	1.75	1.18	65.43	48.00
24-2	121	221.06		34.69	53.12	1.72	1.13	57.43	58.00
24-3	121	222.54		33.24	49.79	1.74	1.17	55.87	67.00
24-4	121	224.01		34.61	52.93	1.72	1.13	57.34	56.00
24-5	11	224.41		35.62	55.33	1.70	1.10	50.40	53.00
24-6	121	227.01		35.86	55.92	1.70	1.10	58.66	55.00
25-1	93	228.76		35.88	55.95	1.70	1.10	58.67	53.00
25-2	121	230.54		34.70	83.14	1.72	1.13	57.44	58.00
25-3	121	232.04		34.21	51.99	1.73	1.14	56.91	44.00
25-4	93	233.24		34.36	52.35	1.72	1.14	57.08	38.00
25-5	121	234.70		33.94	51.39	1.73	1.15	56.63	43.00
26-1	121	238.67		34.06	51.66	1.73	1.15	56.75	35.00
26-2	121	240.17		36.32	57.04	1.69	1.09	59.13	37.00
26-3	121	241.67		35.36	54.71	1.71	1.11	58.13	46.00
26-4	121	243.17		32.62	48.40	1.75	1.19	55.18	53.00
26-5	121	244.67		33.08	49.44	1.74	1.17	55.70	35.00

Table 8. Index-properties and vane-shear-strength data for Hole 664D.

Core/ section	Interval (cm)	Depth (mbsf)	Grain density (g/cm^3)	Wet-water content (%)	Dry-water content (%)	Wet-bulk density (g/cm^3)	Dry-bulk density (g/cm^3)	Porosity (%)	Vane shear strength (kPa)
6-1	121	41.51	2.51	48.28	93.34	1.47	0.80	69.87	25.00
6-2	121	43.01	2.70	44.34	79.66	1.36	0.90	67.99	38.00
6-3	121	44.31	2.63	45.17	82.38	1.54	0.88	68.21	31.00
6-4	121	46.01	2.99	45.08	84.78	1.32	0.87	68.47	30.00
6-5	121	47.31	2.61	43.58	77.24	1.55	0.91	66.62	32.00
6-6	121	48.99	2.68	46.03	85.28	1.53	0.87	69.38	28.00
12-1	121	98.51	2.49	39.84	66.21	1.58	1.02	61.97	35.00
12-2	121	99.89	2.61	39.36	63.44	1.62	1.01	62.84	39.00
12-3	121	101.38	2.62	39.13	64.28	1.62	1.02	62.43	32.00
12-4	121	102.08	2.37	46.02	25.27	1.47	0.84	66.67	37.00
12-5	121	104.38	2.49	40.90	69.21	1.57	0.99	63.00	52.00
12-6	121	105.88	2.70	40.55	68.22	1.62	1.00	64.36	41.00
13-1	121	108.01	2.60	40.90	69.80	1.59	0.99	64.05	36.00
13-2	121	109.47	2.58	39.63	68.65	1.61	1.02	62.62	32.00
13-3	121	110.93	2.38	39.82	66.17	1.60	1.02	62.77	34.00
13-4	121	112.43	2.51	39.99	66.63	1.58	1.01	62.33	34.00
13-5	121	113.89	2.61	38.54	62.70	1.63	1.05	61.81	40.00
13-6	121	115.39	2.69	34.27	32.15	1.72	1.18	88.06	44.00
14-1	121	117.51		34.77	83.31	1.72	1.13	57.51	37.00
14-2	121	118.88		34.06	81.66	1.73	1.15	86.76	38.00
14-3	121	120.38		40.86	68.23	1.62	0.97	63.29	36.00
14-4	121	121.88		40.63	68.42	1.62	0.97	63.35	47.00
14-5	121	123.38		39.62	63.62	1.64	1.00	62.40	35.00
14-6	121	124.85		39.91	66.41	1.63	0.99	62.67	27.00
15-1	121	127.01		40.23	67.32	1.63	0.98	62.98	35.00
15-2	121	128.46		38.36	62.22	1.66	1.03	61.17	65.00
15-3	121	129.96		38.81	63.41	1.65	1.02	61.61	32.00
15-4	121	131.46		38.64	62.97	1.65	1.02	61.45	45.00
15-5	121	132.96		39.45	63.14	1.64	1.00	62.23	37.00
15-6	115	134.40		40.34	67.61	1.62	0.98	63.08	45.00
16-1	96	136.26		40.17	67.15	1.63	0.98	62.92	31.00
16-2	121	137.61		41.13	69.84	1.61	0.96	63.82	38.00
16-3	121	139.11		42.25	73.16	1.60	0.93	64.85	33.00
16-4	121	140.61		30.52	62.66	1.65	1.02	61.33	48.00
16-5	121	142.11		39.86	66.27	1.63	0.99	62.62	45.00
16-6	121	143.61		41.04	69.60	1.61	0.96	63.74	35.00
17-1	121	146.01		30.13	61.63	1.66	1.04	60.94	41.00
17-2	121	147.44		37.95	61.16	1.66	1.04	60.77	48.00
17-3	121	148.94		37.41	89.77	1.67	1.05	60.23	41.00
17-4	121	150.44		39.40	65.03	1.64	1.00	62.19	47.00
17-5	121	151.94		39.09	64.16	1.64	1.01	61.88	26.00
17-6	121	153.44		37.55	60.13	1.67	1.05	60.37	34.00
18-1	121	155.51		40.51	68.09	1.62	0.97	63.24	57.00
18-2	121	156.96		40.06	66.84	1.63	0.99	62.82	84.00
18-3	121	158.46		44.87	81.40	1.56	0.87	67.18	43.00
18-4	121	159.96		41.68	71.46	1.60	0.95	64.33	45.00
18-5	121	161.46		43.38	76.62	1.58	0.90	65.87	35.00
18-6	121	162.96		41.92	72.17	1.60	0.94	64.55	43.00
19-1	121	164.98	2.54	41.25	70.21	1.57	0.97	63.81	39.00
19-2	121	166.48	2.58	41.56	71.13	1.58	0.96	64.49	35.00
19-3	121	167.98	2.57	40.98	69.44	1.58	0.98	63.86	42.00
19-4	121	169.48	2.54	41.12	69.84	1.57	0.98	63.67	40.00
19-5	121	170.98	2.64	40.48	68.02	1.61	1.02	63.94	32.00
19-6	115	172.42	2.64	42.83	74.91	1.57	0.94	66.19	25.00
20-1	121	174.51	2.70	40.99	69.46	1.61	0.99	64.97	39.00
20-2	121	176.01	2.75	41.16	69.94	1.62	0.99	65.50	29.00
20-3	121	177.51	2.56	30.97	63.87	1.61	1.03	61.79	39.00
20-4	121	179.01	2.62	39.94	66.49	1.61	1.00	63.23	37.00
20-5	121	180.31	2.71	36.81	38.26	1.68	1.11	60.93	44.00
20-6	121	182.01	2.68	37.65	60.40	1.66	1.07	61.49	37.00
21-1	121	183.93	2.58	39.47	65.20	1.61	1.03	62.42	47.00
21-2	121	185.40	2.56	37.50	60.01	1.63	1.06	60.26	55.00
21-3	121	186.90	2.60	37.60	60.26	1.64	1.08	60.79	21.00
21-4	121	188.40	2.56	36.93	58.55	1.64	1.08	59.68	51.00
21-5	121	189.90	2.56	39.31	65.31	1.60	1.02	62.32	47.00
21-6	121	191.40	2.59	37.68	60.46	1.64	1.05	60.69	44.00
22-1	121	193.51	2.57	36.17	56.66	1.66	1.11	59.03	70.00
22-2	121	195.01	2.60	35.67	55.44	1.68	1.12	58.76	70.00
22-3	121	196.51	2.54	35.76	55.66	1.66	1.12	58.23	70.00
22-4	121	198.01	2.57	36.80	58.22	1.65	1.09	59.65	84.00
22-5	121	199.31	2.60	36.19	56.70	1.67	1.11	59.27	80.00
22-6	121	201.01	2.54	37.57	60.18	1.63	1.08	60.17	47.00
23-1	121	203.01	2.67	35.66	55.43	1.69	1.11	59.39	56.00
23-2	121	204.51	2.60	35.10	54.09	1.69	1.13	58.17	50.00
23-3	121	206.01	2.43	34.28	52.17	1.65	1.18	55.63	66.00
23-4	121	207.51	2.64	37.39	59.72	1.66	1.08	60.87	54.00

Table 8 (continued).

Core/ section	Interval (cm)	Depth (mbsf)	Grain density (g/cm^3)	Wet-water content (%)	Dry-water content (%)	Wet-bulk density (g/cm^3)	Dry-bulk density (g/cm^3)	Porosity (%)	Vane shear strength (kPa)
23-5	121	209.01	2.55	35.72	55.58	1.66	1.14	58.36	55.00
23-6	121	210.51	2.59	32.96	49.16	1.72	1.21	55.66	96.00
24-1	121	212.47	2.64	35.83	55.83	1.68	1.12	59.25	72.00
24-2	121	213.92	2.61	36.31	57.00	1.67	1.10	59.47	47.00
24-3	121	215.39	2.60	35.51	55.07	1.68	1.13	58.58	46.00
24-4	121	216.87	2.62	34.87	53.55	1.69	1.17	58.11	32.00
24-5	121	218.37	2.58	33.85	51.18	1.70	1.18	56.59	42.00
24-6	121	219.87	2.60	31.68	46.36	1.74	1.24	54.35	68.00
25-1	121	221.97	2.53	34.36	52.36	1.68	1.16	56.65	53.00
25-2	121	223.47	2.96	33.65	50.73	1.81	1.21	59.72	53.00
25-3	121	224.97	2.62	32.96	49.17	1.73	1.20	55.99	52.00
25-4	121	226.47	2.63	34.64	52.99	1.70	1.15	57.94	44.00
25-5	121	227.97	2.61	34.15	51.85	1.70	1.16	57.20	52.00
25-6	121	229.47	2.51	35.06	53.98	1.66	1.13	57.27	38.00
26-1	121	231.51	2.55	35.59	55.26	1.66	1.14	58.17	52.00
26-2	121	233.01	2.48	34.62	52.96	1.66	1.17	56.46	43.00
26-3	121	234.51	2.65	35.44	54.90	1.69	1.16	58.96	43.00
26-4	121	236.01	2.54	33.44	50.25	1.69	1.18	55.72	53.00
26-5	121	237.81	2.59	33.77	50.98	1.70	1.18	56.59	45.00
26-6	121	238.98	2.66	30.32	43.51	1.79	1.27	53.28	50.00
27-1	121	241.01	2.55	32.63	48.44	1.71	1.23	54.95	67.00
27-2	121	242.81	2.51	33.52	50.41	1.69	1.16	55.56	48.00
27-3	121	244.01	2.67	35.34	54.66	1.70	1.14	59.03	43.00
27-4	121	245.51	2.62	35.03	53.92	1.69	1.16	58.22	45.00
27-5	121	247.01		33.07	49.42	1.72	1.15	56.05	45.00
27-6	121	248.51		35.49	55.03	1.68	1.15	58.64	54.00
28-1	121	250.51		34.62	52.94	1.72	1.13	57.35	85.00
28-2	121	251.97		34.37	52.37	1.72	1.14	57.09	75.00
28-3	121	253.44		34.68	53.08	1.72	1.13	57.41	75.00
28-4	121	254.94		30.31	43.49	1.80	1.26	52.56	60.00
29-5	121	256.44		32.92	49.07	1.75	1.18	55.51	74.00
29-1	121	259.97		31.86	46.75	1.77	1.21	54.34	58.00
29-2	121	261.47		33.78	51.01	1.73	1.15	56.45	57.00
29-3	121	262.94		32.55	48.26	1.75	1.19	55.11	62.00
29-4	121	264.44		32.53	48.22	1.75	1.19	55.09	44.00
29-5	121	265.91		31.01	44.94	1.78	1.24	53.37	72.00
29-6	121	267.39		31.86	46.76	1.77	1.21	54.34	52.00
30-1	121	269.46		33.00	49.26	1.75	1.10	55.60	59.00
30-2	121	270.88		33.67	50.76	1.73	1.16	56.33	57.00
30-3	131	272.42		32.44	48.03	1.76	1.19	54.99	58.00
30-4	121	273.82		34.53	52.73	1.72	1.13	57.25	59.00
30-5	121	275.32		32.38	47.88	1.76	1.19	54.92	85.00
30-6	121	276.82		31.39	45.76	1.78	1.22	53.81	67.00
31-1	121	279.01		33.36	50.07	1.74	1.17	56.00	61.00
31-2	121	280.51		34.57	52.82	1.72	1.13	57.29	33.00
31-3	121	282.01		34.27	52.14	1.72	1.14	56.98	34.00
31-4	121	283.49		32.46	48.07	1.76	1.19	55.01	47.00
31-5	121	284.99		32.30	47.71	1.76	1.20	54.83	36.00
31-6	121	286.49		33.28	49.88	1.74	1.17	55.91	36.00
32-1	121	288.49		34.41	52.47	1.72	1.14	57.13	53.00
32-2	121	289.99		33.91	51.30	1.73	1.15	56.59	49.00
32-3	121	291.49		34.04	51.60	1.73	1.15	56.73	33.00
32-4	121	292.99		34.21	52.00	1.73	1.14	56.92	46.00
32-5	121	294.49		32.08	47.22	1.76	1.20	54.58	38.00
32-6	121	295.99		30.13	43.12	1.80	1.26	52.35	52.00

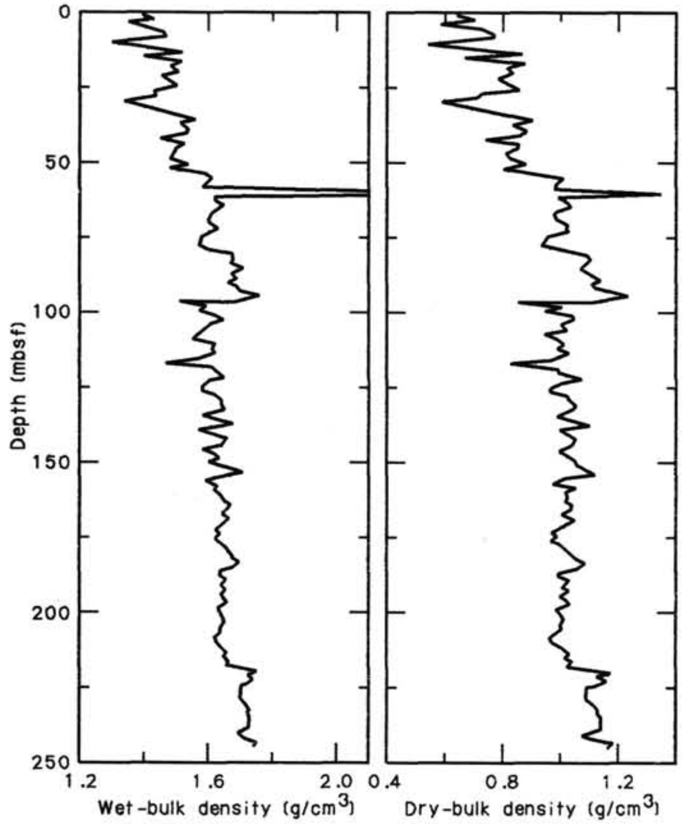

Figure 12. Wet- and dry-bulk-density profiles for Hole 664B.

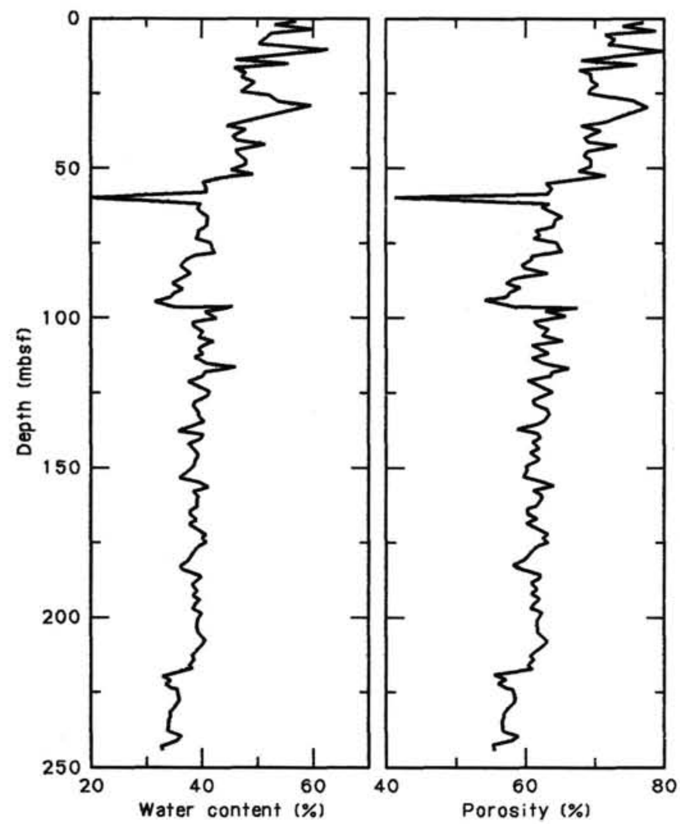

Figure 13. Water-content and porosity profiles for Hole 664B.

Table 9. *P*-wave-logger velocity data for Hole 664B.

Depth (m)	*P*-wave velocity (km/s)	Depth (m)	*P*-wave velocity (km/s)	Depth (m)	*P*-wave velocity (km/s)
0.20	1.541	70.50	1.536	145.40	1.569
0.30	1.517	72.80	1.527	145.90	1.529
1.40	1.558	73.70	1.569	147.00	1.560
2.20	1.520	75.20	1.540	149.00	1.552
2.60	1.550	77.00	1.560	151.40	1.573
2.70	1.520	78.00	1.552	153.00	1.550
2.90	1.549	78.30	1.617	153.50	1.580
3.30	1.515	79.00	1.538	155.00	1.548
3.70	1.538	80.00	1.550	157.50	1.524
4.10	1.521	82.00	1.580	160.00	1.550
4.40	1.561	83.00	1.555	162.50	1.555
5.00	1.512	84.70	1.548	165.50	1.532
6.20	1.511	85.80	1.578	169.50	1.540
7.00	1.530	86.50	1.550	172.00	1.540
8.00	1.540	87.90	1.575	172.90	1.566
10.00	1.506	89.30	1.539	175.10	1.529
11.40	1.541	90.10	1.600	175.40	1.555
12.20	1.510	90.80	1.550	178.20	1.533
12.90	1.545	91.50	1.598	178.50	1.560
13.20	1.509	94.00	1.564	181.20	1.540
14.70	1.529	95.20	1.624	182.90	1.570
15.30	1.505	95.50	1.587	186.30	1.540
16.10	1.557	95.80	1.623	188.80	1.561
17.20	1.530	96.10	1.553	189.40	1.538
20.00	1.520	96.20	1.646	190.70	1.559
20.90	1.509	96.50	1.530	192.00	1.542
21.60	1.552	97.90	1.555	193.50	1.540
23.00	1.522	98.30	1.536	194.20	1.617
24.30	1.521	99.60	1.565	194.40	1.550
24.70	1.589	100.00	1.530	195.00	1.575
25.70	1.520	101.00	1.560	195.40	1.540
27.00	1.540	101.80	1.521	197.40	1.545
27.30	1.501	102.50	1.569	200.50	1.562
29.50	1.538	103.50	1.525	201.10	1.530
30.90	1.514	105.50	1.550	202.00	1.565
31.20	1.569	107.70	1.558	203.50	1.535
32.70	1.521	108.00	1.523	204.60	1.570
34.20	1.512	109.20	1.575	205.50	1.550
35.50	1.537	109.70	1.526	208.50	1.542
37.20	1.555	110.30	1.551	209.30	1.587
37.70	1.518	111.00	1.517	210.00	1.552
39.40	1.540	112.50	1.549	211.20	1.575
40.30	1.550	113.60	1.560	212.00	1.540
44.70	1.548	115.00	1.532	216.00	1.542
45.60	1.570	117.00	1.540	219.30	1.560
46.70	1.518	118.40	1.528	220.20	1.570
48.30	1.559	118.60	1.595	221.50	1.547
49.40	1.519	119.00	1.560	223.50	1.570
50.00	1.560	120.70	1.587	223.80	1.547
52.00	1.515	121.50	1.562	225.90	1.562
52.50	1.570	122.90	1.564	227.50	1.570
54.40	1.530	124.00	1.604	229.00	1.551
55.00	1.628	125.80	1.526	229.30	1.640
55.50	1.548	127.80	1.550	229.40	1.540
58.00	1.564	129.60	1.570	230.70	1.563
59.10	1.540	129.90	1.530	232.00	1.552
59.60	1.572	130.10	1.564	234.50	1.552
62.00	1.570	131.90	1.528	236.30	1.551
62.60	1.638	134.00	1.542	238.00	1.572
62.80	1.565	135.50	1.611	239.50	1.557
64.90	1.536	136.00	1.567	241.50	1.533
65.40	1.560	137.00	1.583	242.40	1.560
65.70	1.540	137.70	1.623	242.80	1.531
67.50	1.540	140.00	1.542	244.90	1.572
68.90	1.532	142.00	1.536	245.50	1.559
69.70	1.569	143.50	1.565		

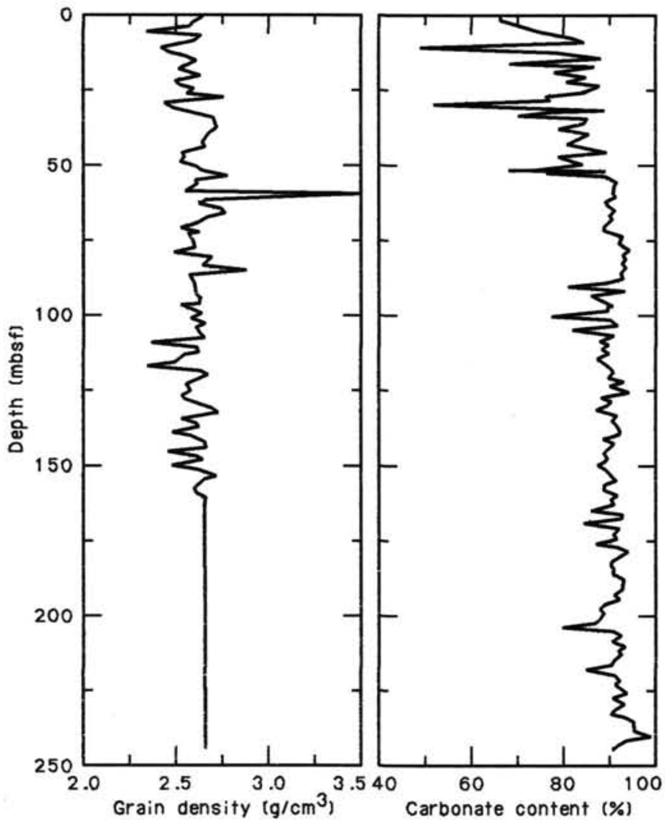

Figure 14. Grain-density and carbonate contents for Hole 664B.

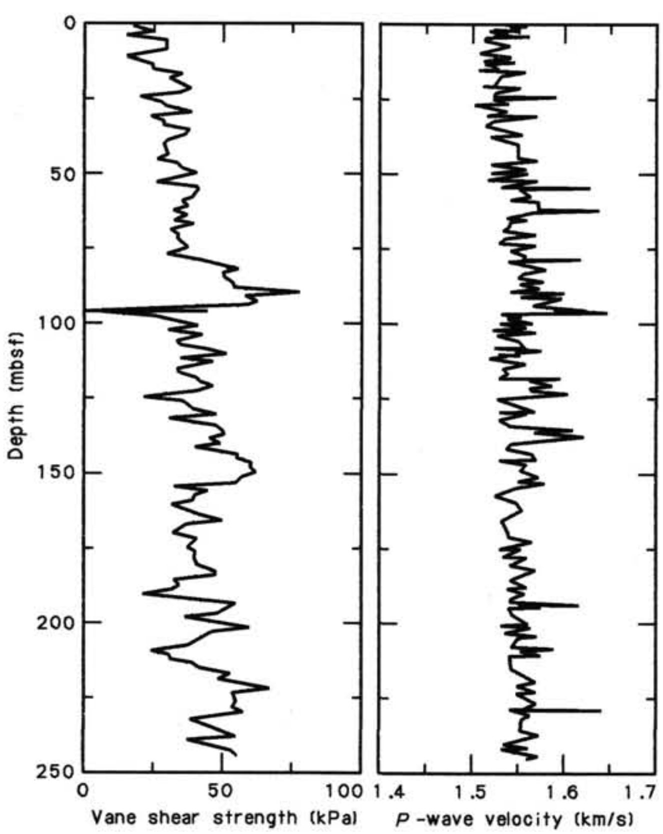

Figure 15. Vane-shear-strength and P-wave-velocity profiles for Hole 664B.

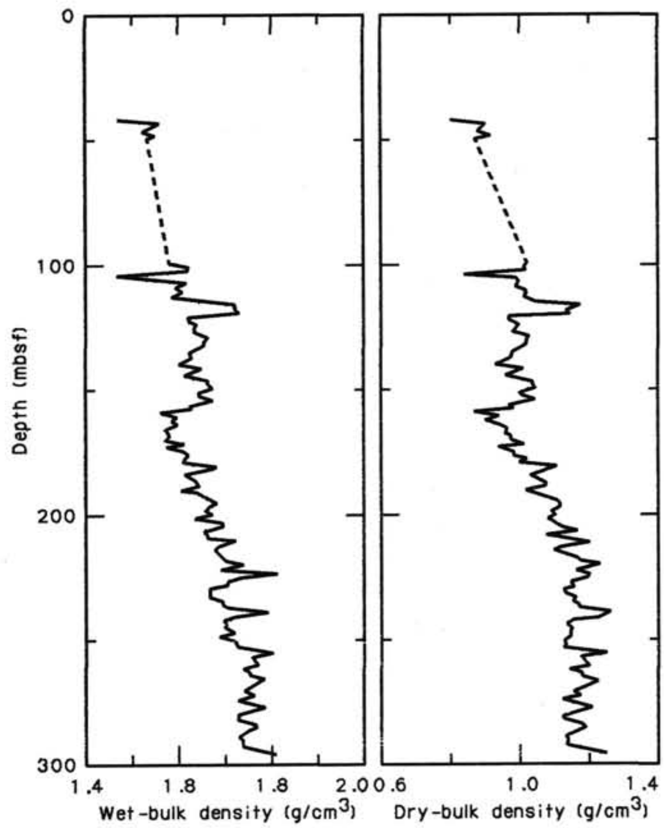

Figure 16. Wet- and dry-bulk-density profiles for Hole 664D.

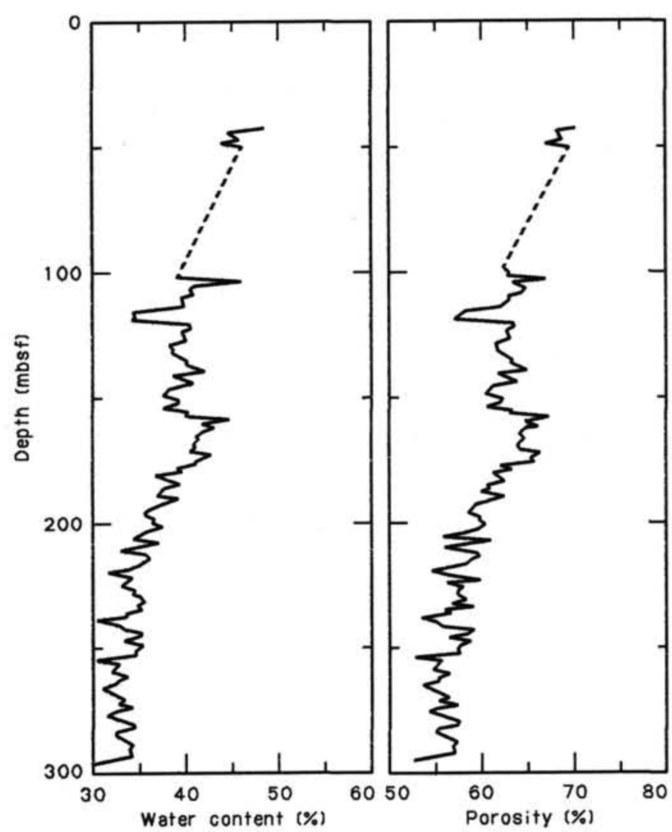

Figure 17. Water-content and porosity profiles for Hole 664D.

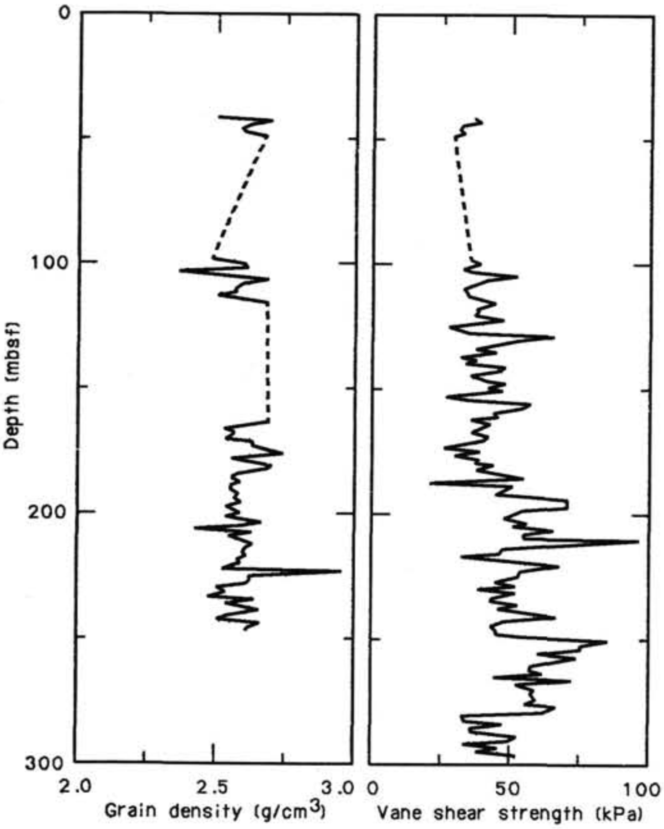

Figure 18. Grain-density and vane-shear-strength profiles for Hole 664D.

Table 10. Composite-depth sections between Hole 664B and Holes 664C and 664D.

Hole 664B core/section interval (cm)	Hole 664C core/section interval (cm)	Composite depth (mbsf)	Hole 664B core/section interval (cm)	Hole 664D core/section interval (cm)	Composite depth (mbsf)
—	1H-1, 0	0	—	12H-3, 25	100.55
1H-1, 50	1H-1, 120	1.20	12H-6, 45	12H-7, 42	106.72
1H-7, 22	2H-4, 25	9.92	12H-7, 35	13H-2, 45	108.12
2H-1, 52	2H-5, 55	11.72		13H-3, 22	109.39
2H-7, 0	3H-3, 125	20.20			
3H-1, 30	3H-4, 60	21.05			
3H-6, 145	4H-3, 65	29.70			
4H-1, 75	4H-4, 58	31.13			
4H-7, 30	5H-3, 140	39.68			
5H-1, 75	5H-4, 100	40.78			
5H-7, 31	6H-3, 50	49.34			
6H-1, 105	6H-5, 37	[a]51.26			
6H-4, 0	—	54.71			

[a] A turbidite from Cores 108-664C-4-0 through -664C-4-95 was removed from the composite depth.

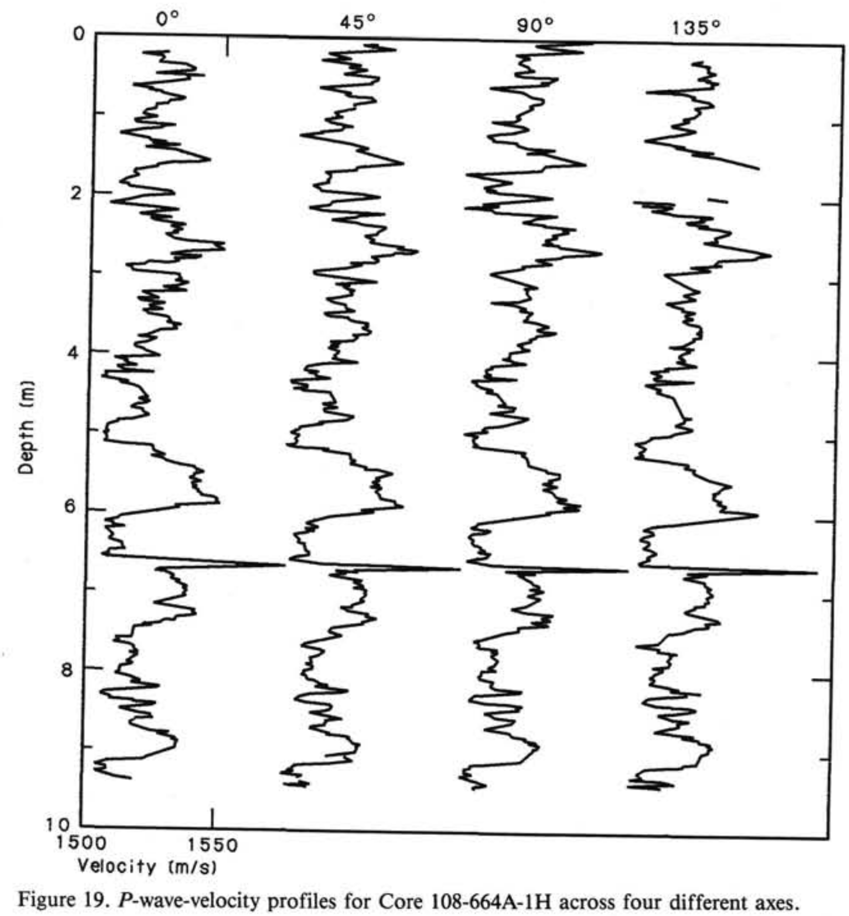

Figure 19. *P*-wave-velocity profiles for Core 108-664A-1H across four different axes.

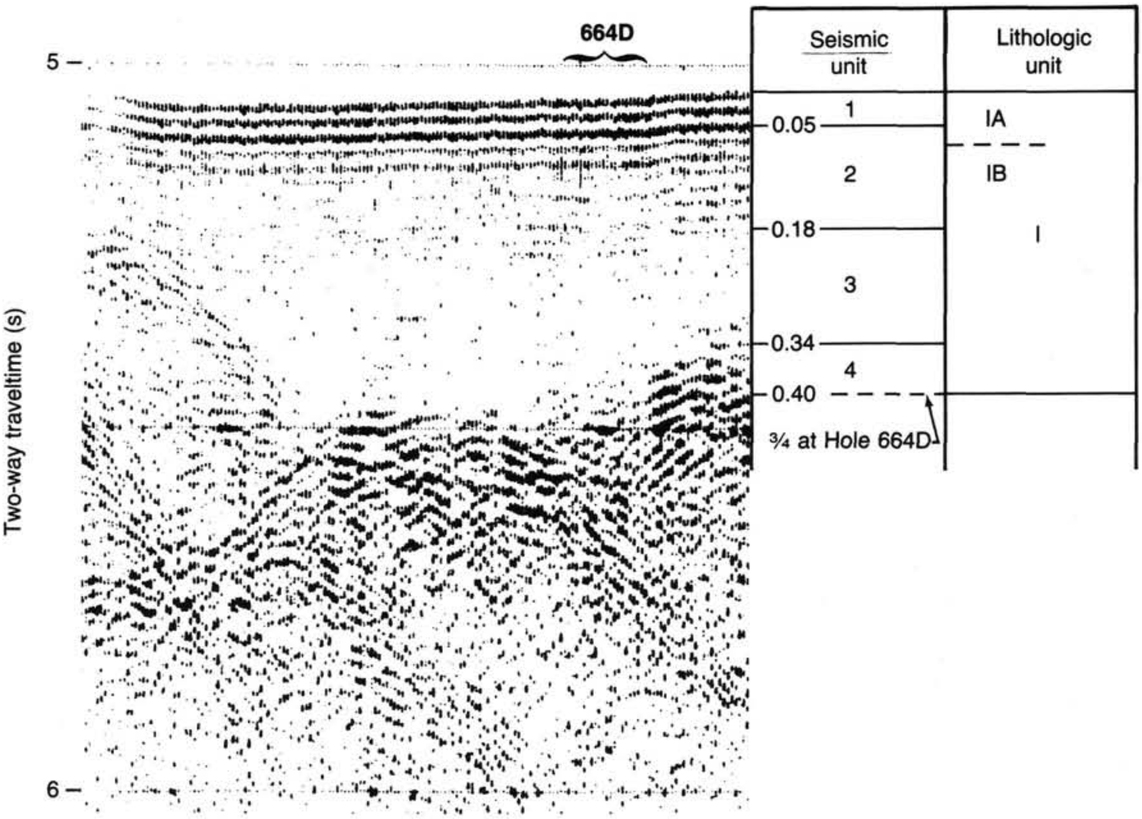

Figure 20. Comparison of Site 664 seismic units with lithologic units. Hole 664D lies off this seismic line and deeper in the sediment pond; the most nearly equivalent position within the sediment pond is indicated by the bracket. Estimated depth to the acoustic basement (the boundary between seismic units 3 and 4) at Hole 664D is indicated by the designation "3/4."

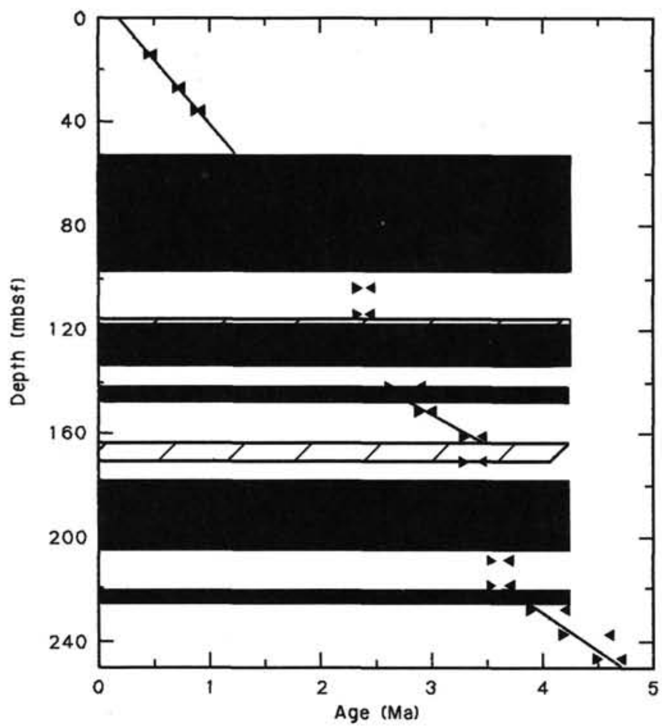

Figure 21. Age-depth curve for Hole 664B (also applies to Holes 664A and 664C). Black layers represent gravity-deposited sediments (slumps); white layers represent pelagic deposition; diagonal pattern indicates slight deformation (tilting) of pelagic sediments. Age-depth biostratigraphic control points are shown by triangles.

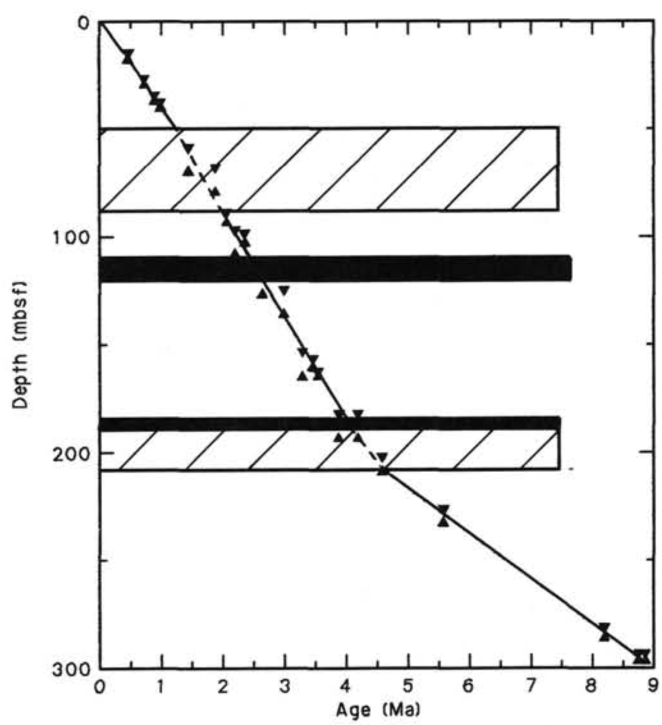

Figure 22. Age-depth curve for Hole 664D. Black layers represent gravity-deposited sediments (slumps); white layers represent pelagic deposition; diagonal pattern indicates slight deformation (tilting) of pelagic sediments. Age-depth biostratigraphic control points are shown by triangles.

SITE 664 HOLE B CORE 1 H CORED INTERVAL 3806.3-3815.8 mbsl; 0-9.5 mbsf

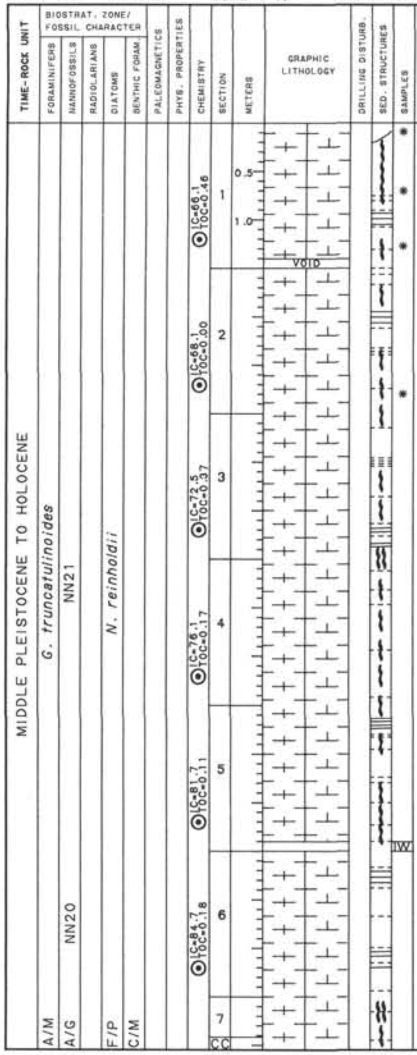

LITHOLOGIC DESCRIPTION

FORAMINIFER-NANNOFOSSIL OOZE and MUD-BEARING FORAMINIFER-NANNOFOSSIL OOZE, alternating with CLAY-BEARING, FORAMINIFER-BEARING NANNOFOSSIL OOZE

Foraminifer-nannofossil ooze and mud-bearing foraminifer-nannofossil ooze, white, light-gray, and gray (5Y 8/1, 7/1, 6/1), alternating with clay-bearing, foraminifer-bearing nannofossil ooze, white to light-gray (7.5YR 8/0, 5Y 7/2); weakly to moderately bioturbated throughout; black and green microlaminations and burrows; laminations most common in Sections 5, 6, and 7. Minor voids in Section 1, 144–150 cm, and Section 5, 146–150 cm.

SMEAR SLIDE SUMMARY (%):

	1, 10 D	1, 70 D	11, 130 D	12, 130 D
TEXTURE:				
Sand	25	20	20	15
Silt	15	10	15	15
Clay	65	70	65	70
COMPOSITION:				
Quartz	Tr	—	—	—
Clay	<5	5	10	15
Accessory Minerals	5	5	5	Tr
Foraminifers	25	25	25	15
Nannofossils	60	65	55	70
Diatoms	2	Tr	Tr	Tr
Radiolarians	3	Tr	5	Tr

Chemistry: IC here refers to weight % $CaCO_3$.

SITE 664 HOLE B CORE 2 H CORED INTERVAL 3815.8-3825.3 mbsl; 9.5-19.0 mbsf

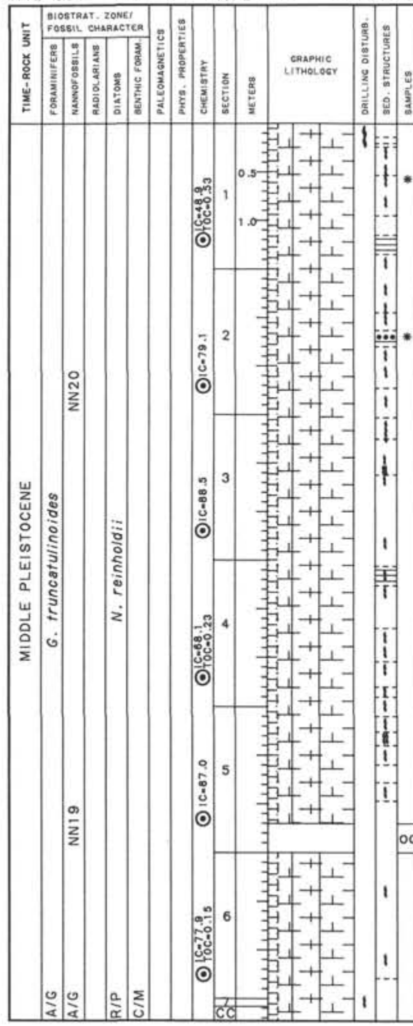

LITHOLOGIC DESCRIPTION

FORAMINIFER-NANNOFOSSIL OOZE and MUD-BEARING FORAMINIFER-NANNOFOSSIL OOZE, alternating with CLAY-BEARING, FORAMINIFER-BEARING NANNOFOSSIL OOZE and MUD-BEARING NANNOFOSSIL OOZE

Foraminifer-nannofossil ooze and mud-bearing foraminifer-nannofossil ooze, white, light-gray or gray (5Y 8/1, 7/1, 6/1), alternating with clay-bearing foraminifer-bearing nannofossil ooze, white to light-gray (7.5YR 8/0, 5Y 7/2) and mud-bearing nannofossil ooze, gray (5Y 6/1); weakly bioturbated throughout; green laminations in Sections 1 and 4. Turbidite or contourite in Section 2, 70 cm.

SMEAR SLIDE SUMMARY (%):

	1, 60 D	2, 75 D
TEXTURE:		
Sand	10	5
Silt	15	10
Clay	75	85
COMPOSITION:		
Clay	10	20
Accessory Minerals	<5	5
Foraminifers	10	5
Nannofossils	75	65
Diatoms	Tr	5
Radiolarians	Tr	—

SITE 664 HOLE B CORE 3 H CORED INTERVAL 3825.3-3834.8 mbsl; 19.0-28.5 mbsf

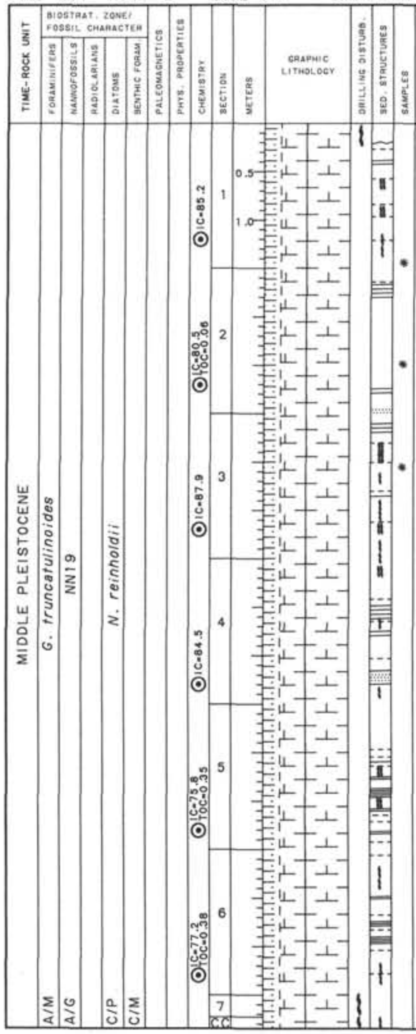

LITHOLOGIC DESCRIPTION

CLAY-BEARING, FORAMINIFER-BEARING NANNOFOSSIL OOZE, alternating with MUDDY NANNOFOSSIL OOZE

Clay-bearing, foraminifer-bearing nannofossil ooze, light-gray to white (5Y 7/1, 8/1), alternating with muddy nannofossil ooze, olive-gray to gray (10Y 5/2, 5Y 5/1); weakly bioturbated; green laminations common throughout, but particularly in Sections 5 and 6. Section 2, 145 cm, and Section 4, 125 cm, contain coarse foraminifer sands, the latter with sharp lower and upper contacts. Minor void in Section 6, 144–150 cm.

SMEAR SLIDE SUMMARY (%):

	1, 140 D	2, 100 D	3, 60 D
TEXTURE:			
Sand	25	5	—
Silt	25	15	15
Clay	50	80	85
COMPOSITION:			
Quartz	Tr	—	—
Clay	20	20	20
Accessory Minerals	Tr	5	5
Foraminifers	30	5	5
Nannofossils	50	70	70
Diatoms	—	Tr	—
Radiolarians	—	Tr	—

SITE 664 HOLE B CORE 4 H CORED INTERVAL 3834.8-3844.3 mbsl; 28.5-38.0 mbsf

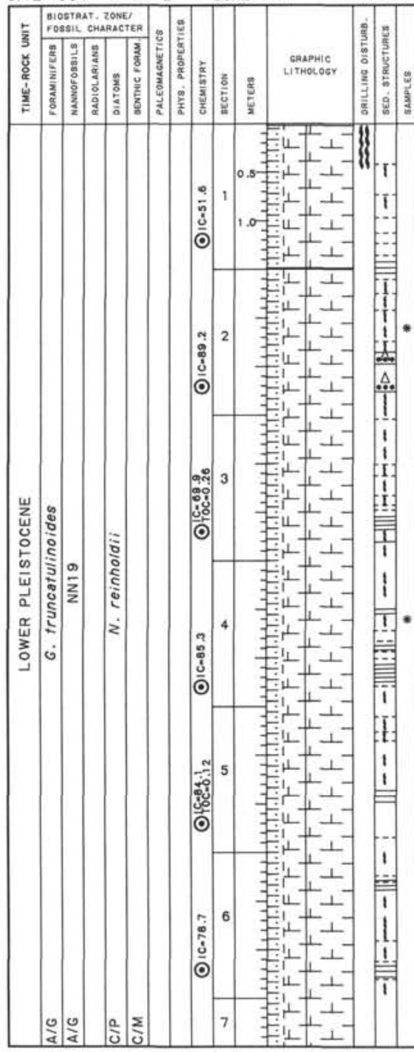

LITHOLOGIC DESCRIPTION

CLAY-BEARING, FORAMINIFER-BEARING NANNOFOSSIL OOZE, alternating with MUDDY NANNOFOSSIL OOZE

Clay-bearing, foraminifer-bearing nannofossil ooze, light-gray to white (5Y 7/1, 8/1), alternating with muddy nannofossil ooze, olive-gray to gray (10Y 5/2, 5Y 5/1); weak to moderate bioturbation; green, black, and purple laminations common throughout core. Two turbidites in Section 2, one at 88–98 cm, and one at 98–125 cm. Minor voids in Section 1, 0–3 and 148–150 cm.

SMEAR SLIDE SUMMARY (%):

	2, 60 D	4, 60 D
TEXTURE:		
Sand	5	15
Silt	10	20
Clay	85	65
COMPOSITION:		
Clay	25	15
Accessory Minerals	5	5
Foraminifers	5	15
Nannofossils	65	60
Diatoms	—	5
Radiolarians	—	

SITE 664 HOLE B CORE 5 H CORED INTERVAL 3844.3-3853.8 mbsl; 38.0-47.5 mbsf

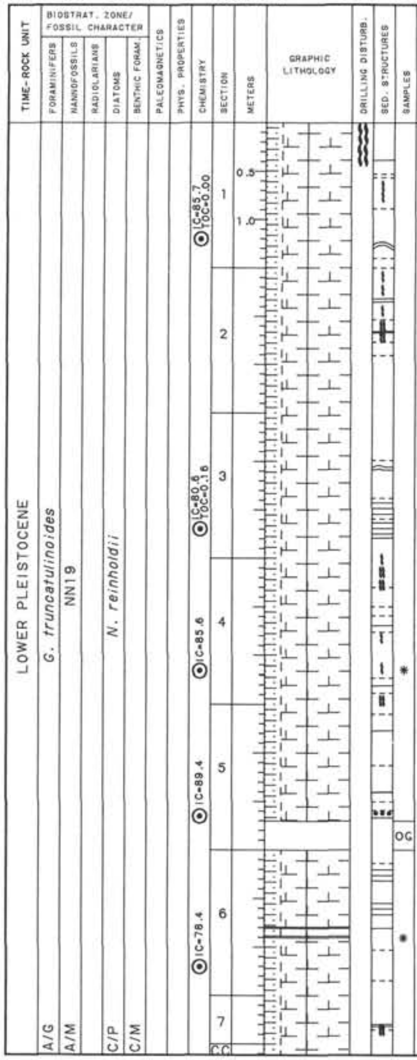

LITHOLOGIC DESCRIPTION

CLAY-BEARING, FORAMINIFER-BEARING NANNOFOSSIL OOZE, alternating with MUDDY NANNOFOSSIL OOZE

Clay-bearing, foraminifer-bearing nannofossil ooze, light-gray to white (5Y 7/1, 8/1), alternating with muddy nannofossil ooze, olive-gray to gray (10Y 5/2, 5Y 5/1); weak to moderate bioturbation; green, black and purple laminations common throughout core. A turbidite (?) in Section 5, 110 cm. Minor voids in Section 6, 77–78 and 85–87 cm.

SMEAR SLIDE SUMMARY (%):

	4, 115 D	6, 100 D
TEXTURE:		
Sand	15	5
Silt	20	15
Clay	65	80
COMPOSITION:		
Quartz	Tr	5
Clay	15	20
Accessory Minerals	Tr	5
Foraminifers	20	10
Nannofossils	65	60
Diatoms	—	Tr
Radiolarians	—	Tr

SITE 664 HOLE B CORE 6 H CORED INTERVAL 3853.8-3863.3 mbsl; 47.5-57.0 mbsf

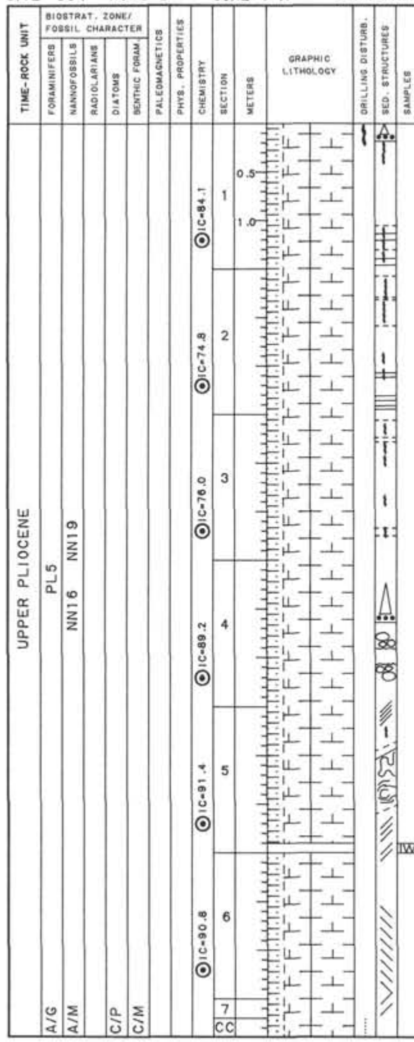

LITHOLOGIC DESCRIPTION

CLAY-BEARING, FORAMINIFER-BEARING NANNOFOSSIL OOZE and MUDDY NANNOFOSSIL OOZE

Clay-bearing, foraminifer-bearing nannofossil ooze, light-gray to white (5Y 7/1, 8/1). Muddy nannofossil ooze, olive-gray to gray (10Y 5/2, 5Y 5/1). A slump occurs from Section 4, 70 cm, through CC; brecciated in Section 4. Two turbidites; one in Section 4, 0–73 cm, and another in Section 1, 0–20 cm. Weak to moderate bioturbation in sections not disturbed by slumping; green, black, and purple laminations are common throughout core. Minor void in Section 5, 145–150 cm.

SITE 664 HOLE B CORE 7 H CORED INTERVAL 3863.3-3872.8 mbsl; 57.0-66.5 mbsf

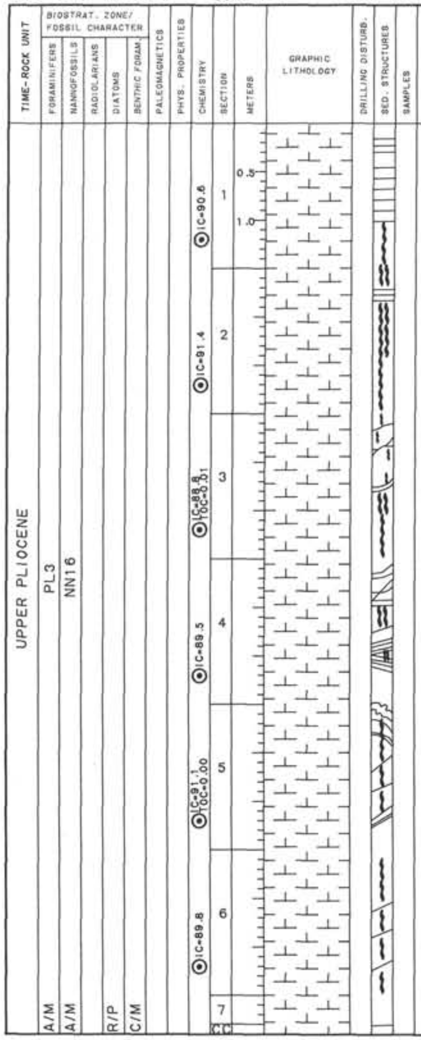

LITHOLOGIC DESCRIPTION

CLAY-BEARING, FORAMINIFER-BEARING NANNOFOSSIL OOZE

Clay-bearing, foraminifer-bearing nannofossil ooze, light-gray to white (5Y 7/1, 8/1, 7.5YR 8/0). Most of core exhibits slump features including dipping beds, microfaults, and convoluted bedding. Green and black laminations common and generally dip 10° or more.

SITE 664 HOLE B CORE 8 H CORED INTERVAL 3872.8-3882.3 mbsl; 66.5-76.0 mbsf

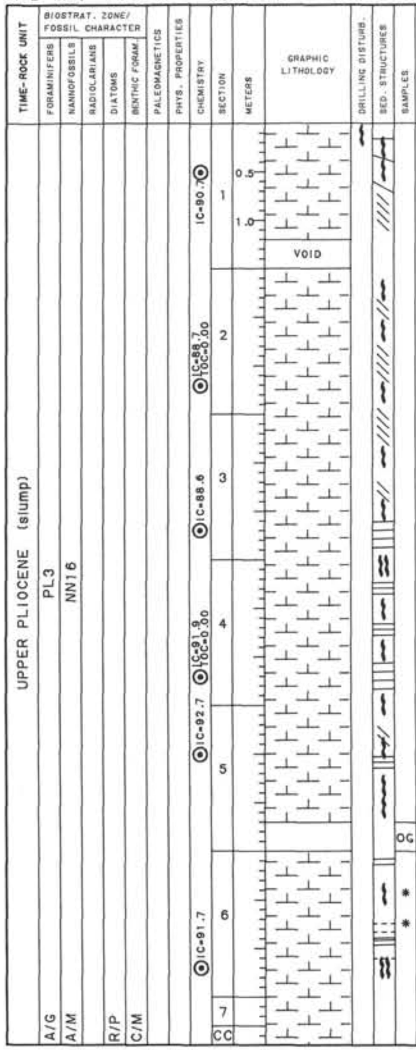

LITHOLOGIC DESCRIPTION

CLAY-BEARING, FORAMINIFER-BEARING NANNOFOSSIL OOZE

Clay-bearing, foraminifer-bearing nannofossil ooze, light-gray to white (5Y 7/1, 8/1, 7.5YR 8/0); weak to moderate bioturbation; green, black, and purple laminations are common throughout core, dipping approximately 10°. All of core is probably a slump.

SMEAR SLIDE SUMMARY (%):

	6, 50 D	6, 82 D
TEXTURE:		
Sand	5	5
Silt	20	20
Clay	75	75
COMPOSITION:		
Clay	—	10
Foraminifers	25	20
Nannofossils	75	65
Radiolarians	Tr	5
Sponge spicules	—	Tr

SITE 664 HOLE B CORE 9 H CORED INTERVAL 3882.3-3891.8 mbsl; 76.0-85.5 mbsf

TIME-ROCK UNIT	FORAMINIFERS	NANNOFOSSILS	RADIOLARIANS	DIATOMS	BENTHIC FORAM.	PALEOMAGNETICS	PHYS. PROPERTIES	CHEMISTRY	SECTION	METERS
UPPER PLIOCENE (WITH LOWER PLIOCENE SLUMP)	M13	NN15						IC=94.4	1	0.5, 1.0
								IC=92.6 TOC=0.00	2	
								IC=93.5	3	
								IC=92.4 TOC=0.00	4	
								IC=93.5	5	
								IC=92.4	6	
									7	
	A/G	A/M		B	C/M				CC	

BIOSTRAT. ZONE/ FOSSIL CHARACTER

GRAPHIC LITHOLOGY / DRILLING DISTURB. / SED. STRUCTURES / SAMPLES

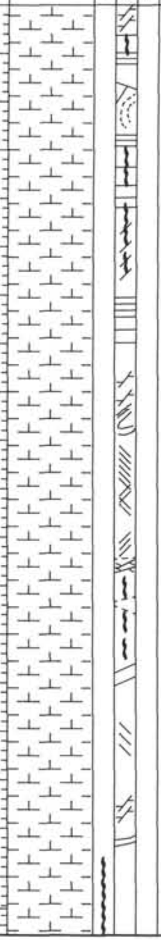

LITHOLOGIC DESCRIPTION

CLAY-BEARING, FORAMINIFER-BEARING NANNOFOSSIL OOZE

Clay-bearing, foraminifer-bearing nannofossil ooze, light-gray to white (5Y 7/1, 8/1, 7.5YR 8/0); weak to moderate bioturbation; green, black, and purple laminations common throughout core, dipping approximately 10°. Microfaults and contorted and folded beds are common throughout. Most of core is part of a slump.

SITE 664 HOLE B CORE 10 H CORED INTERVAL 3891.8-3901.3 mbsl; 85.5-95.0 mbsf

TIME-ROCK UNIT	FORAMINIFERS	NANNOFOSSILS	RADIOLARIANS	DIATOMS	BENTHIC FORAM.	PALEOMAGNETICS	PHYS. PROPERTIES	CHEMISTRY	SECTION	METERS
UPPER PLIOCENE (WITH LOWER PLIOCENE SLUMP)	PL1	NN15		N. marina?				IC=93.1	1	0.5, 1.0
								IC=89.3	2	
								IC=80.8	3	
								IC=93.2	4	
								IC=85.7 TOC=0.00	5	
								IC=88.0	6	
	A/G	A/M		F/P	C/M				CC	

BIOSTRAT. ZONE/ FOSSIL CHARACTER

GRAPHIC LITHOLOGY / DRILLING DISTURB. / SED. STRUCTURES / SAMPLES

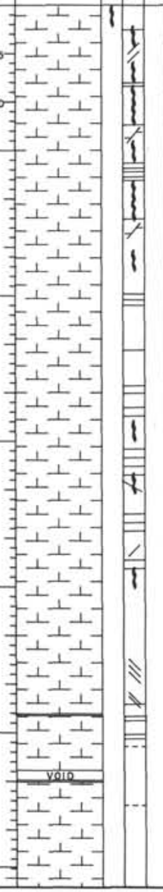

LITHOLOGIC DESCRIPTION

CLAY-BEARING, FORAMINIFER-BEARING NANNOFOSSIL OOZE

Clay-bearing, foraminifer-bearing nannofossil ooze, light-gray to white (5Y 7/1, 8/1, 7.5YR 8/0); weak to moderate bioturbation; green, black, and purple laminations common throughout core, dipping approximately 10°; microfaulting common; core part of a slump. Minor voids in Section 5, 130–133 cm, and Section 6, 40–44 and 55–57 cm.

SITE 664 HOLE B CORE 11 H CORED INTERVAL 3901.3-3910.8 mbsl; 95.0-104.5

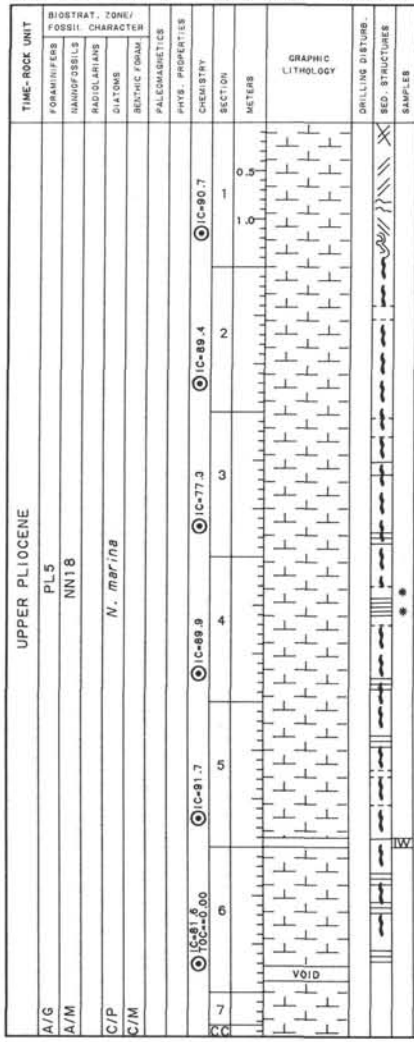

LITHOLOGIC DESCRIPTION

FORAMINIFER-BEARING NANNOFOSSIL OOZE to NANNOFOSSIL OOZE

Foraminifer-bearing nannofossil ooze to nannofossil ooze, white (2.5Y 8/0) to light-gray (10Y 7/1); weak to moderate bioturbation; green, black, and purple laminations common throughout core. Section 1 is part of a slump.

SMEAR SLIDE SUMMARY (%):

	4, 29 D	4, 57 D
TEXTURE:		
Sand	10	10
Silt	15	15
Clay	75	75
COMPOSITION:		
Quartz	Tr	Tr
Clay	5	5
Accessory Minerals	—	Tr
Foraminifers	20	20
Nannofossils	75	70
Diatoms	Tr	—
Radiolarians	Tr	Tr
Sponge spicules	Tr	5

SITE 664 HOLE B CORE 12 H CORED INTERVAL 3910.8-3920.3 mbsl; 104.5-114.0 mbsf

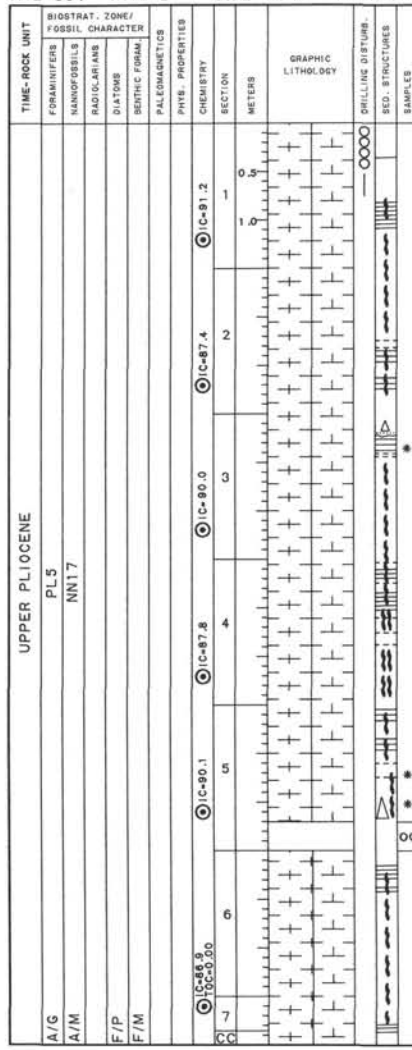

LITHOLOGIC DESCRIPTION

FORAMINIFER-BEARING NANNOFOSSIL OOZE, alternating with FORAMINIFER-NANNOFOSSIL OOZE

Foraminifer-bearing nannofossil ooze, white (2.5YR 8/0) to light-greenish-gray (5GY 7/1), alternating with foraminifer-nannofossil ooze, white (2.5YR 8/0) to light greenish gray (5GY 7/1); weak bioturbation; faint green and black laminations throughout core. Graded bedding and erosional contacts in Section 3, 25 cm, and Section 5, 120 cm.

SMEAR SLIDE SUMMARY (%):

	3, 41 M	5, 80 D	5, 114 D
TEXTURE:			
Sand	5	—	10
Silt	20	20	30
Clay	75	80	50
COMPOSITION:			
Quartz	10	Tr	5
Clay	10	10	—
Foraminifers	10	15	45
Nannofossils	70	80	50
Diatoms	—	Tr	—
Radiolarians	—	5	—

SITE 664 HOLE B CORE 13 H CORED INTERVAL 3920.3-3929.8 mbsl; 114.123.5 mbsf

TIME-ROCK UNIT	FORAMINIFERS	NANNOFOSSILS	RADIOLARIANS	DIATOMS	BENTHIC FORAM	PALEOMAGNETICS	PHYS. PROPERTIES	CHEMISTRY	SECTION	METERS
UPPER PLIOCENE	PL3	NN16		N. marina				IC=89.2	1	0.5, 1.0
								IC=90.4	2	
								IC=90.9, TOC=0.00	3	
								IC=89.5	4	
								IC=93.0	5	
								IC=89.4	6	
									7	
	A/G	A/M		F/P	F/M				CC	

GRAPHIC LITHOLOGY / DRILLING DISTURB. / SED. STRUCTURES / SAMPLES

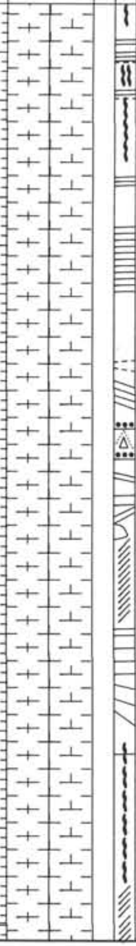

LITHOLOGIC DESCRIPTION

FORAMINIFER-BEARING NANNOFOSSIL OOZE, alternating with FORAMINIFER-NANNOFOSSIL OOZE

Foraminifer-bearing nannofossil ooze, white (2.5YR 8/0) to light-greenish-gray (5GY 7/1), alternating with foraminifer-nannofossil ooze, white (2.5YR 8/0) to light-greenish-gray (5GY 7/1). Sections 3 through 6 have erosional contacts, tilted and contorted beds, and are part of a slump; remainder of core, weak to moderate bioturbation and black pyritic blebs throughout.

SITE 664 HOLE B CORE 14 H CORED INTERVAL 3929.8-3939.3 mbsl; 123.5-133.0 mbsf

TIME-ROCK UNIT	FORAMINIFERS	NANNOFOSSILS	RADIOLARIANS	DIATOMS	BENTHIC FORAM	PALEOMAGNETICS	PHYS. PROPERTIES	CHEMISTRY	SECTION	METERS
UPPER PLIOCENE	PL4	NN16		N. jouseae				IC=94.2	1	0.5, 1.0
								IC=87.7	2	
								IC=90.5	3	
								IC=89.3	4	
								IC=86.9	5	
								IC=81.9, TOC=0.00	6	
	A/G	A/M		C/M	R/M				CC	

GRAPHIC LITHOLOGY / DRILLING DISTURB. / SED. STRUCTURES / SAMPLES

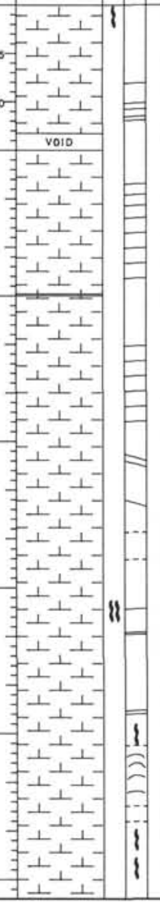

LITHOLOGIC DESCRIPTION

FORAMINIFER-BEARING NANNOFOSSIL OOZE

Foraminifer-bearing nannofossil ooze, white (2.5YR 8/0), with purple and greenish-gray laminations throughout core: weak bioturbation; pyritic burrows common. Minor void in Section 2, 144–150 cm.

SITE 664 HOLE B CORE 15 H CORED INTERVAL 3939.3-3948.8 mbsl; 133.-142.5 mbsf

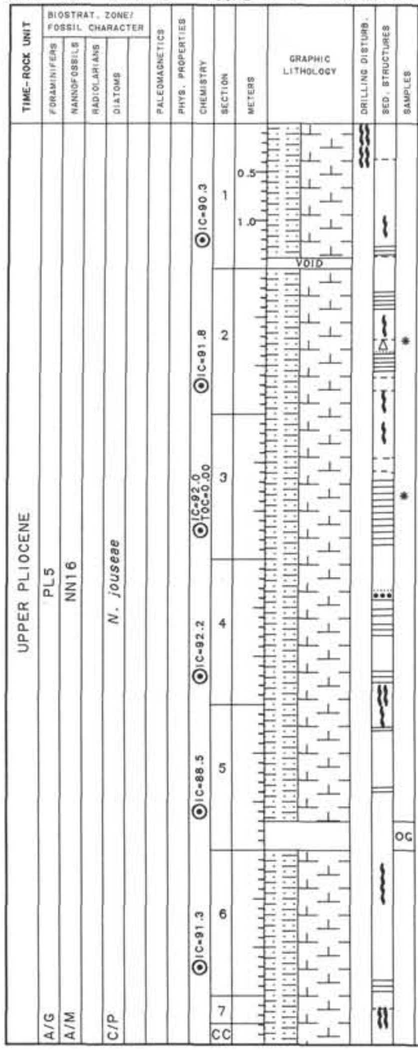

LITHOLOGIC DESCRIPTION

FORAMINIFER-BEARING MUDDY NANNOFOSSIL OOZE

Foraminifer-bearing, muddy nannofossil ooze, white (7.5YR 8/0); weak bioturbation with purple and green laminations throughout. Turbidites in Sections 2 and 4.

SMEAR SLIDE SUMMARY (%):

	2, 85 D	3, 80 D
TEXTURE:		
Sand	20	15
Silt	15	15
Clay	65	70
COMPOSITION:		
Clay	15	25
Accessory Minerals	Tr	—
Foraminifers	15	15
Nannofossils	70	60

SITE 664 HOLE B CORE 16 H CORED INTERVAL 3948.8-3958.3 mbsl; 142.5-152 mbsf

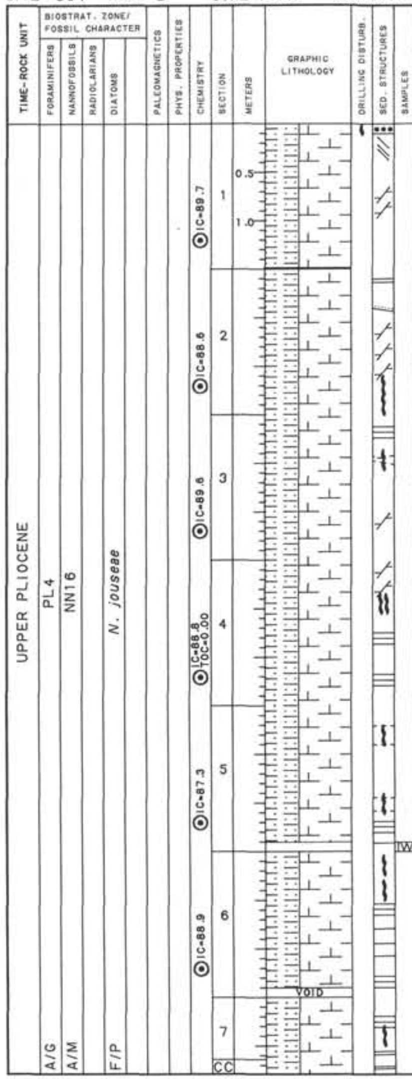

LITHOLOGIC DESCRIPTION

FORAMINIFER-BEARING, MUDDY NANNOFOSSIL OOZE

Foraminifer-bearing, mud-bearing nannofossil ooze, white (7.5YR 8/0); weak bioturbation with green laminations commonly occuring in Section 4 to CC. Sections 1 through 3 have numerous microfaults. Turbidites present at top of Sections 1 and 2. Minor voids in Section 1, 146–150 cm, and Section 6, 140–150 cm.

SITE 664 HOLE B CORE 17 H CORED INTERVAL 3958.3-3967.8 mbsl; 152.0-161.5 mbsf

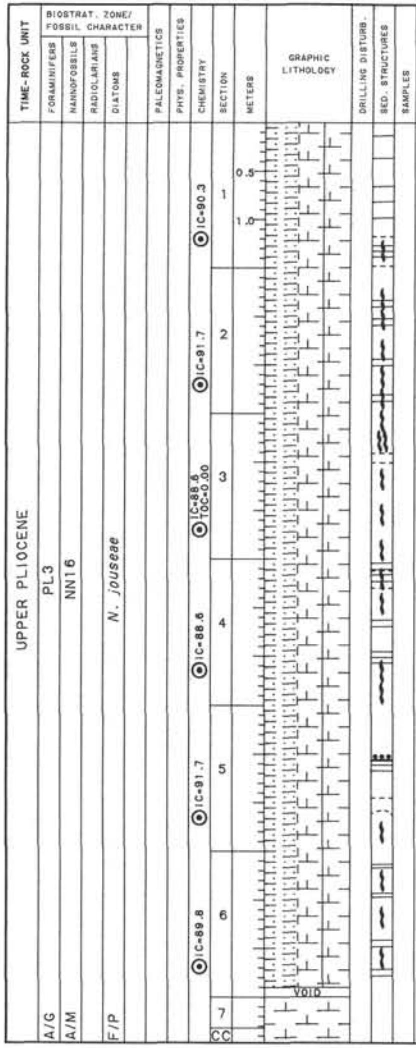

LITHOLOGIC DESCRIPTION

FORAMINIFER-BEARING, MUD-BEARING NANNOFOSSIL OOZE, alternating with CLAY-BEARING, FORAMINIFER-BEARING NANNOFOSSIL OOZE and MUD-BEARING, FORAMINIFER- BEARING NANNOFOSSIL OOZE

Foraminifer-bearing, mud-bearing nannofossil ooze, white (7.5YR 8/0); alternating with clay-bearing, foraminifer-bearing nannofossil ooze, white (5Y 8/1, 7.5Y 8/0), and mud-bearing, foraminifer-bearing nannofossil ooze, white (7.5YR 8/0); weak to moderate bioturbation with green and purple laminations and occasional nodules (manganese?). Minor void in Section 6, 142–150 cm.

SITE 664 HOLE B CORE 18 H CORED INTERVAL 3967.8-3977.3 mbsl; 161.5-171.0 mbsf

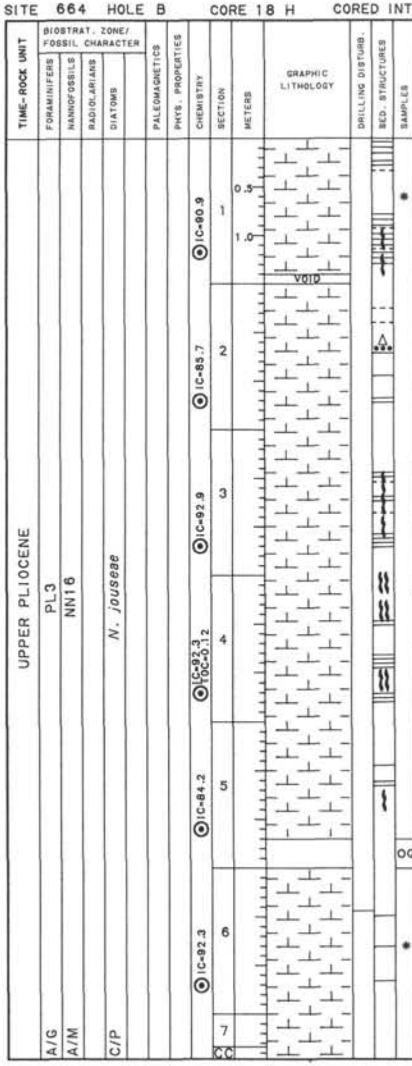

LITHOLOGIC DESCRIPTION

MUD-BEARING, FORAMINIFER-BEARING NANNOFOSSIL OOZE

Mud-bearing, foraminifer-bearing nannofossil ooze, white (7.5YR 8/0); weak to moderate bioturbation with purple and green laminations that dip slightly throughout. Turbidite in Section 2, 70 cm.

SMEAR SLIDE SUMMARY (%):

	1, 60 D	6, 70 D
TEXTURE:		
Sand	15	15
Silt	15	20
Clay	70	65
COMPOSITION:		
Clay	15	10
Accessory Minerals	5	5
Foraminifers	15	20
Nannofossils	60	60
Diatoms	5	—

SITE 664 HOLE B CORE 19 H CORED INTERVAL 3977.3-3986.8 mbsl; 171.0-180.5 mbsf

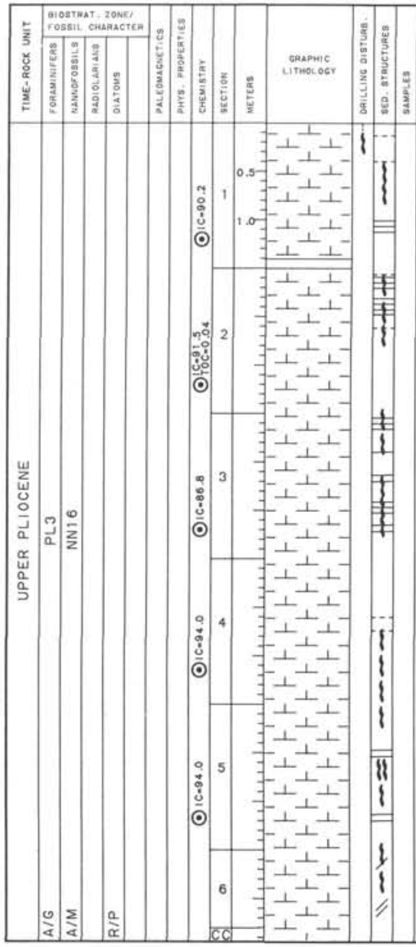

LITHOLOGIC DESCRIPTION

MUD-BEARING, FORAMINIFER-BEARING NANNOFOSSIL OOZE

Mud-bearing, foraminifer-bearing nannofossil ooze, white (7.5YR 8/0); weak bioturbation with occasional purple and green laminations.

SITE 664 HOLE B CORE 20 H CORED INTERVAL 3986.8-3996.3 mbsl; 180.5-190.0 mbsf

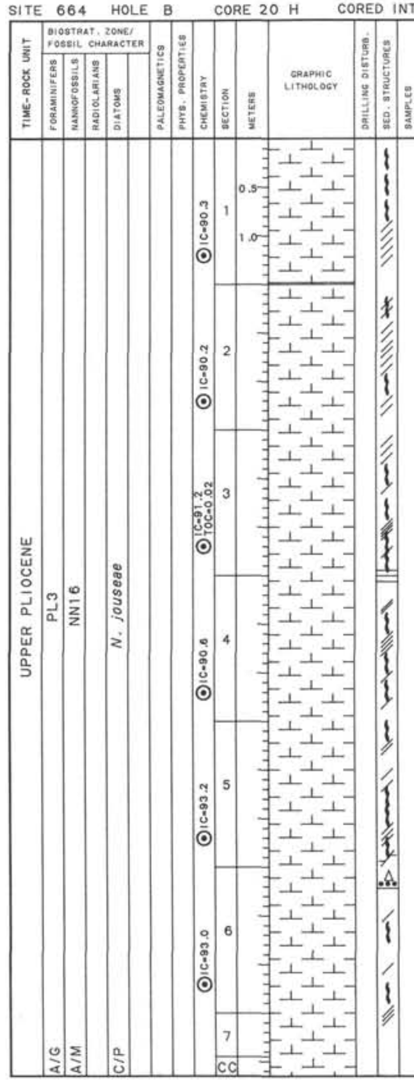

LITHOLOGIC DESCRIPTION

MUD-BEARING, FORAMINIFER-BEARING NANNOFOSSIL OOZE

Mud-bearing, foraminifer-bearing nannofossil ooze, white (7.5YR 8/0); weak bioturbation with purple and green, slightly dipping laminations. Core is part of slump. Minor void in Section 1, 148–150 cm.

SITE 664 HOLE B CORE 21 H CORED INTERVAL 3996.3-4003.8 mbsl; 190.0-199.5 mbsf

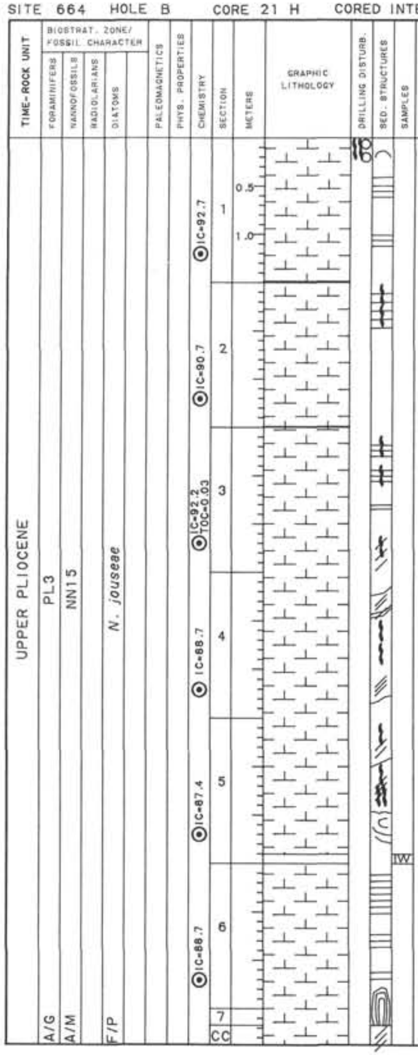

LITHOLOGIC DESCRIPTION

MUD-BEARING, FORAMINIFER-BEARING NANNOFOSSIL OOZE

Mud-bearing, foraminifer-bearing nannofossil ooze, white (7.5YR 8/0); weak bioturbation with occasional purple and green, slightly dipping laminations. Core is part of slump. Minor voids in Section 1, 143–150 cm, and Section 2, 148–150 cm.

SITE 664 HOLE B CORE 22 H CORED INTERVAL 4005.8-4015.3 mbsl; 199.5-209.0 mbsf

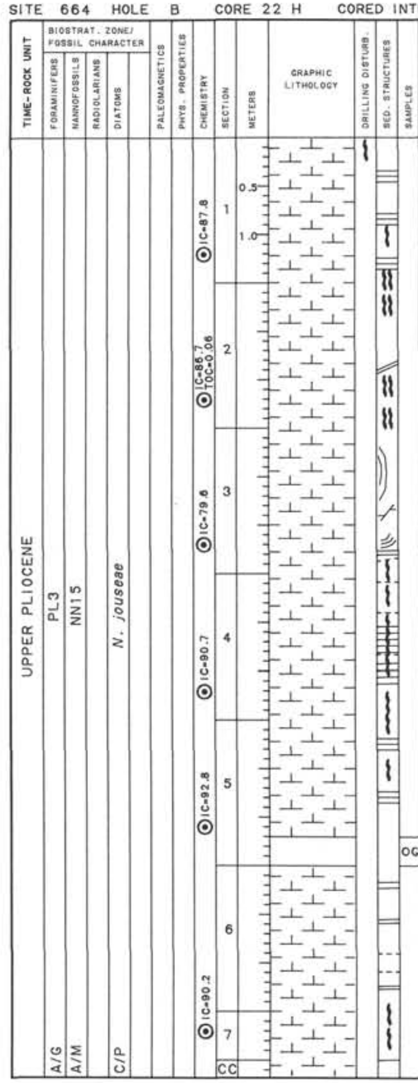

LITHOLOGIC DESCRIPTION

MUD-BEARING, FORAMINIFER-BEARING NANNOFOSSIL OOZE

Mud-bearing, foraminifer-bearing nannofossil ooze, white (7.5YR 8/0); weak bioturbation with occasional purple and green, slightly dipping laminations. Core is part of slump.

SITE 664 HOLE B CORE 23 H CORED INTERVAL 4015.3-4024.8 mbsl; 209.0-218.5 mbsf

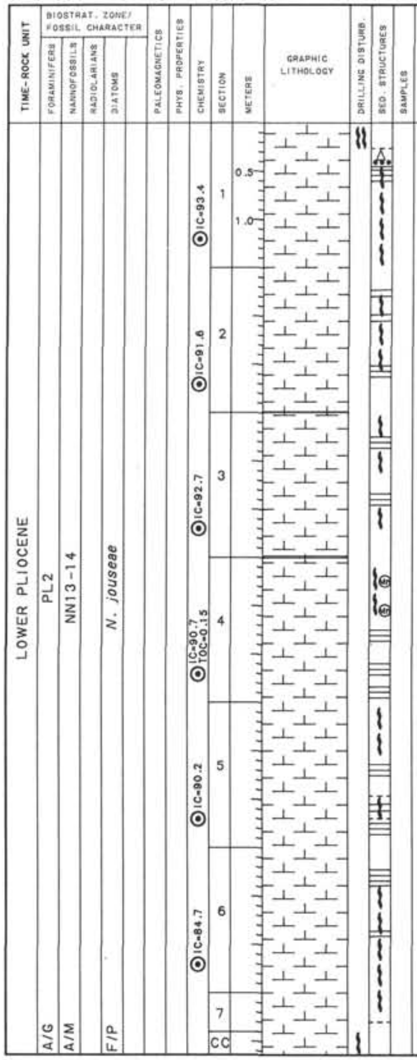

LITHOLOGIC DESCRIPTION

MUD-BEARING, FORAMINIFER-BEARING NANNOFOSSIL OOZE

Mud-bearing, foraminifer-bearing nannofossil ooze, white (7.5YR 8/0); weak bioturbation with occasional purple and green laminations. Turbidite in Section 1, 30 cm. Minor void in Section 2, 148–150 cm, and Section 3, 148–150 cm.

SITE 664 HOLE B CORE 24 H CORED INTERVAL 4024.8-4034.3 mbsl; 218.5-228 mbsf

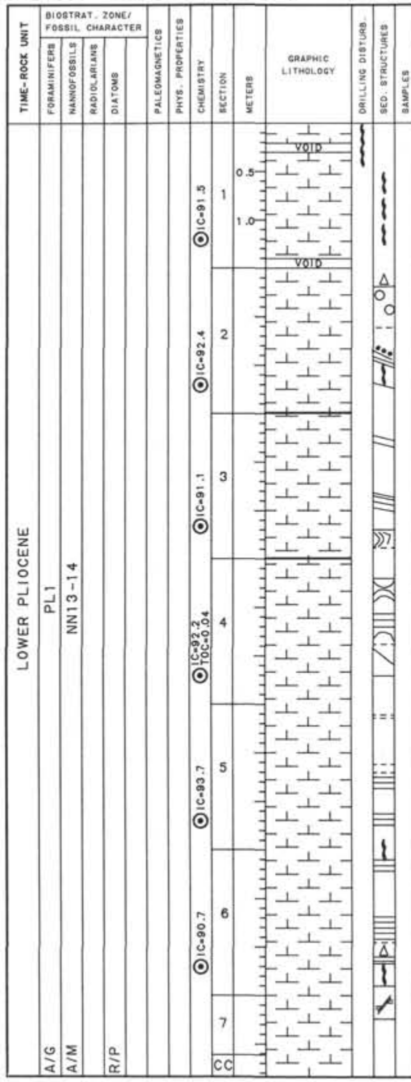

LITHOLOGIC DESCRIPTION

MUD-BEARING, FORAMINIFER-BEARING NANNOFOSSIL OOZE

Mud-bearing, foraminifer-bearing nannofossil ooze, white (7.5YR 8/0); weak bioturbation with occasional purple and green laminations. Turbidite in Section 2, 80 cm. Beds are strongly deformed in Sections 2 through 4. Minor voids in Section 2, 148–150 cm, and Section 3, 147 cm.

SITE 664 HOLE B CORE 25 H CORED INTERVAL 4034.3-4043.8 mbsl; 228-237.5 mbsf

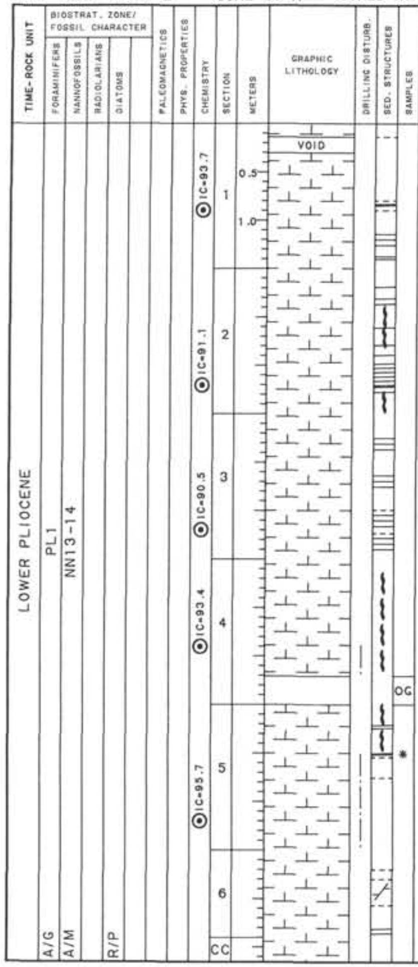

LITHOLOGIC DESCRIPTION

MUD-BEARING, FORAMINIFER-BEARING NANNOFOSSIL OOZE

Mud-bearing, foraminifer-bearing nannofossil ooze, white (7.5YR 8/0); weak bioturbation with occasional purple and green laminations. Microfault occurs in Section 6, 30 cm.

SMEAR SLIDE SUMMARY (%):

	5, 50
	D
TEXTURE:	
Sand	—
Silt	15
Clay	85
COMPOSITION:	
Clay	10
Foraminifers	15
Nannofossils	75

SITE 664 HOLE B CORE 26 H CORED INTERVAL 4043.8-4053.3 mbsl; 237.5-247.0 mbsf

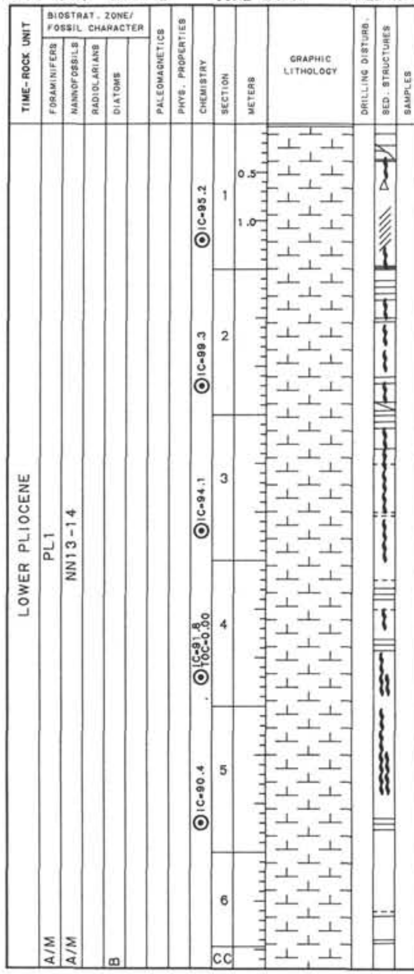

LITHOLOGIC DESCRIPTION

MUD-BEARING, FORAMINIFER-BEARING NANNOFOSSIL OOZE

Mud-bearing, foraminifer-bearing nannofossil ooze, white (7.5YR 8/0); weak bioturbation with occasional purple and green laminations. Microfault occurs in Section 1, 30 cm, and in Section 2, 140 cm. Minor void in Section 1, 0–5 cm.

SITE 664 HOLE C CORE 1 H CORED INTERVAL 3806.8-3811 mbsl; 0-4.2 mbsf

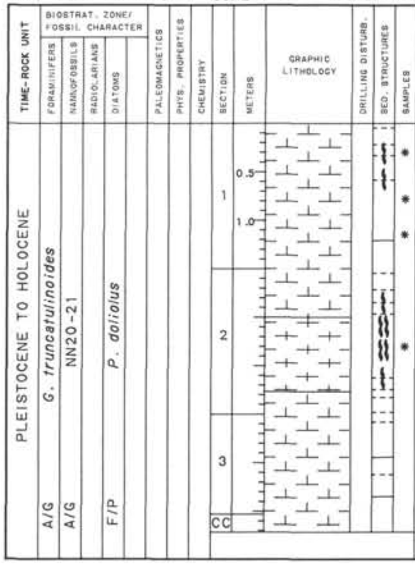

LITHOLOGIC DESCRIPTION

FORAMINIFER-BEARING, SILICEOUS, MUD-BEARING NANNOFOSSIL OOZE to CLAY-BEARING, FORAMINIFER-BEARING NANNOFOSSIL OOZE to FORAMINIFER-BEARING NANNOFOSSIL OOZE and FORAMINIFER-NANNOFOSSIL OOZE

Foraminifer-bearing, siliceous, mud-bearing nannofossil ooze, pale-brown (10YR 6/3) or light-yellowish-brown, to clay-bearing, foraminifer-bearing nannofossil ooze, olive-gray (10Y 5/2) or gray (10Y 5/1), to foraminifer-bearing nannofossil ooze, gray (5Y 5/1) or light-gray (5Y 7/1), and foraminifer-nannofossil ooze, light-gray (10Y 7/1), mottled with (10Y 6/1, 5/1); weak to moderate bioturbation.

SMEAR SLIDE SUMMARY (%):

	1, 28 D	1, 80 D	1, 131 D	2, 91 D
TEXTURE:				
Sand	5	5	5	10
Silt	30	20	20	20
Clay	65	75	75	70
COMPOSITION:				
Quartz	5	Tr	Tr	Tr
Clay	10	10	5	—
Accessory Minerals	Tr	Tr	—	—
Foraminifers	10	15	20	30
Nannofossils	65	70	70	70
Diatoms				
Radiolarians	10	5	5	Tr
Sponge Spicules				

SITE 664 HOLE C CORE 2 H CORED INTERVAL 3811.0-3820.5 mbsl; 4.2-13.7 mbsf

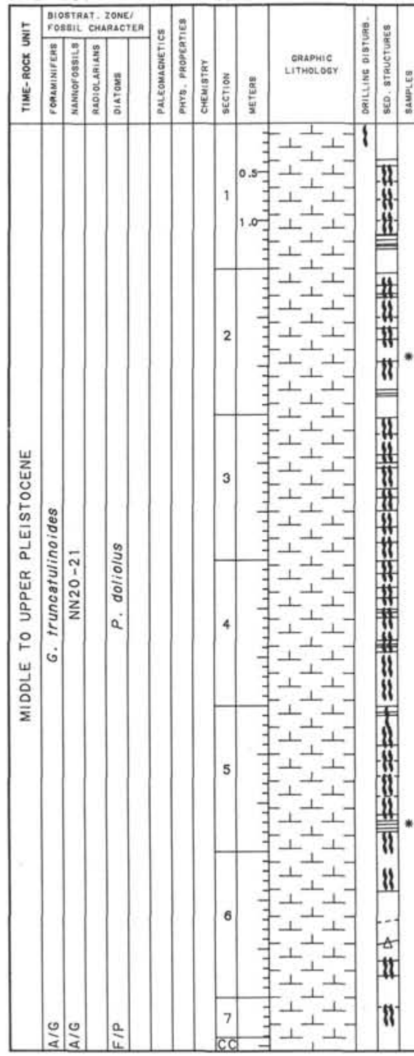

LITHOLOGIC DESCRIPTION

FORAMINIFER-BEARING, CLAY-BEARING, NANNOFOSSIL OOZE to FORAMINIFER-BEARING NANNOFOSSIL OOZE

Foraminifer-bearing, clay-bearing, nannofossil ooze to foraminifer-bearing nannofossil ooze, gray (5Y 5/1,6/1), light-gray (5Y 7/1), or light-olive-gray (5Y 6/2); moderate to heavy bioturbation with occasional purple and green laminations.

SMEAR SLIDE SUMMARY (%):

	2, 95 D	5, 129 D
TEXTURE:		
Sand	5	—
Silt	15	15
Clay	80	85
COMPOSITION:		
Quartz	2	3
Clay	3	15
Accessory Minerals	Tr	—
Foraminifers	20	10
Nannofossils	75	72
Diatoms	Tr	Tr
Radiolarians	Tr	Tr
Sponge spicules	Tr	Tr

SITE 664 HOLE C CORE 3 H CORED INTERVAL 3820.5-3830.0 mbsl; 13.7-23.2 mbsf

TIME-ROCK UNIT	FORAMINIFERS	NANNOFOSSILS	RADIOLARIANS	DIATOMS	PALEOMAGNETICS	PHYS. PROPERTIES	CHEMISTRY	SECTION	METERS	GRAPHIC LITHOLOGY	DRILLING DISTURB.	SED. STRUCTURES	SAMPLES	LITHOLOGIC DESCRIPTION
MIDDLE PLEISTOCENE	*G. truncatulinoides*	NN20-21 / NN19		*N. reinholdii*				1, 2, 3, 4, 5, 6, CC	0.5, 1.0					FORAMINIFER-NANNOFOSSIL OOZE, alternating with CLAY-BEARING, FORAMINIFER-BEARING NANNOFOSSIL OOZE Foraminifer-nannofossil ooze, white (5Y 8/1), alternating with clay-bearing, foraminifer-bearing nannofossil ooze, gray (5Y 6/1), light-gray (5Y 7/1), or olive-gray (5Y 5/2); weak to moderate bioturbation with occasional purple laminations.
	A/M	A/G		F/P										

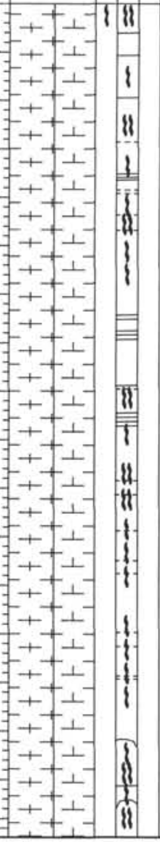

SITE 664 HOLE C CORE 4 H CORED INTERVAL 3830.0-3839.5 mbsl; 23.2-32.7 mbsf

TIME-ROCK UNIT	FORAMINIFERS	NANNOFOSSILS	RADIOLARIANS	DIATOMS	PALEOMAGNETICS	PHYS. PROPERTIES	CHEMISTRY	SECTION	METERS	GRAPHIC LITHOLOGY	DRILLING DISTURB.	SED. STRUCTURES	SAMPLES	LITHOLOGIC DESCRIPTION
MIDDLE PLEISTOCENE	*G. truncatulinoides*	NN19		*N. reinholdii*				1, 2, 3, 4, 5, 6, CC	0.5, 1.0					CLAY-BEARING, FORAMINIFER-BEARING NANNOFOSSIL OOZE to FORAMINIFER-BEARING NANNOFOSSIL OOZE Clay-bearing, foraminifer-bearing nannofossil ooze to foraminifer-bearing nannofossil ooze, light-gray (5Y 7/1), gray (5Y 6/1, 5/1), or white (5Y 8/1); weak to moderate bioturbation with occasional purple and black laminations. Turbidites in Section 1, 70 cm, and Section 5, 100 cm. Minor voids in Section 1, 0–7 and 145–150 cm.
	A/G	A/G		C/M										

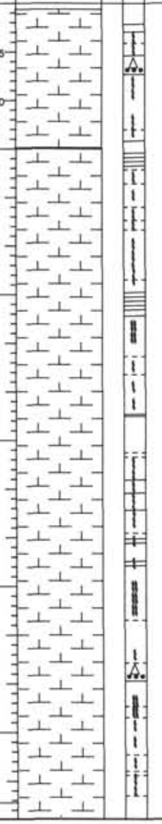

SITE 664 HOLE C CORE 5 H CORED INTERVAL 3839.5-3849.0 mbsl; 32.7-42.2 mbsf

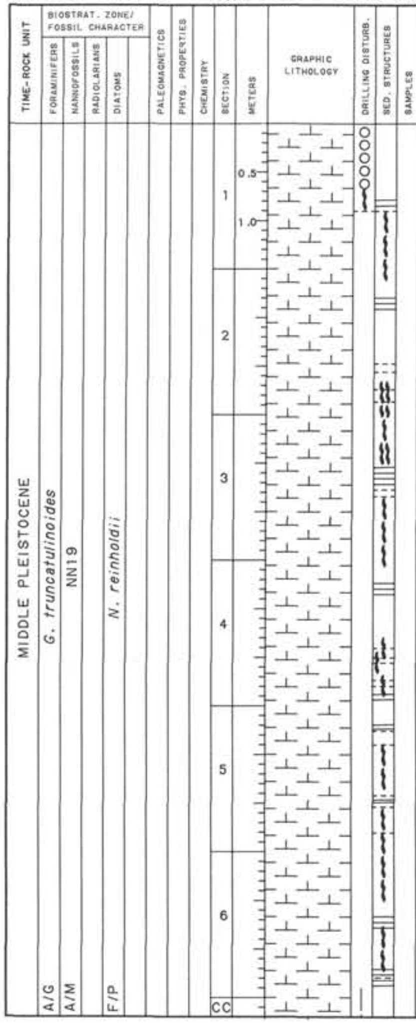

LITHOLOGIC DESCRIPTION

CLAY-BEARING, FORAMINIFER-BEARING NANNOFOSSIL OOZE to FORAMINIFER-BEARING, CLAY-BEARING NANNOFOSSIL OOZE

Clay-bearing, foraminifer-bearing nannofossil ooze to foraminifer-bearing, clay-bearing nannofossil ooze, light-gray (5Y 7/1), gray (5Y 6/1, 5/1), or white (5Y 8/1, 7.5YR 8/0); weak to moderate bioturbation with occasional purple and black laminations.

SITE 664 HOLE C CORE 6 H CORED INTERVAL 3849.0-3858.5 mbsl; 42.2-51.7 mbsf

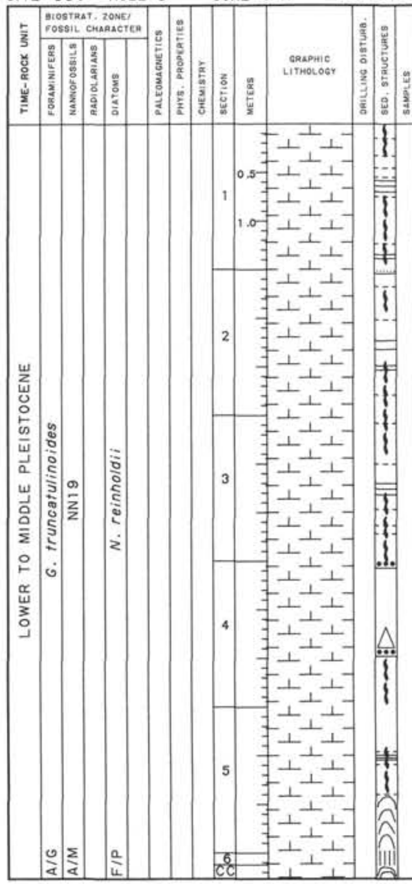

LITHOLOGIC DESCRIPTION

CLAY-BEARING, FORAMINIFER-BEARING NANNOFOSSIL OOZE to FORAMINIFER-BEARING NANNOFOSSIL OOZE

Clay-bearing, foraminifer-bearing nannofossil ooze to foraminifer-bearing nannofossil ooze, light-gray (5Y 7/1), gray (5Y 6/1, 5/1), or white (5Y 8/1); weak to moderate bioturbation with occasional purple and black laminations. Turbidites in Section 2, 5 cm, and Section 4, 10 and 97 cm. Section 5, 90 cm, to CC, is a slump.

SITE 664 HOLE C CORE 7 H CORED INTERVAL 3858.5-3868.0 mbsl; 51.7-61.2 mbsf

TIME-ROCK UNIT	FORAMINIFERS	NANNOFOSSILS	RADIOLARIANS	DIATOMS	PALEOMAGNETICS	PHYS. PROPERTIES	CHEMISTRY	SECTION	METERS	GRAPHIC LITHOLOGY	DRILLING DISTURB.	SED. STRUCTURES	SAMPLES	LITHOLOGIC DESCRIPTION
LOWER TO MIDDLE PLEISTOCENE	PL5	NN19		*N. reinholdii*				1, 2, 3, 4, 5, 6, 7, CC	0.5, 1.0	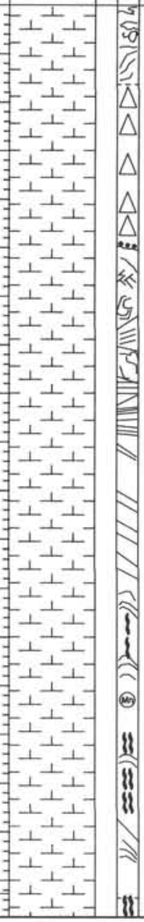				CLAY-BEARING, FORAMINIFER-BEARING NANNOFOSSIL OOZE to FORAMINIFER-BEARING NANNOFOSSIL OOZE Clay-bearing, foraminifer-bearing nannofossil ooze to foraminifer-bearing nannofossil ooze, light-gray (5Y 7/1), gray (5Y 6/1, 5/1), or white (5Y 8/1); beds are folded, contorted, and stretched. Internal shear planes common throughout slumped sections. Large turbidite between Section 1, 86 cm, and Section 2, 110 cm.
	A/G	A/M		F/P										

BIOSTRAT. ZONE/ FOSSIL CHARACTER

SITE 664 HOLE D CORE 1 H CORED INTERVAL 3801.7-3804.0 mbsl; 0-2.3 mbsf

TIME-ROCK UNIT	FORAMINIFERS	NANNOFOSSILS	RADIOLARIANS	DIATOMS	PALEOMAGNETICS	PHYS. PROPERTIES	CHEMISTRY	SECTION	METERS	GRAPHIC LITHOLOGY	DRILLING DISTURB.	SED. STRUCTURES	SAMPLES	LITHOLOGIC DESCRIPTION
PLEISTOCENE TO HOLOCENE	A/G *G. truncatulinoides*	A/G NN20-21		C/P *P. doliolus*				1, 2, CC	0.5, 1.0				* * *	see below

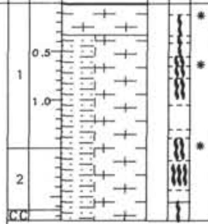

MUDDY FORAMINIFER-NANNOFOSSIL OOZE

Muddy foraminifer-nannofossil ooze, gray (5Y 6/1, 5/1) or light-gray (5Y 7/1); moderate to heavy bioturbation. Minor void in Section 1, 0–4 cm.

Minor lithology: Section 1, 4–32 cm: mud-bearing foraminifer-nannofossil ooze, light-gray (5Y 7/2); weak to moderate bioturbation.

SMEAR SLIDE SUMMARY (%):

	1, 20 M	1, 62 M	2, 3 D
TEXTURE:			
Sand	20	10	20
Silt	25	30	30
Clay	55	60	50
COMPOSITION:			
Quartz	5	10	5
Clay	10	15	20
Foraminifers	40	30	25
Nannofossils	45	45	45
Diatoms	Tr	Tr	
Radiolarians	Tr	Tr	5
Sponge spicules			

SITE 664 HOLE D CORE 2 H CORED INTERVAL 3804.0-3813.5 mbsl; 2.3-11.8 mbsf

TIME-ROCK UNIT	FORAMINIFERS	NANNOFOSSILS	RADIOLARIANS	DIATOMS	PALEOMAGNETICS	PHYS. PROPERTIES	CHEMISTRY	SECTION	METERS	GRAPHIC LITHOLOGY	DRILLING DISTURB.	SED. STRUCTURES	SAMPLES	LITHOLOGIC DESCRIPTION
MIDDLE TO UPPER PLEISTOCENE	*G. truncatulinoides* A/G	NN20-21 A/G		R/P				1, 2, 3, 4, 5, 6, 7, CC	0.5, 1.0					see below

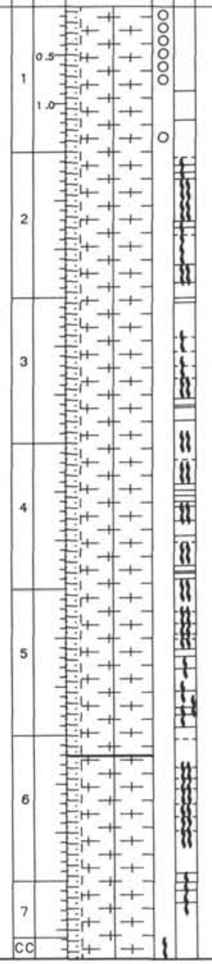

MUD-BEARING FORAMINIFER-NANNOFOSSIL OOZE, alternating with MUDDY FORAMINIFER-NANNOFOSSIL OOZE

Mud-bearing foraminifer-nannofossil ooze, white (5Y 8/1) or light-gray (5Y 7/1), alternating with muddy foraminifer-nannofossil ooze, gray (5Y 6/1, 5/1); moderate to heavy bioturbation with occasional purple and black laminations. Minor void in Section 6, 19–23 cm.

SITE 664 HOLE D CORE 3 H CORED INTERVAL 3813.5-3823.0 mbsl; 11.8-21.3 mbsf

TIME-ROCK UNIT	FORAMINIFERS	NANNOFOSSILS	RADIOLARIANS	DIATOMS	PALEOMAGNETICS	PHYS. PROPERTIES	CHEMISTRY	SECTION	METERS	GRAPHIC LITHOLOGY	DRILLING DISTURB.	SED. STRUCTURES	SAMPLES
MIDDLE PLEISTOCENE	*G.. truncatulinoides* A/G	NN19 A/G		*N. reinholdii* R/P				1, 2, 3, 4, 5, 6, 7, CC	0.5, 1.0				

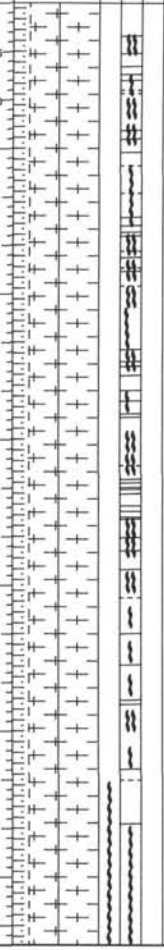

LITHOLOGIC DESCRIPTION

MUD-BEARING FORAMINIFER-NANNOFOSSIL OOZE and MUDDY FORAMINIFER-NANNOFOSSIL OOZE

Mud-bearing foraminifer-nannofossil ooze, white (5Y 8/1) or light-gray (5Y 7/1), alternating with muddy foraminifer-nannofossil ooze, gray (5Y 6/1, 5/1); moderate to heavy bioturbation with occasional purple and black laminations.

SITE 664 HOLE D CORE 4 H CORED INTERVAL 3823.0-3832.5 mbsl; 21.3-30.8 mbsf

TIME-ROCK UNIT	FORAMINIFERS	NANNOFOSSILS	RADIOLARIANS	DIATOMS	PALEOMAGNETICS	PHYS. PROPERTIES	CHEMISTRY	SECTION	METERS	GRAPHIC LITHOLOGY	DRILLING DISTURB.	SED. STRUCTURES	SAMPLES
MIDDLE PLEISTOCENE	*G. truncatulinoides* A/G	NN19 A/G		*N. reinholdii* R/P				1, 2, 3, 4, 5, 6, 7, CC	0.5, 1.0				

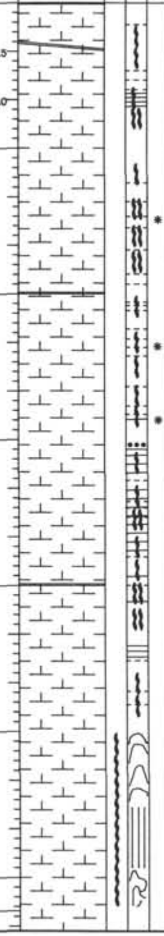

LITHOLOGIC DESCRIPTION

CLAY-BEARING, SILICEOUS-BEARING, FORAMINIFER-BEARING NANNOFOSSIL OOZE

Clay-bearing, siliceous-bearing, foraminifer-bearing nannofossil ooze, dark-gray (10Y 4/1), to foraminifer-bearing nannofossil ooze, white (2.5Y 8/0); moderate to heavy bioturbation with occasional purple and black laminations. Flow-in from Section 6 through CC. Minor voids in Section 1, 0–2 and 41–43 cm, and Section 2, 146–150 cm.

SMEAR SLIDE SUMMARY (%):

	2, 70 M	3, 56 D	5, 98 D
TEXTURE:			
Sand	5	10	5
Silt	15	30	25
Clay	80	60	70
COMPOSITION:			
Clay	10	10	—
Volcanic Glass	Tr	—	—
Accessory Minerals	Tr	Tr	—
Foraminifers	15	25	10
Nannofossils	75	70	70
Diatoms	Tr		
Radiolarians	Tr	5	10
Sponge spicules			

SITE 664 HOLE D CORE 5 H CORED INTERVAL 3832.5-3842.0 mbsl; 30.8-40.3 mbsf

TIME-ROCK UNIT	FORAMINIFERS	NANNOFOSSILS	RADIOLARIANS	DIATOMS	PALEOMAGNETICS	PHYS. PROPERTIES	CHEMISTRY	SECTION	METERS	GRAPHIC LITHOLOGY	DRILLING DISTURB.	SED. STRUCTURES	SAMPLES
LOWER TO MIDDLE PLEISTOCENE	*G. truncatulinoides* A/G	NN19 A/M		*N. reinholdii* F/P				1, 2, 3, 4, 5, 6, 7, CC	0.5, 1.0				*

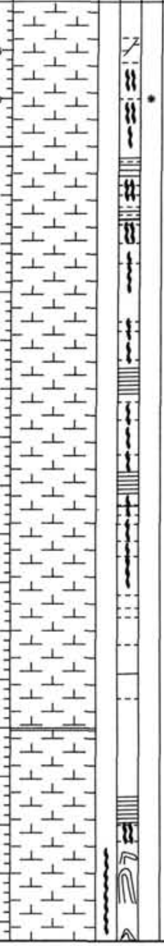

LITHOLOGIC DESCRIPTION

MUD-BEARING, SILICEOUS-BEARING, FORAMINIFER-BEARING NANNOFOSSIL OOZE

Mud-bearing, siliceous-bearing, foraminifer-bearing nannofossil ooze, light-gray (5Y 7/1), gray (5Y 6/1, 5/1), or white (10Y 8/0); moderately bioturbated with gray, greenish-purple, or black laminations throughout core. Flow-in from Section 6, 120 cm, through CC. Minor void in Section 6, 0–2 cm.

SMEAR SLIDE SUMMARY (%):

	1, 78 D
TEXTURE:	
Sand	10
Silt	20
Clay	70
COMPOSITION:	
Quartz	5
Clay	5
Foraminifers	15
Nannofossils	65
Diatoms	Tr
Radiolarians	5
Sponge spicules	5

SITE 664 HOLE D CORE 6 H CORED INTERVAL 3842.0-3851.1 mbsl; 40.3-49.8 mbsf

TIME-ROCK UNIT	FORAMINIFERS	NANNOFOSSILS	RADIOLARIANS	DIATOMS	PALEOMAGNETICS	PHYS. PROPERTIES	CHEMISTRY	SECTION	METERS	GRAPHIC LITHOLOGY	DRILLING DISTURB.	SED. STRUCTURES	SAMPLES
LOWER PLEISTOCENE	*G. truncatulinoides* A/G	NN19 A/M		*N. reinholdii* C/P				1, 2, 3, 4, 5, 6, 7, CC	0.5, 1.0				

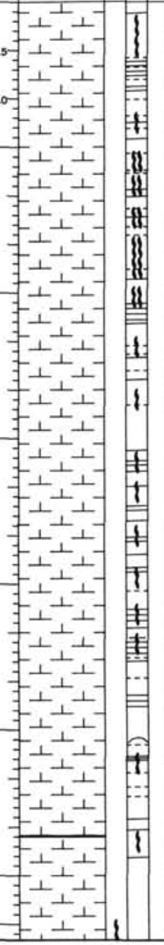

LITHOLOGIC DESCRIPTION

MUD-BEARING, SILICEOUS-BEARING, FORAMINIFER-BEARING NANNOFOSSIL OOZE

Mud-bearing, siliceous-bearing, foraminifer-bearing nannofossil ooze, light-gray (5Y 7/1), gray (5Y 6/1, 5/1), to white (10Y 8/0); moderately bioturbated with gray, greenish-purple, or black laminations throughout core. Flow-in from Section 6, 120 cm, through CC. Minor void in Section 6, 107–110 cm.

SITE 664 HOLE D CORE 7 H CORED INTERVAL 3851.5-3861.0 mbsl; 49.8-59.3 mbsf

TIME-ROCK UNIT: LOWER PLEISTOCENE

BIOSTRAT. ZONE/FOSSIL CHARACTER: FORAMINIFERS: *G. truncatulinoides* A/G; NANNOFOSSILS: NN19 A/M; RADIOLARIANS; DIATOMS: *N. reinholdii* C/P

PALEOMAGNETICS | PHYS. PROPERTIES | CHEMISTRY | SECTION: 1, 2, 3, 4, 5, 6, 7, CC | METERS: 0.5, 1.0

GRAPHIC LITHOLOGY | DRILLING DISTURB. | SED. STRUCTURES | SAMPLES

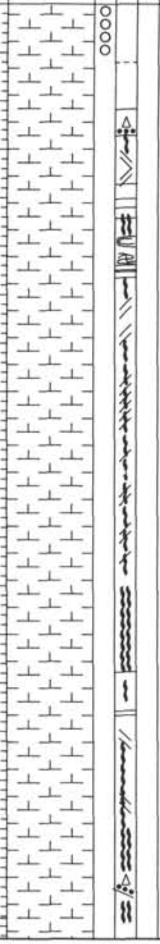

LITHOLOGIC DESCRIPTION

MUD-BEARING, SILICEOUS-BEARING, FORAMINIFER-BEARING NANNOFOSSIL OOZE

Mud-bearing, siliceous-bearing, foraminifer-bearing nannofossil ooze, light-gray (5Y 7/1), gray (5Y 6/1, 5/1), or white (10Y 8/0); moderately bioturbated with gray, greenish-purple, or black laminations throughout core. Sections 2 through 7 have dipping and folded beds; part of a slump.

SITE 664 HOLE D CORE 8 H CORED INTERVAL 3861.0-3870.5 mbsl; 59.3-68.8 mbsf

TIME-ROCK UNIT: UPPER PLIOCENE TO LOWER PLEISTOCENE

BIOSTRAT. ZONE/FOSSIL CHARACTER: FORAMINIFERS: *G. truncatulinoides* A/G; NANNOFOSSILS: NN19 A/M; RADIOLARIANS; DIATOMS: *N. reinholdii* C/P

PALEOMAGNETICS | PHYS. PROPERTIES | CHEMISTRY | SECTION: 1, 2, 3, 4, 5, 6, 7, CC | METERS: 0.5, 1.0

GRAPHIC LITHOLOGY | DRILLING DISTURB. | SED. STRUCTURES | SAMPLES

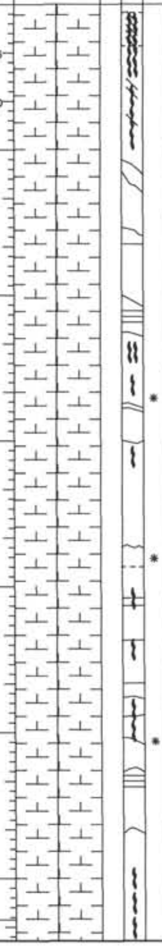

LITHOLOGIC DESCRIPTION

FORAMINIFER-NANNOFOSSIL OOZE, alternating with MUD-BEARING, FORAMINIFER-BEARING NANNOFOSSIL OOZE and CLAY-BEARING, FORAMINIFER-BEARING NANNOFOSSIL OOZE

Foraminifer-nannofossil ooze, white (2.5Y 8/0), alternating with mud-bearing, foraminifer-bearing nannofossil ooze and clay-bearing, foraminifer-bearing nannofossil ooze, greenish-gray (5GY 5/1) to gray (10Y 6/2); weakly bioturbated with occasional purple and green, slightly dipping laminations; probably part of a slump.

SMEAR SLIDE SUMMARY (%):

	3, 112 D	4, 126 D	6, 7 D
TEXTURE:			
Sand	15	10	5
Silt	30	25	10
Clay	55	65	85
COMPOSITION:			
Quartz	—	2	Tr
Clay	—	10	10
Accessory Minerals	—	Tr	—
Foraminifers	30	23	10
Nannofossils	70	65	75
Diatoms	Tr	Tr	
Radiolarians	Tr	Tr	5
Sponge spicules	Tr	Tr	

SITE 664 HOLE D CORE 9 H CORED INTERVAL 3870.5-3880.0 mbsl; 68.8-78.3 mbsf

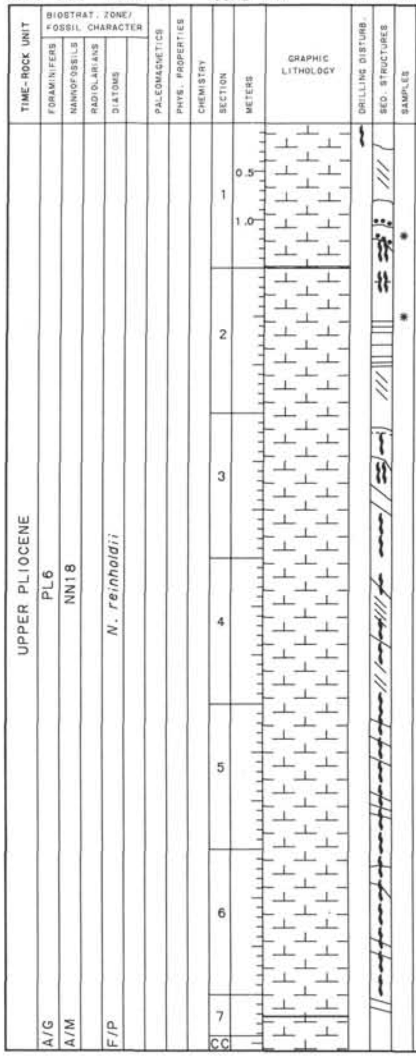

LITHOLOGIC DESCRIPTION

CLAY-BEARING, FORAMINIFER-BEARING NANNOFOSSIL OOZE

Clay-bearing, foraminifer-bearing nannofossil ooze, white (5Y 8/1), light-olive-gray (5Y 6/2), or light-gray (5Y 7/1); weakly bioturbated; green laminations common throughout; bedding planes and laminations slightly dipping; core probably part of a slump. Two turbidites in Section 1. Minor voids in Section 1, 148–150 cm, and Section 7, 25–30 cm.

SMEAR SLIDE SUMMARY (%):

	1, 130 D	2, 70 D
TEXTURE:		
Sand	15	10
Silt	10	15
Clay	75	75
COMPOSITION:		
Clay	15	20
Accessory Minerals	Tr	Tr
Foraminifers	10	10
Nannofossils	70	70
Diatoms	Tr	Tr
Radiolarians	5	Tr

SITE 664 HOLE D CORE 10 H CORED INTERVAL 3880.0-3889.5 mbsl; 78.3-87.8 mbsf

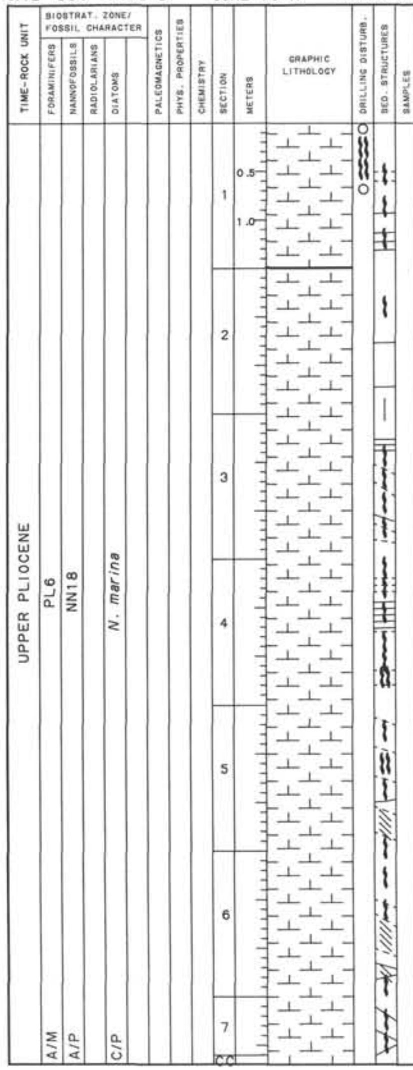

LITHOLOGIC DESCRIPTION

CLAY-BEARING, FORAMINIFER-BEARING NANNOFOSSIL OOZE

Clay-bearing, foraminifer-bearing nannofossil ooze, white (7.5Y 8/0) or light-gray (5Y 7/1); weakly bioturbated; purple (N 7) laminations common; bedding planes and laminations slightly dipping; core part of a slump. Minor void in Section 1, 146–150 cm.

SITE 664 HOLE D CORE 11 H CORED INTERVAL 3889.5-3899.0 mbsl; 87.8-97.3 mbsf

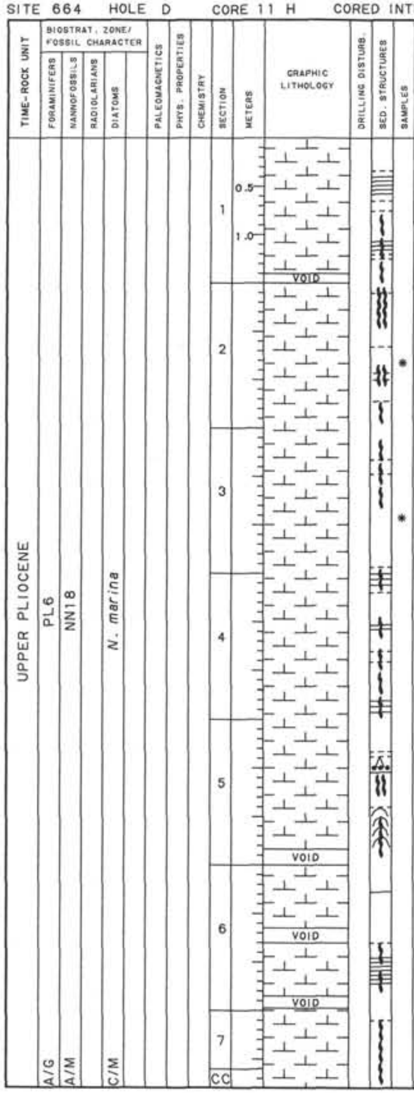

LITHOLOGIC DESCRIPTION

CLAY-BEARING, FORAMINIFER-BEARING NANNOFOSSIL OOZE

Clay-bearing, foraminifer-bearing nannofossil ooze, white (5Y 8/1, 7.5Y 8/0), light-olive-gray (5Y 6/2), or light-gray (5Y 7/1); bioturbation weak to moderate; purple (N 7) laminations common. Turbidite in Section 5, 50 cm. Minor void in Section 1, 147–150 cm.

SMEAR SLIDE SUMMARY (%):

	2, 80 D	3, 90 D
TEXTURE:		
Sand	20	25
Silt	15	15
Clay	65	60
COMPOSITION:		
Clay	20	20
Accessory Minerals	Tr	Tr
Foraminifers	20	20
Nannofossils	60	60

SITE 664 HOLE D CORE 12 H CORED INTERVAL 3899.0-3908.5 mbsl; 97.3-106.8 mbsf

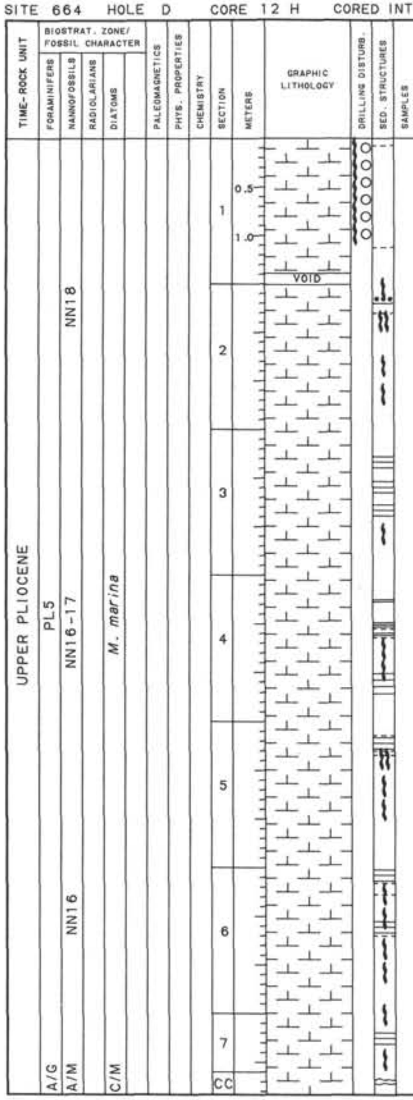

LITHOLOGIC DESCRIPTION

CLAY-BEARING, FORAMINIFER-BEARING NANNOFOSSIL OOZE

Clay-bearing, foraminifer-bearing nannofossil ooze, white (5Y 8/1), light-olive-gray (5Y 6/2), or light-gray (5Y 7/1); bioturbation relatively weak; well-defined, horizontal green and purple laminations common. Turbidite in Section 2, 20 cm.

SITE 664 HOLE D CORE 13 H CORED INTERVAL 3908.5-3918.0 mbsl; 106.8-116.3 mbsf

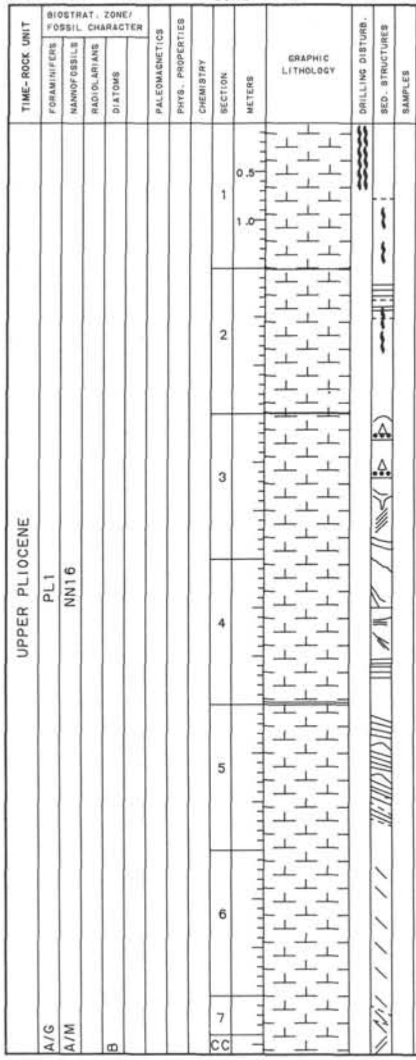

LITHOLOGIC DESCRIPTION

CLAY-BEARING, FORAMINIFER-BEARING NANNOFOSSIL OOZE

Clay-bearing, foraminifer-bearing nannofossil ooze, white (5Y 8/1, 7.5Y 8/0) or light-gray (5Y 7/1); weakly bioturbated with occasional green and purple laminations. Below Section 2 bedding planes and laminations generally dip or contort. Several shear planes in Section 4. Two turbidites in Section 3; one at 10–25 cm, and one at 25–60 cm. Minor voids in Section 1, 146–150 cm; Section 2, 146–150 cm, and Section 4, 146–150 cm.

SITE 664 HOLE D CORE 14 H CORED INTERVAL 3918.0-3927.5 mbsl; 116.3-125.8 mbsf

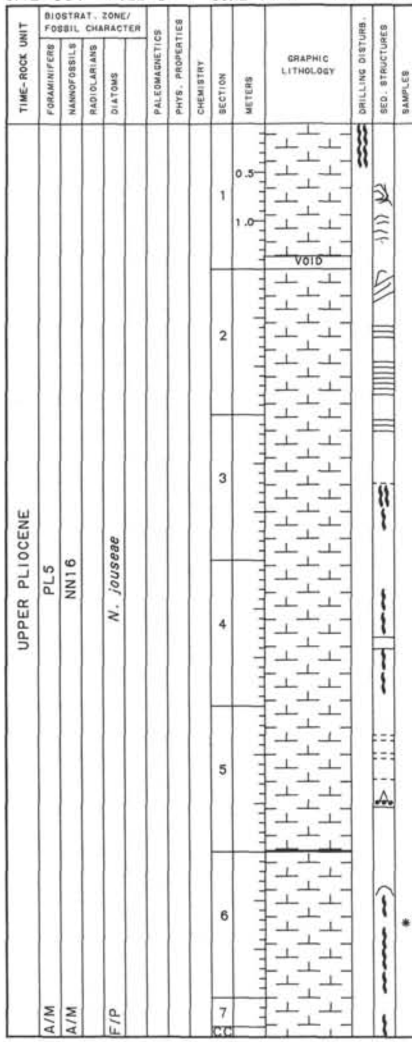

LITHOLOGIC DESCRIPTION

CLAY-BEARING, FORAMINIFER-BEARING, DIATOM-BEARING NANNOFOSSIL OOZE

Clay-bearing, foraminifer-bearing, diatom-bearing nannofossil ooze, white (5Y 8/1, 7.5Y 8/0) or gray (5Y 6/1); Section 1, 0–150 cm, and Section 2, 0–75 cm, weakly bioturbated; laminations common. Bedding planes and laminations dip or fold. Section 2, 75 cm, through CC, weakly to moderately bioturbated; laminations and bedding planes horizontal. Turbidites in Section 4, 85 cm, and Section 5, 105 cm. Minor void in Section 5, 147–150 cm.

SMEAR SLIDE SUMMARY (%):

	3, 70 D	6, 70 D
TEXTURE:		
Sand	5	15
Silt	15	15
Clay	80	70
COMPOSITION:		
Quartz	—	Tr
Clay	15	10
Accessory Minerals	5	Tr
Foraminifers	10	20
Nannofossils	70	60
Diatoms	5	10

SITE 664 HOLE D CORE 15 H CORED INTERVAL 3927.5-3937.0 mbsl; 125.8-135.3 mbsf

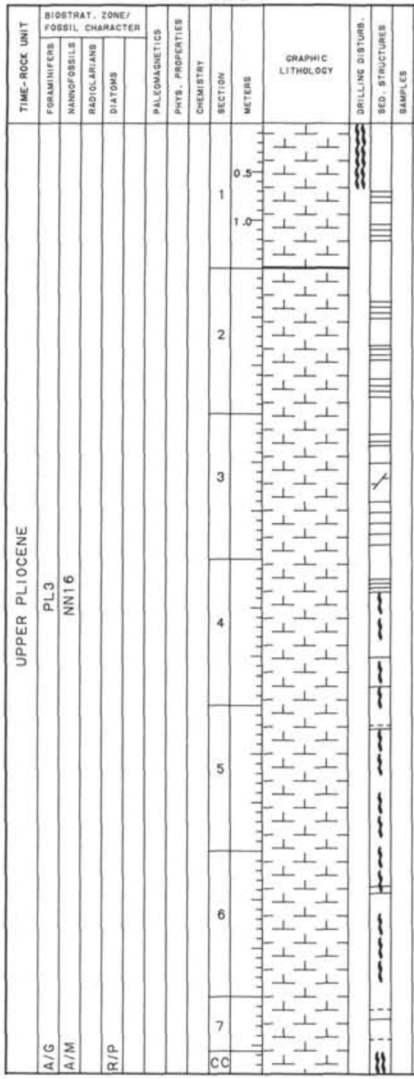

LITHOLOGIC DESCRIPTION

CLAY-BEARING, FORAMINIFER-BEARING, DIATOM-BEARING NANNOFOSSIL OOZE

Clay-bearing, foraminifer-bearing, diatom-bearing nannofossil ooze, white (7.5Y 8/0); purple and green laminations common in Sections 1 through 3. Section 4 through CC, weak to moderate bioturbation with occasional laminations. Minor void in Section 1, 145–150 cm.

SITE 664 HOLE D CORE 16 H CORED INTERVAL 3937.0-3946.5 mbsl; 135.3-144.8 mbsf

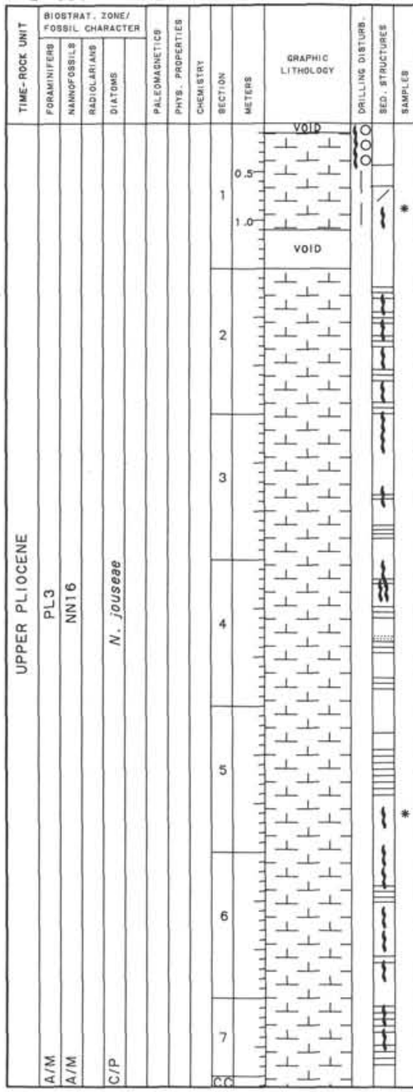

LITHOLOGIC DESCRIPTION

CLAY-BEARING, FORAMINIFER-BEARING NANNOFOSSIL OOZE

Clay-bearing, foraminifer-bearing nannofossil ooze, white (5Y 8/1, 7.5Y 8/0) or light-gray (5Y 7/1); bioturbation relatively weak; green and purple laminations common. Turbidite in Section 4, 75 cm.

SMEAR SLIDE SUMMARY (%):

	1, 80 D	5, 130 D
TEXTURE:		
Sand	15	25
Silt	15	15
Clay	70	60
COMPOSITION:		
Clay	20	15
Accessory Minerals	Tr	Tr
Foraminifers	10	20
Nannofossils	65	65
Diatoms	<5	Tr

SITE 644 HOLE D CORE 17 H CORED INTERVAL 3946.5-3956.0 mbsl; 144.8-154.3 mbsf

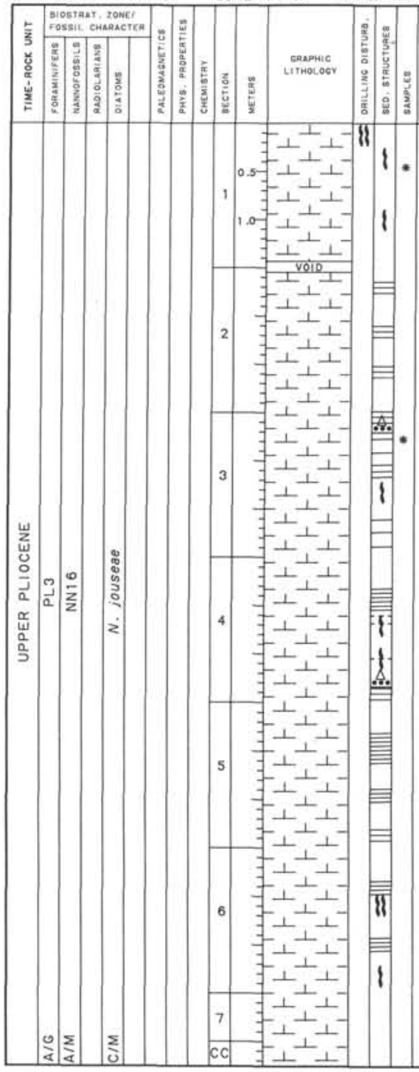

LITHOLOGIC DESCRIPTION

CLAY-BEARING, FORAMINIFER-BEARING NANNOFOSSIL OOZE

Clay-bearing, foraminifer-bearing nannofossil ooze, white (5Y 8/1, 7.5Y 8/0) or light-gray (5Y 7/1); very weak bioturbation; green and purple laminations abundant. Turbidites in Section 3, 0–5 cm, and Section 4, 108–133 cm.

SMEAR SLIDE SUMMARY (%):

	1, 50 D	3, 20 D
TEXTURE:		
Sand	15	10
Silt	15	20
Clay	70	70
COMPOSITION:		
Clay	15	15
Accessory Minerals	—	Tr
Foraminifers	10	10
Nannofossils	70	75
Diatoms	<5	—

SITE 664 HOLE D CORE 18 H CORED INTERVAL 3956.0-3965.5 mbsl; 154.3-163.8 mbsf

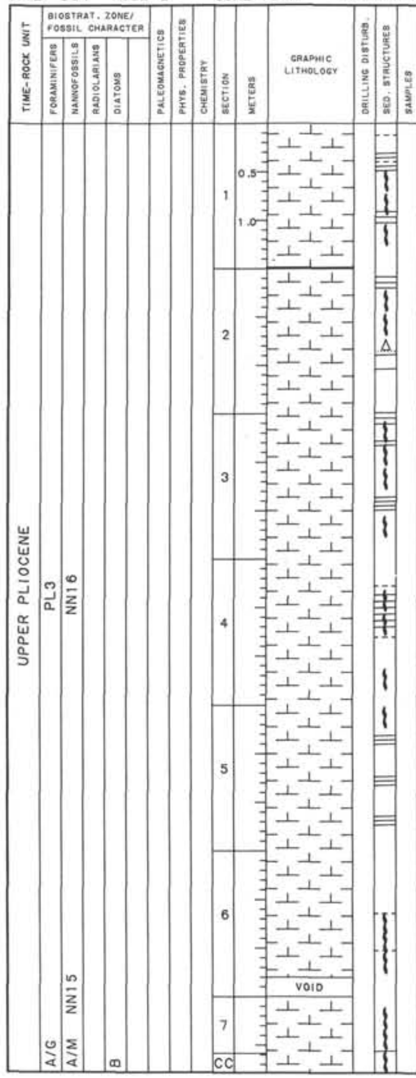

LITHOLOGIC DESCRIPTION

CLAY-BEARING, FORAMINIFER-BEARING NANNOFOSSIL OOZE and FORAMINIFER-BEARING, CLAY-BEARING NANNOFOSSIL OOZE

Clay-bearing, foraminifer-bearing nannofossil ooze and foraminifer-bearing, clay-bearing nannofossil ooze, white (5Y 8/1, 7.5Y 8/0) or light-gray (5Y 7/1); bioturbation weak to moderate; green and purple laminations common. Turbidite in Section 2, 100–110 cm. Minor void in Section 1, 145–150 cm.

SITE 664 HOLE D CORE 19 H CORED INTERVAL 3965.5-3975.0 mbsl; 163.8-173.3 mbsf

TIME-ROCK UNIT	FORAMINIFERS	NANNOFOSSILS	RADIOLARIANS	DIATOMS	PALEOMAGNETICS	PHYS. PROPERTIES	CHEMISTRY
UPPER PLIOCENE	PL3	NN15					
	A/G	A/M		F/P			

BIOSTRAT. ZONE/FOSSIL CHARACTER

SECTION · METERS · GRAPHIC LITHOLOGY · DRILLING DISTURB. · SED. STRUCTURES · SAMPLES

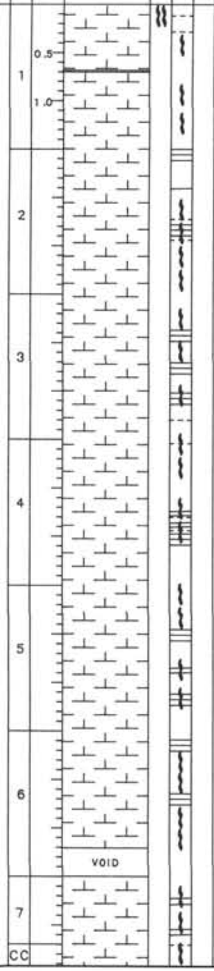

LITHOLOGIC DESCRIPTION

CLAY-BEARING, FORAMINIFER-BEARING NANNOFOSSIL OOZE and FORAMINIFER-BEARING, CLAY-BEARING NANNOFOSSIL OOZE

Clay-bearing, foraminifer-bearing nannofossil ooze and foraminifer-bearing, clay-bearing nannofossil ooze, white (5Y 8/1, 7.5Y 8/0) or light-gray (5Y 7/1); bioturbation weak to moderate; green and purple laminations common. Minor void in Section 1, 68–71 cm.

SITE 664 HOLE D CORE 20 H CORED INTERVAL 3975.0-3984.5 mbsl; 173.3-182.8 mbsf

TIME-ROCK UNIT	FORAMINIFERS	NANNOFOSSILS	RADIOLARIANS	DIATOMS	PALEOMAGNETICS	PHYS. PROPERTIES	CHEMISTRY
LOWER PLIOCENE	PL2	NN14-15					
	A/G	A/M		R/P			

BIOSTRAT. ZONE/FOSSIL CHARACTER

SECTION · METERS · GRAPHIC LITHOLOGY · DRILLING DISTURB. · SED. STRUCTURES · SAMPLES

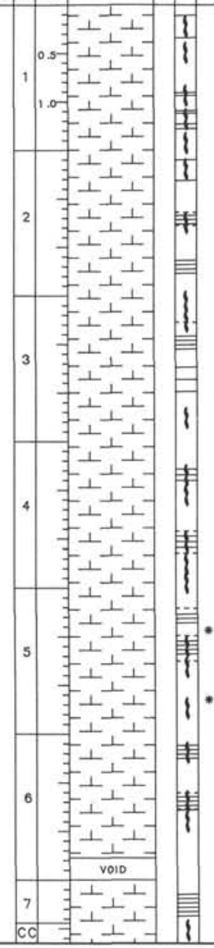

LITHOLOGIC DESCRIPTION

MUD-BEARING, FORAMINIFER-BEARING NANNOFOSSIL OOZE

Mud-bearing, foraminifer-bearing nannofossil ooze, white (5Y 8/1, 7.5Y 8/0) or light-gray (5Y 7/1); bioturbation weak to moderate; green and purple laminations common.

SMEAR SLIDE SUMMARY (%):

	5, 50 D	5, 110 D
TEXTURE:		
Sand	20	15
Silt	15	15
Clay	65	70
COMPOSITION:		
Clay	15	15
Accessory Minerals	5	5
Foraminifers	20	20
Nannofossils	50	60
Diatoms	5	—

SITE 664 HOLE D CORE 21 H CORED INTERVAL 3984.5-3994.0 mbsl; 182.8-192.3 mbsf

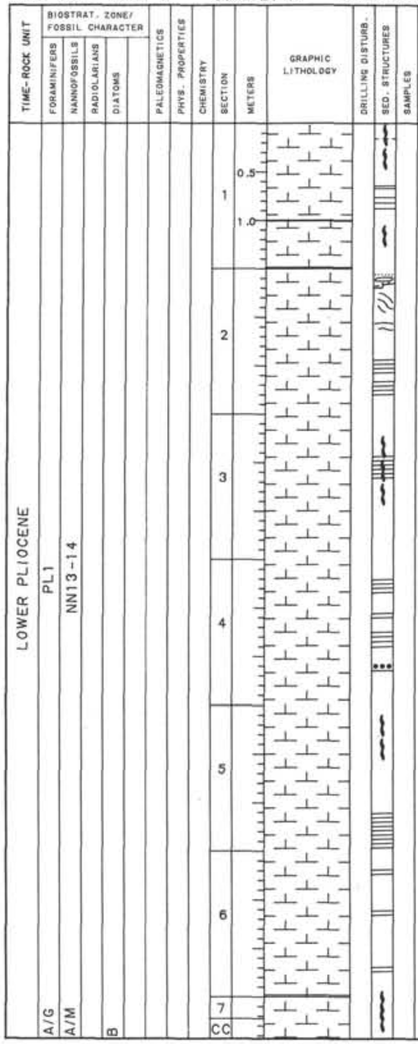

LITHOLOGIC DESCRIPTION

MUD-BEARING, FORAMINIFER-BEARING NANNOFOSSIL OOZE

Mud-bearing, foraminifer-bearing nannofossil ooze, white (5Y 8/1, 7.5Y 8/0) or light-gray (5Y 7/1); bioturbation very weak; green and purple laminations common. Folded and dipping bedding planes and laminations in Section 2. Turbidites in Section 2, 10–20 cm, and in Section 4, 110–120 cm. Minor voids in Section 1, 147–150 cm, and Section 6, 147–150 cm.

SITE 664 HOLE D CORE 22 H CORED INTERVAL 3994.0-4003.5 mbsl; 192.3-201.8 mbsf

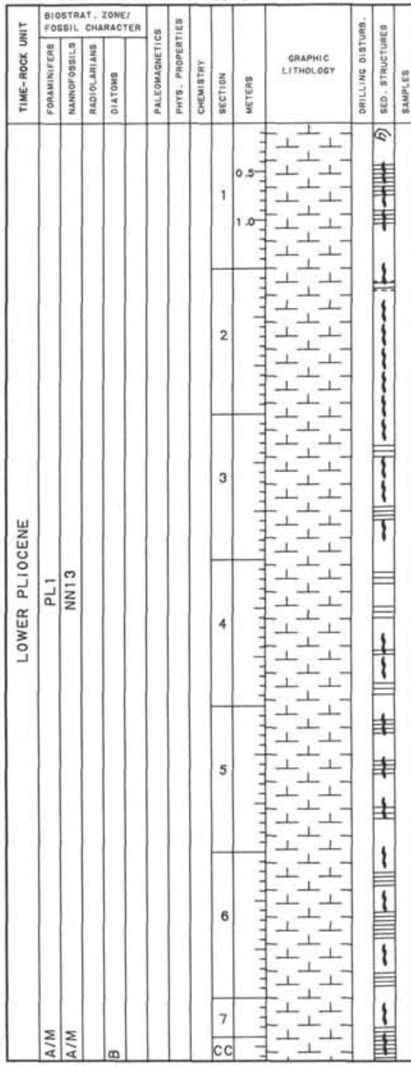

LITHOLOGIC DESCRIPTION

MUD-BEARING, FORAMINIFER-BEARING NANNOFOSSIL OOZE

Mud-bearing, foraminifer-bearing nannofossil ooze, white (5Y 8/1, 7.5Y 8/0) or light-gray (5Y 7/1); bioturbation very weak; green and purple laminations common.

SITE 664 HOLE D CORE 23 H CORED INTERVAL 4003.5-4013.5 mbsl; 201.8-211.3 mbsf

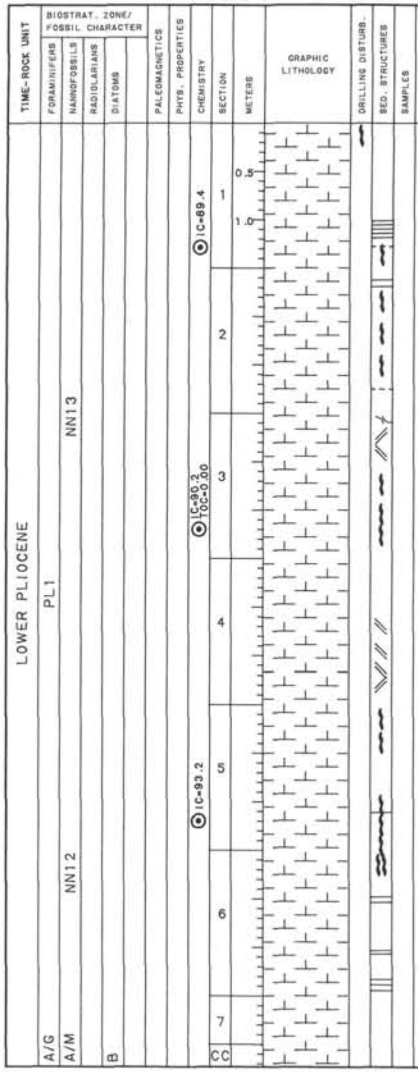

LITHOLOGIC DESCRIPTION

MUD-BEARING, FORAMINIFER-BEARING NANNOFOSSIL OOZE

Mud-bearing, foraminifer-bearing nannofossil ooze, white (5Y 8/1, 7.5Y 8/0); bioturbation very weak; green and purple laminations common; Sections 3 and 4 slightly deformed.

SITE 664 HOLE D CORE 24 H CORED INTERVAL 4013.0-4022 mbsl; 211.3-220.8 mbsf

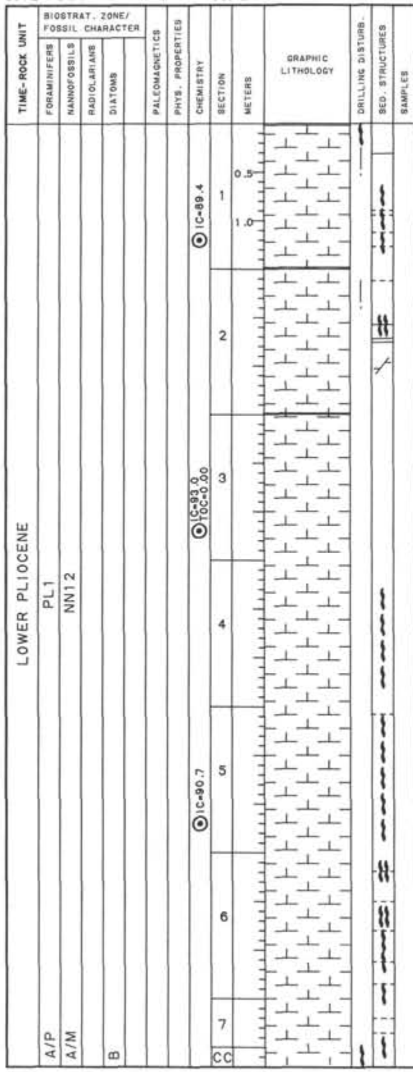

LITHOLOGIC DESCRIPTION

MUD-BEARING, FORAMINIFER-BEARING NANNOFOSSIL OOZE

Mud-bearing, foraminifer-bearing nannofossil ooze, white (5Y 8/1, 7.5Y 8/0); bioturbation very weak in Sections 1 through 3 and weak to moderate in Section 3 through CC; laminations rare. Minor voids in Section 1, 0–4 and 145–150 cm, and Section 2, 146–150 cm.

SITE 664 HOLE D CORE 25 H CORED INTERVAL 4022.5-4032.0 mbsl; 220.8-230.3 mbsf

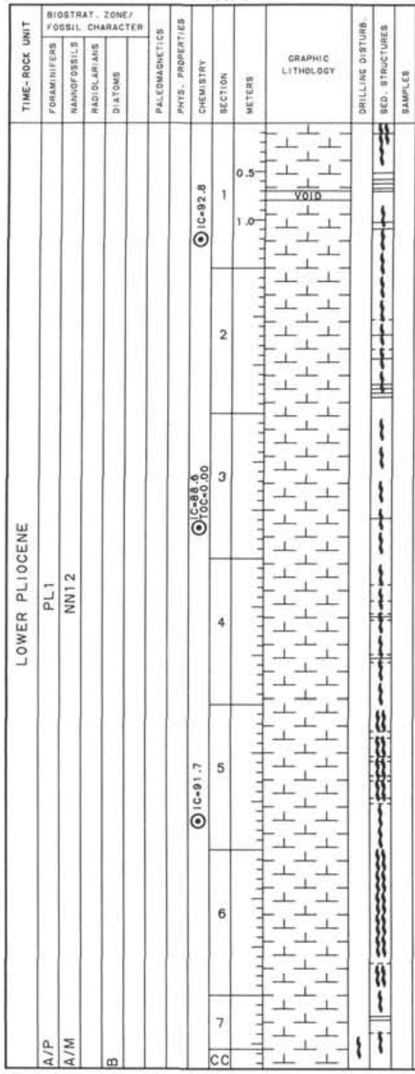

LITHOLOGIC DESCRIPTION

MUD-BEARING, FORAMINIFER-BEARING NANNOFOSSIL OOZE

Mud-bearing, foraminifer-bearing nannofossil ooze, white (5Y 8/1, 7.5Y 8/0) or light-gray (5Y 7/0); bioturbation moderate to heavy; occasional green and purple laminations.

SITE 664 HOLE D CORE 26 H CORED INTERVAL 4032.0-4041.5 mbsl; 230.3-239.8 mbsf

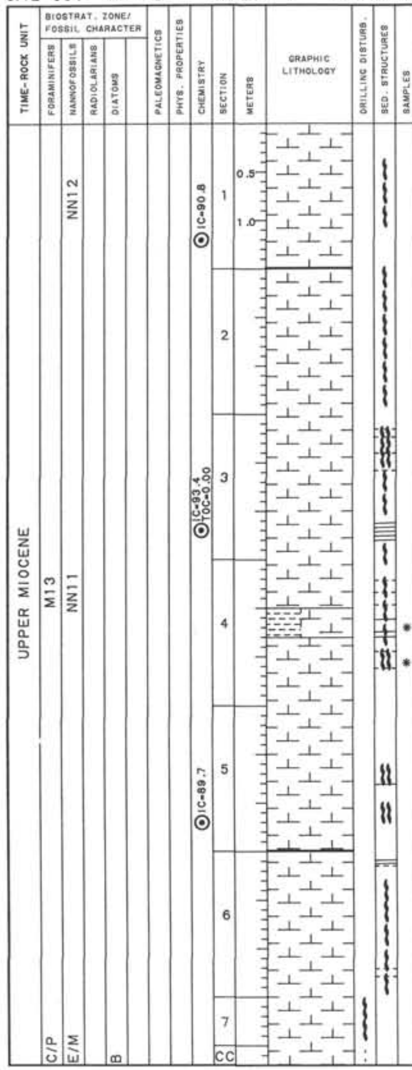

LITHOLOGIC DESCRIPTION

CLAY-BEARING, FORAMINIFER-BEARING NANNOFOSSIL OOZE

Clay-bearing, foraminifer-bearing nannofossil ooze, white (5Y 8/1, 7.5Y 8/0) or light-gray (5Y 7/0); bioturbation weak to moderate; occasional green and purple laminations. Minor void in Section 1, 146–150 cm, and Section 5, 149–150 cm.

Minor lithology: Section 4, 50–80 cm: clayey nannofossil ooze, light-gray (7.5YR 7/0).

SMEAR SLIDE SUMMARY (%):

	4, 68 D	4, 110 D
TEXTURE:		
Sand	—	—
Silt	—	10
Clay	100	90
COMPOSITION:		
Clay	25	10
Foraminifers	—	10
Nannofossils	75	80

SITE 664 HOLE D CORE 27 H CORED INTERVAL 4041.5-4051.0 mbsl; 239.8-249.3 mbsf

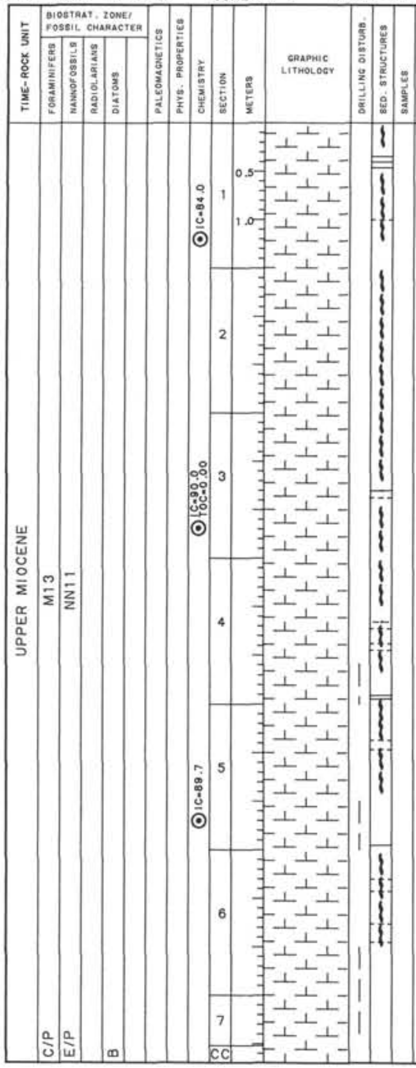

LITHOLOGIC DESCRIPTION

CLAY-BEARING, FORAMINIFER-BEARING NANNOFOSSIL OOZE

Clay-bearing, foraminifer-bearing nannofossil ooze, white (5Y 8/1, 7.5Y 8/0); bioturbation weak to moderate; laminations rare; *Zoophycos* burrows common

SITE 664 HOLE D CORE 28 H CORED INTERVAL 4051.0-4060.5 mbsl; 249.3-258.8 mbsf

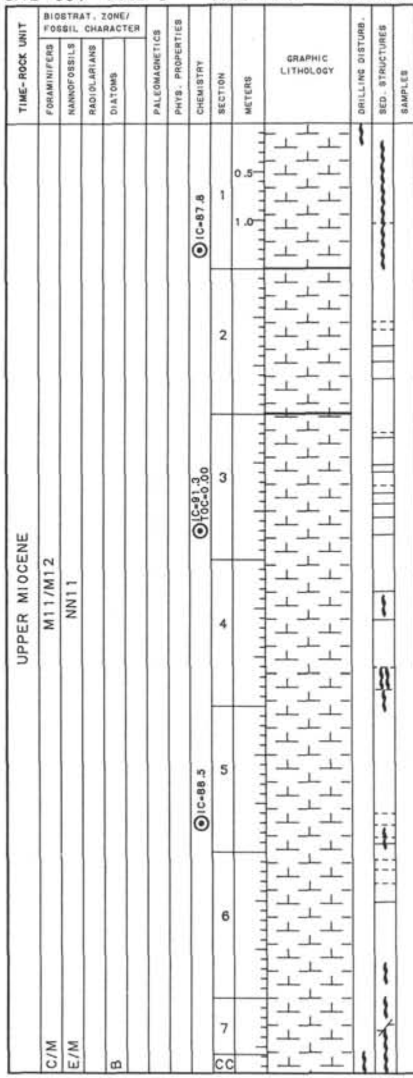

LITHOLOGIC DESCRIPTION

CLAY-BEARING, FORAMINIFER-BEARING NANNOFOSSIL OOZE

Clay-bearing, foraminifer-bearing nannofossil ooze, white (5Y 8/1, 7.5Y 8/0); bioturbation very weak; laminations rare; burrows pyritized; microfault in Section 7, 25 cm. Minor voids in Section 1, 145–150 cm, and Section 2, 147–150 cm.

SITE 664 HOLE D CORE 29 H CORED INTERVAL 4060.5-4070.0 mbsl; 258.8-268.3 mbsf

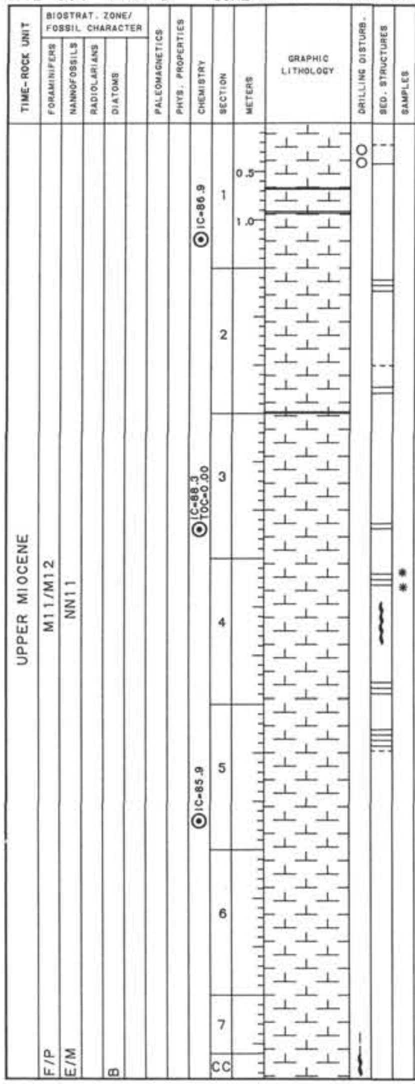

LITHOLOGIC DESCRIPTION

MUD-BEARING, FORAMINIFER-BEARING NANNOFOSSIL OOZE

Mud-bearing, foraminifer-bearing nannofossil ooze, white (10Y 8/1, 7.5Y 8/0); bioturbation very weak; laminations rare. Minor voids in Section 1, 67–69 and 91–93 cm, and Section 2, 148–150 cm.

SMEAR SLIDE SUMMARY (%):

	4, 17 D	4, 31 M
TEXTURE:		
Sand	—	Tr
Silt	5	15
Clay	95	85
COMPOSITION:		
Quartz	5	10
Clay	10	10
Foraminifers	Tr	5
Nannofossils	85	75

SITE 664 HOLE D CORE 30 H CORED INTERVAL 4070.0-4079.5 mbsl; 268.3-277.8 mbsf

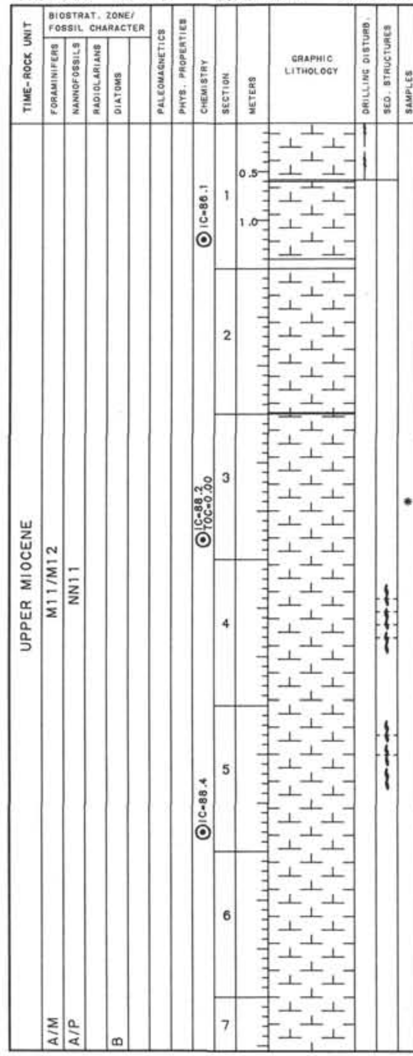

LITHOLOGIC DESCRIPTION

MUD-BEARING, FORAMINIFER-BEARING NANNOFOSSIL OOZE

Mud-bearing, foraminifer-bearing nannofossil ooze, white (10Y 8/1, 7.5Y 8/0). Minor void in Section 2, 145–150 cm.

SMEAR SLIDE SUMMARY (%):

	3, 63 D
TEXTURE:	
Sand	—
Silt	5
Clay	95
COMPOSITION:	
Clay	10
Nannofossils	90

SITE 664 HOLE D CORE 31 H CORED INTERVAL 4079.5-4089.0 mbsl; 277.8-287.3 mbsf

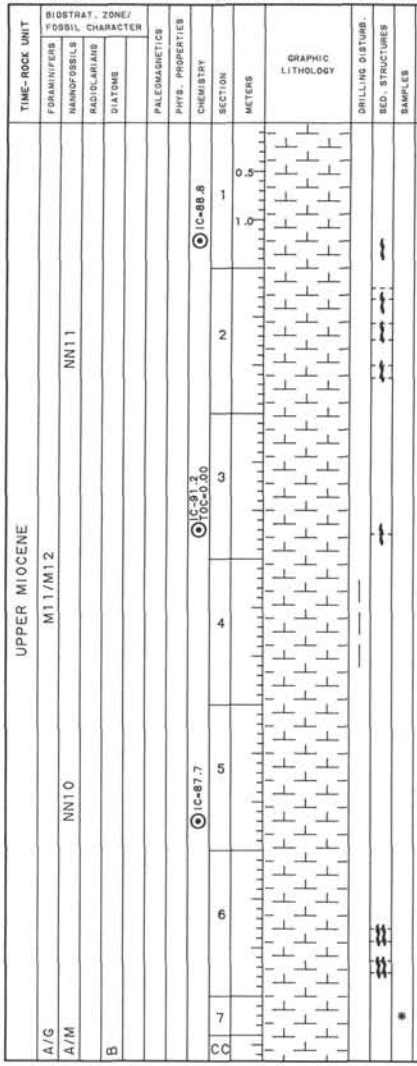

LITHOLOGIC DESCRIPTION

MUD-BEARING, FORAMINIFER-BEARING NANNOFOSSIL OOZE

Mud-bearing, foraminifer-bearing nannofossil ooze, white (10Y 8/1, 7.5Y 8/0); bioturbation very weak; laminations rare; pyrite blebs common throughout.

SMEAR SLIDE SUMMARY (%):

	7, 57 M
TEXTURE:	
Sand	—
Silt	5
Clay	15
COMPOSITION:	
Quartz	Tr
Clay	15
Nannofossils	85

SITE 664 HOLE D CORE 32 H CORED INTERVAL 4089.0-4098.5 mbsl; 287.3-296.8 mbsf

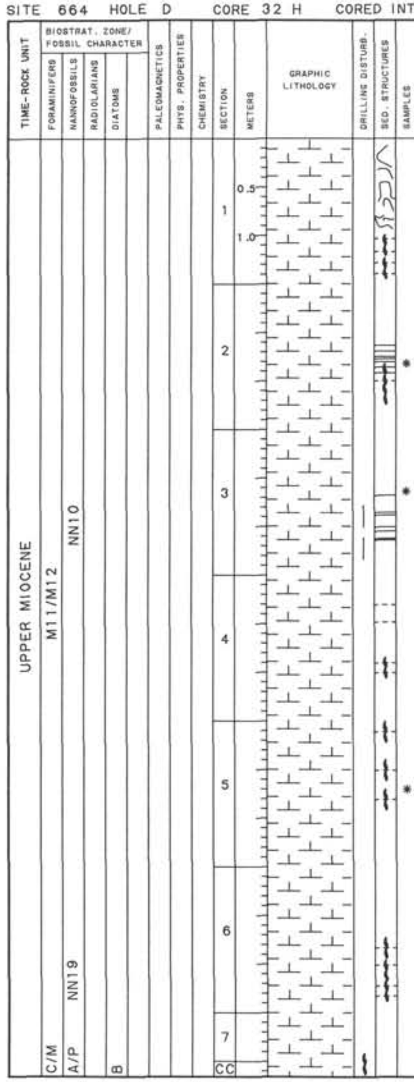

LITHOLOGIC DESCRIPTION

CLAY-BEARING, FORAMINIFER-BEARING NANNOFOSSIL OOZE

Clay-bearing, foraminifer-bearing nannofossil ooze, white (10Y 8/1, 2.5Y 8/0); bioturbation very weak; laminations rare; pyrite blebs common throughout.

SMEAR SLIDE SUMMARY (%):

	2, 82 M	3, 60 D	5, 62 D
TEXTURE:			
Sand	—	5	—
Silt	15	15	10
Clay	85	80	90
COMPOSITION:			
Quartz	Tr	Tr	Tr
Clay	15	10	15
Foraminifers	10	10	0
Nannofossils	75	75	75

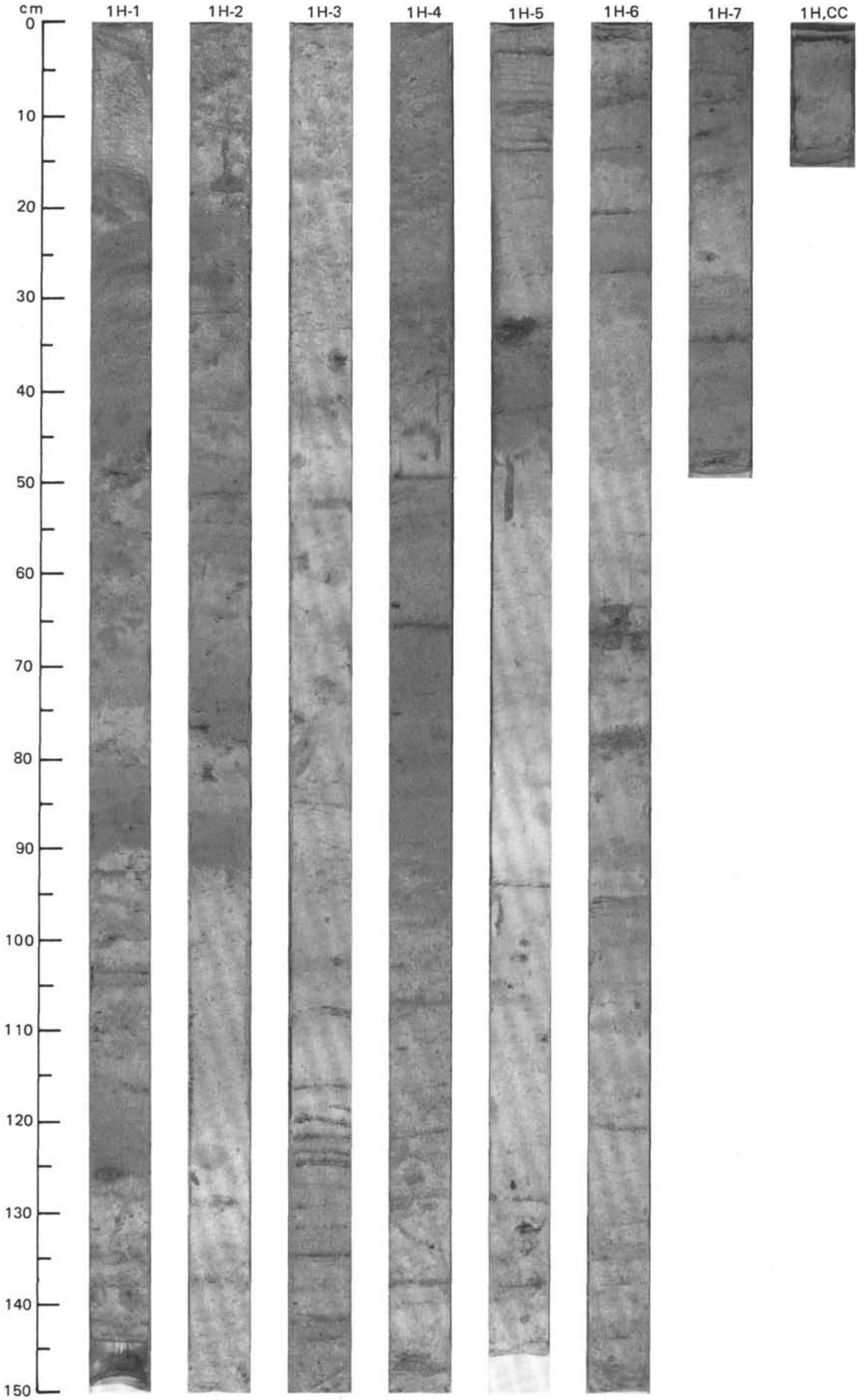
cm
0
10
20
30
40
50
60
70
80
90
100
110
120
130
140
150
1H-1
1H-2
1H-3
1H-4
1H-5
1H-6
1H-7
1H,CC

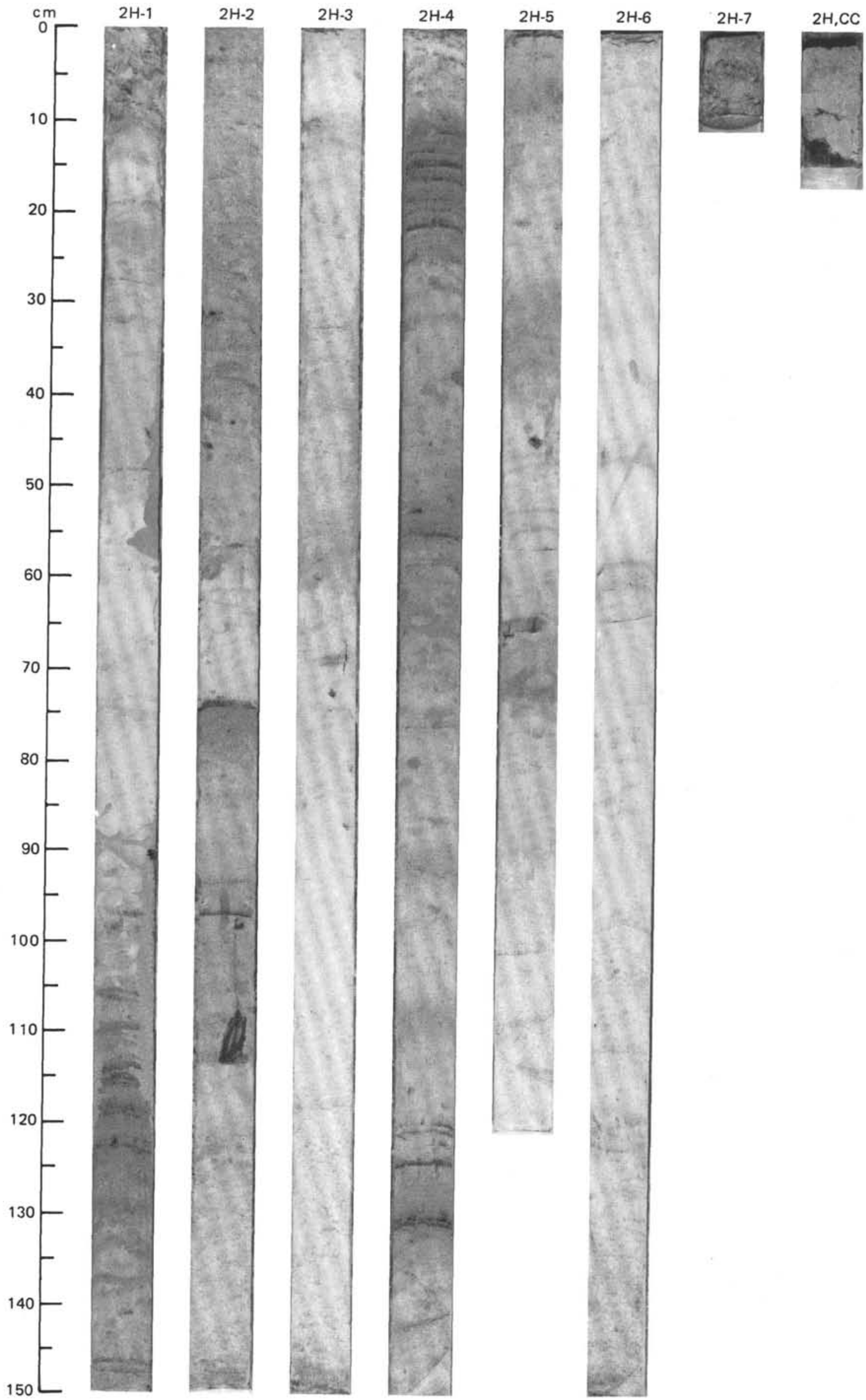
cm
0
10
20
30
40
50
60
70
80
90
100
110
120
130
140
150
2H-1
2H-2
2H-3
2H-4
2H-5
2H-6
2H-7
2H,CC

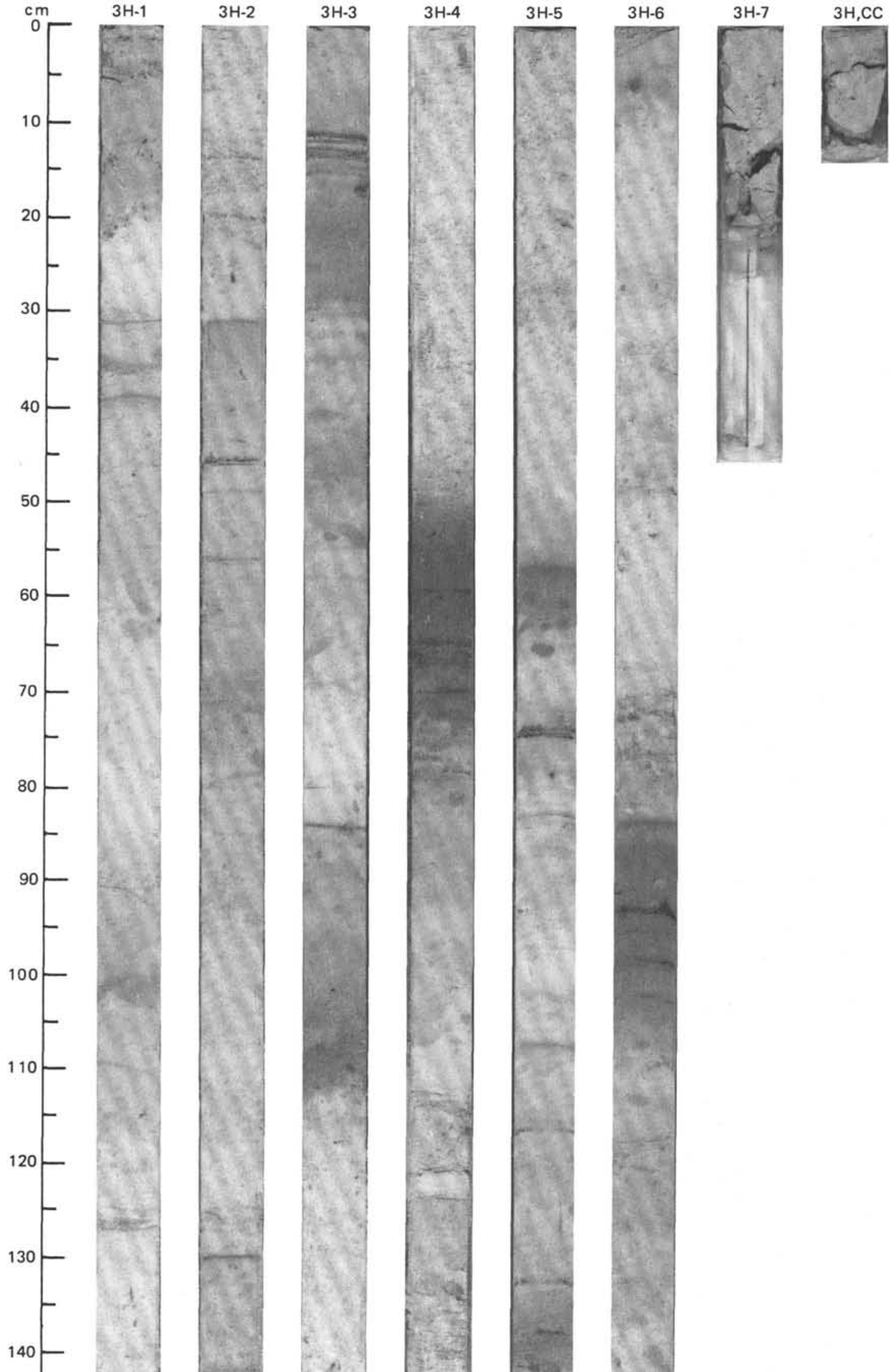
cm
0
10
20
30
40
50
60
70
80
90
100
110
120
130
140
150
3H-1
3H-2
3H-3
3H-4
3H-5
3H-6
3H-7
3H,CC

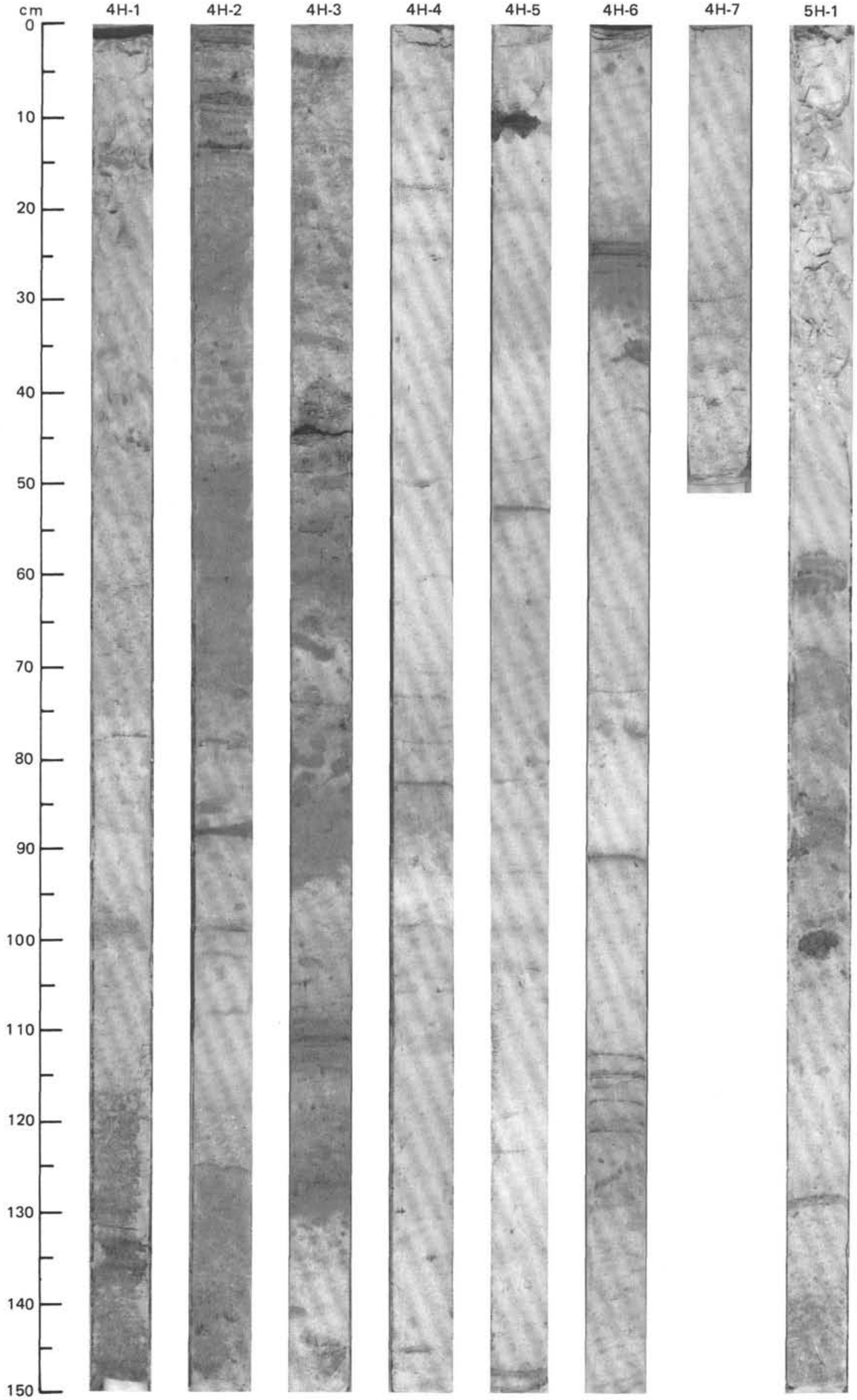
cm
0
10
20
30
40
50
60
70
80
90
100
110
120
130
140
150
4H-1
4H-2
4H-3
4H-4
4H-5
4H-6
4H-7
5H-1

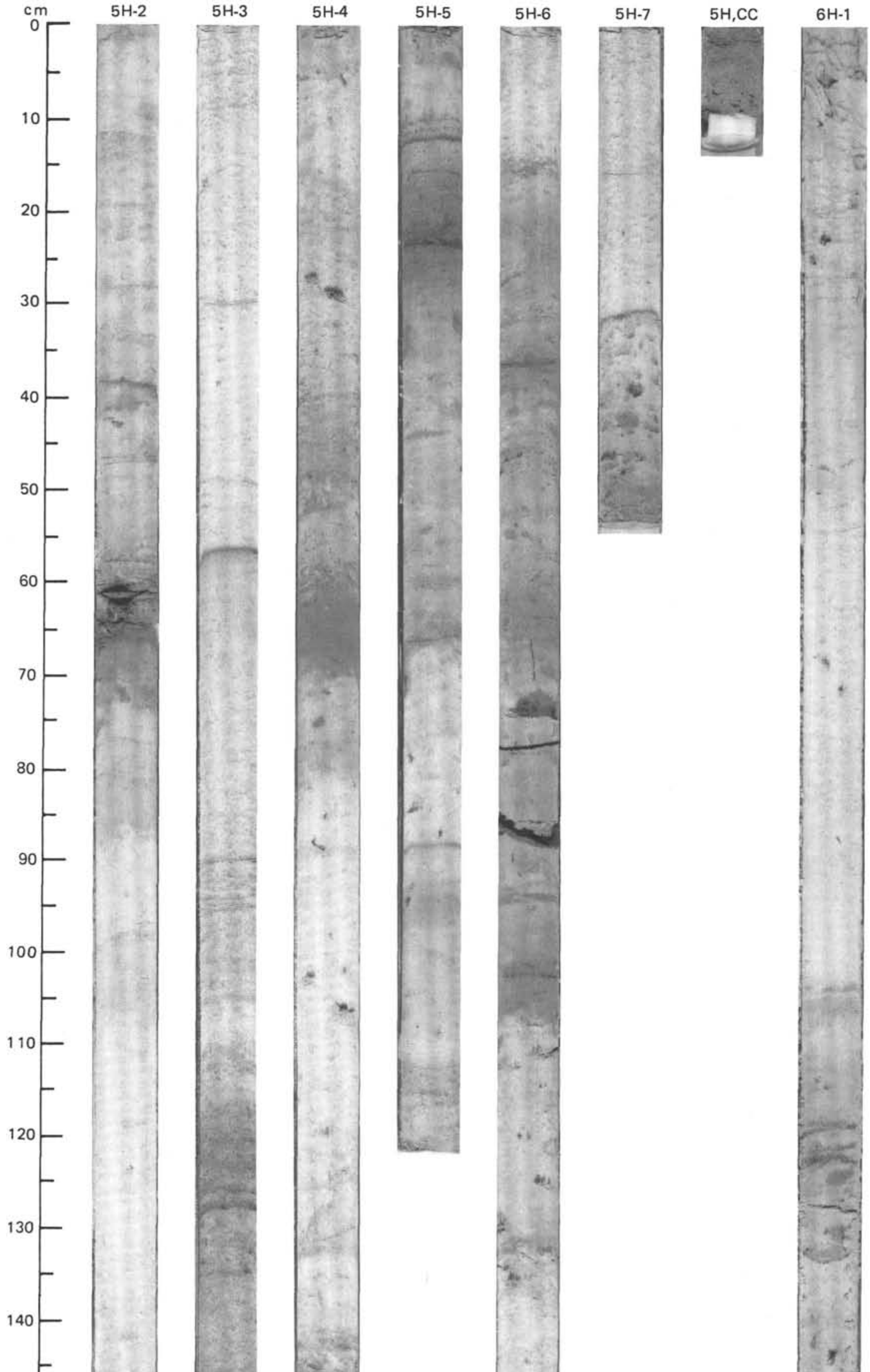
cm
0
10
20
30
40
50
60
70
80
90
100
110
120
130
140
150
5H-2
5H-3
5H-4
5H-5
5H-6
5H-7
5H,CC
6H-1

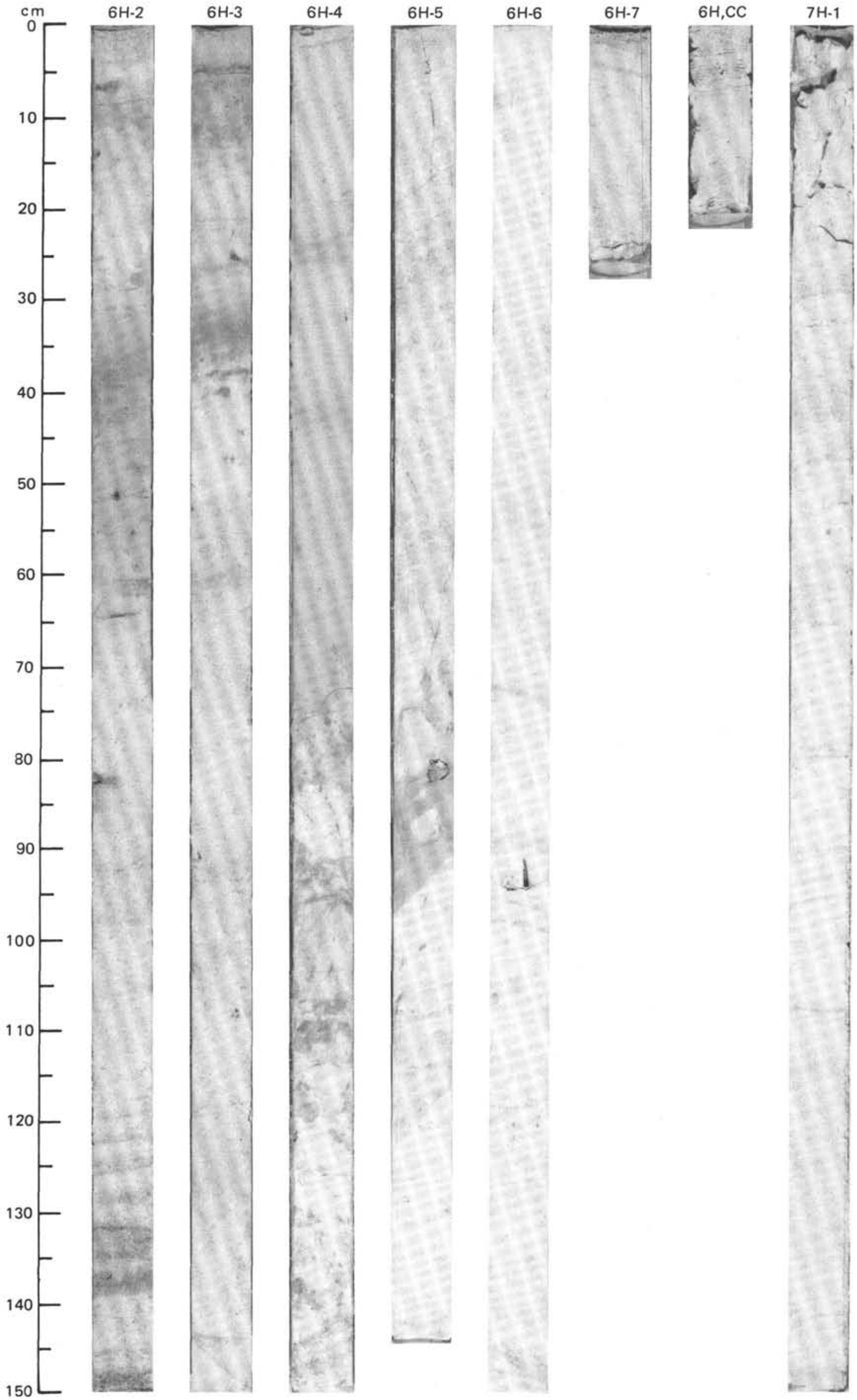
cm
0
10
20
30
40
50
60
70
80
90
100
110
120
130
140
150
6H-2
6H-3
6H-4
6H-5
6H-6
6H-7
6H,CC
7H-1

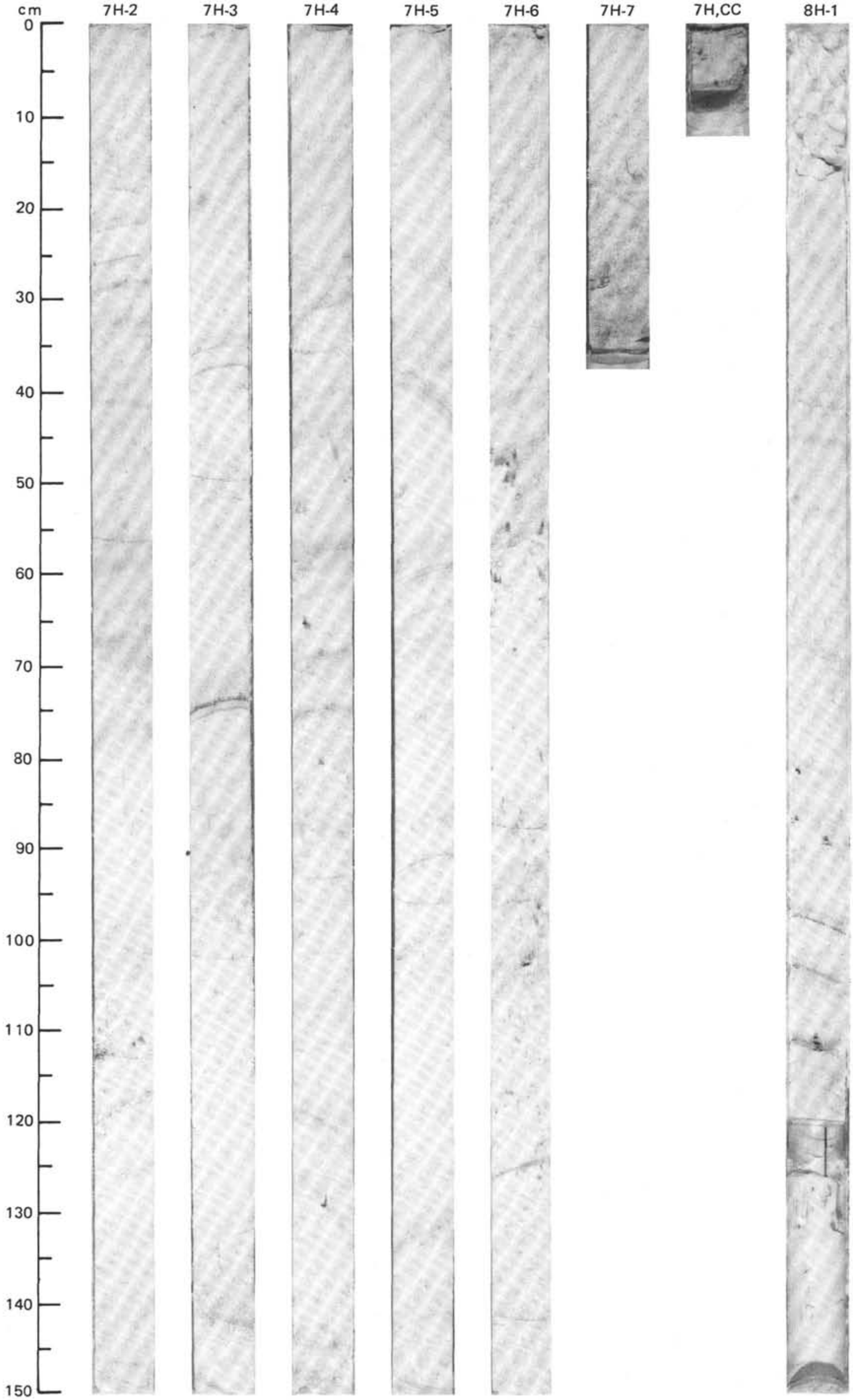
cm
0
10
20
30
40
50
60
70
80
90
100
110
120
130
140
150
7H-2
7H-3
7H-4
7H-5
7H-6
7H-7
7H,CC
8H-1

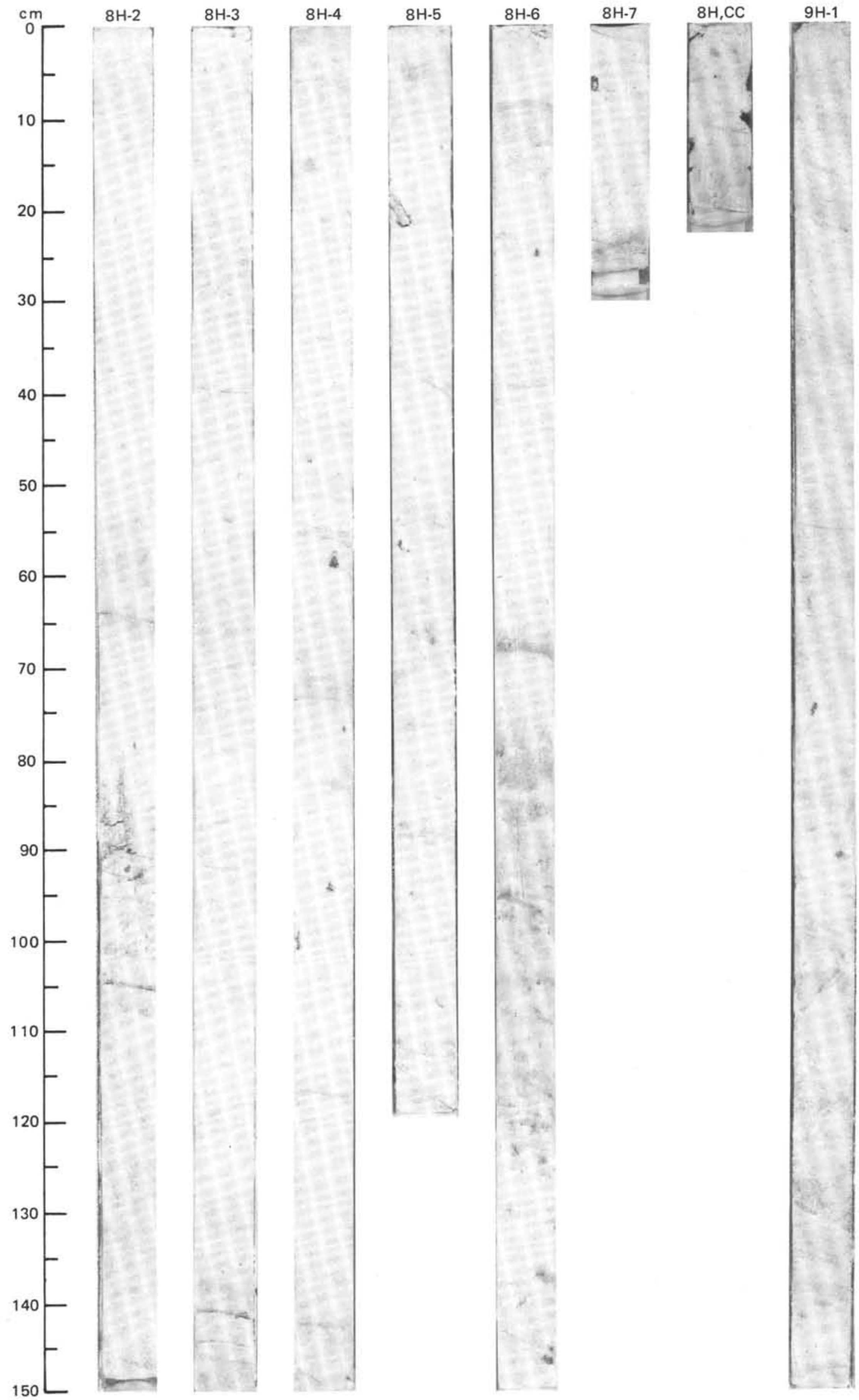
cm
0
10
20
30
40
50
60
70
80
90
100
110
120
130
140
150
8H-2
8H-3
8H-4
8H-5
8H-6
8H-7
8H,CC
9H-1

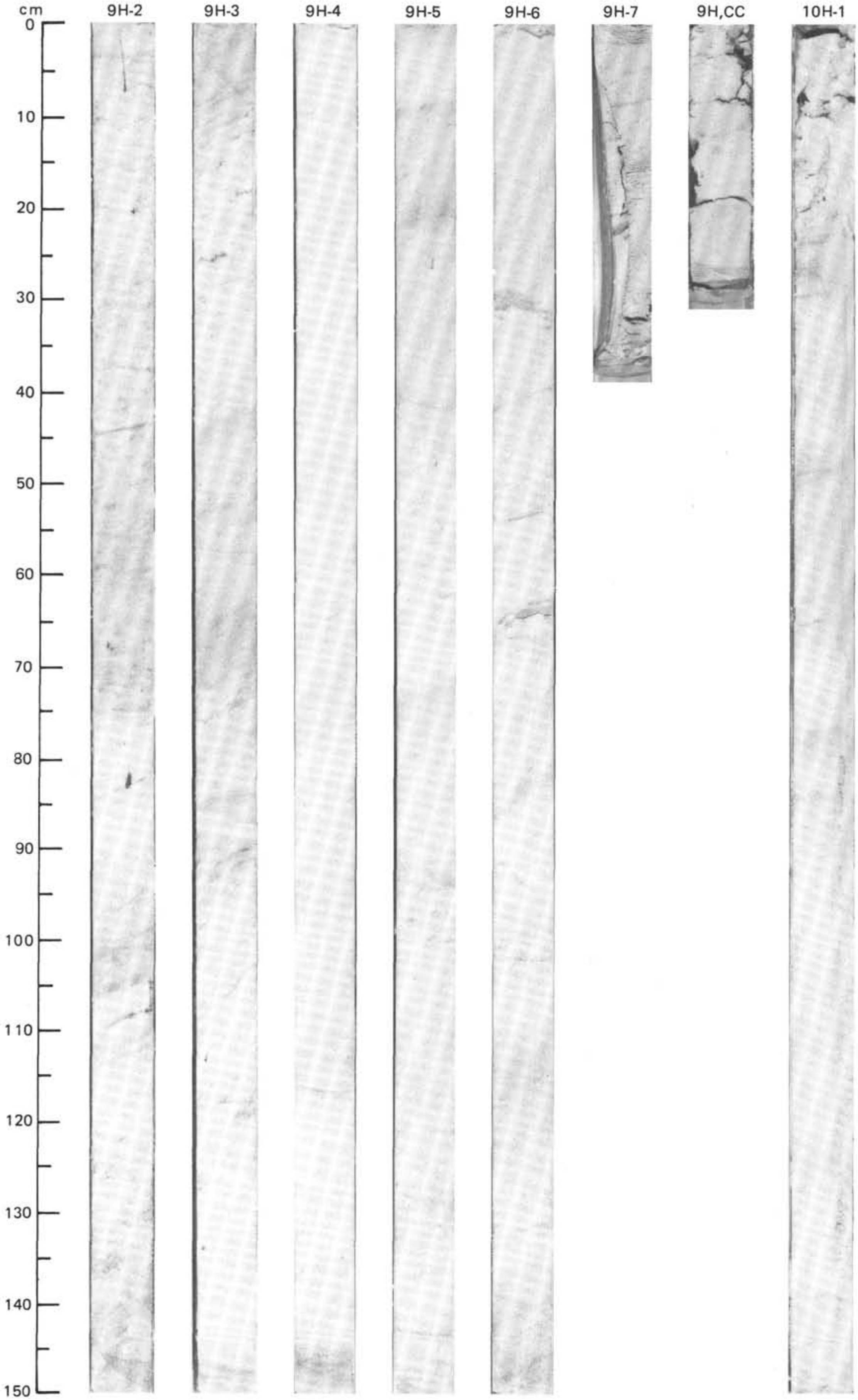
cm
0
10
20
30
40
50
60
70
80
90
100
110
120
130
140
150
9H-2
9H-3
9H-4
9H-5
9H-6
9H-7
9H,CC
10H-1

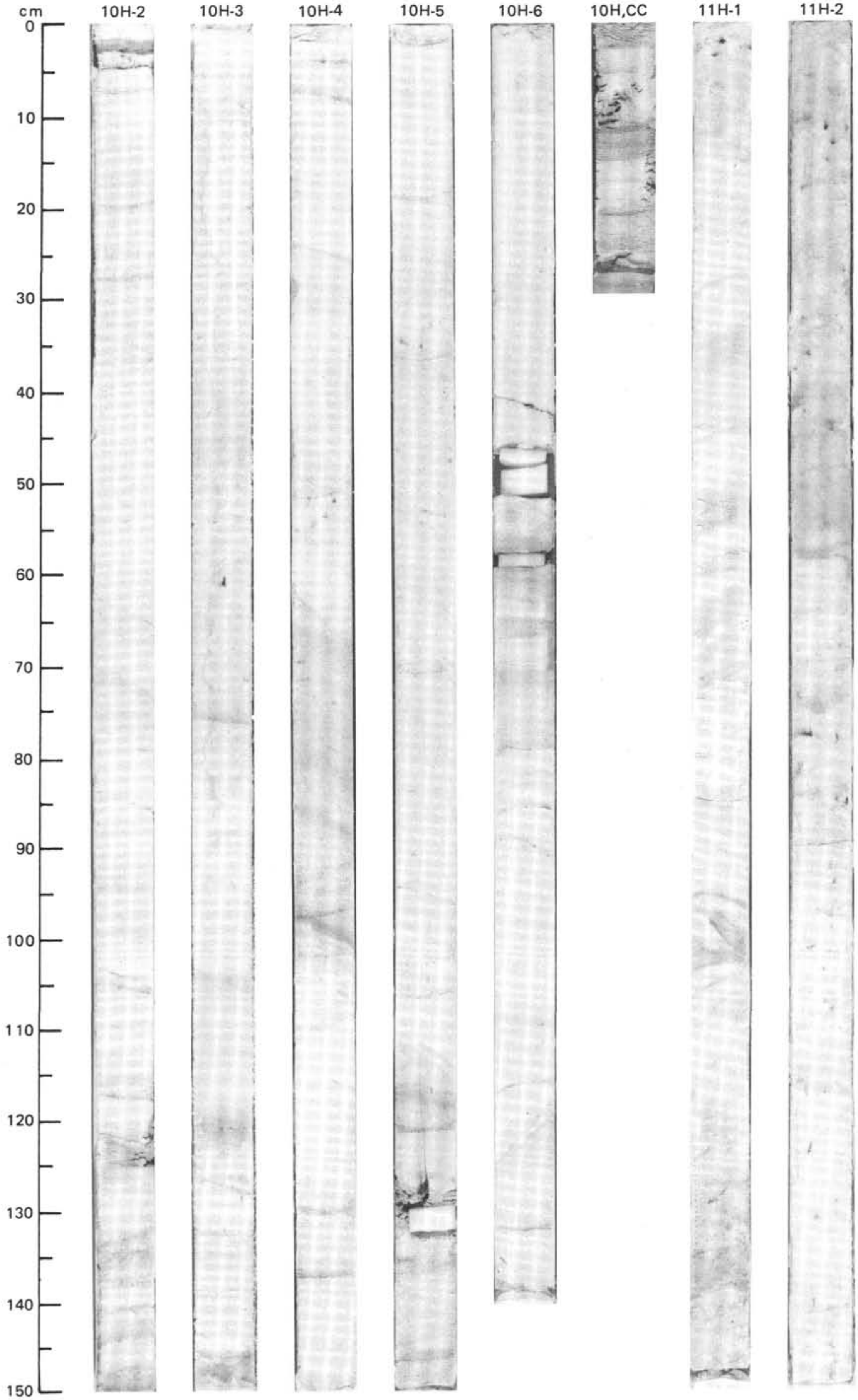
cm
0
10
20
30
40
50
60
70
80
90
100
110
120
130
140
150
10H-2
10H-3
10H-4
10H-5
10H-6
10H,CC
11H-1
11H-2

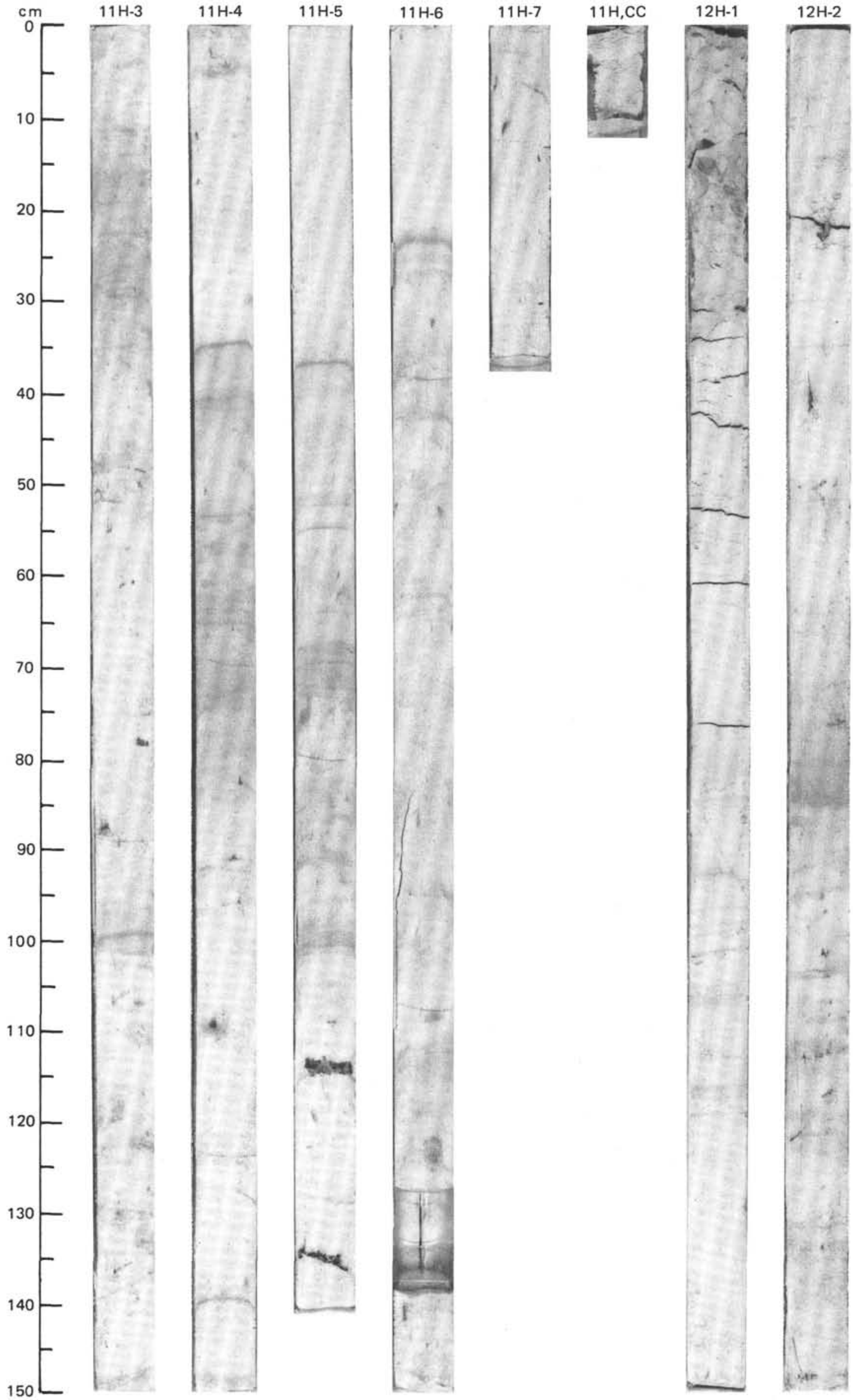
cm
0
10
20
30
40
50
60
70
80
90
100
110
120
130
140
150
11H-3
11H-4
11H-5
11H-6
11H-7
11H,CC
12H-1
12H-2

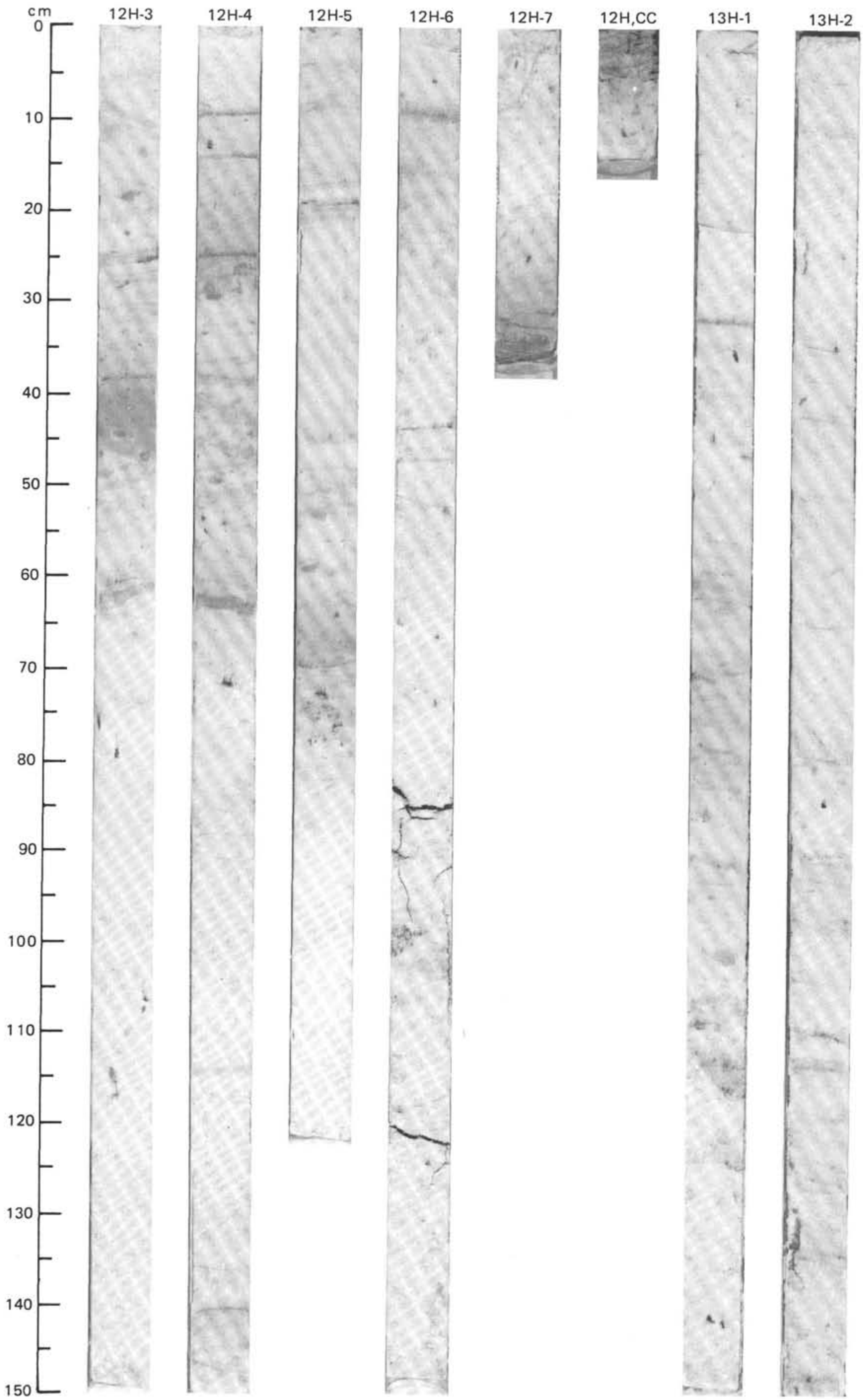
cm
0
10
20
30
40
50
60
70
80
90
100
110
120
130
140
150
12H-3
12H-4
12H-5
12H-6
12H-7
12H,CC
13H-1
13H-2

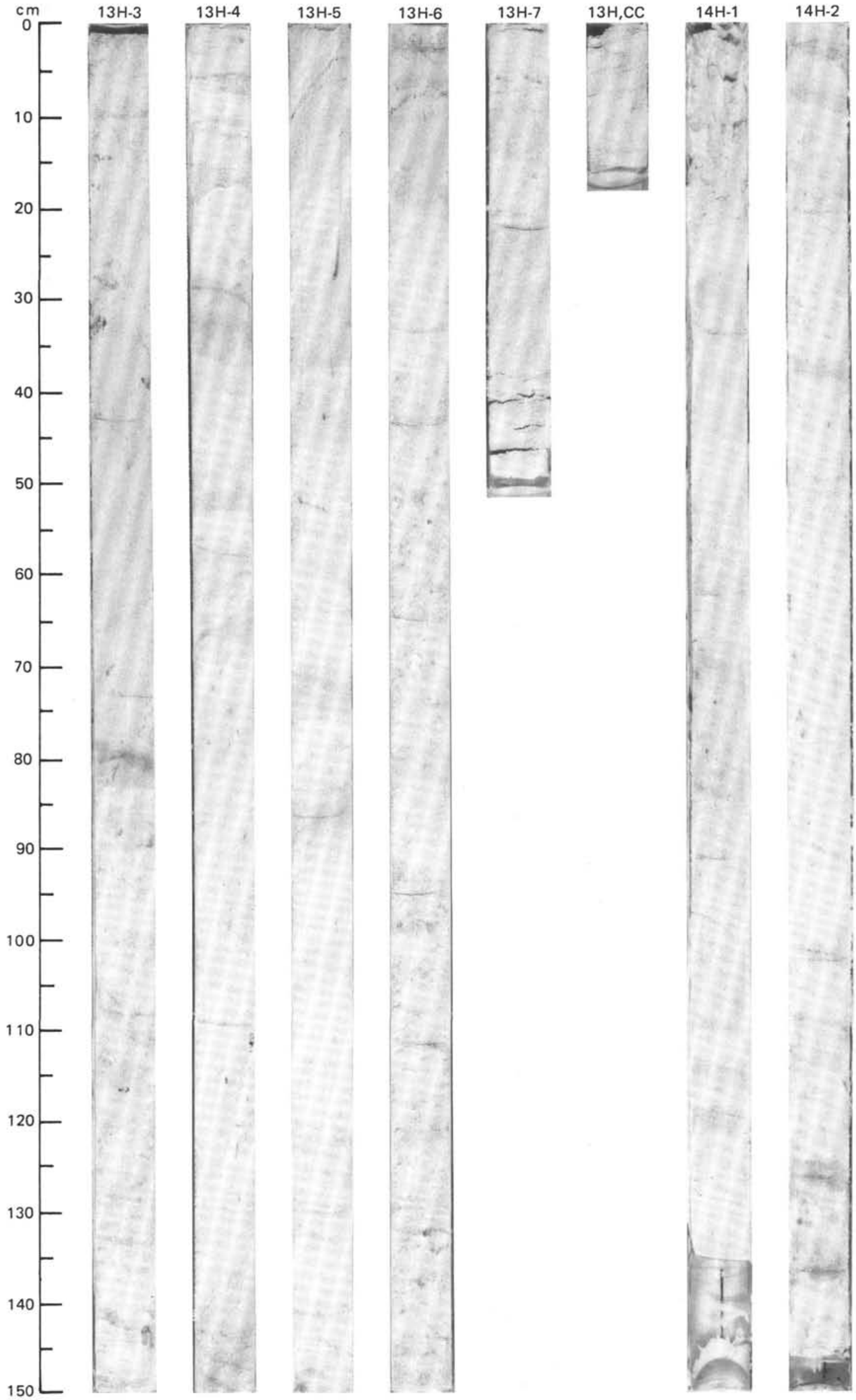
cm
0
10
20
30
40
50
60
70
80
90
100
110
120
130
140
150
13H-3
13H-4
13H-5
13H-6
13H-7
13H,CC
14H-1
14H-2

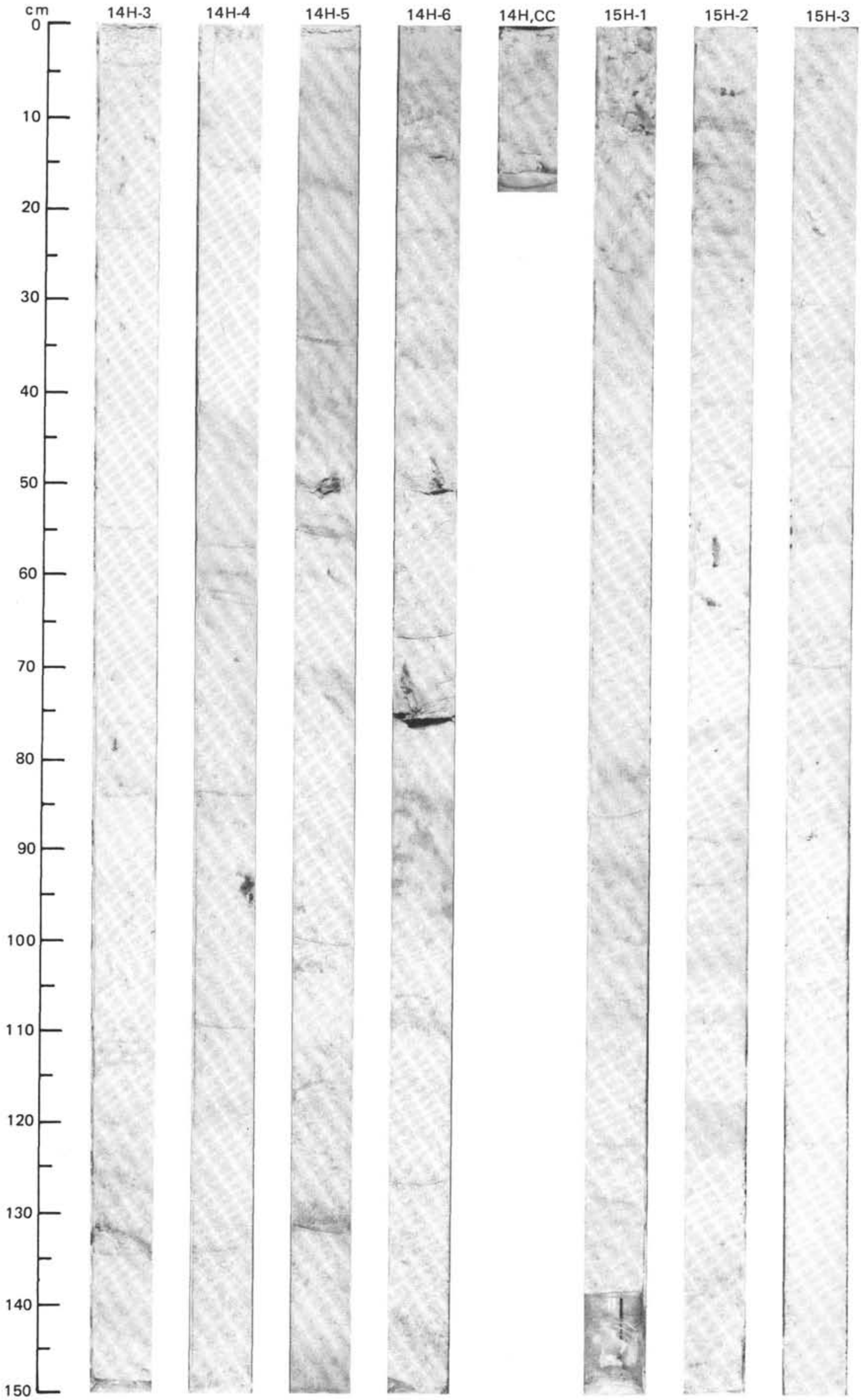
cm
0
10
20
30
40
50
60
70
80
90
100
110
120
130
140
150
14H-3
14H-4
14H-5
14H-6
14H,CC
15H-1
15H-2
15H-3

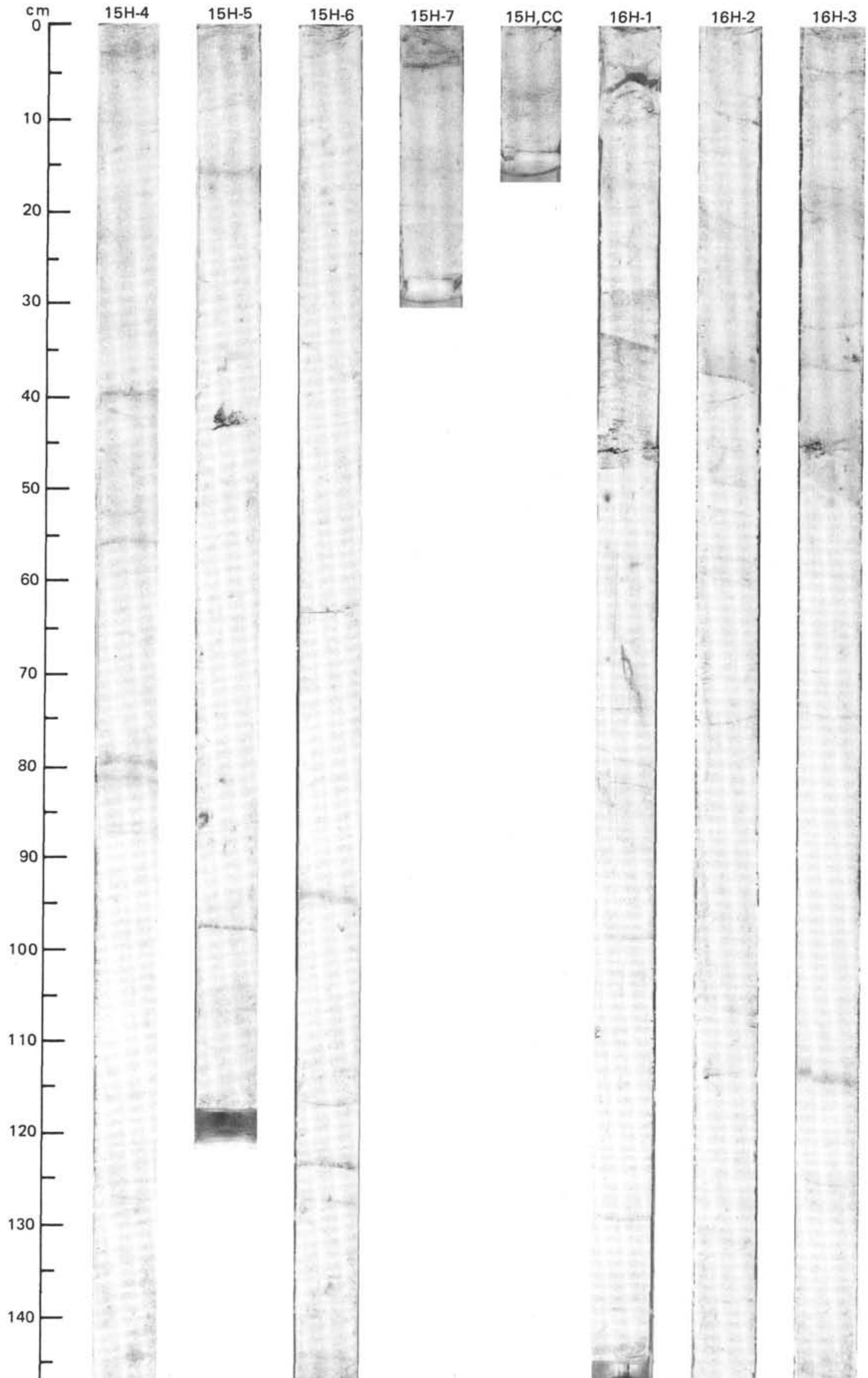
cm
0
10
20
30
40
50
60
70
80
90
100
110
120
130
140
150
15H-4
15H-5
15H-6
15H-7
15H,CC
16H-1
16H-2
16H-3

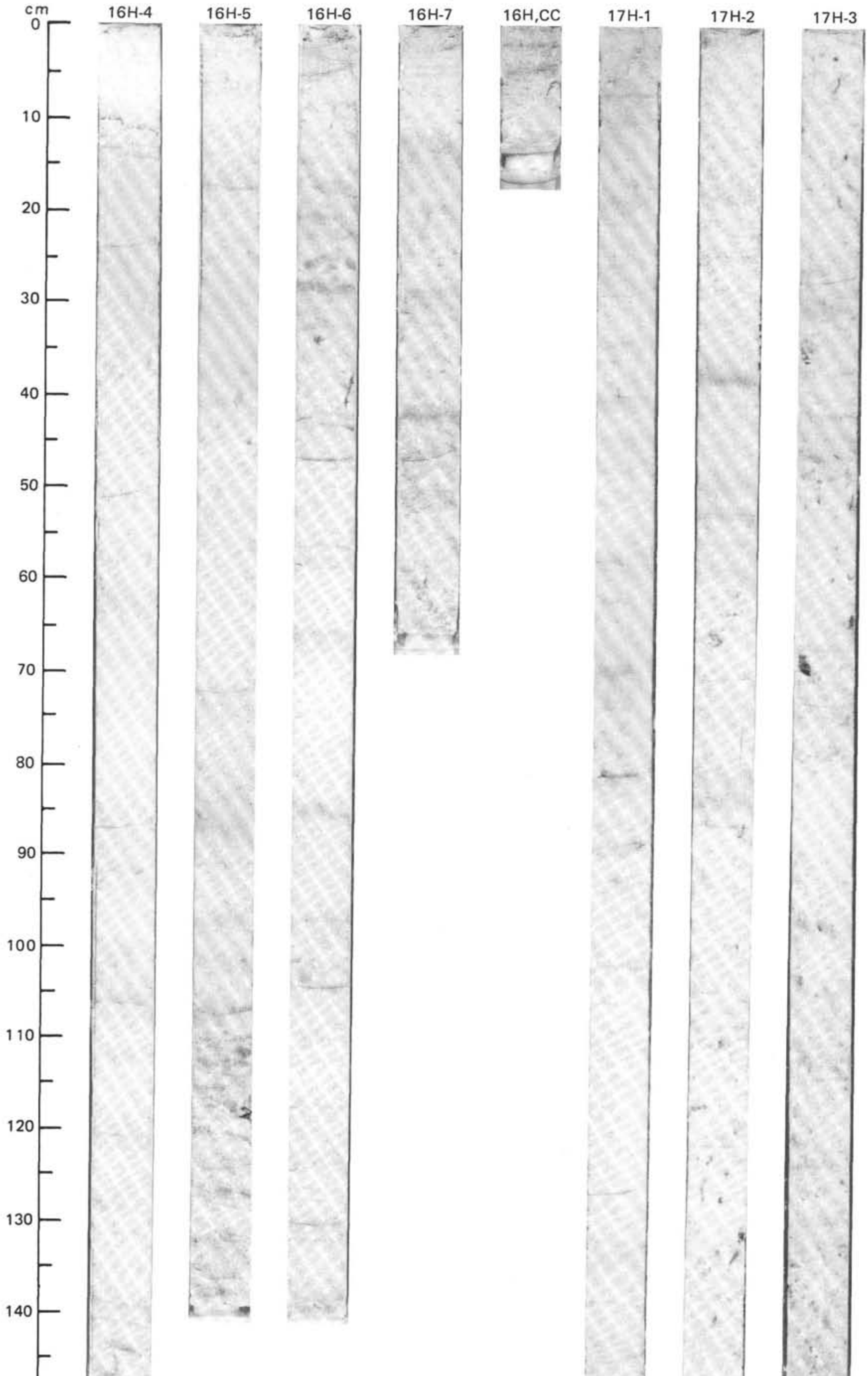
cm
0
10
20
30
40
50
60
70
80
90
100
110
120
130
140
150
16H-4
16H-5
16H-6
16H-7
16H,CC
17H-1
17H-2
17H-3

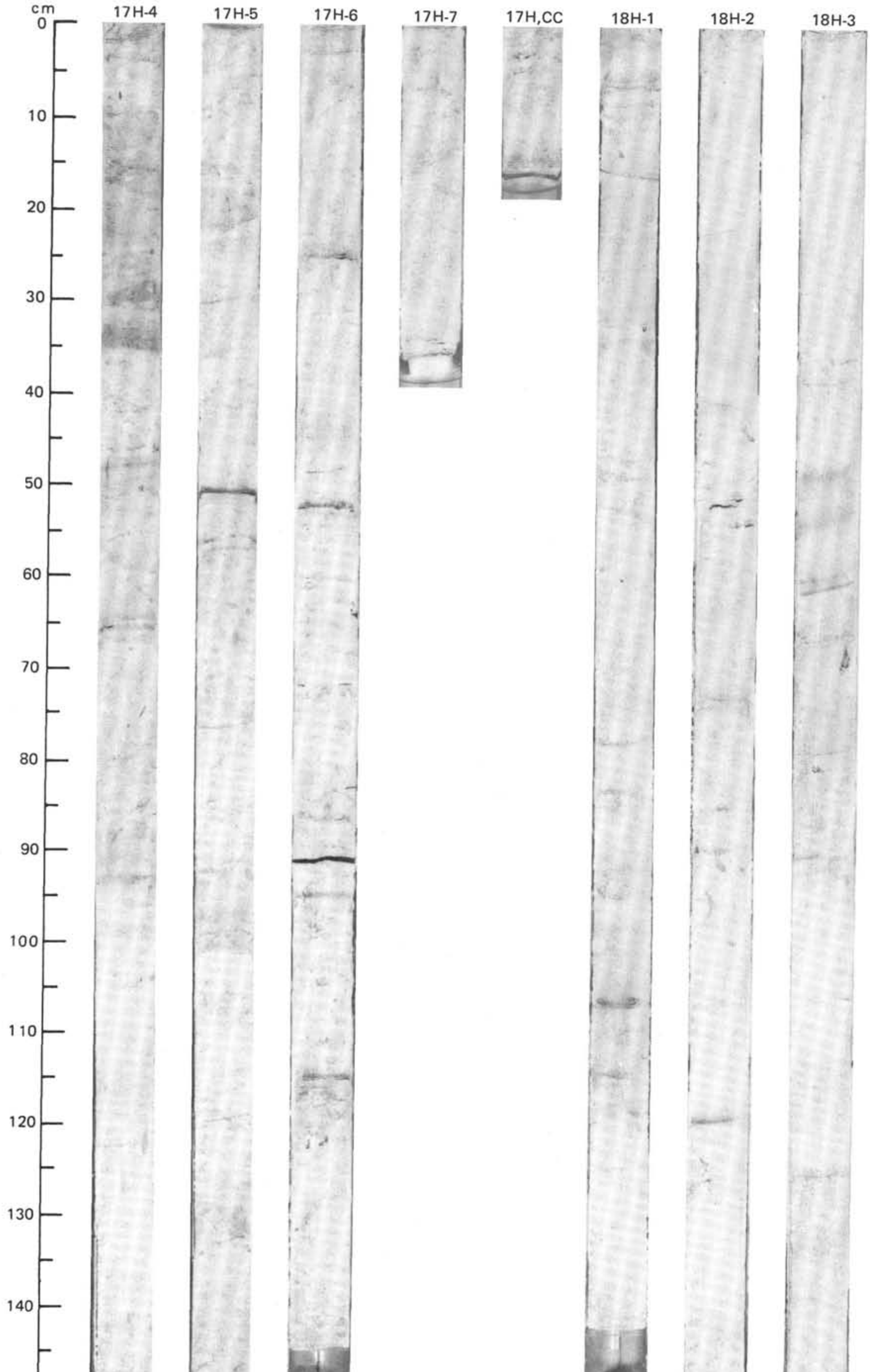
cm
17H-4
17H-5
17H-6
17H-7
17H,CC
18H-1
18H-2
18H-3
0
10
20
30
40
50
60
70
80
90
100
110
120
130
140
150

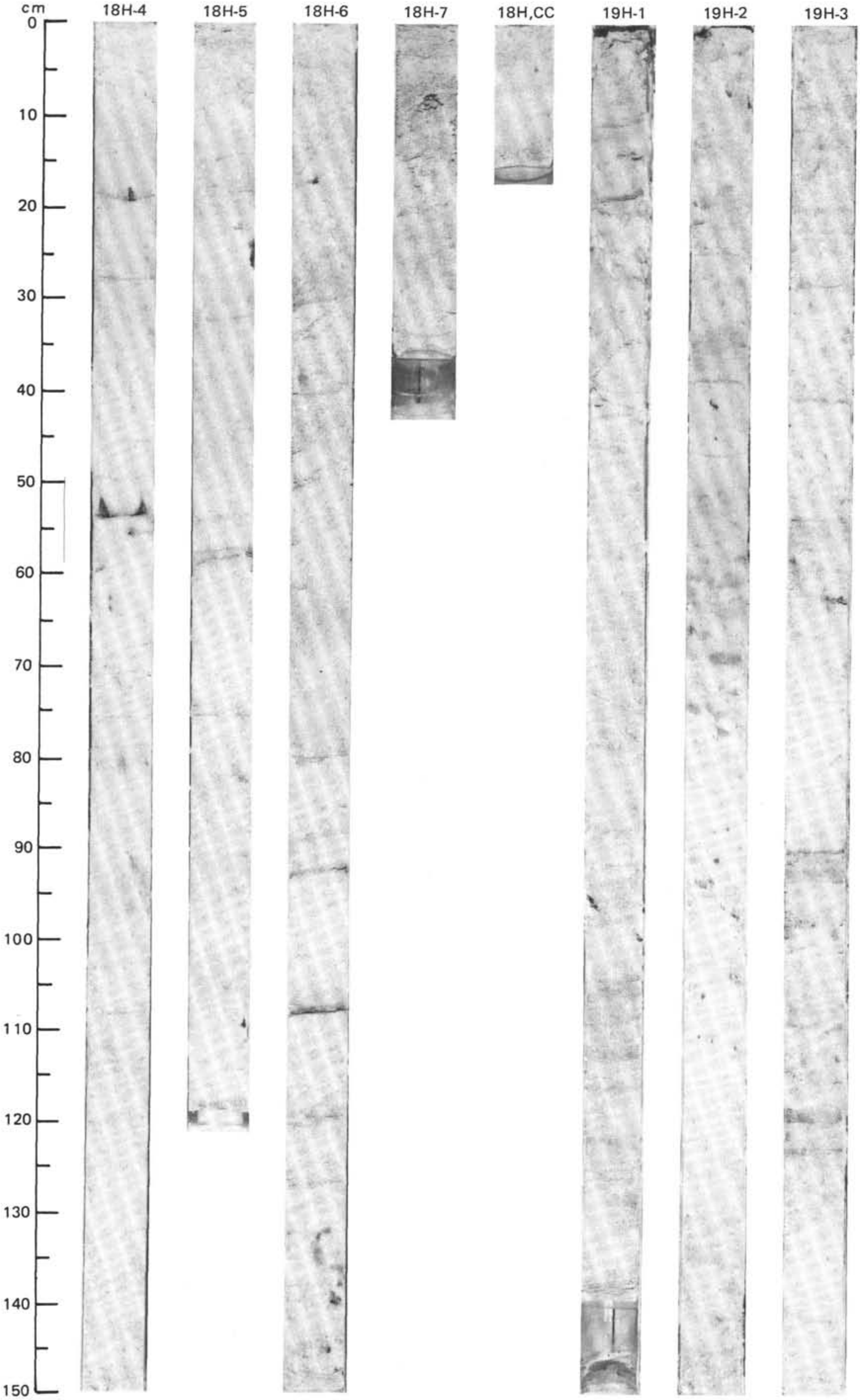
cm
18H-4
18H-5
18H-6
18H-7
18H,CC
19H-1
19H-2
19H-3
0
10
20
30
40
50
60
70
80
90
100
110
120
130
140
150

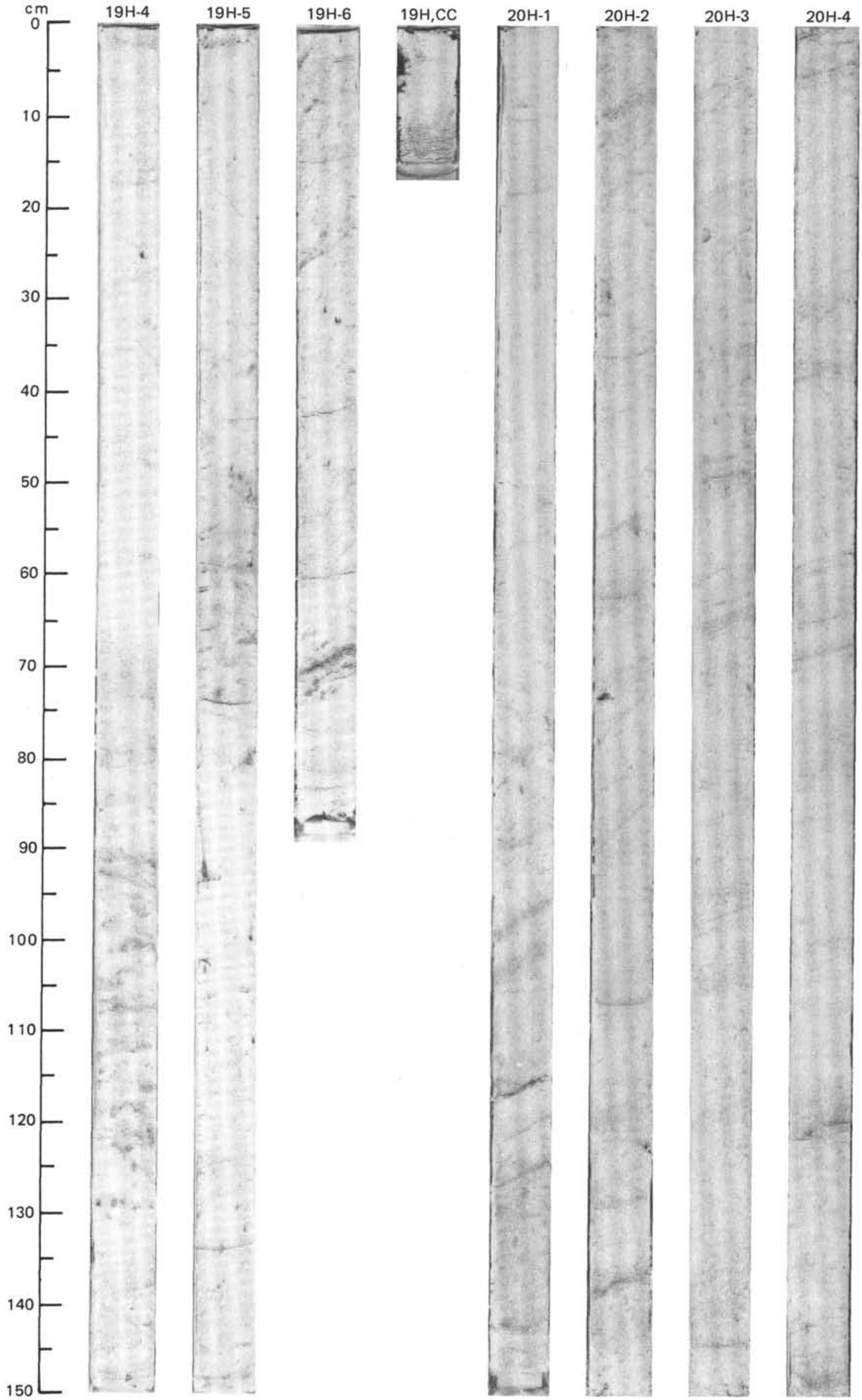
cm
0
10
20
30
40
50
60
70
80
90
100
110
120
130
140
150
19H-4
19H-5
19H-6
19H,CC
20H-1
20H-2
20H-3
20H-4

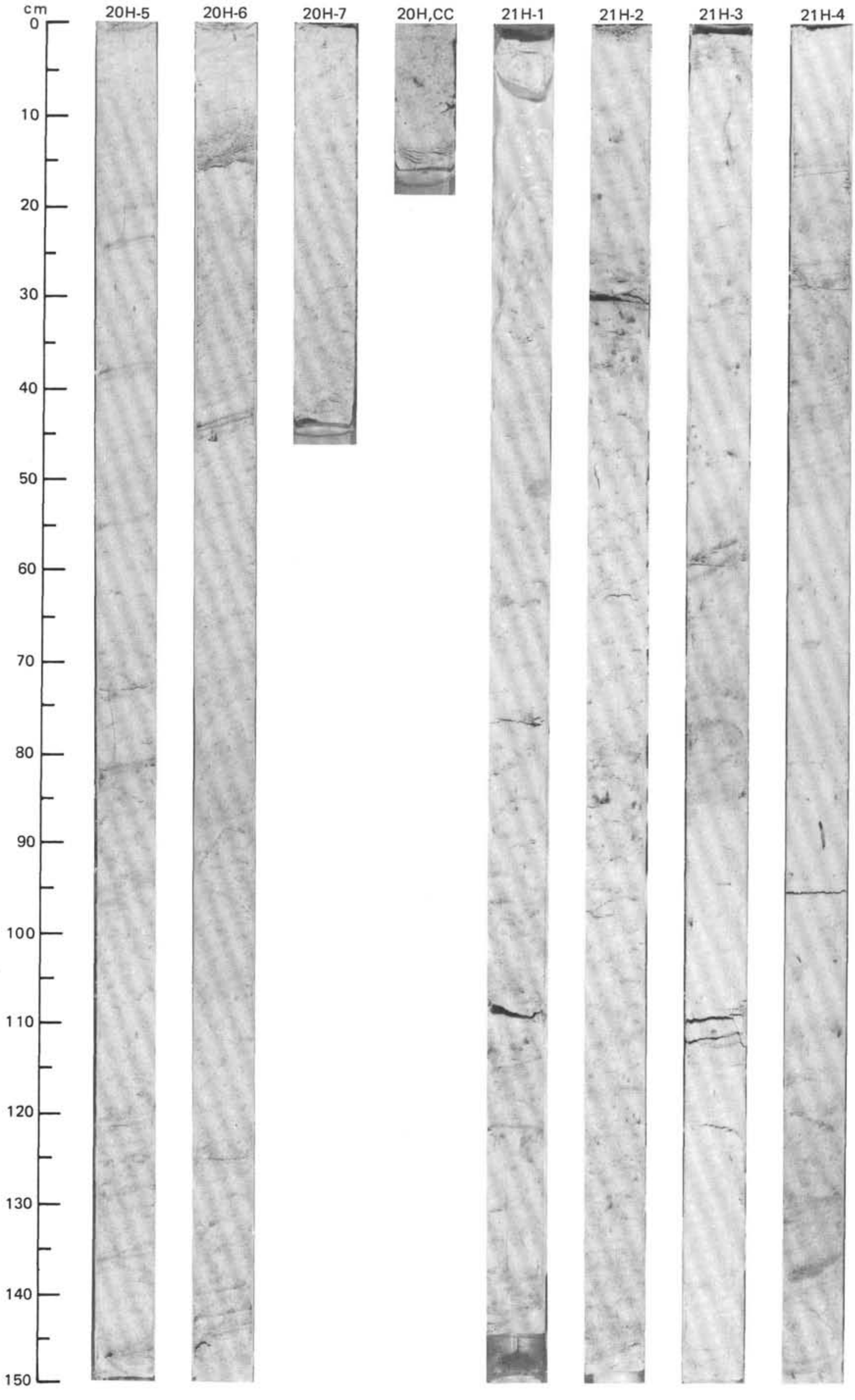
cm
0
10
20
30
40
50
60
70
80
90
100
110
120
130
140
150
20H-5
20H-6
20H-7
20H,CC
21H-1
21H-2
21H-3
21H-4

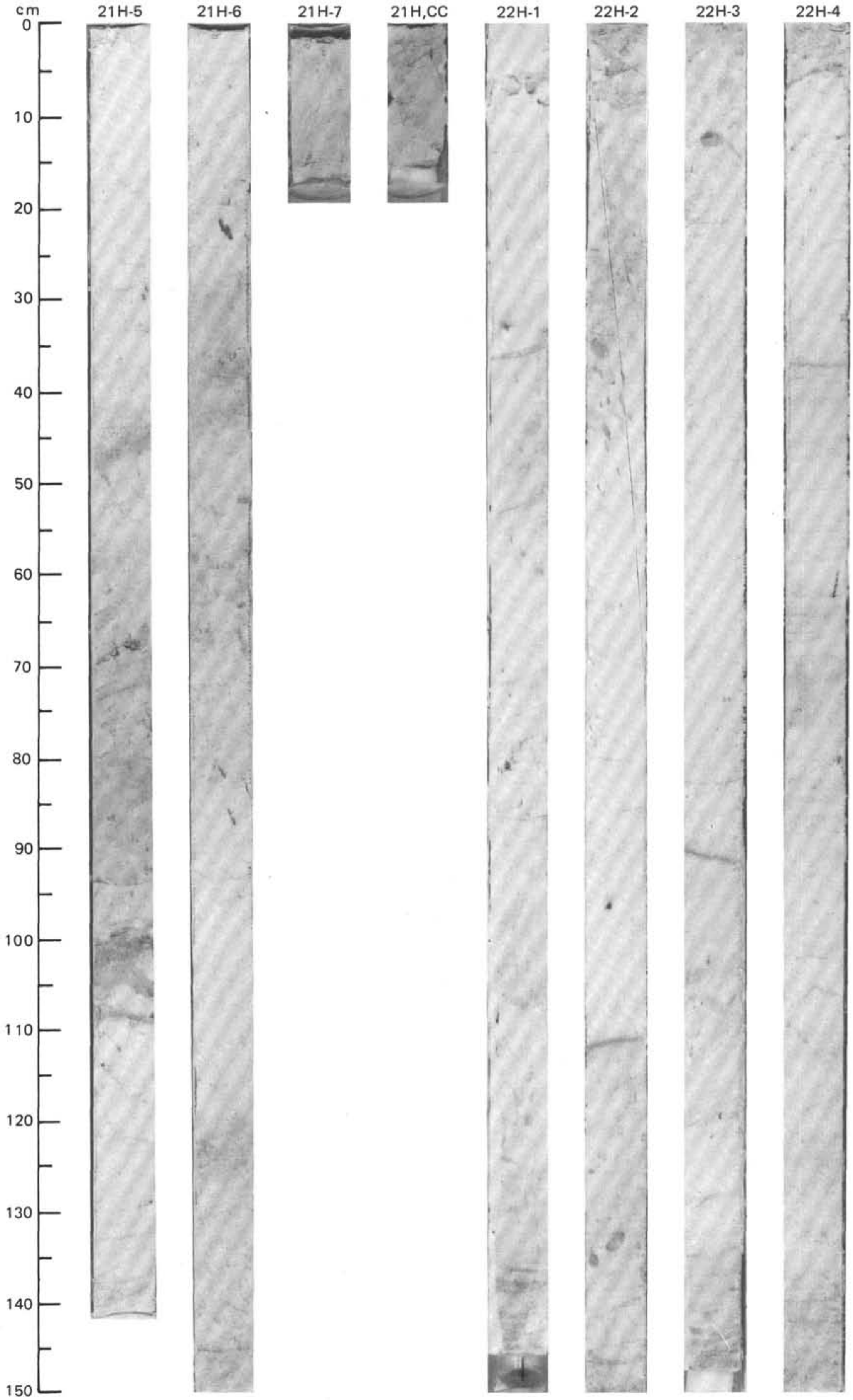
cm
21H-5
21H-6
21H-7
21H,CC
22H-1
22H-2
22H-3
22H-4
0
10
20
30
40
50
60
70
80
90
100
110
120
130
140
150

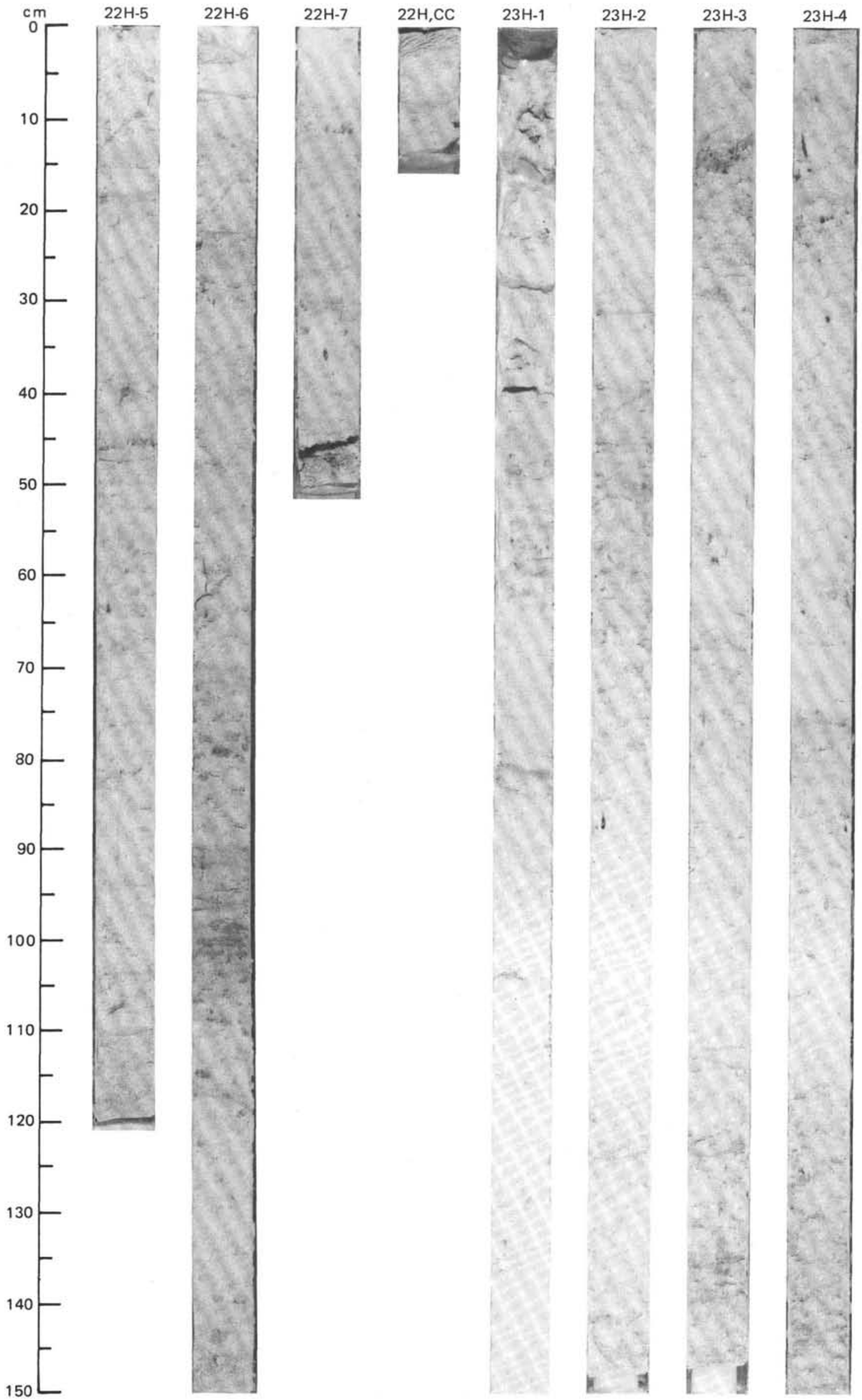
cm
0
10
20
30
40
50
60
70
80
90
100
110
120
130
140
150
22H-5
22H-6
22H-7
22H,CC
23H-1
23H-2
23H-3
23H-4

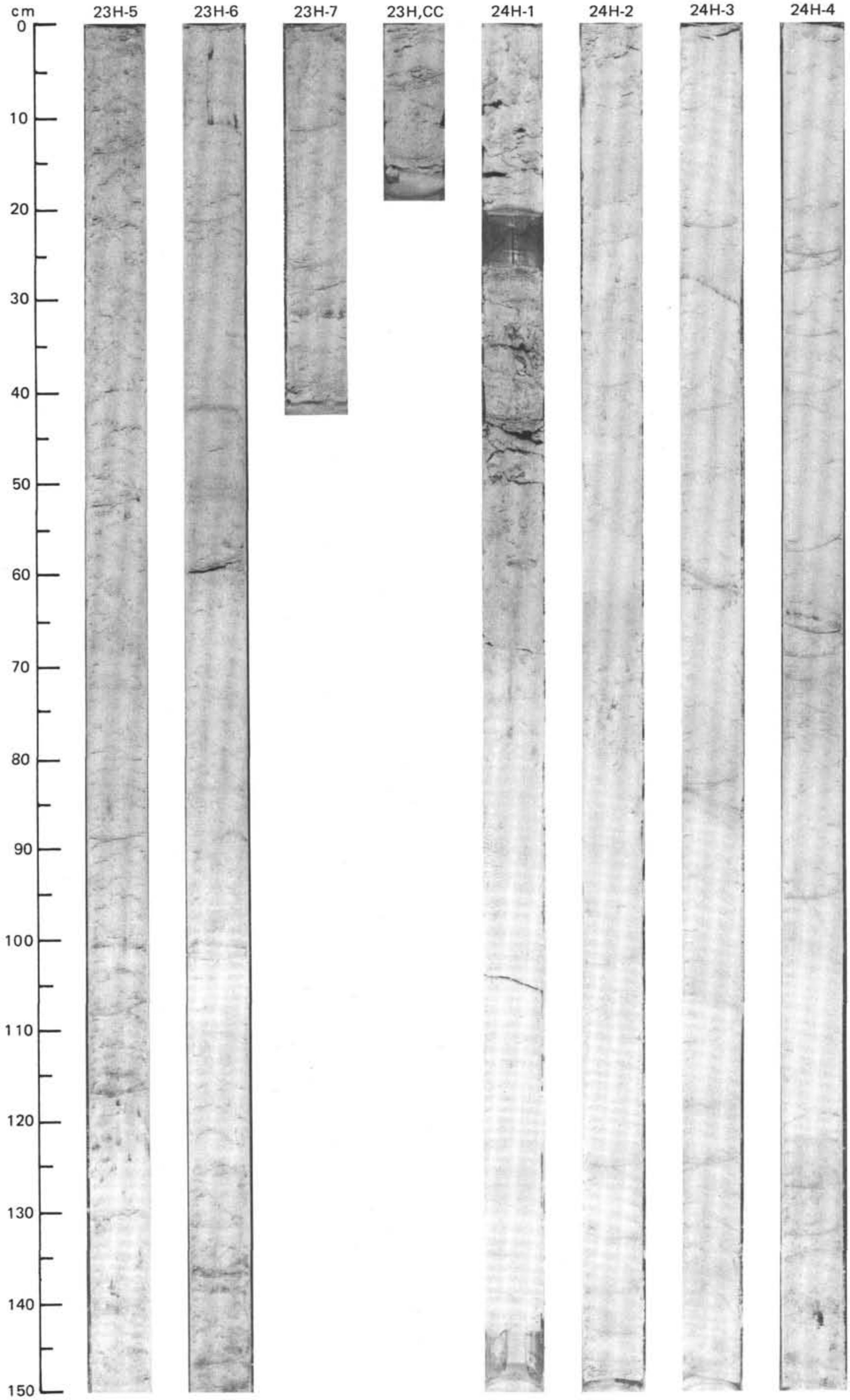
cm
0
10
20
30
40
50
60
70
80
90
100
110
120
130
140
150
23H-5
23H-6
23H-7
23H,CC
24H-1
24H-2
24H-3
24H-4

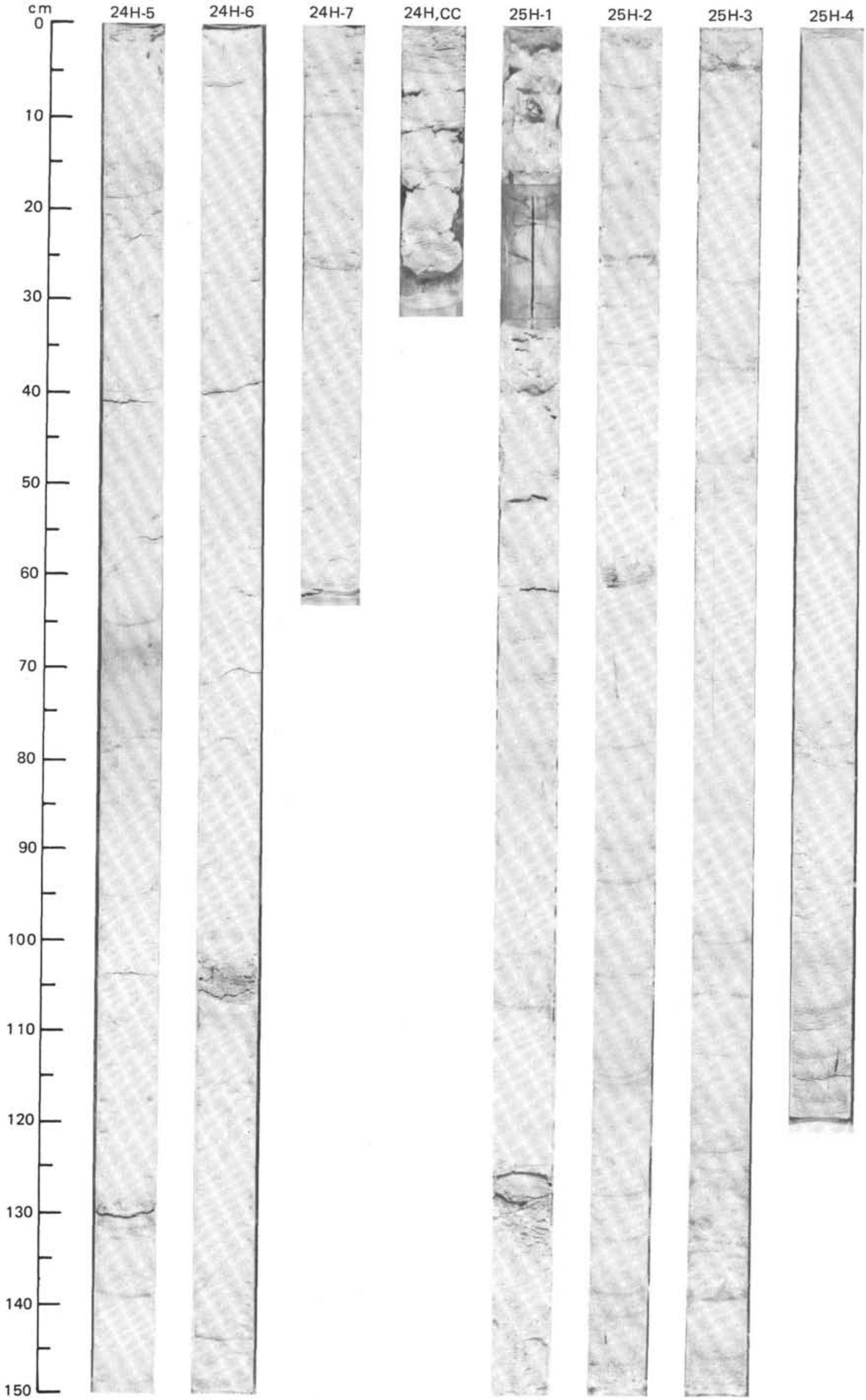
cm
0
10
20
30
40
50
60
70
80
90
100
110
120
130
140
150
24H-5
24H-6
24H-7
24H,CC
25H-1
25H-2
25H-3
25H-4

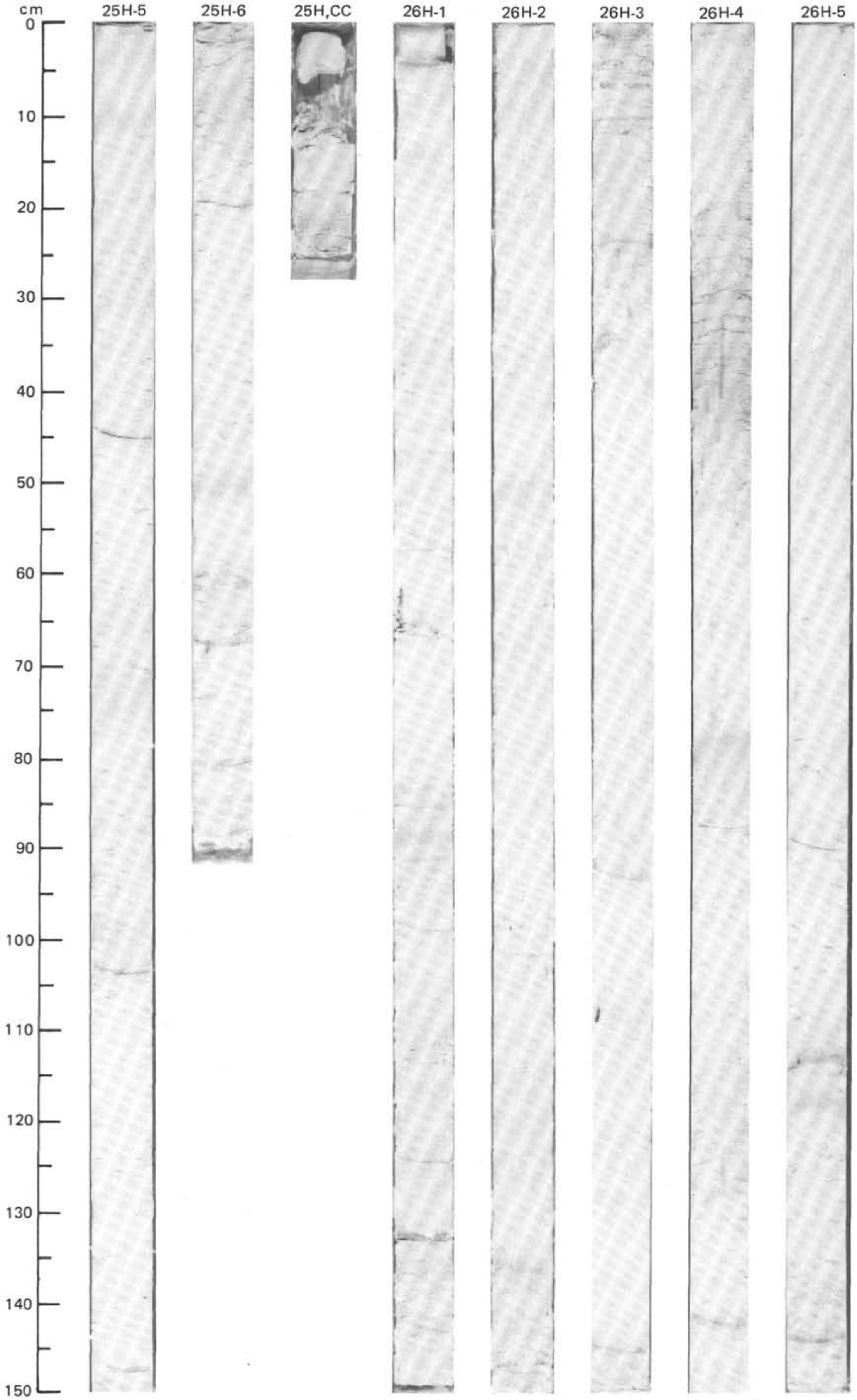
cm
0
10
20
30
40
50
60
70
80
90
100
110
120
130
140
150
25H-5
25H-6
25H,CC
26H-1
26H-2
26H-3
26H-4
26H-5

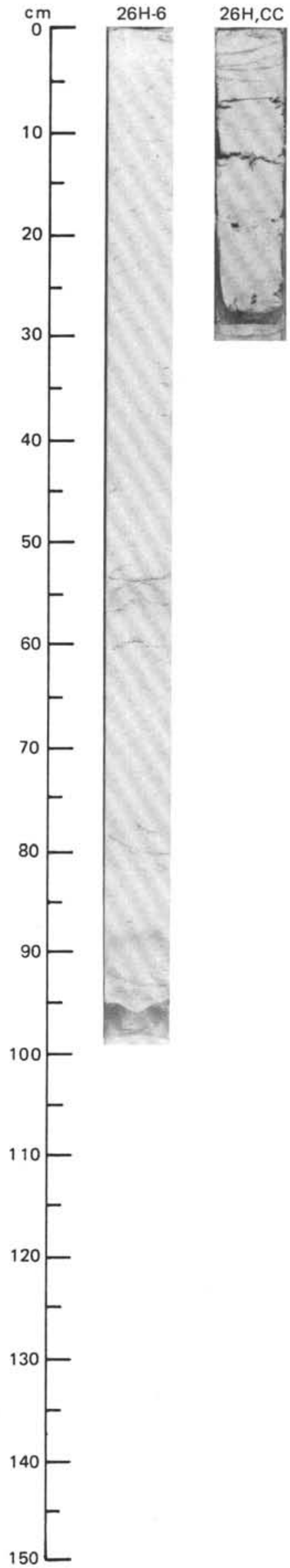
cm
26H-6
26H,CC
0
10
20
30
40
50
60
70
80
90
100
110
120
130
140
150

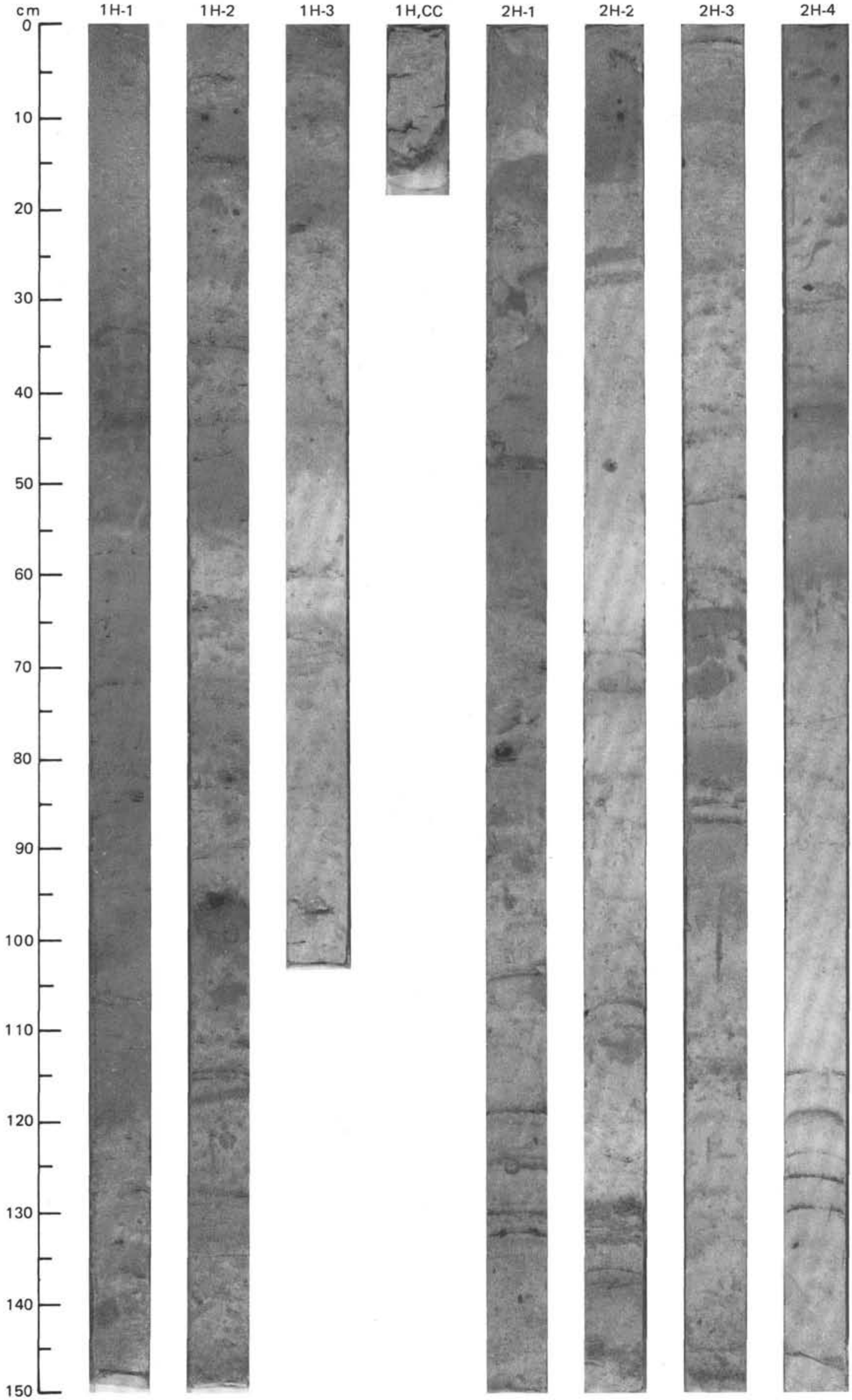
cm
0
10
20
30
40
50
60
70
80
90
100
110
120
130
140
150
1H-1
1H-2
1H-3
1H,CC
2H-1
2H-2
2H-3
2H-4

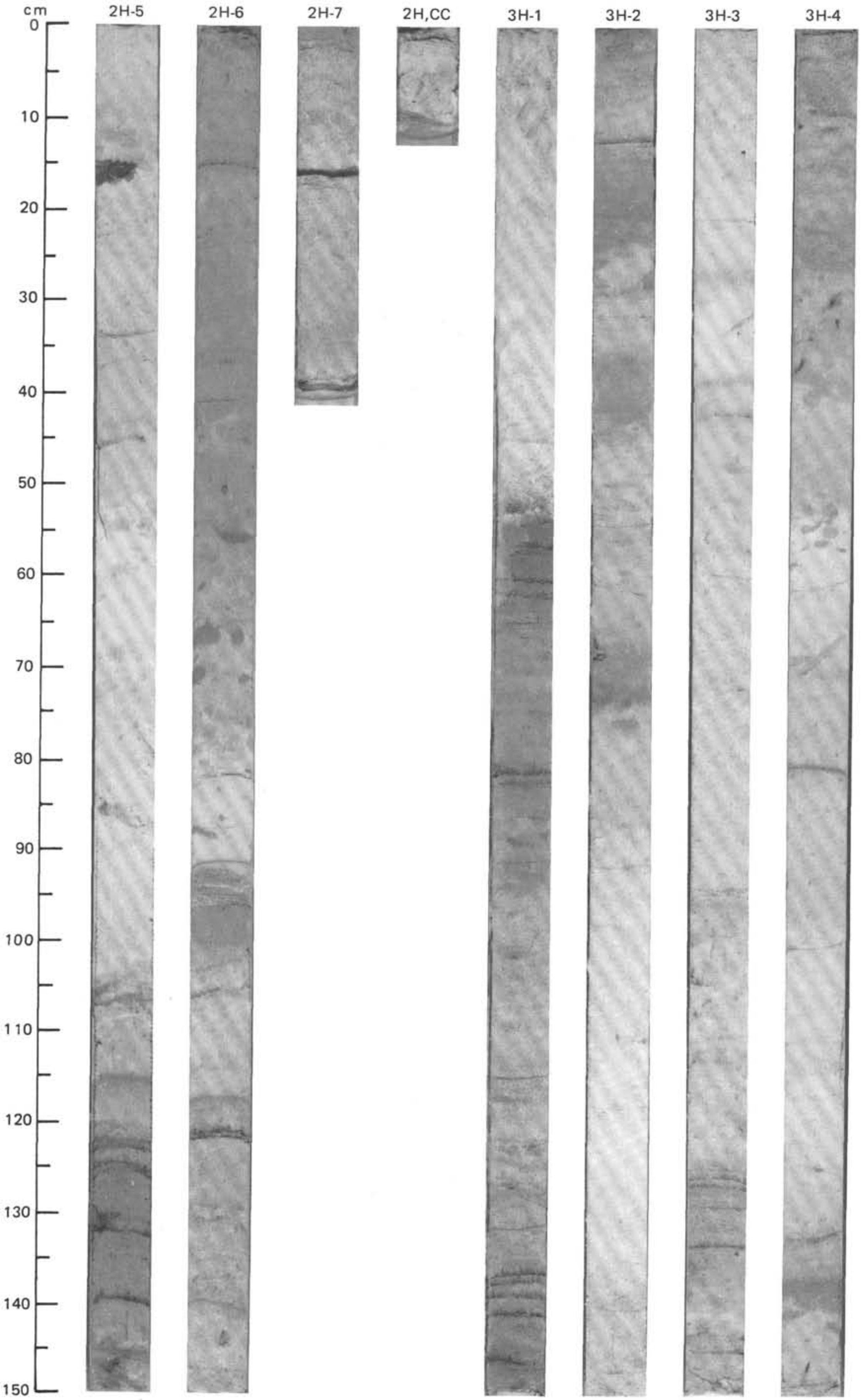
cm
0
10
20
30
40
50
60
70
80
90
100
110
120
130
140
150
2H-5
2H-6
2H-7
2H,CC
3H-1
3H-2
3H-3
3H-4

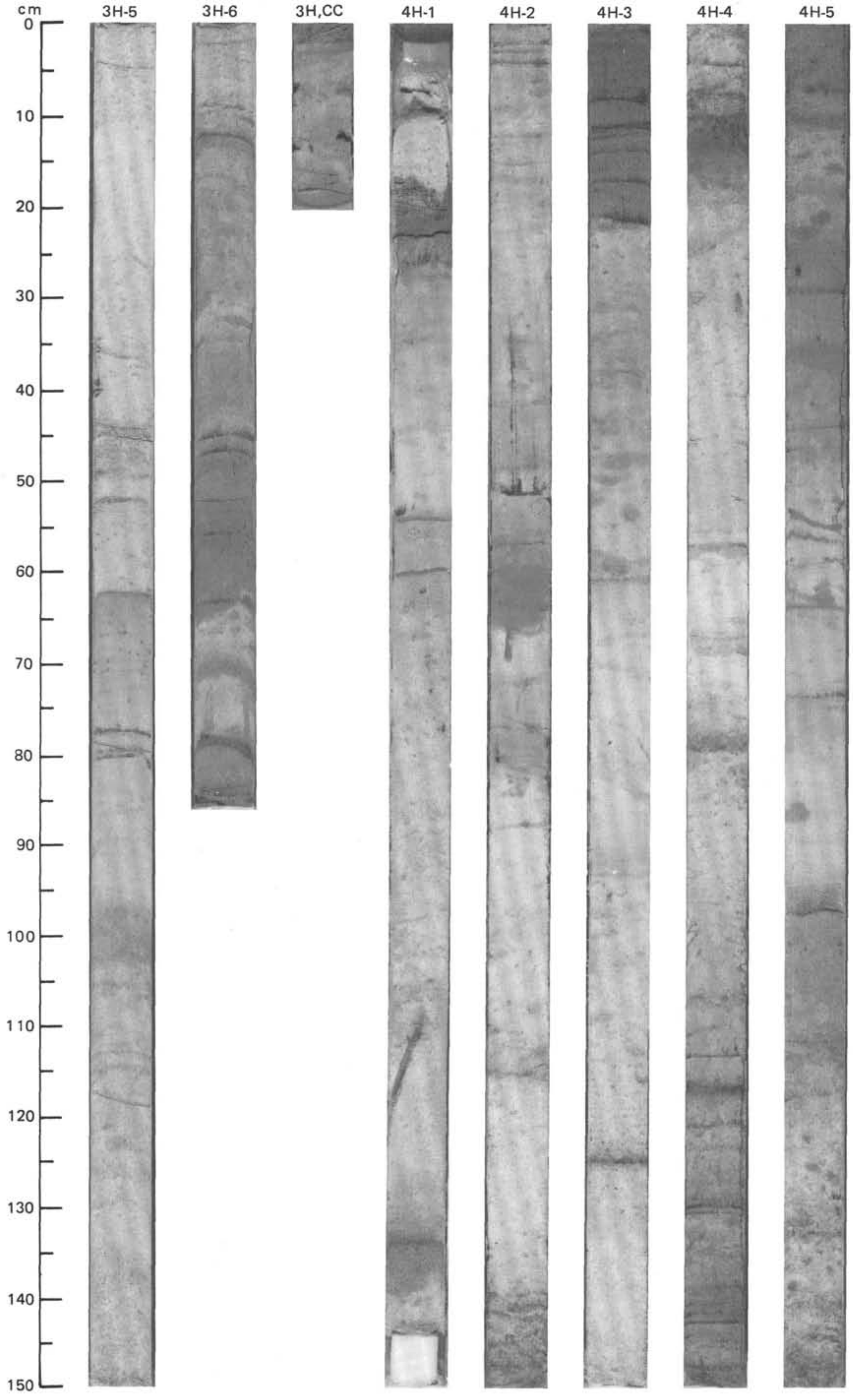
cm
0
10
20
30
40
50
60
70
80
90
100
110
120
130
140
150
3H-5
3H-6
3H,CC
4H-1
4H-2
4H-3
4H-4
4H-5

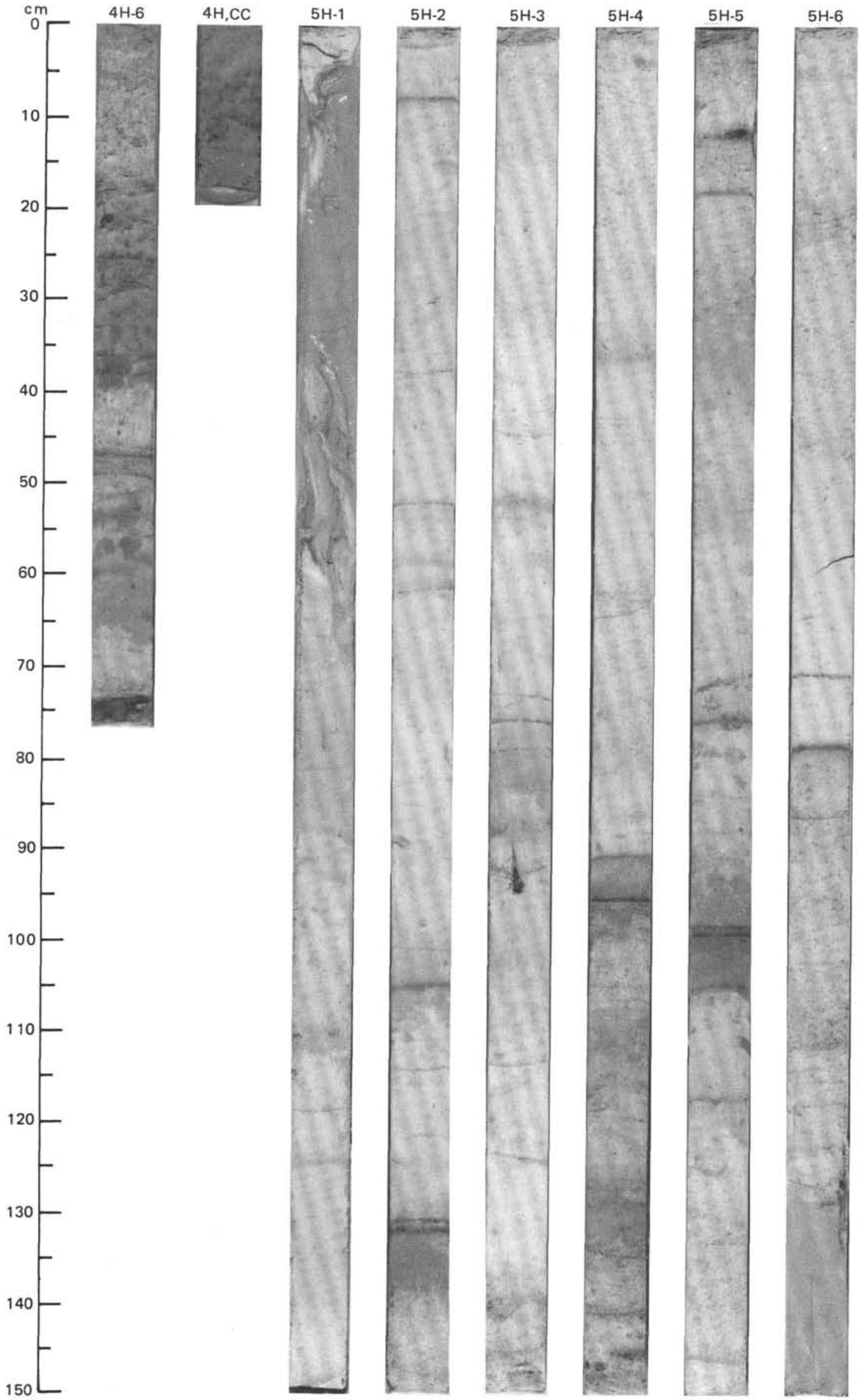
cm
0
10
20
30
40
50
60
70
80
90
100
110
120
130
140
150
4H-6
4H,CC
5H-1
5H-2
5H-3
5H-4
5H-5
5H-6

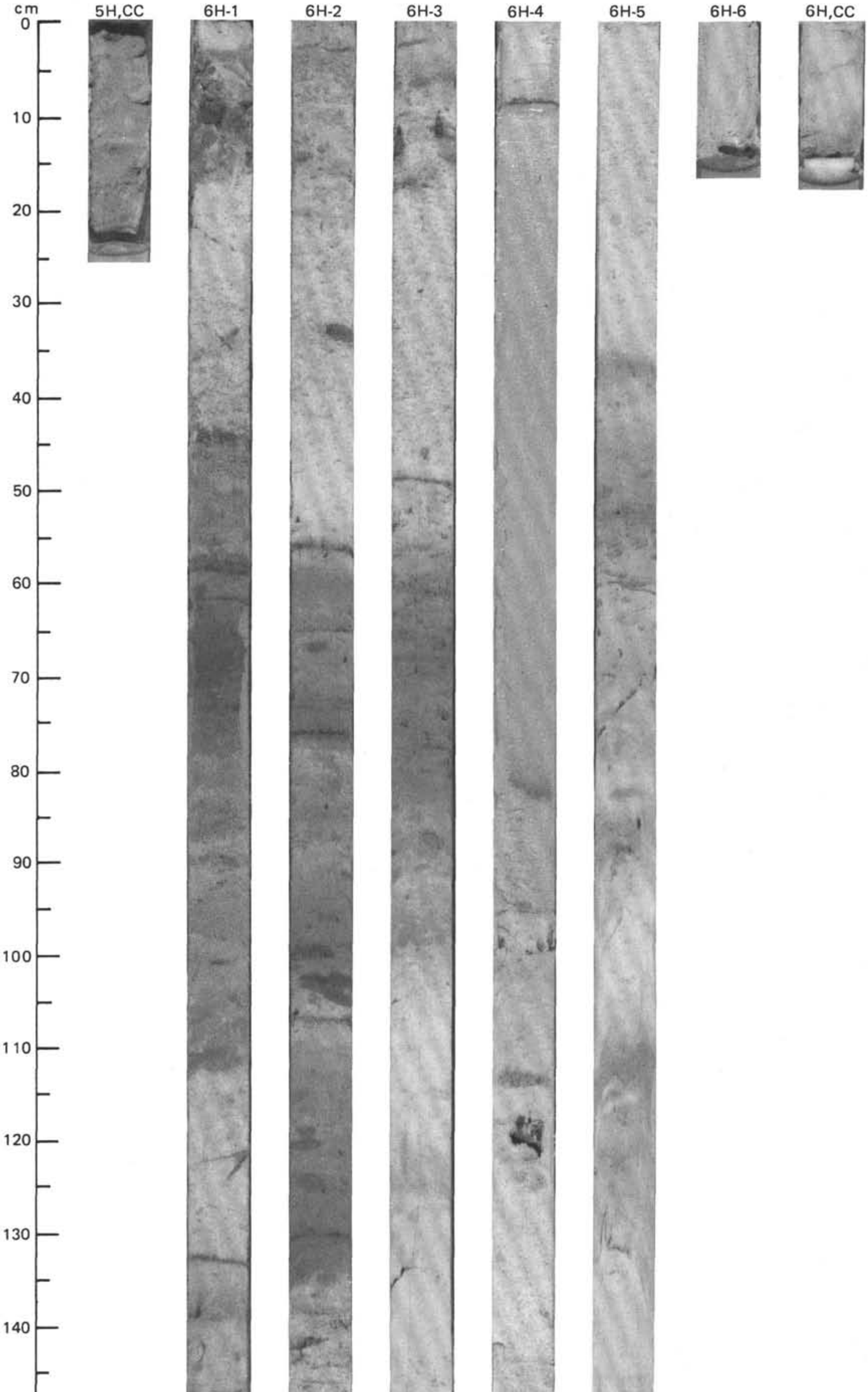
cm
0
10
20
30
40
50
60
70
80
90
100
110
120
130
140
150
5H,CC
6H-1
6H-2
6H-3
6H-4
6H-5
6H-6
6H,CC

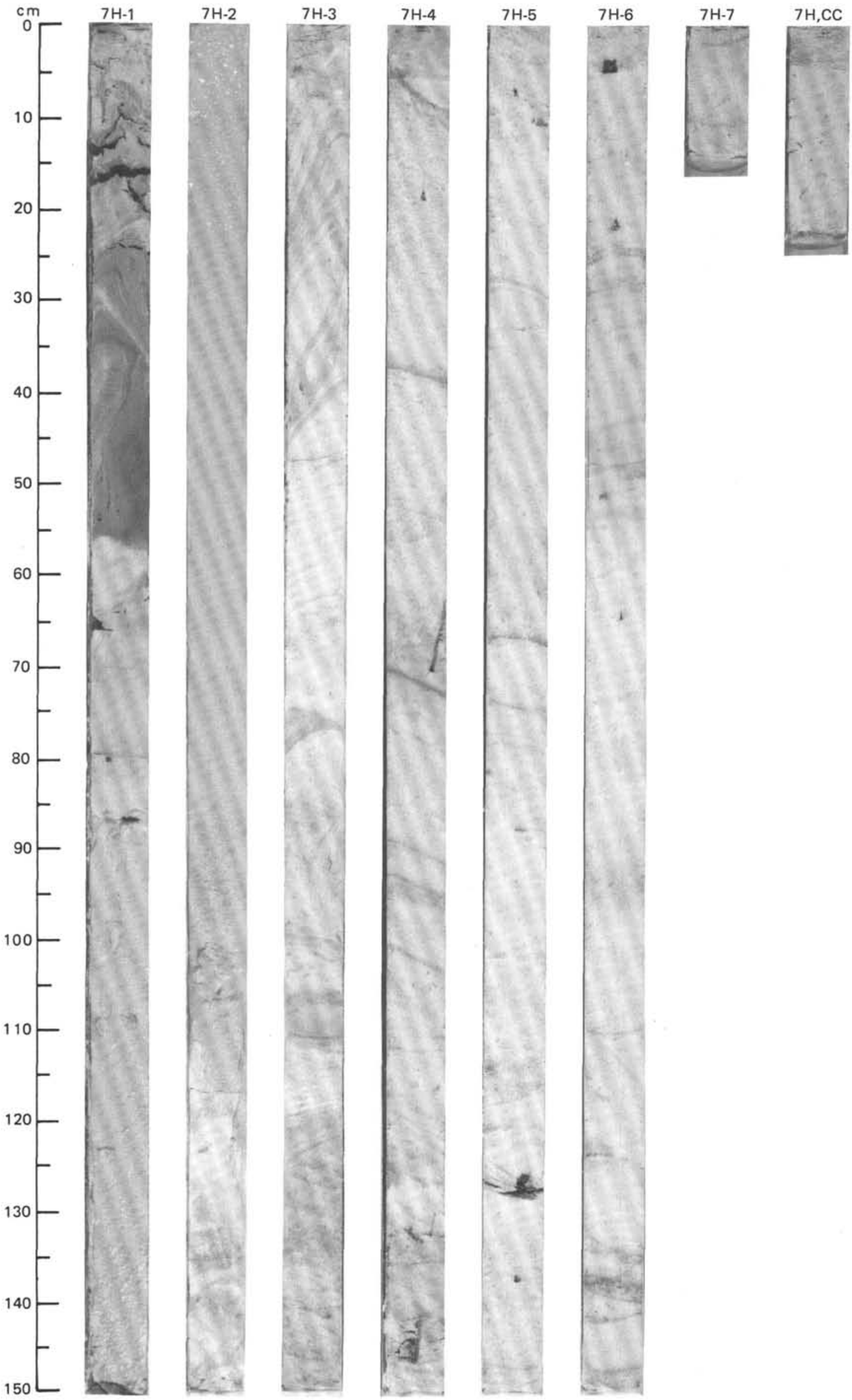
cm
0
10
20
30
40
50
60
70
80
90
100
110
120
130
140
150
7H-1
7H-2
7H-3
7H-4
7H-5
7H-6
7H-7
7H,CC

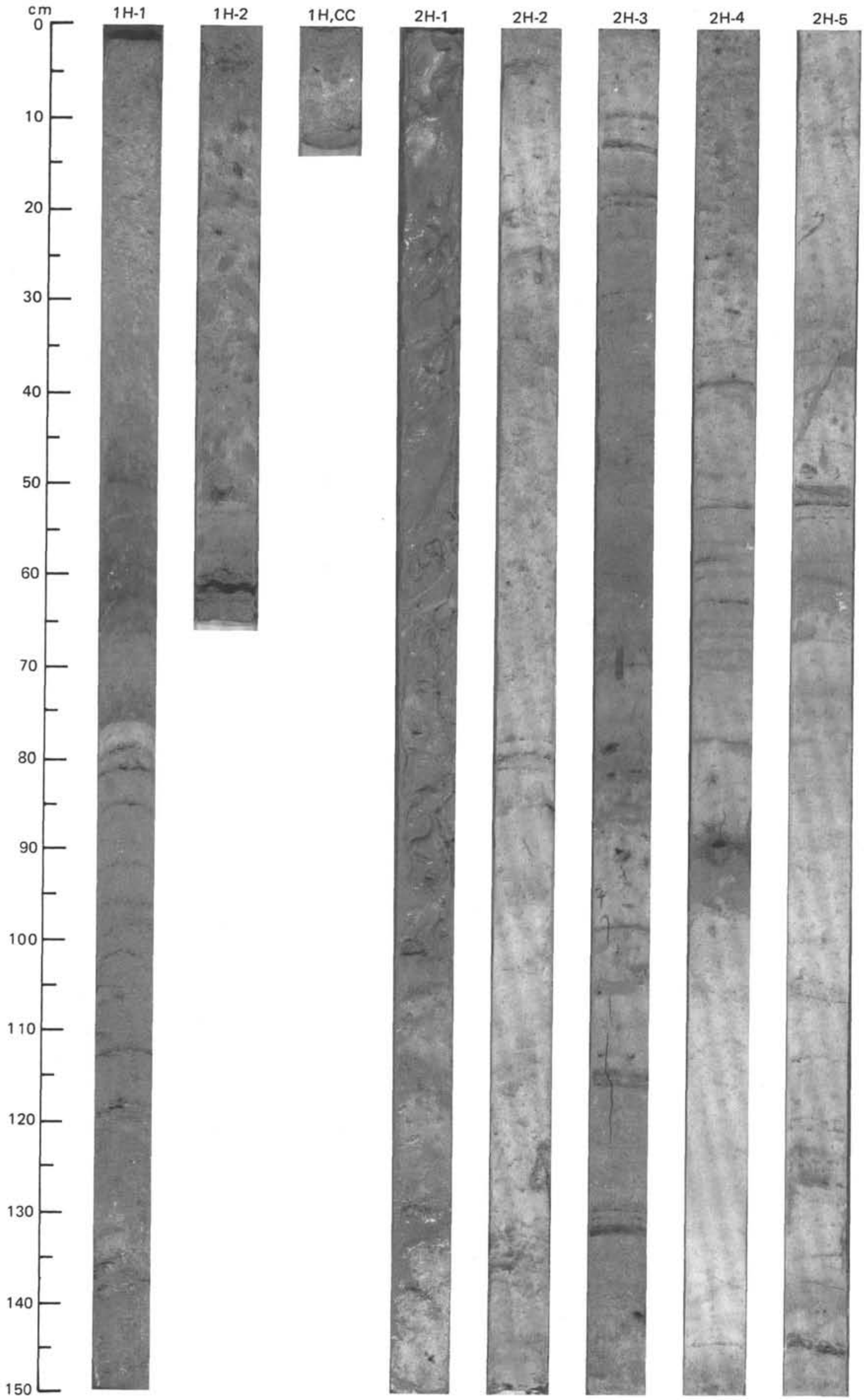
cm
0
10
20
30
40
50
60
70
80
90
100
110
120
130
140
150
1H-1
1H-2
1H,CC
2H-1
2H-2
2H-3
2H-4
2H-5

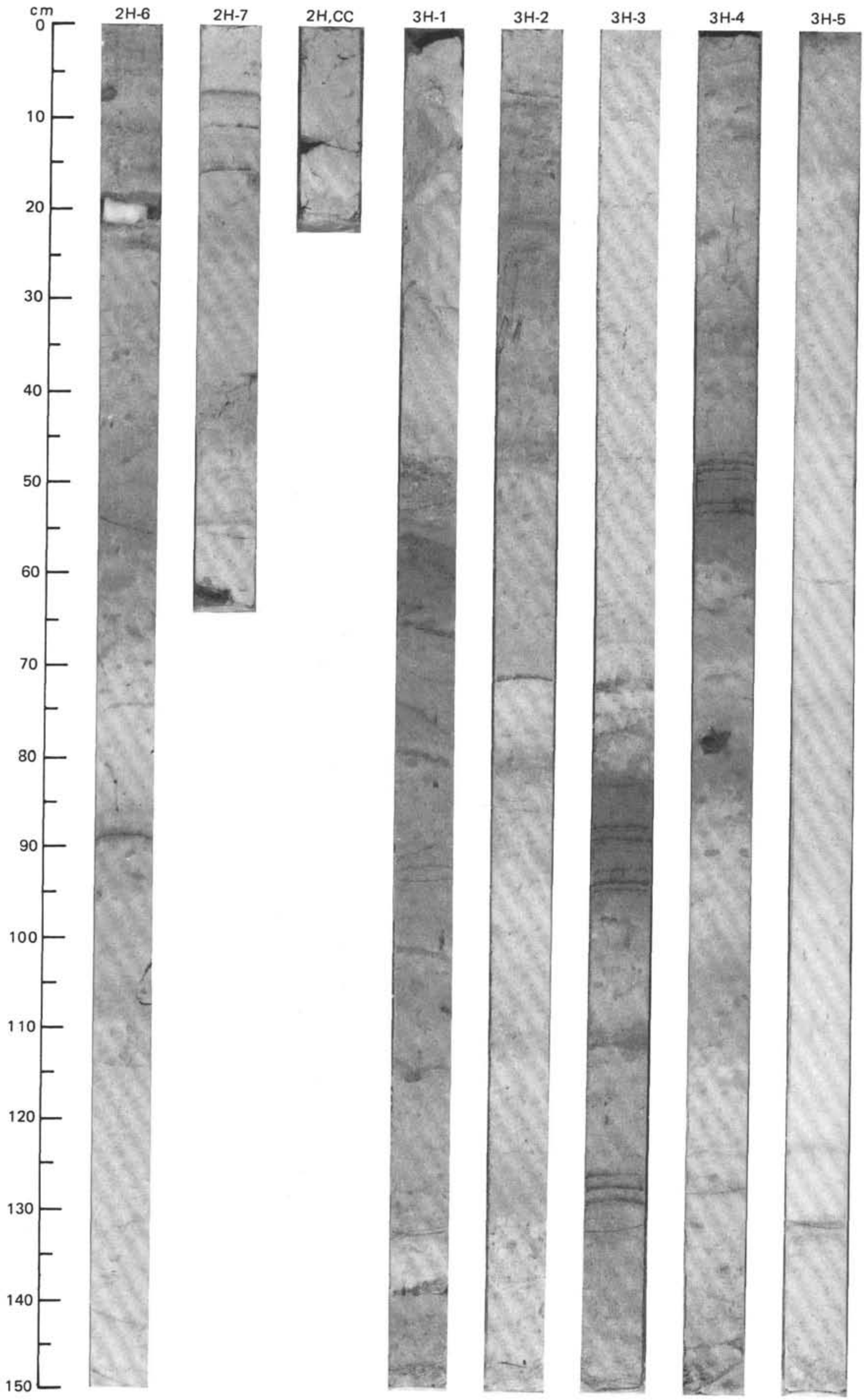
cm
0
10
20
30
40
50
60
70
80
90
100
110
120
130
140
150
2H-6
2H-7
2H,CC
3H-1
3H-2
3H-3
3H-4
3H-5

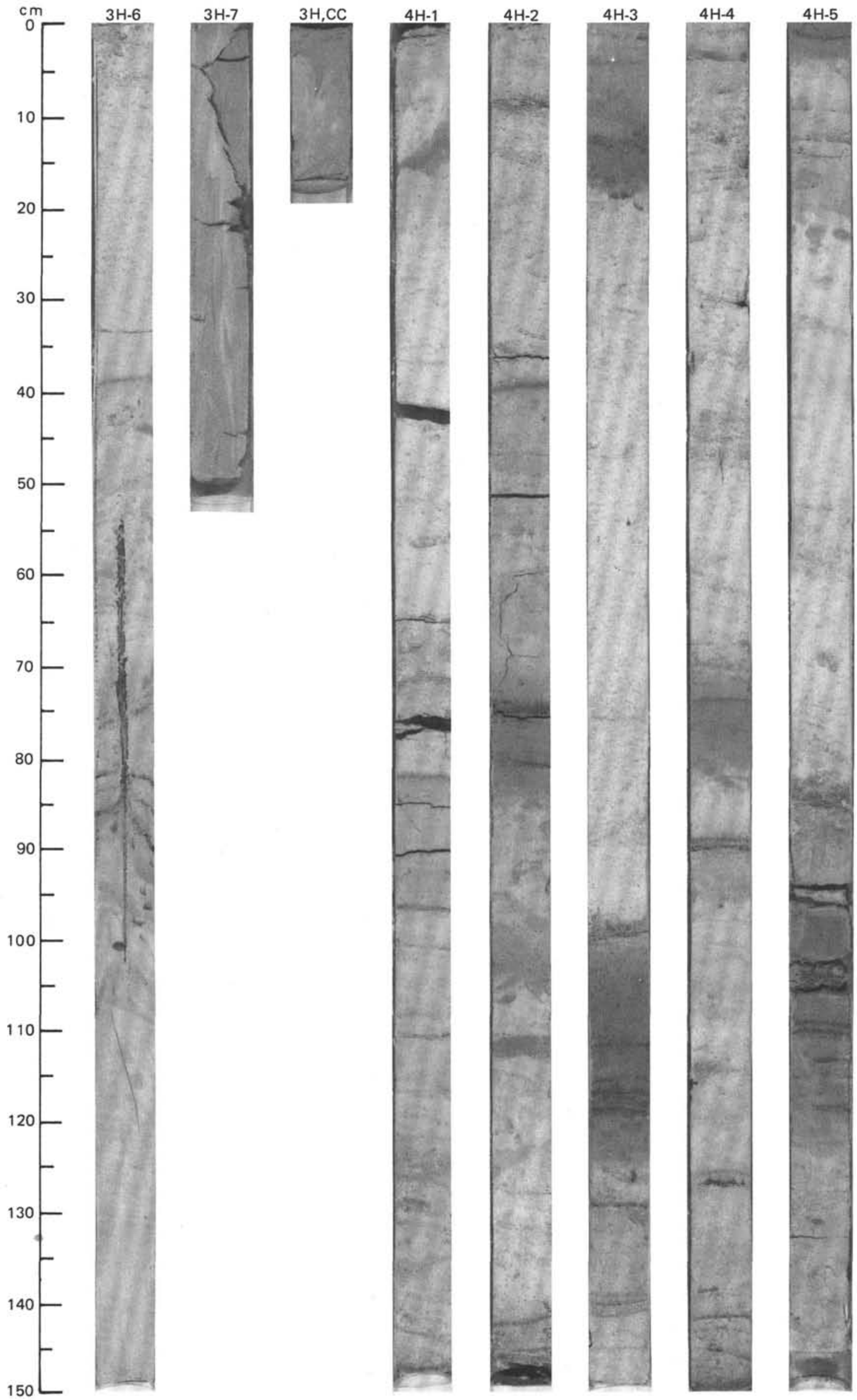
cm
0
10
20
30
40
50
60
70
80
90
100
110
120
130
140
150
3H-6
3H-7
3H,CC
4H-1
4H-2
4H-3
4H-4
4H-5

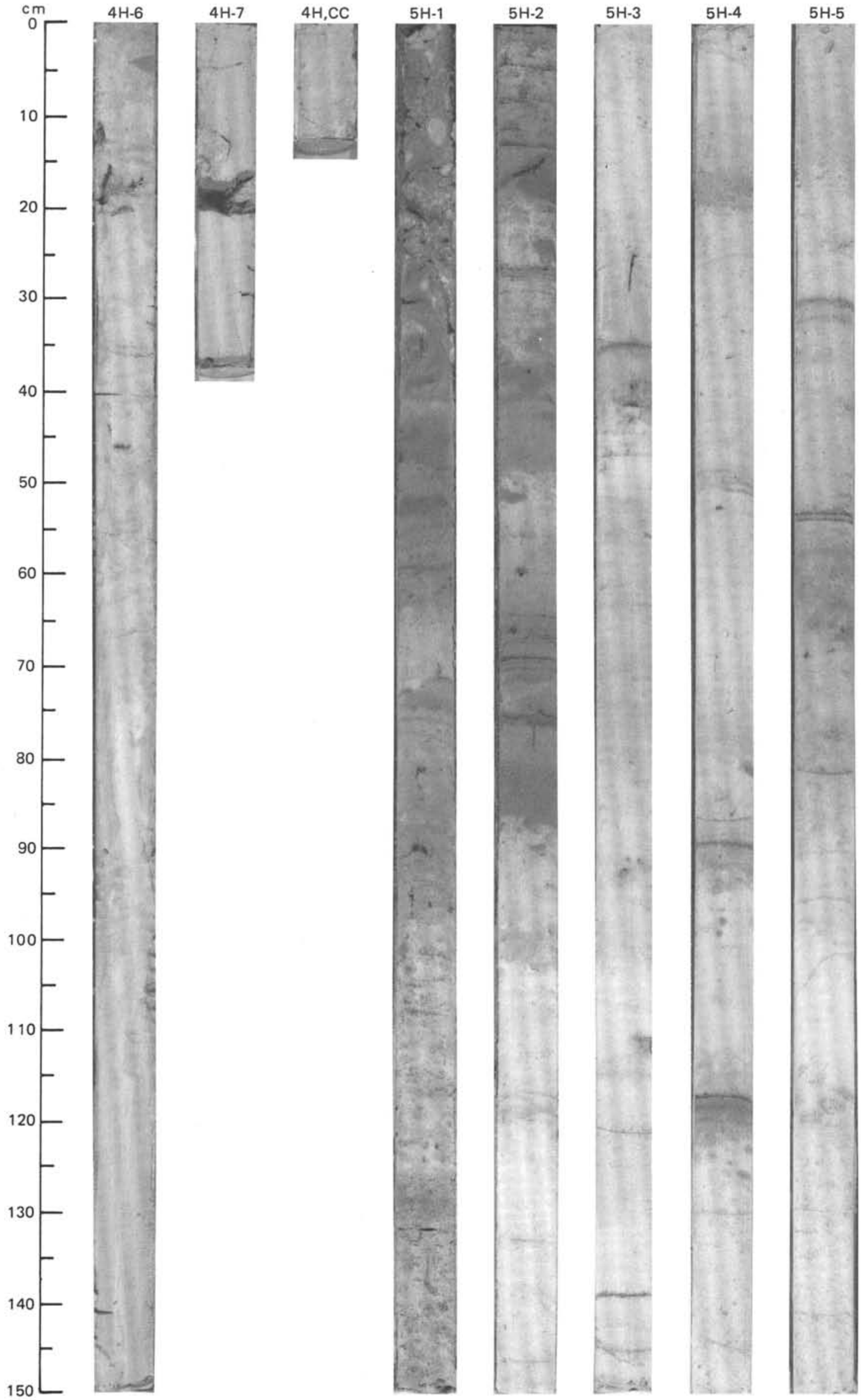
cm
0
10
20
30
40
50
60
70
80
90
100
110
120
130
140
150
4H-6
4H-7
4H,CC
5H-1
5H-2
5H-3
5H-4
5H-5

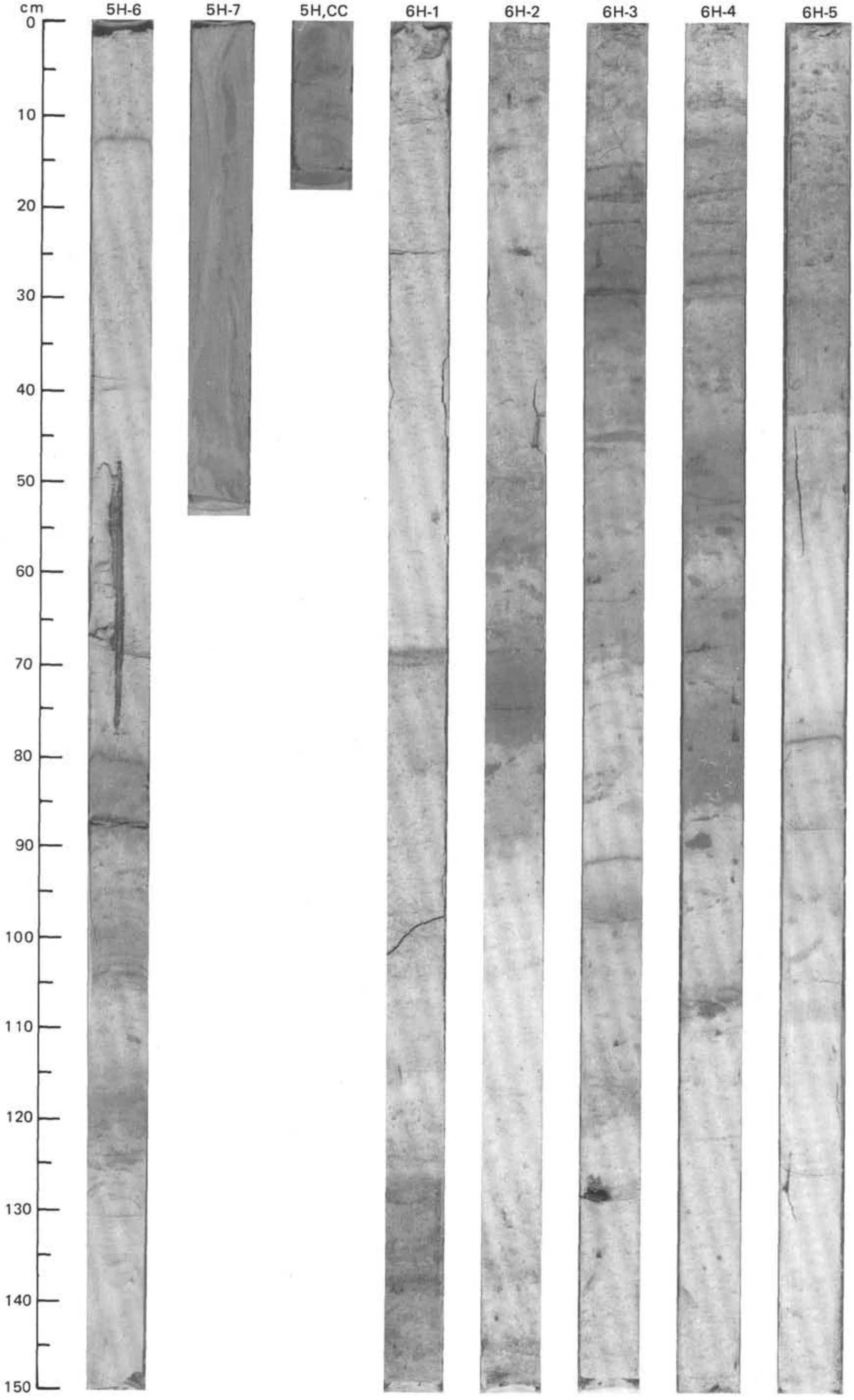
cm
0
10
20
30
40
50
60
70
80
90
100
110
120
130
140
150
5H-6
5H-7
5H,CC
6H-1
6H-2
6H-3
6H-4
6H-5

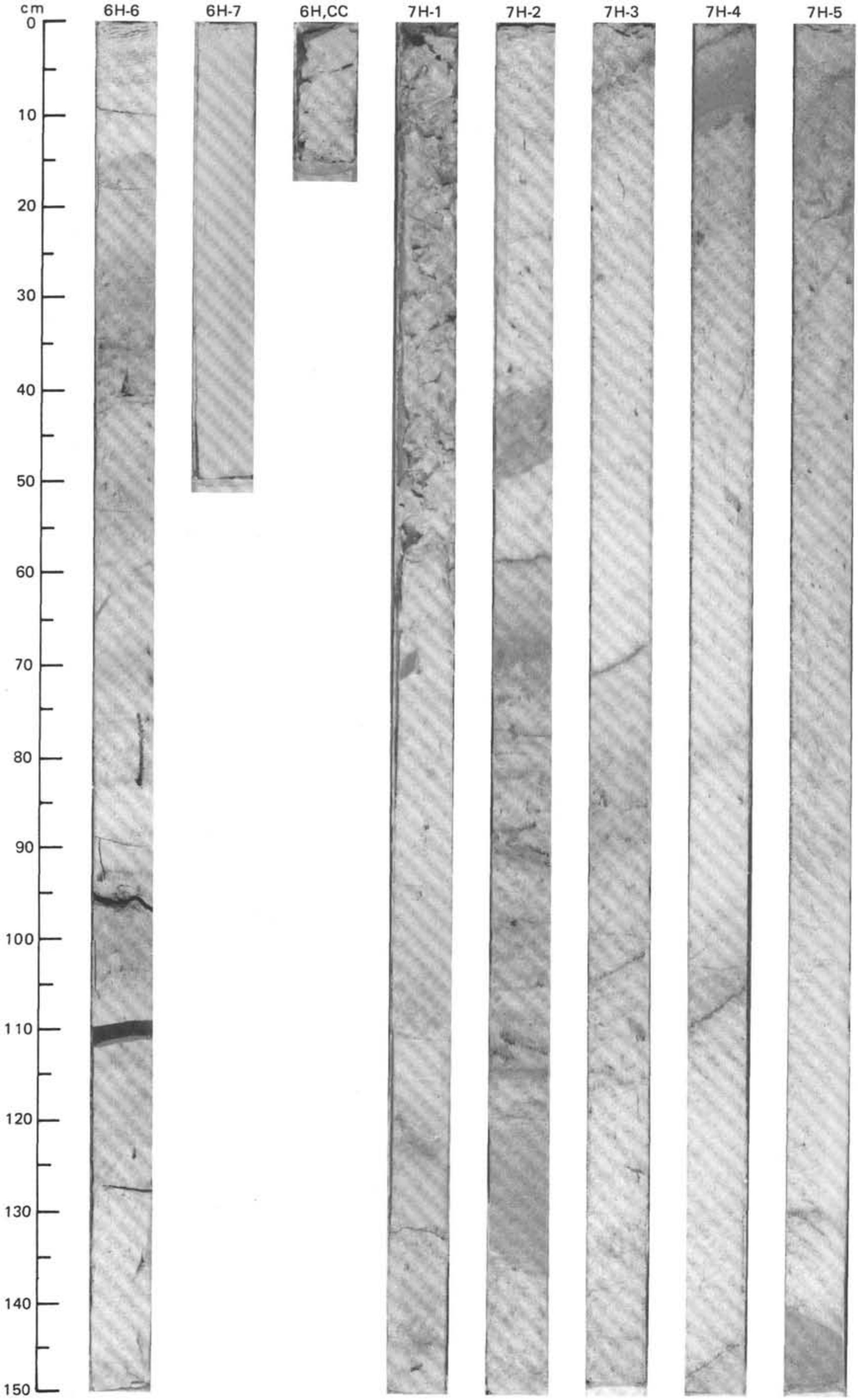
cm
0
10
20
30
40
50
60
70
80
90
100
110
120
130
140
150
6H-6
6H-7
6H,CC
7H-1
7H-2
7H-3
7H-4
7H-5

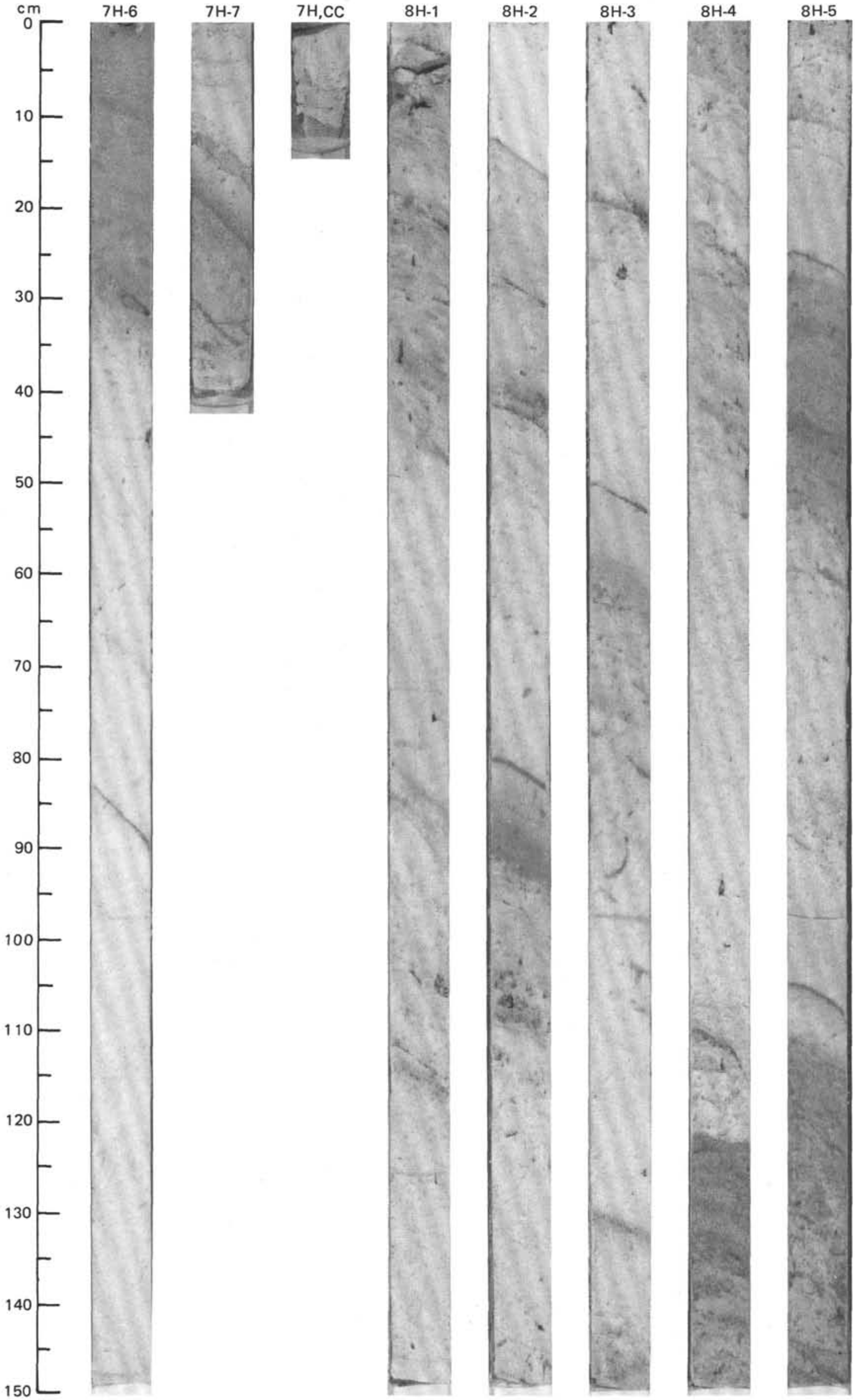
cm
0
10
20
30
40
50
60
70
80
90
100
110
120
130
140
150
7H-6
7H-7
7H,CC
8H-1
8H-2
8H-3
8H-4
8H-5

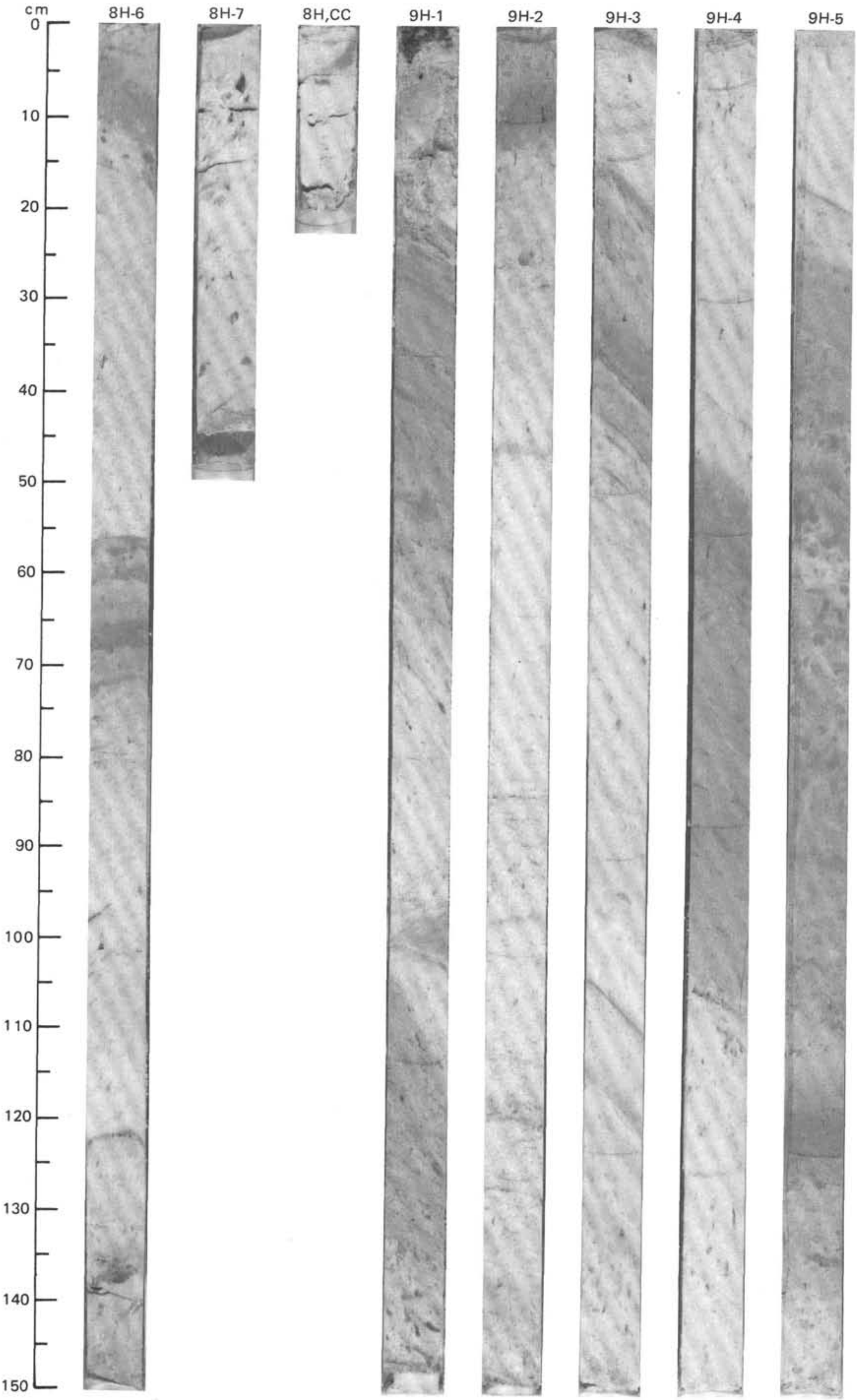
cm
0
10
20
30
40
50
60
70
80
90
100
110
120
130
140
150
8H-6
8H-7
8H,CC
9H-1
9H-2
9H-3
9H-4
9H-5

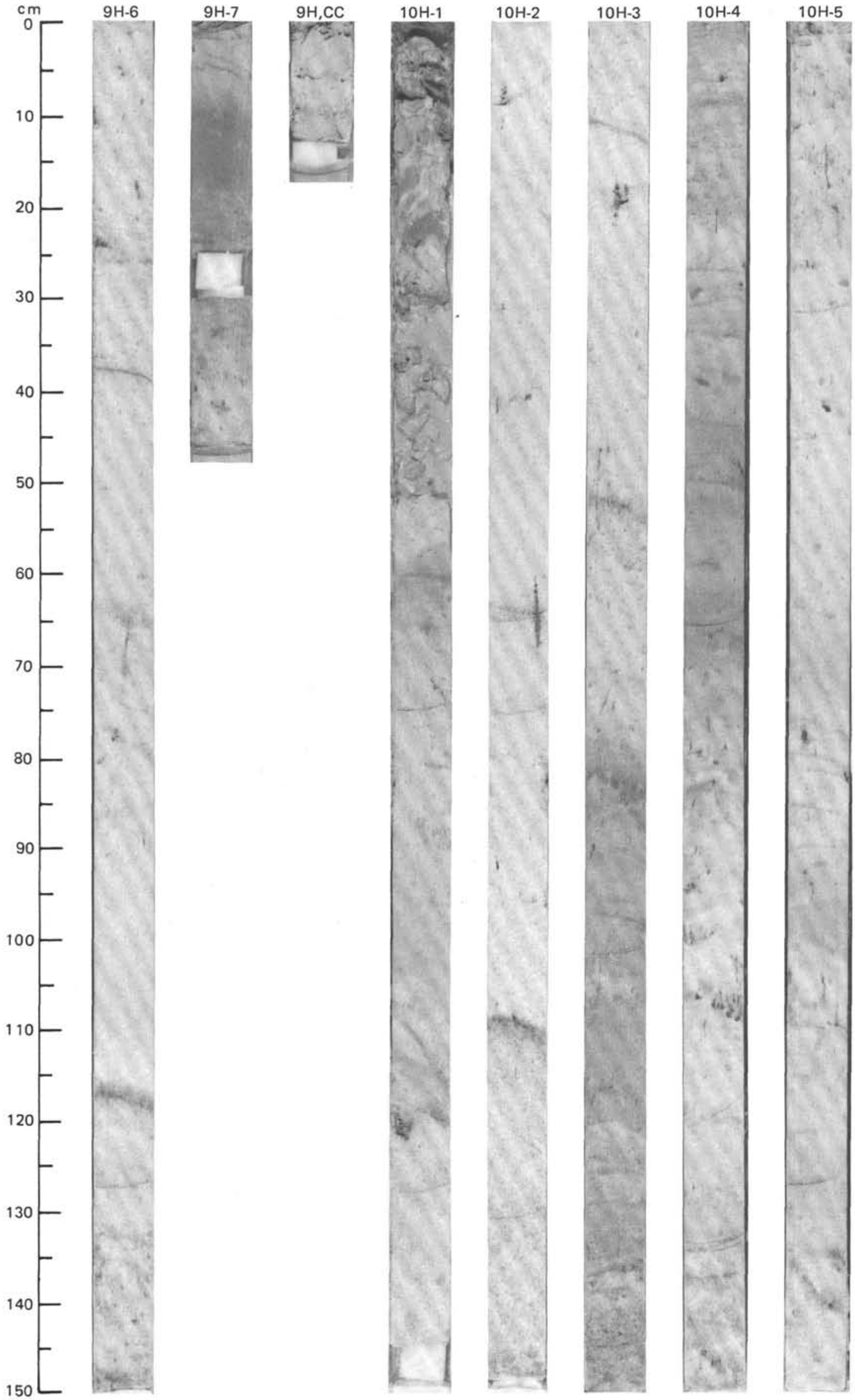
cm
0
10
20
30
40
50
60
70
80
90
100
110
120
130
140
150
9H-6
9H-7
9H,CC
10H-1
10H-2
10H-3
10H-4
10H-5

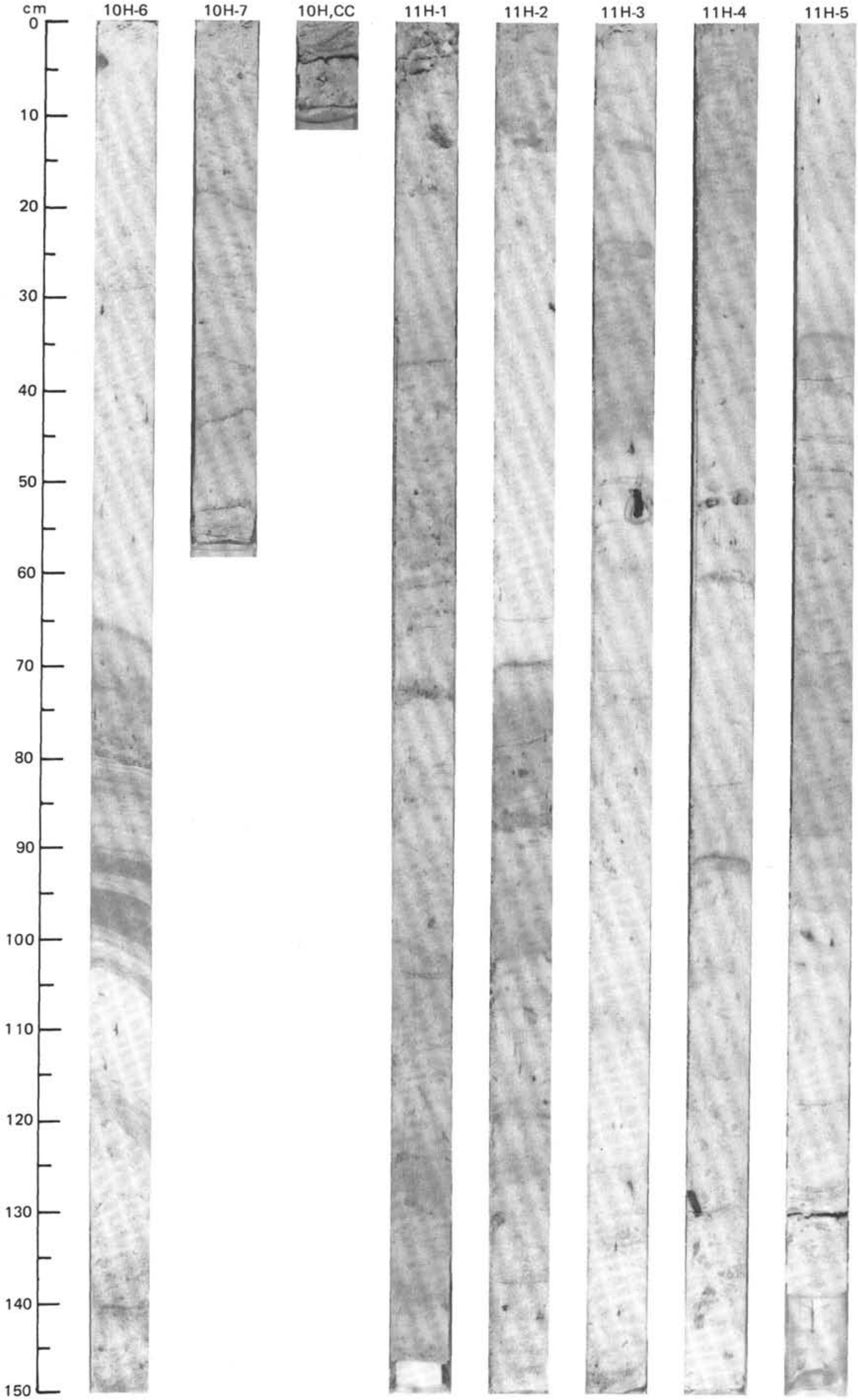
cm
0
10
20
30
40
50
60
70
80
90
100
110
120
130
140
150
10H-6
10H-7
10H,CC
11H-1
11H-2
11H-3
11H-4
11H-5

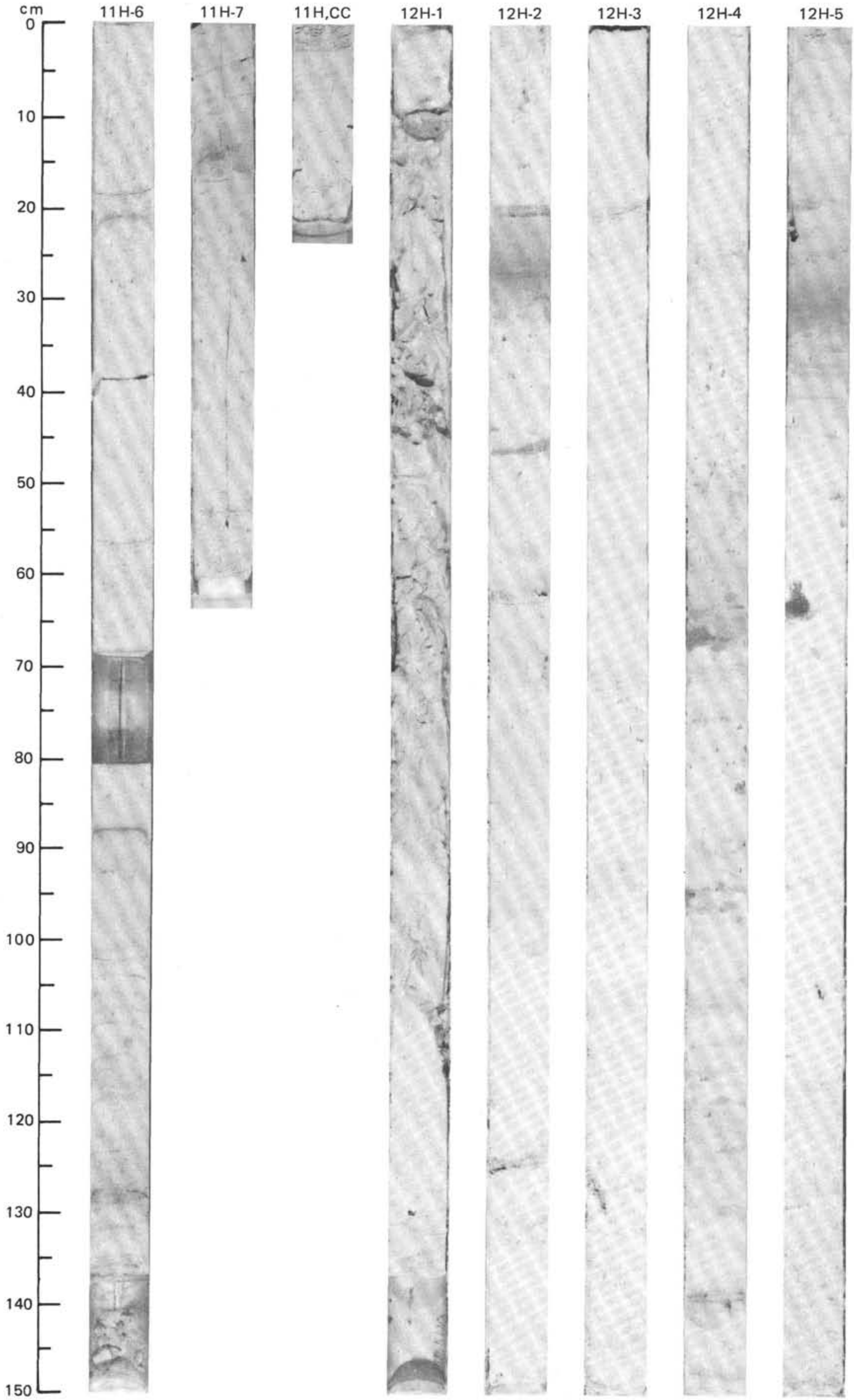
cm
0
10
20
30
40
50
60
70
80
90
100
110
120
130
140
150
11H-6
11H-7
11H,CC
12H-1
12H-2
12H-3
12H-4
12H-5

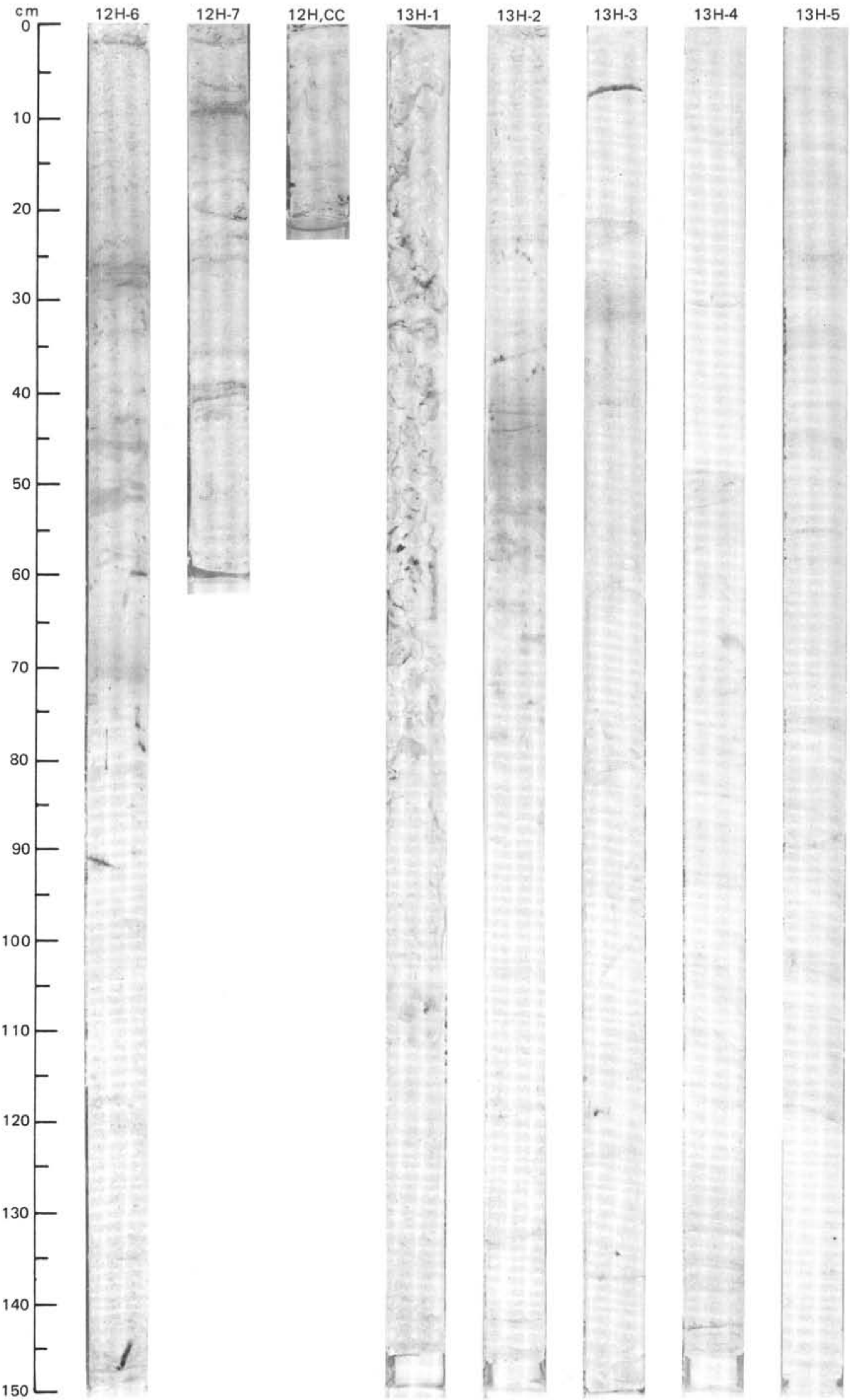
cm
0
10
20
30
40
50
60
70
80
90
100
110
120
130
140
150
12H-6
12H-7
12H,CC
13H-1
13H-2
13H-3
13H-4
13H-5

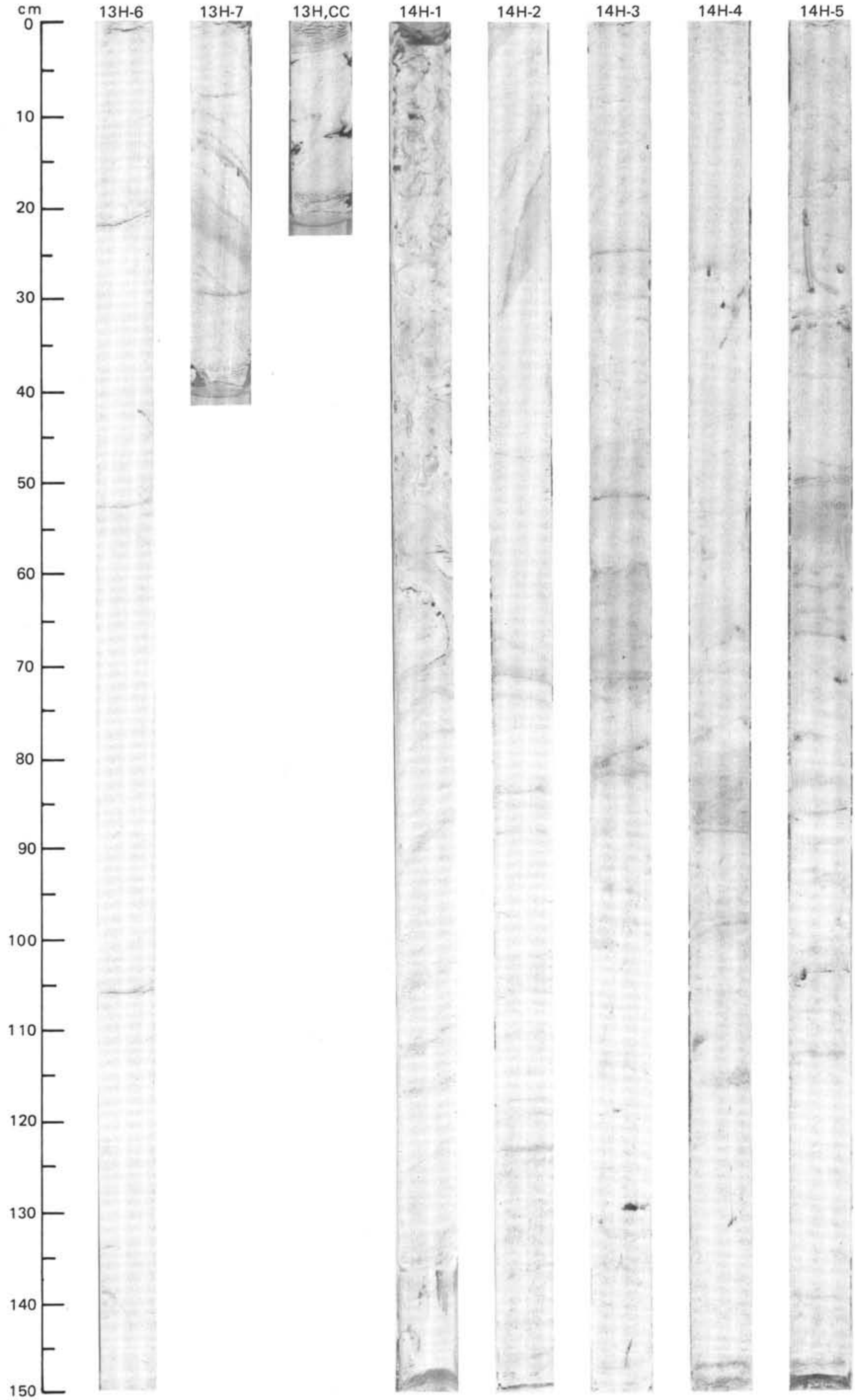
cm
0
10
20
30
40
50
60
70
80
90
100
110
120
130
140
150
13H-6
13H-7
13H,CC
14H-1
14H-2
14H-3
14H-4
14H-5

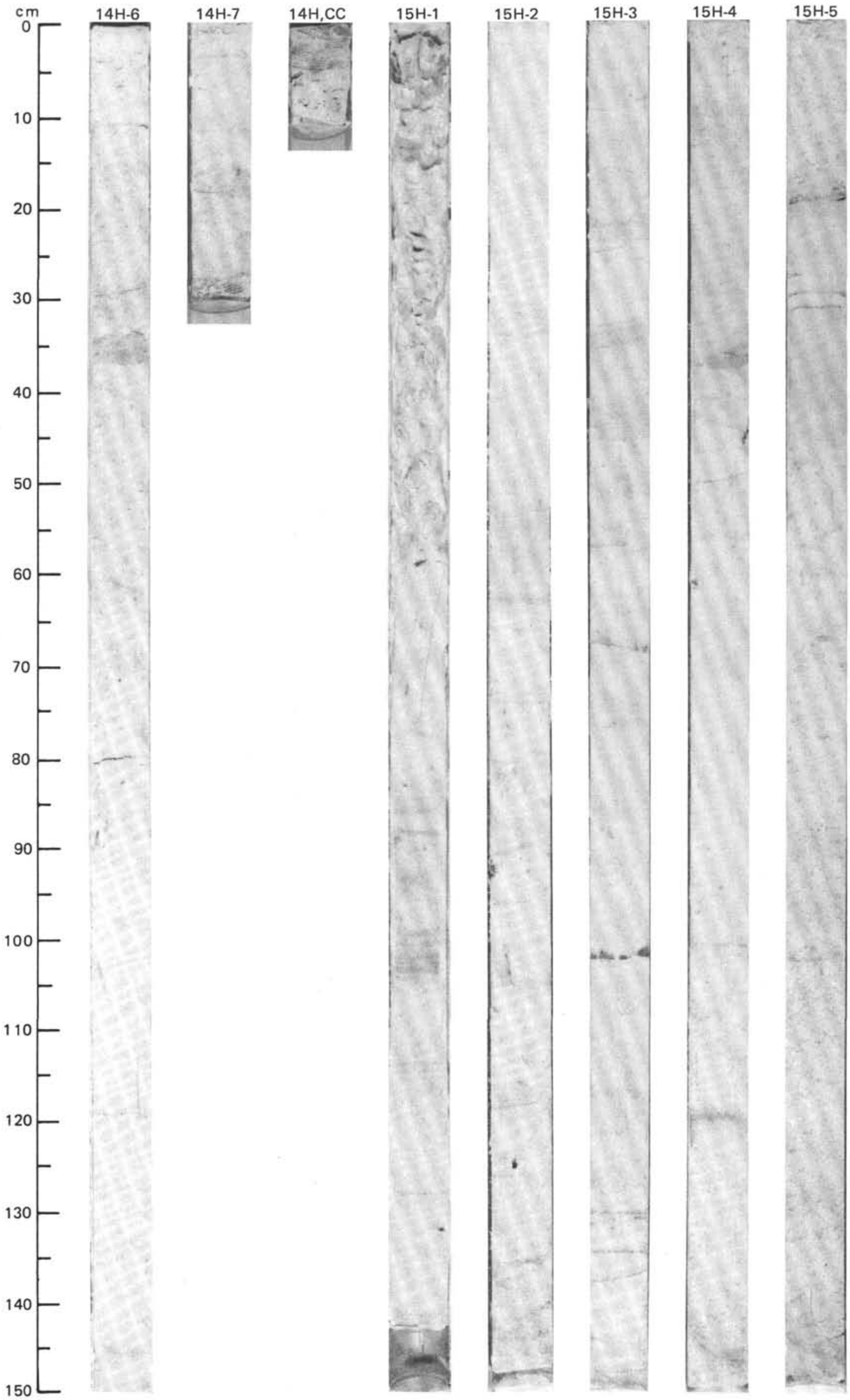
cm
0
10
20
30
40
50
60
70
80
90
100
110
120
130
140
150
14H-6
14H-7
14H,CC
15H-1
15H-2
15H-3
15H-4
15H-5

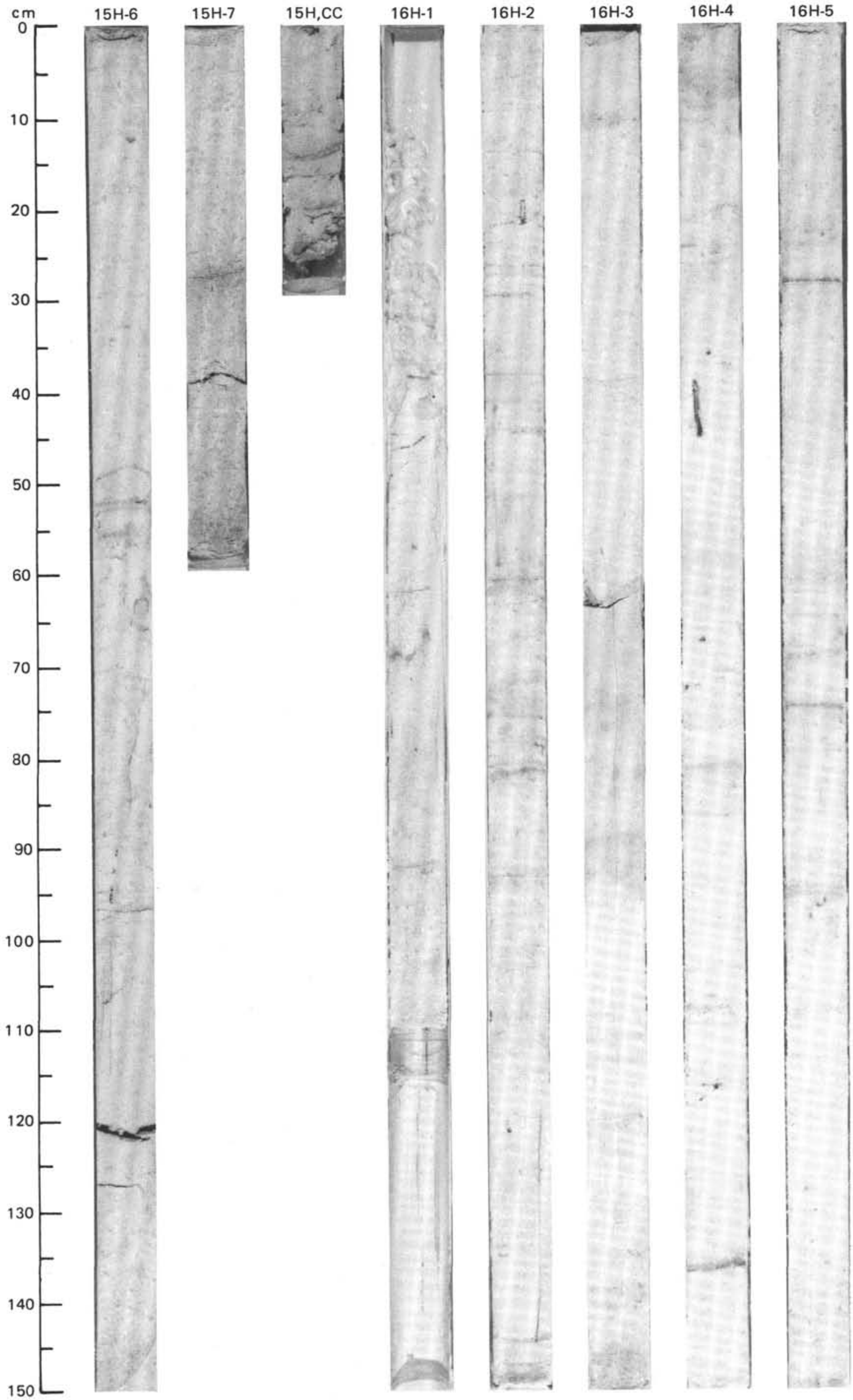
cm
0
10
20
30
40
50
60
70
80
90
100
110
120
130
140
150
15H-6
15H-7
15H,CC
16H-1
16H-2
16H-3
16H-4
16H-5

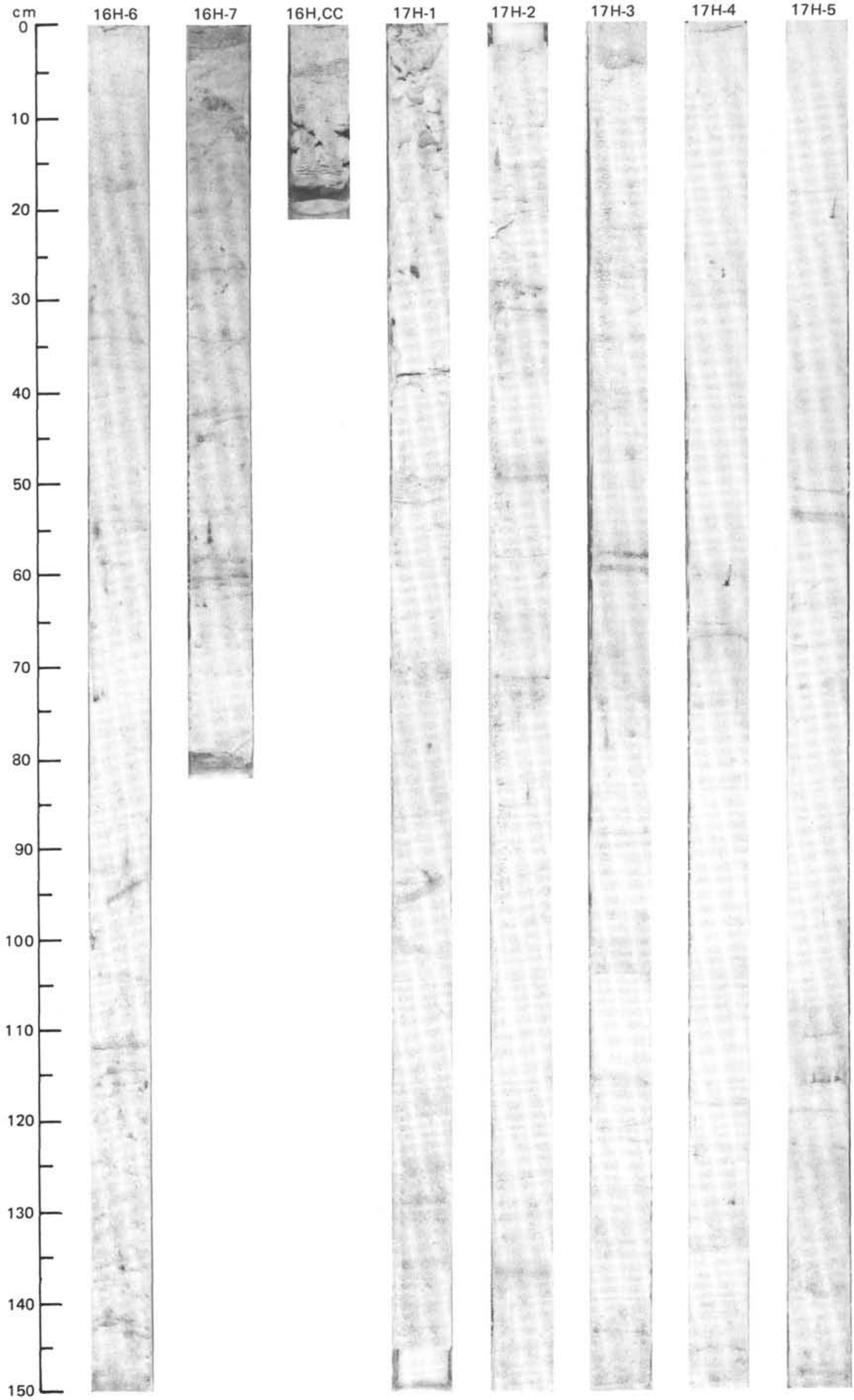
cm
0
10
20
30
40
50
60
70
80
90
100
110
120
130
140
150
16H-6
16H-7
16H,CC
17H-1
17H-2
17H-3
17H-4
17H-5

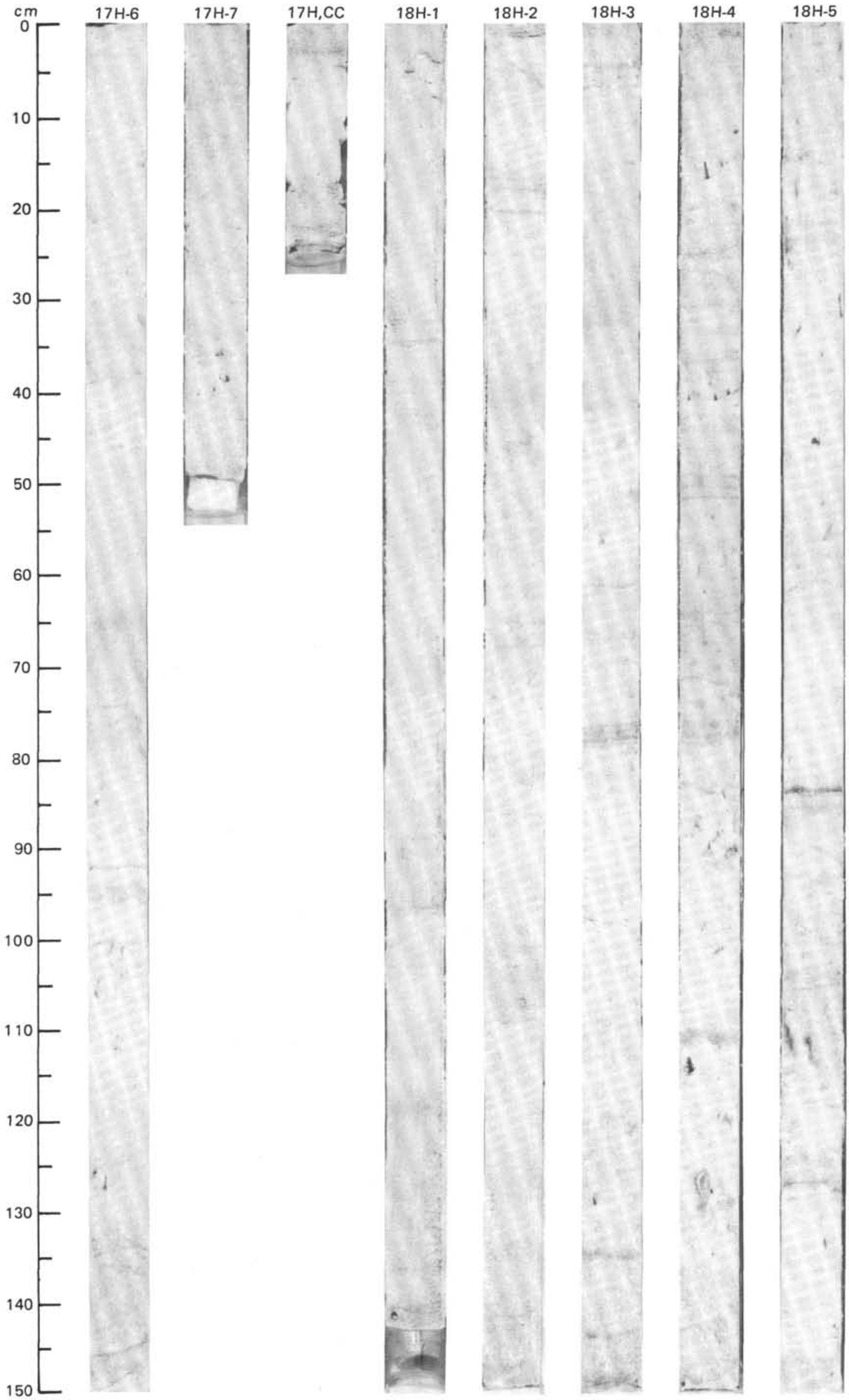
cm
0
10
20
30
40
50
60
70
80
90
100
110
120
130
140
150
17H-6
17H-7
17H,CC
18H-1
18H-2
18H-3
18H-4
18H-5

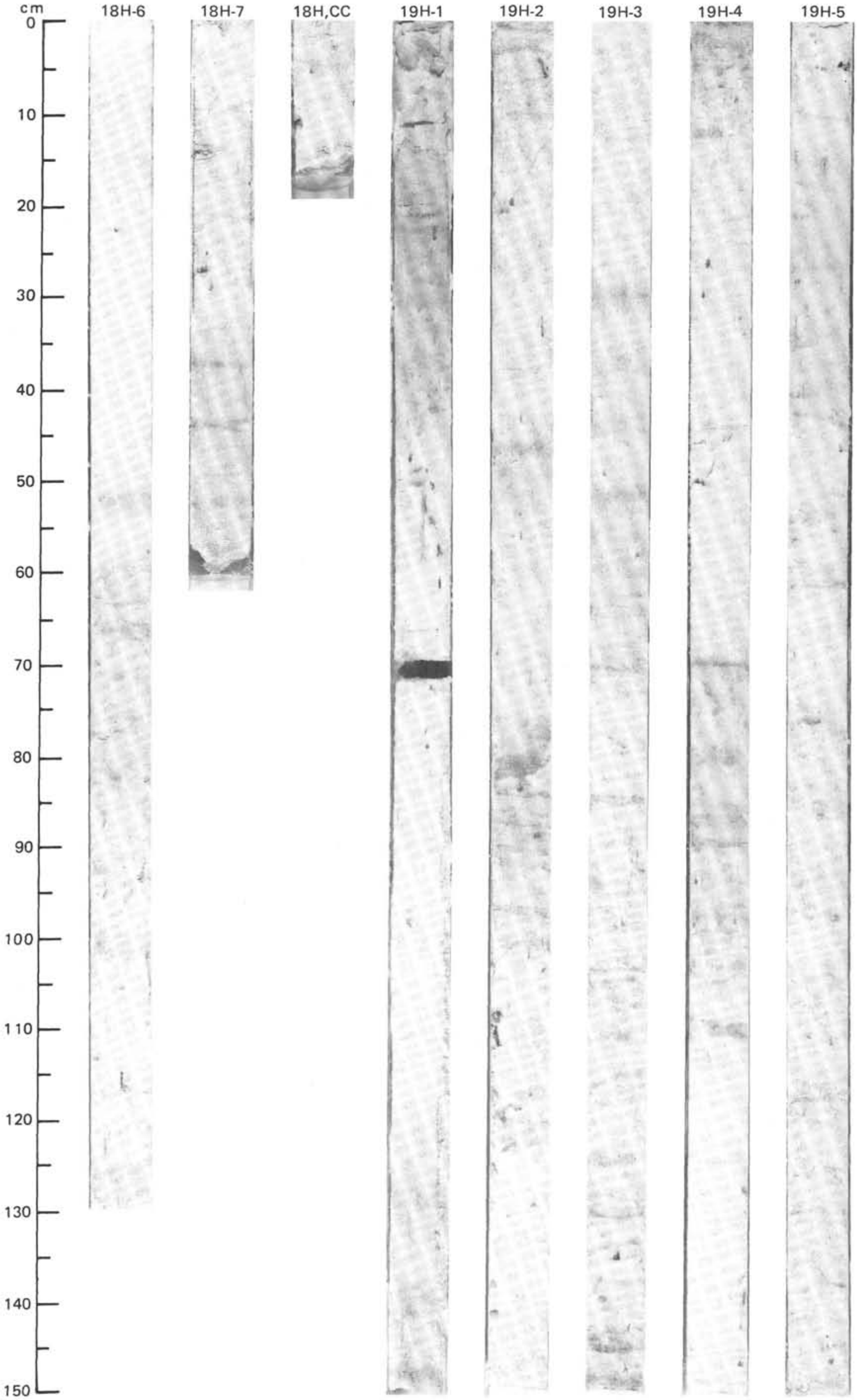
cm
0
10
20
30
40
50
60
70
80
90
100
110
120
130
140
150
18H-6
18H-7
18H,CC
19H-1
19H-2
19H-3
19H-4
19H-5

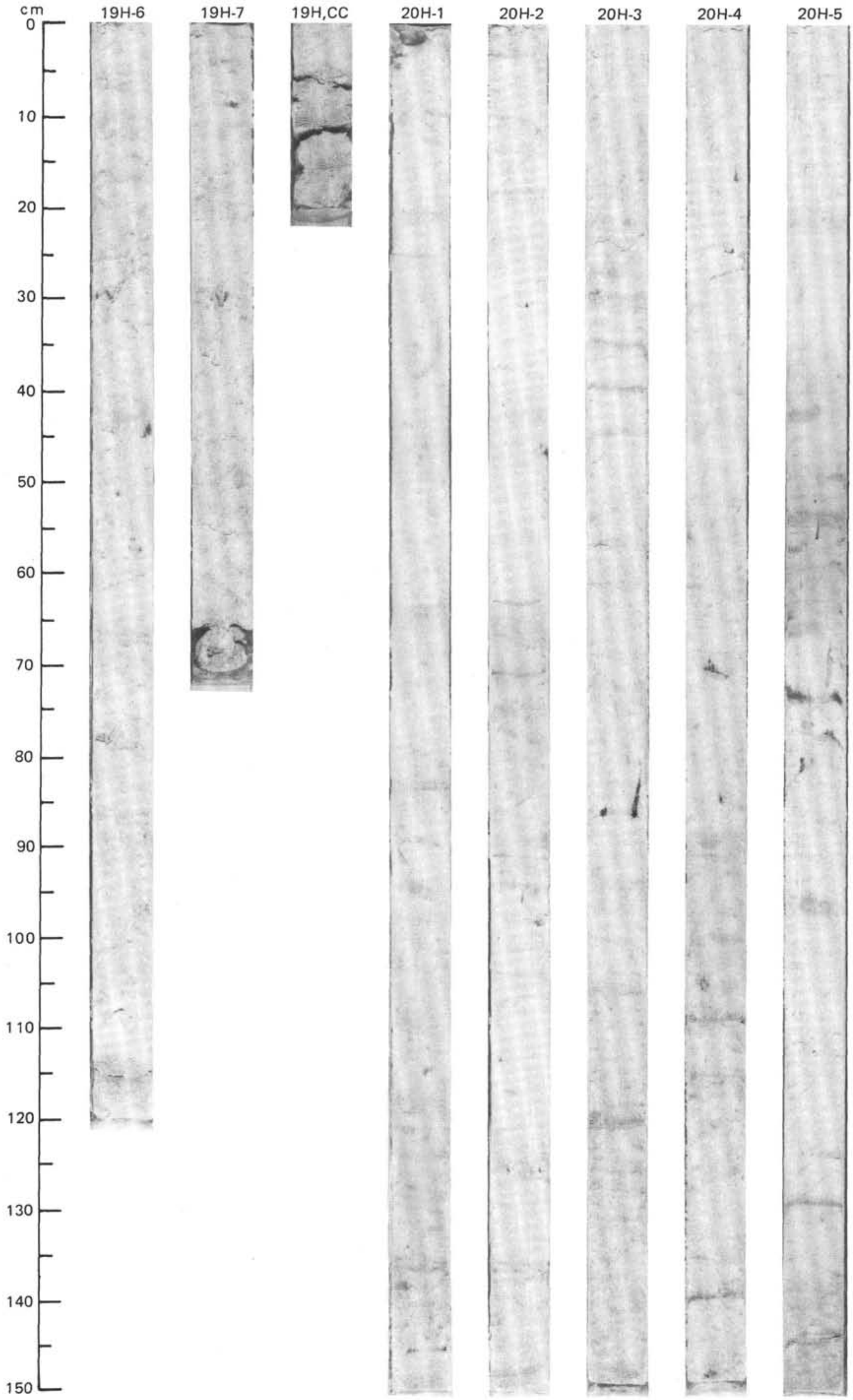
cm
0
10
20
30
40
50
60
70
80
90
100
110
120
130
140
150
19H-6
19H-7
19H,CC
20H-1
20H-2
20H-3
20H-4
20H-5

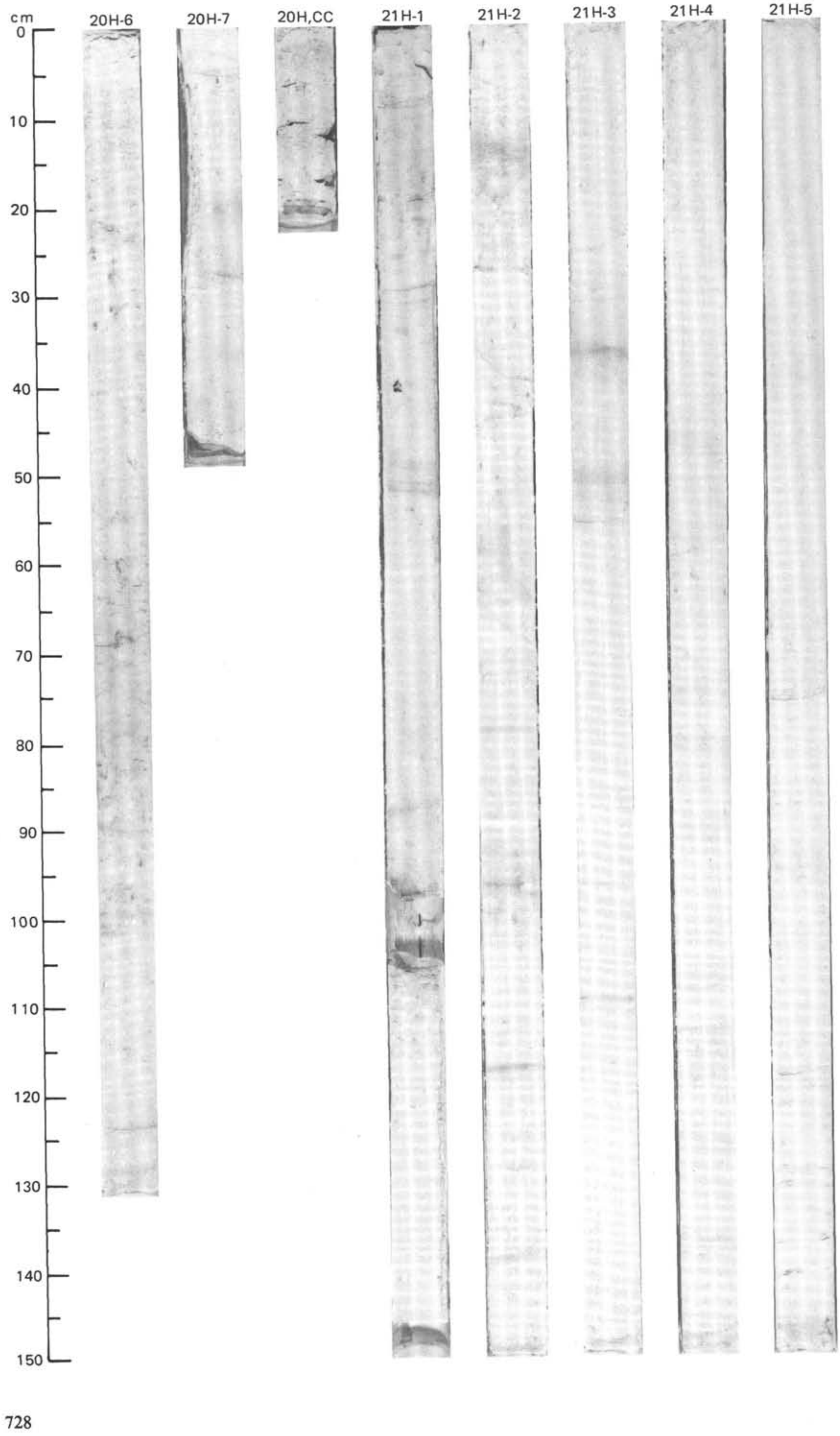
cm
0
10
20
30
40
50
60
70
80
90
100
110
120
130
140
150
20H-6
20H-7
20H,CC
21H-1
21H-2
21H-3
21H-4
21H-5

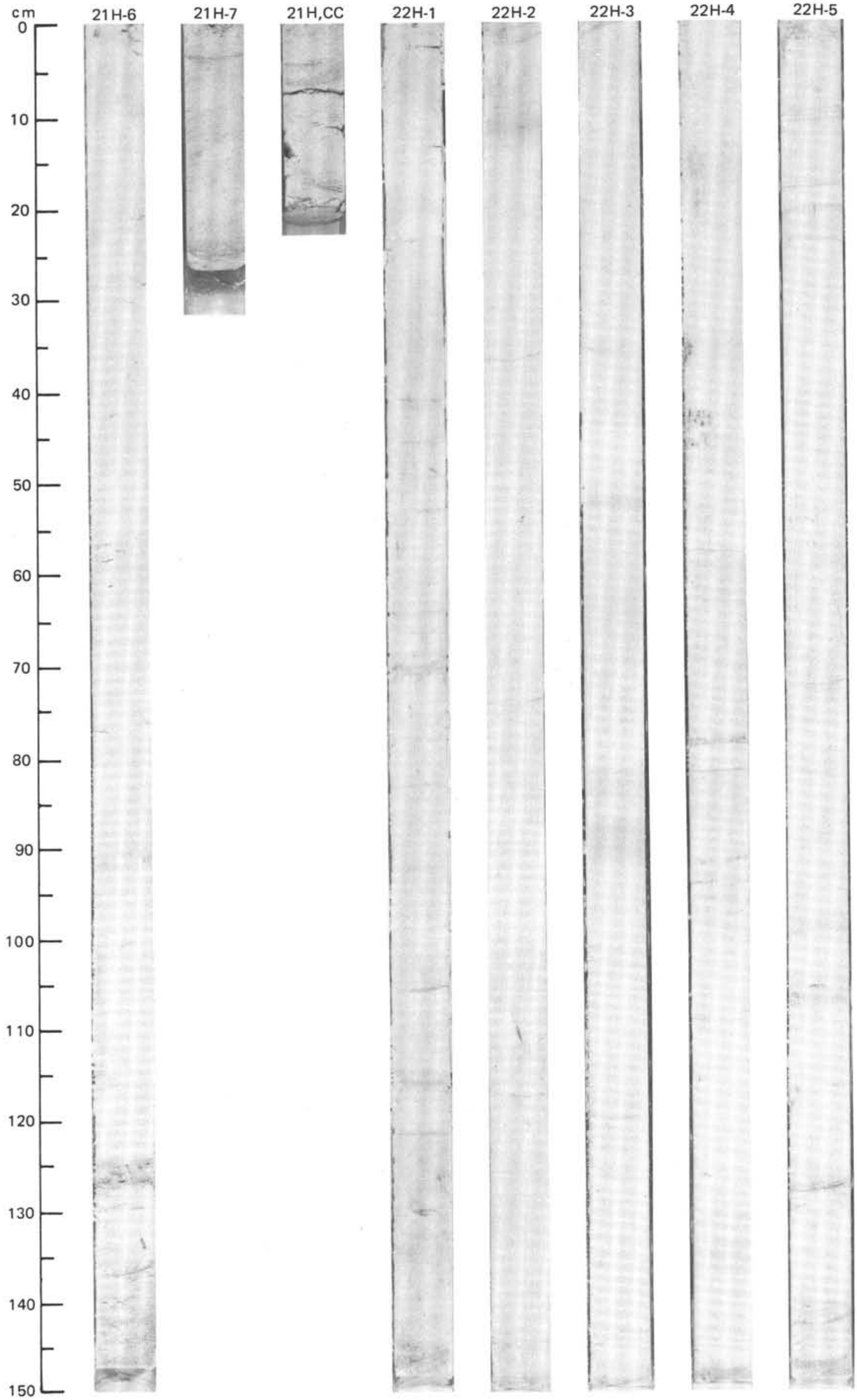
cm
0
10
20
30
40
50
60
70
80
90
100
110
120
130
140
150
21H-6
21H-7
21H,CC
22H-1
22H-2
22H-3
22H-4
22H-5

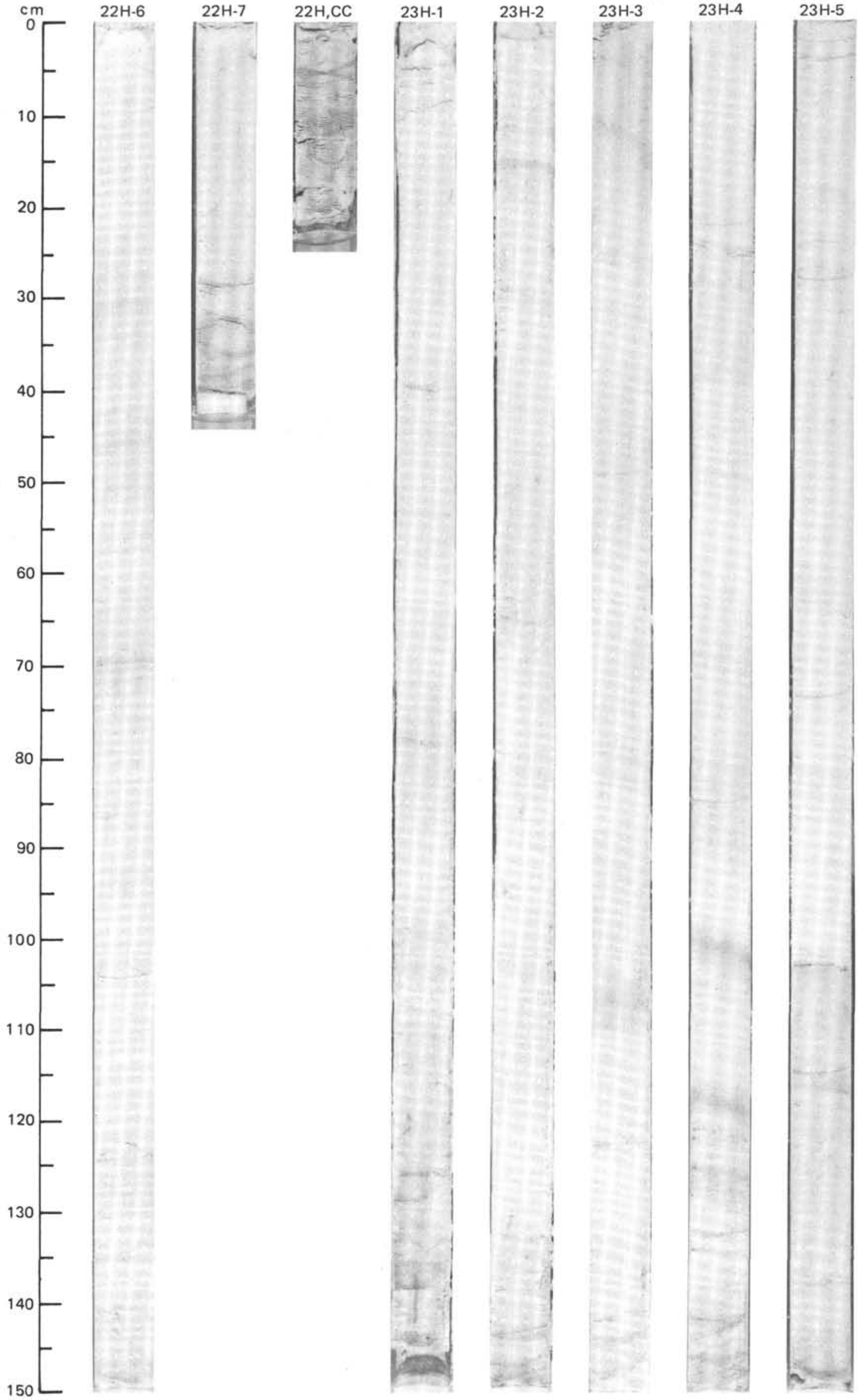
cm
0
10
20
30
40
50
60
70
80
90
100
110
120
130
140
150
22H-6
22H-7
22H,CC
23H-1
23H-2
23H-3
23H-4
23H-5

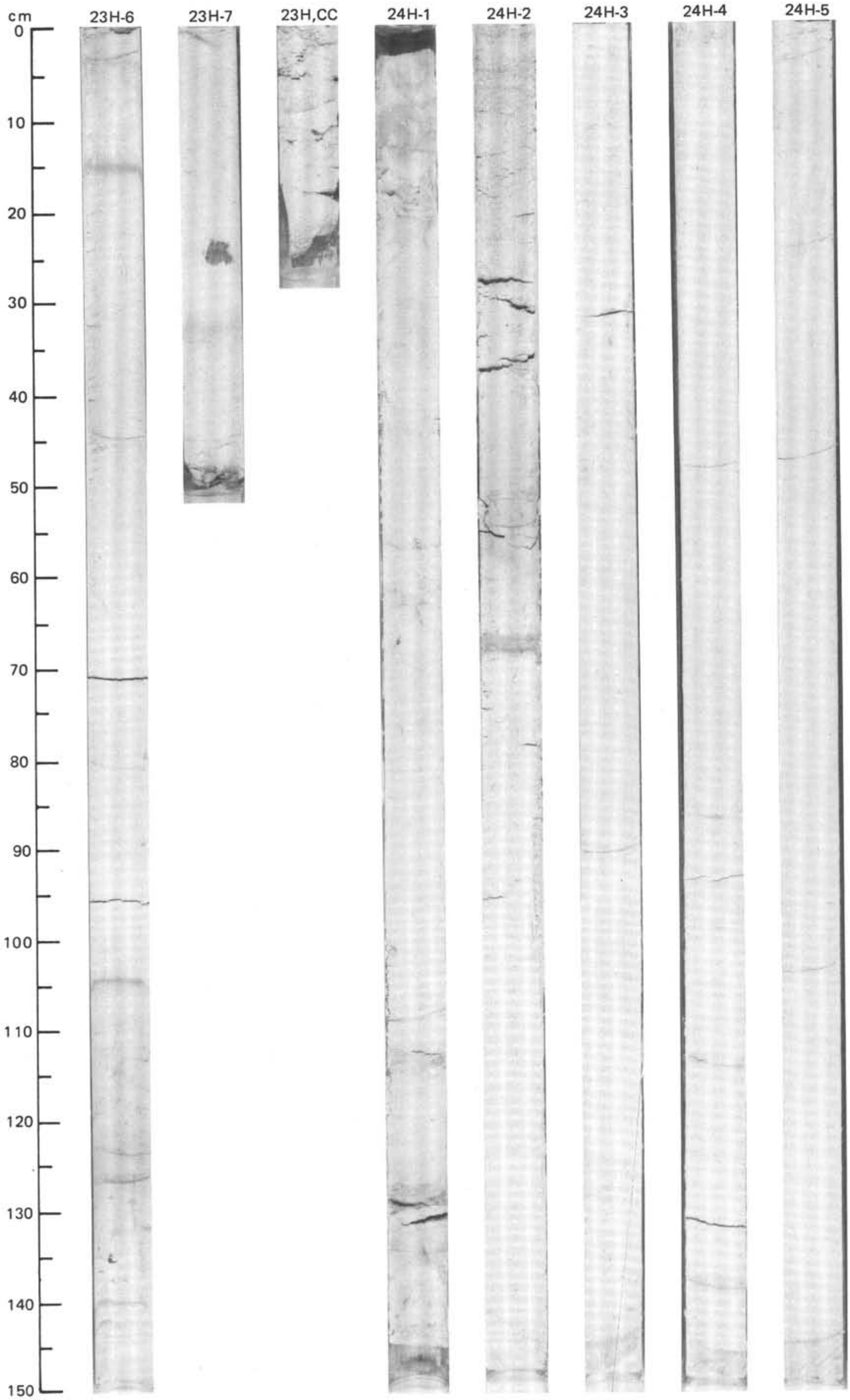
cm
0
10
20
30
40
50
60
70
80
90
100
110
120
130
140
150
23H-6
23H-7
23H,CC
24H-1
24H-2
24H-3
24H-4
24H-5

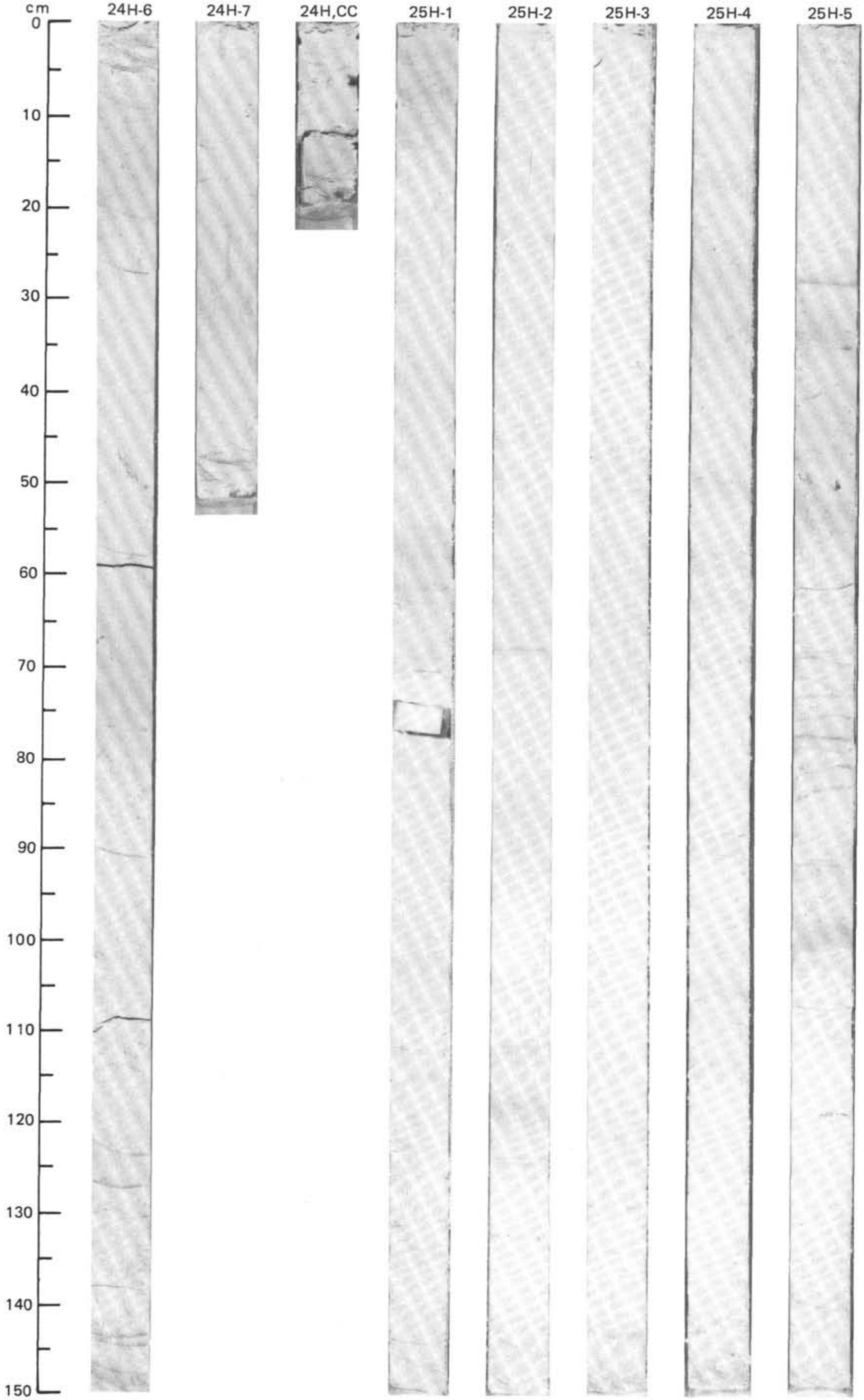
cm
0
10
20
30
40
50
60
70
80
90
100
110
120
130
140
150
24H-6
24H-7
24H,CC
25H-1
25H-2
25H-3
25H-4
25H-5

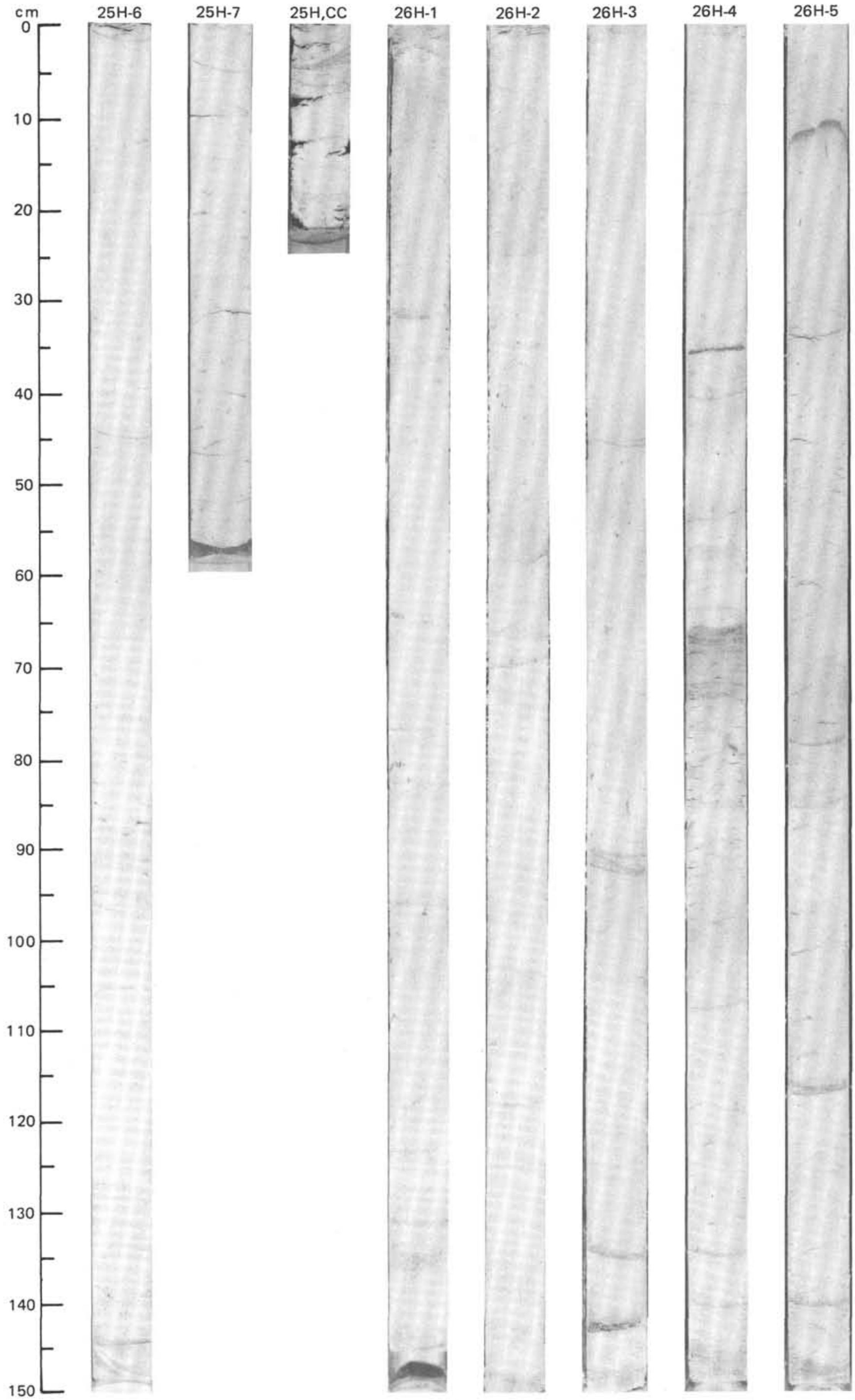
cm
0
10
20
30
40
50
60
70
80
90
100
110
120
130
140
150
25H-6
25H-7
25H,CC
26H-1
26H-2
26H-3
26H-4
26H-5

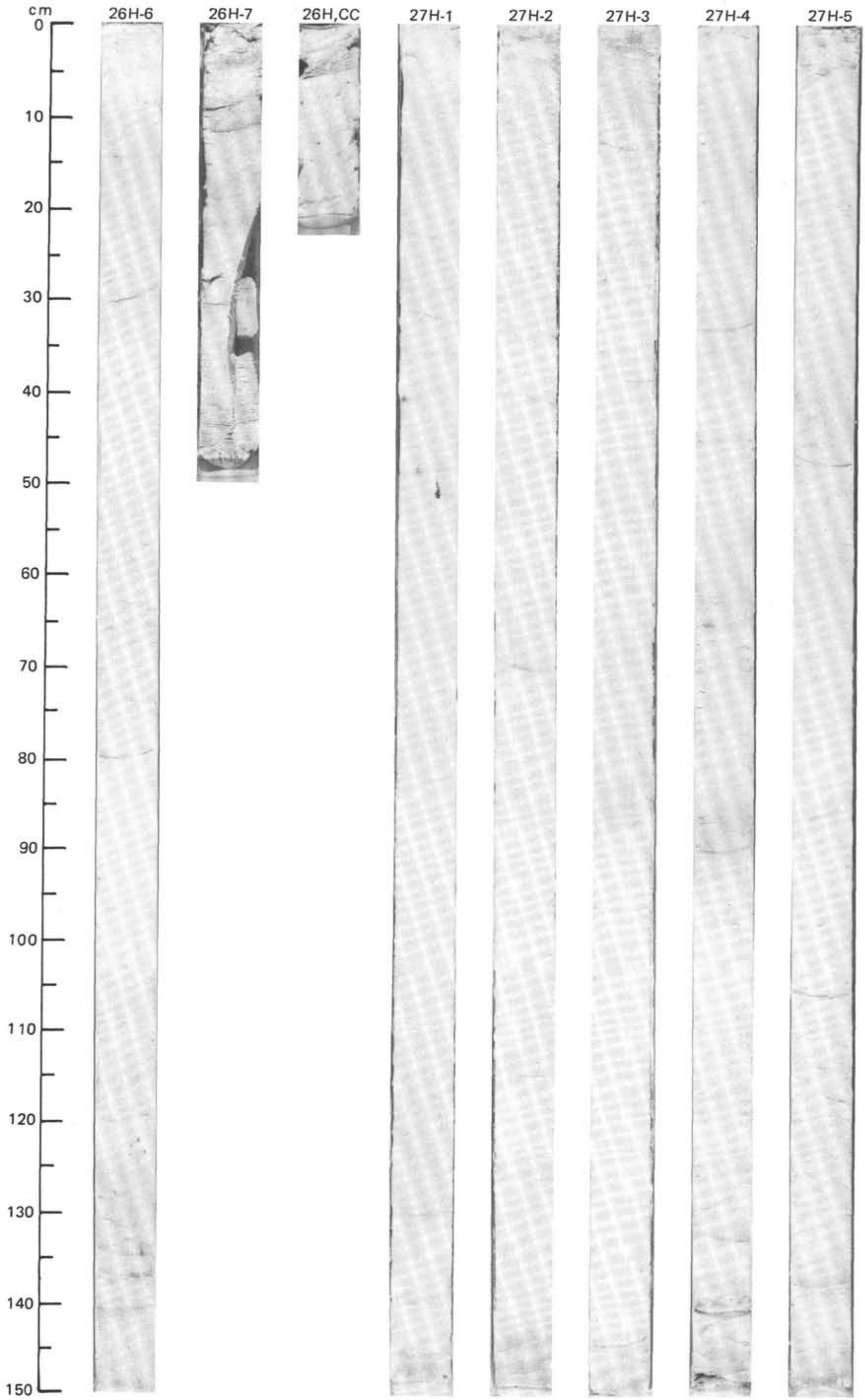
cm
0
10
20
30
40
50
60
70
80
90
100
110
120
130
140
150
26H-6
26H-7
26H,CC
27H-1
27H-2
27H-3
27H-4
27H-5

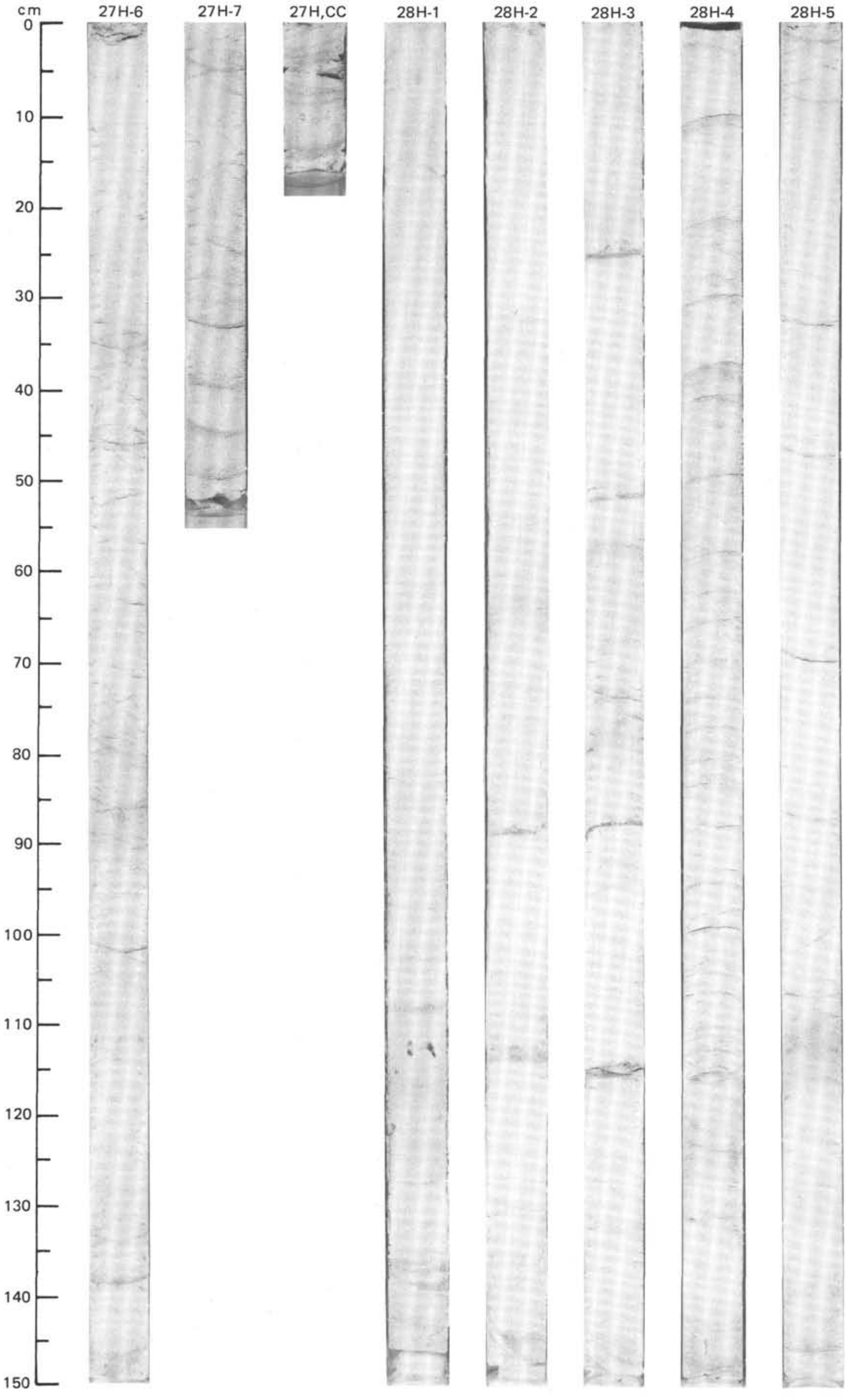
cm
0
10
20
30
40
50
60
70
80
90
100
110
120
130
140
150
27H-6
27H-7
27H,CC
28H-1
28H-2
28H-3
28H-4
28H-5

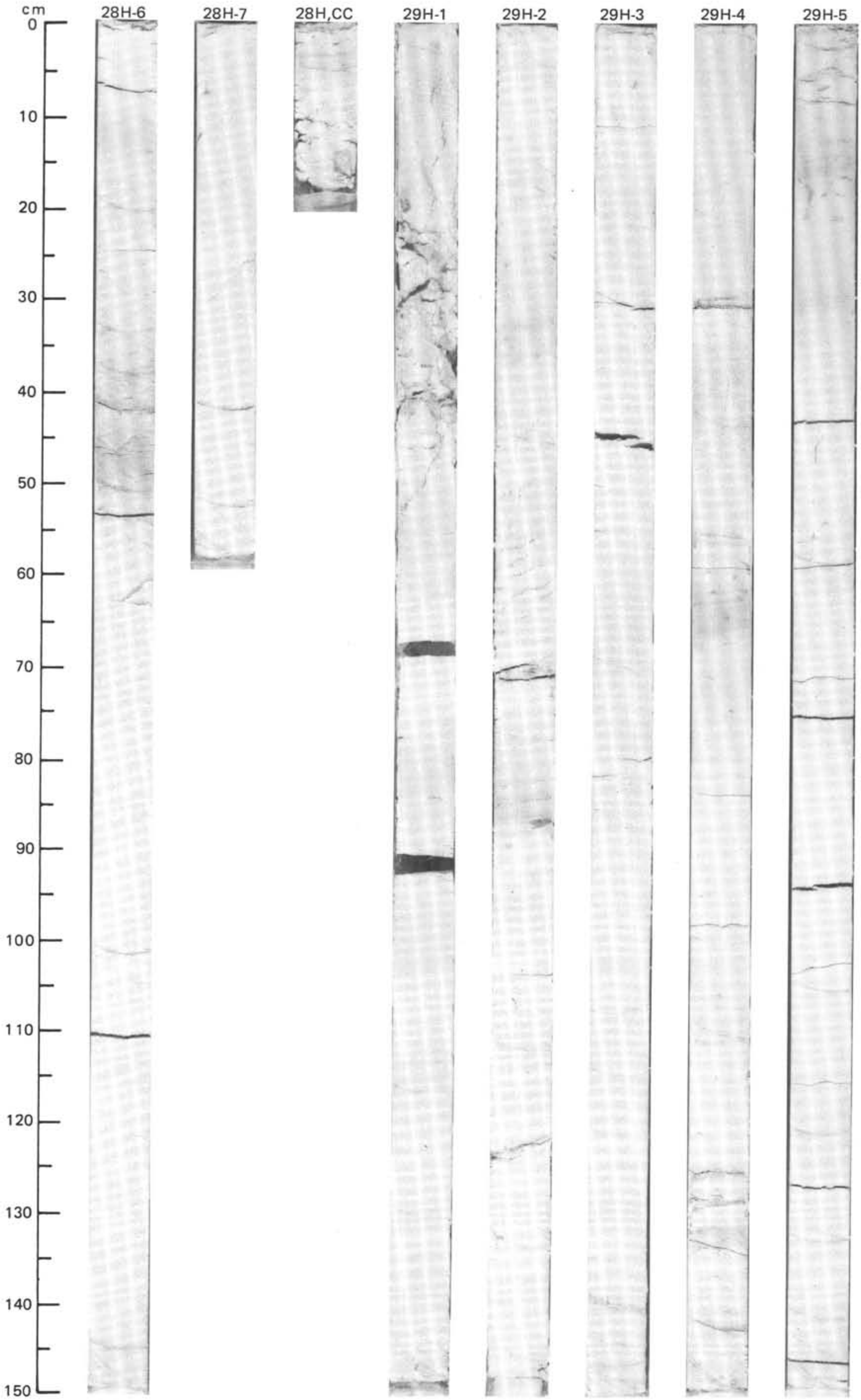
cm
0
10
20
30
40
50
60
70
80
90
100
110
120
130
140
150
28H-6
28H-7
28H,CC
29H-1
29H-2
29H-3
29H-4
29H-5

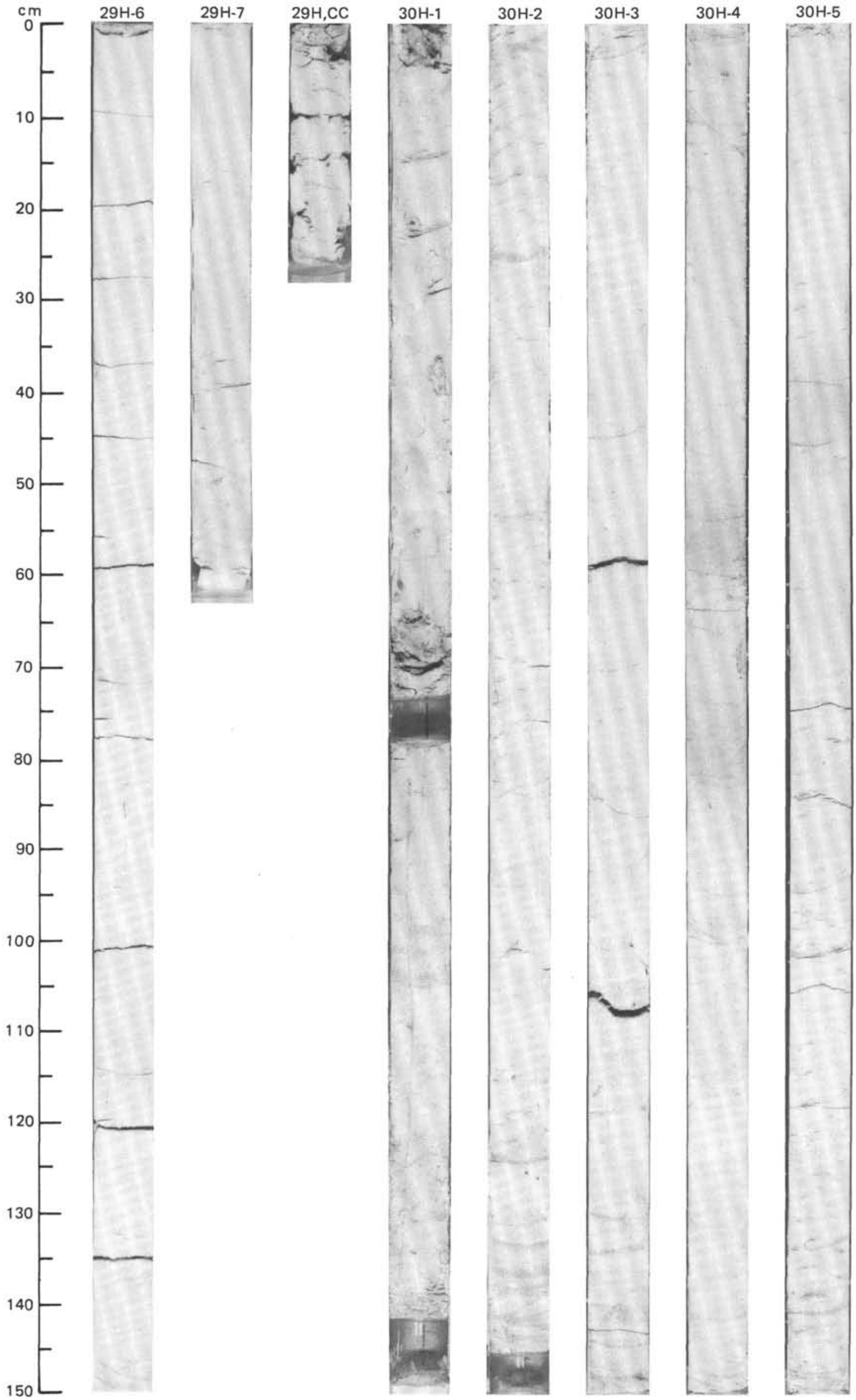
cm
0
10
20
30
40
50
60
70
80
90
100
110
120
130
140
150
29H-6
29H-7
29H,CC
30H-1
30H-2
30H-3
30H-4
30H-5

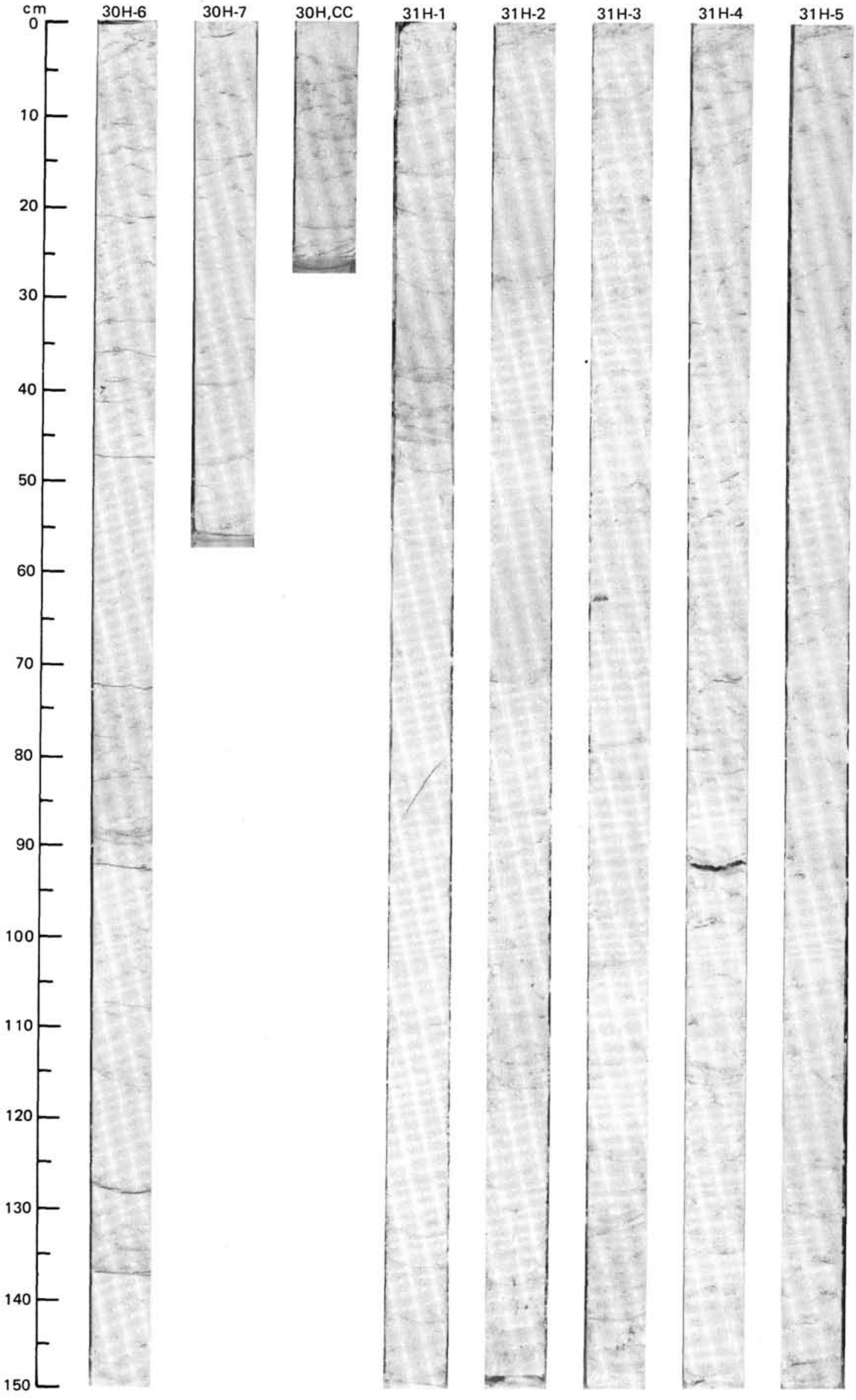
cm
0
10
20
30
40
50
60
70
80
90
100
110
120
130
140
150
30H-6
30H-7
30H,CC
31H-1
31H-2
31H-3
31H-4
31H-5

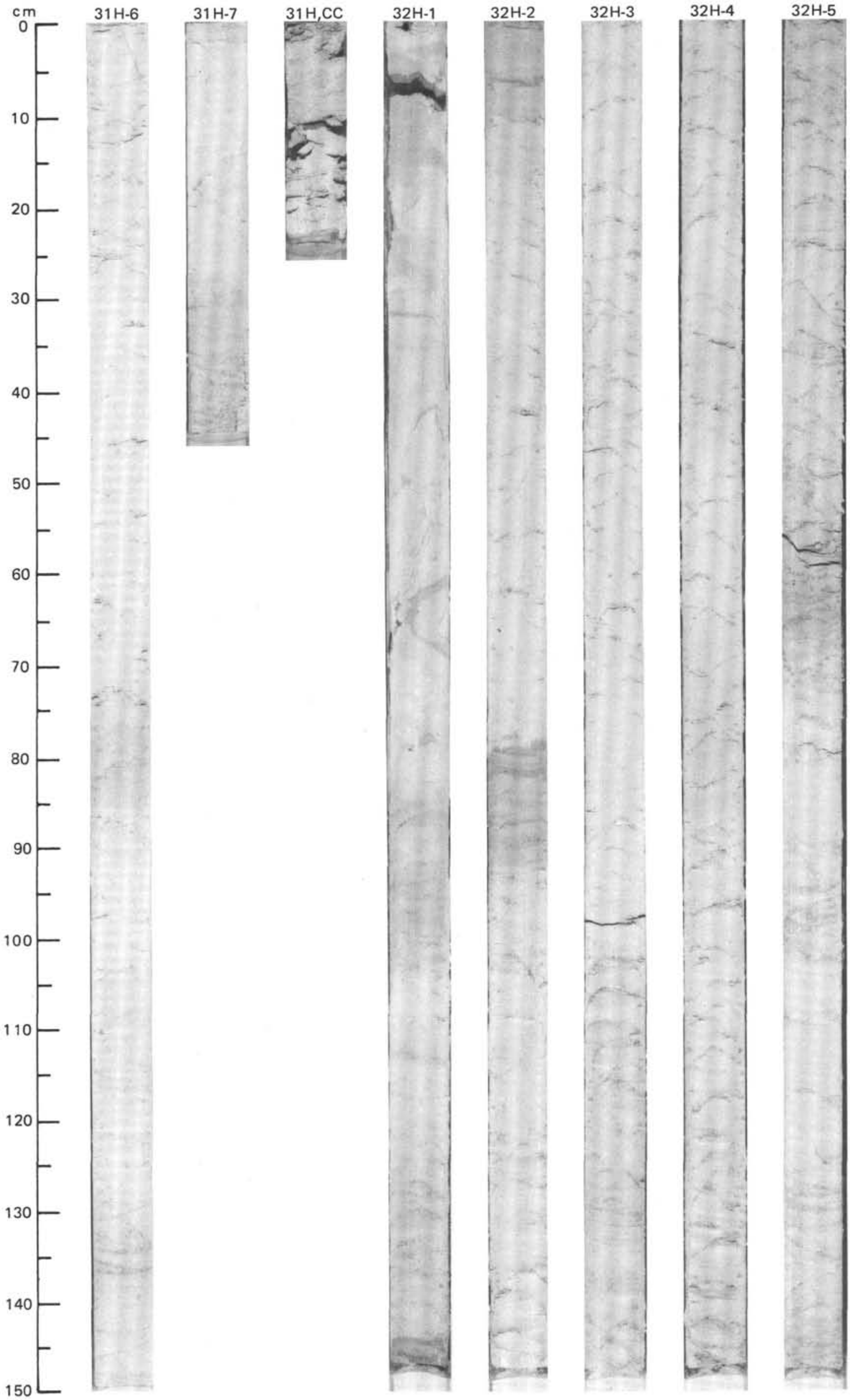
cm
31H-6
31H-7
31H,CC
32H-1
32H-2
32H-3
32H-4
32H-5
0
10
20
30
40
50
60
70
80
90
100
110
120
130
140
150

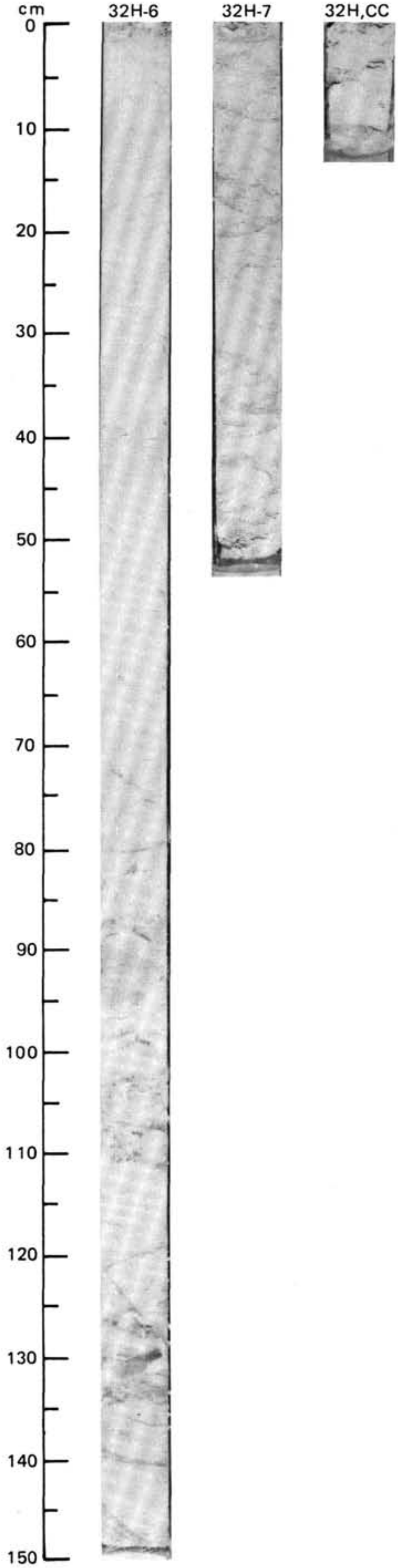
cm
0
10
20
30
40
50
60
70
80
90
100
110
120
130
140
150
32H-6
32H-7
32H,CC